

Protein oxidation by the attack of OH radicals / OH
erradikalen erasoen bidezko proteinen oxidazioa

Jon Uranga Barandiaran

Protein oxidation by the attack of OH radicals
OH erradikalen erasoen bidezko proteinen oxidazioa

Jon Uranga Barandiaran

Doctoral Dissertation

2017

Director: Jesus M. Ugalde Uribe-Etxebarria

co-Director: Jon M. Matxain Beraza

eman ta zabal zazu



Universidad del País Vasco Euskal Herriko Unibertsitatea



Eskerrik beroenak

Igaro dira jada tesiko urteak, eta ze abiadan gainera! Betidanik gustatu izan zait kimika, eta ez neukan zalantza gehiegi doktoredutza bat egiterakoan. Kimika gustuko izatearen zati handi bat izeba Maria Asuni dagokio, etxean egiten zizkidan experimentu guzti horien ondorioz. Ez ditut inoiz ahaztuko. Hortaz, eskerrik asko, izeba!

Bizipen ugari tesi garaian, batzuk gozoak eta besteak mingontsak, eta hona iritsitakoan esker ona erakutsi nahi nuke alboan izan ditudan guztiei. Beti izan bait zaituztet ondoan guraso eta lagunak, eskua luzaturik. 2012ko udan hasi nintzen masterra egiten, Txonirekin hitz egin ostean, gonbita luzatu bait zenidan aurreko udan praktikak egiteko, eta beranduago jarraipena egiteko. Bulegoan sartu, eta bertakoei zer esan? Zertaz hitz egin? Hor nire ardura! Txonik aurkeztu zizkidan bertakoak eta berehala ohartu nintzen talde atsegina zela eta halako mamuak nire buruan baino ez zeudela. Orduz gero, entzun behar izan naute! Duda, txiste edo broma eta hortaz, eskerrik beroenak eman nahi dizkizuet, GUZTIOI!!

Bereziki Jon Mikel eskertu nahiko nuke, izan bait zara niretzako erreferentzia. Hor, txokoan eserita bisera kendu gabe eta Mac teklatuari fuerte sakatuz. A ze nolako kolpeak! Noiz behinka *Cazzo!* ozen bat aterata eta beste batzuetan:

- Ostirala da, eta *reggaeton* pixkat jarri behar da, animatzeko!

Tipo adeitsua eta prestua beti izan zenuen laguntzeko denbora. Lanerako ez ezik noizbaitean garagardo bat edo beste hartu eta edozertaz hitz egiteko aukera izan genuen, izan zen plazerra! Eskerrik beroenak zuri!

Ezin ahaztu zutaz, Txema. Beti izan bait duzu laguntzeko denbora, ordenagailuko arazo eta dudekin, nahiz eta telefonoan deika izan dituzun. Eskerrik asko denbora hartu izana, pazientziaz azalduz. Txema, nola jartzen da...? Txema, zergatik ezin dut...? Txema, nola konpondu...? Txema, zer da...? Ezin egin, zure laguntzarik gabe! *Txema Mercero, El mejor del mundo entero!*

Txoni entzun eta lagundu didazu tesi urteetako garaian eta praktikoago izatearen garrantzia ikusi dut zugaran. Askotan aldrebestu bait dut nire burua... Ez dut ahaztuko zenbakiz eta taulaz josi nuen lehen “draft” hura. Nik neri buruari esaten bainion “zenbat eta gehio orduan eta hobe, seguru!”. Hori bai sarturiko zenbaki mordoa... eta zenbat kosta zitzaidan. Zenbat lerrotako excell-a! Erabat ulertezina, halako organizazio saiakera txiki batekin, letra grekoz betea: $\alpha, \beta, \dots, \lambda$ eta alfabeto greko gabe geratuta, zenbakien bidez eginiko labelak: 1, 2, ..., 17. Hori bai digeritzeko zaila! Ez pentsa diskusioa askoz xamurragoa zenik. Ba hara, hura entregatu eta lasi geratu nintzen. Ostera, komentario bakarra jaso nuen:

- Historio bat idatzi behar duzu!

“¡Laaaa Virgen!” neronek nire buruari. Esfortzu guzti hura eta bueltan zenbakien erdia kentzeko... *Terapia de choque* deituko diote honi. Kezkak eta dudak kontatu dizkizut eta beti aurkitu didazu irtenbide bat, nahiz eta askotan erreboluzionatua ibili naizen. Lagundu didazu gelditzen eta gauzak prespektibaz begiratzen. Hortaz, eskerrik asko, Txoni!

Era beran, Joni, beti egon zara entzuteko prest, irrifarre batekin ahoan eta ikaragarri eskertzen dizut halako txapak entzun izana! TheoBio kongresuak tarteko, 2015ekoa gogoan. A ze nolako irriak Txoniren kontura, afarian. Anisakisari alergia eta afarian ateratako plater guztiak arraina ziren! Gizarajoa, postre gisa atera zuten apioarekin konformatu behar izan zuen!



Mil gracias Mario. Siempre tuviste tiempo para hablar de *Los mayores problemas de la Química Cuántica*. Desde los primeros días que me ayudaste con los problemas de Fortran, siempre he podido contar contigo tanto en lo profesional como en aspectos de índole más personal. ¡Has sido una gran referencia! Echaré de menos las historias del mortero sin tripode y los mosquitos gigantes de la jungla. Aún cuando la historia fuera repetida siempre había un nuevo detalle para sacarle punta. Hay que decir que ninguna historia estaba exagerada ni moldeada a tu gusto. Simpre recordaré aquel día que llegué “demasiado temprano” a la oficina y donde todavía no estaban ni TXabi ni Txoni... Madre mia, ¡qué sensación de estar cumpliendo un papelón! Ocho de la mañana y aún con legañas en los ojos, escucharte hablar de los estados. “¿De qué estará hablando este? Lleva ya cinco minutos y aún sigue. La novela de Miguel Delibes se va a quedar corta como siga así. Tu por si a caso pon buena cara y asiente, que no se entere que tengo sueño” me decía a mi mismo. “Espero que no

haya una preguntita al final de la lección, que este me pilla y parece que tiene bastante mala leche...”. Hasta que apareció Fernando, “¡*Yasta*, le está hablando a él! Yo me voy de aquí, que nadie sabe que estoy ni que dejo de estar... ¡Uffff, vaya librada!” Y por eso te estoy agradecido, Fernando. Bueno, también porque siempre tuviste tiempo para mis dudas ya fueran con Molcas o sobre el futuro laboral pero eso lo doy por saldado tras la tarta que traje.

Muchas gracias a Rafa, que siempre encontraste tiempo para escuchar y buscar respuesta a mis preguntas. Jesus, Elena, David eta Xabi eskerrik asko zuei ere. Entzun behar izan nauzue ofizinan eta lagundu didazue aurkitzen irtenbidea. “Barkatu, galdera bat egiterik bai?” ez dakit zenbat aldiz errepikatu dizuedan galdera hori. Xabiren ofizinako txistuak eta historiak faltan botako ditut! Elisa, Eider, Eli, Maru eta Ion Mitxelena, eskerrik asko zuei ere! Beti aurkitu dut zuengan sustengua. Quisiera también agradecer a Eloy, Sławek, Andreas, Ivan, Noelia, Mauricio (Mr Shannon), Irene, Mireia y claro a Matito. *Muchs gracies!*

I would also like to thank to the theoretical chemistry groups where I have stayed at. Ulf, Paulius, Svante, Maria, Petter and Samuel thank you for your patience at my begining steps. Daryna, Athanasios, Ana, Peter, Servaas and Arnout, many thanks to all of you. I will never forget about the *meetings* in *Café Belge*. I have learned many things and had a fabulous time over there. I would also like to thank the group in Piscataway, Maria Panteva, George, Erich, Kenneth, Darrin and all of the group! I felt very pleased to having been there with you and feel that have learned a lot during my short period, many many thanks!

Ezin naiteke zuetaz ahaztu, kuadrilakoak eta *Guaratxa* osoaz. Larunbatetako futbol partidak, soziedadeko afariak eta diskurtso filosofikoak eta ez horren filosofikoak. *Today in the spotlight...* Lagundu didazue gehien behar izan dudanean eta kontaezinak diren momentu ederrak elkarbanatu ditugu! *Mute! Mañana va en bici Txus!*

Azkenik, gertukoenak, guraso, arreba eta familia osoa, eskertu nahi nituzke. Eman bait didazue dudan guztia eta gaur egun naiz zuengatik naizena. Eskerrik asko!! Askok maite zaituztet!

Contents

1	Laburpena	1
1.1	Arnasketa zelularra eta espezie erreaktiboak	1
1.1.1	Espezie erreaktiboen klasifikazioa	2
1.1.2	Espezie erreaktiboen produkzioa	2
1.1.3	Espezie erreaktiboak eta estres oxidatiboa	3
1.2	Antioxidatzaileak	4
1.3	Osagai zelularren oxidazioa	5
1.3.1	Proteinak	5
1.3.2	Proteinen oxidazioa	6
1.4	Lanaren helburua	9
1.5	Metodoak	9
1.5.1	Dentsitate Funtzionalaren Teoria	9
1.6	Erabilitako modelo eta protokoloa	12
1.6.1	Modeloa	13
1.7	Amino azidoen oxidatzeko joera	13
1.7.1	Sufrea duten amino azidoen oxidazioa	15
1.7.2	Alkohola duten amino azidoak	20
1.7.3	Amino azido aromatikoak	20
1.7.4	Amino azido azido eta basikoak	28
1.7.5	Beste amino azidoak	39
1.7.6	Amino azidoen bizkarrezurra	44
1.8	Ondorioak	50
2	Introduction	53
2.1	Cellular respiration and Reactive species	53
2.1.1	Classification of reactive species	53
2.1.2	Production of reactive species	54
2.1.3	Reactive species and oxidative stress	55
2.2	Antioxidants	56
2.3	Oxidation of cell constituents	57
2.3.1	Proteins	57
2.4	Scope of the work	64

3	Methods	67
3.1	Historical perspective	67
3.2	Density functional theory	69
3.2.1	Hohenberg-Kohn	69
3.2.2	Kohn-Sham (KS)	70
3.2.3	Approximations to exchange-correlation energy	73
3.2.3.1	Local Density Approximation (LDA)	73
3.2.3.2	Generalized Gradient Approximation (GGA)	73
3.2.3.3	Meta Generalized Gradient Approximation (mGGA)	74
3.2.3.4	Hybrid functionals	74
3.2.4	Final remarks on DFT	75
3.3	Basis sets	76
3.3.1	Basis set superposition error (BSSE)	77
3.4	Molecular Space Partitions	77
3.4.1	Mulliken	77
3.4.2	Fuzzy Atom Scheme	78
3.5	Solvation	79
3.6	Employed method and protocol	80
3.6.1	The model	80
4	Protein Backbone Homolytic Dissociation By $\bullet OH$	83
4.1	Introduction	83
4.2	Results and discussion	84
4.2.1	Step 1: H abstraction	84
4.2.1.1	Energies of the intermediate species.	84
4.2.1.2	Rationalizing intermediate's stability	86
4.2.2	Step 2: homolytic bond dissociation.	88
4.2.2.1	Origin of the Ser and Thr preference for the Step ₂ ^{NC} step	90
4.3	Conclusion	91
5	The Attack Of $\bullet OH$ Onto Aromatic Amino Acids	95
5.1	Introduction	95
5.2	Results	96
5.2.1	Phenylalanine	96
5.2.2	Tyrosine	100
5.2.3	Tryptophan	103
5.3	Discussion	106
5.4	Conclusions	108
6	$\bullet OH$ Oxidation Towards S- and OH- Containing Amino Acids	113
6.1	Introduction	113
6.2	Methodology for the electron transfer reactions	115
6.3	Results and discussion	117
6.3.1	Alcohol containing amino acids	118
6.3.1.1	Serine	118
6.3.1.2	Threonine	119

6.3.2	Sulfur-containing amino acids	121
6.3.2.1	Cysteine	121
6.3.2.2	Cystine	122
6.3.2.3	Methionine	124
6.4	Conclusions	128
7	•OH Attack Towards Acid, Base And Amide Side Chains	131
7.1	Introduction	131
7.2	Results	132
7.2.1	Acid containing amino acids	133
7.2.1.1	Aspartic acid	134
7.2.1.2	Glutamic acid	136
7.2.2	Base containing amino acids	137
7.2.2.1	Arginine	137
7.2.2.2	Lysine	138
7.2.3	Amide containing amino acids	139
7.2.3.1	Asparagine	139
7.2.3.2	Glutamine	140
7.3	Conclusions	141
8	Final Conclusions	151

Chapter 1

Laburpena

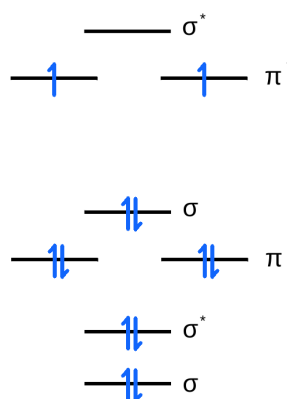
Organismo bizidunak sistema oso konplexuak dira, zeinetan erreakzio kimiko ugari gertatzen diren. Gu geu, erreakzio kimikoz osatuak gaude, erreakzio ugariz! Hala, biokimika organismoen barnean gertatzen diren erreakzio kimikoak aztertzen dituen zientzia da. Mugaturiko atomo kopurua konbinatuz ia muga gabeko molekulak (biomolekulak) osatu daitezke zeinak organismo bizidunen parte diren. Biomolekula bakoitzak bete behar zehatz bat du eta hala eratzen da bizitza ezagutzen dugun moduan.

1.1 Arnasketa zelularra eta espezie erreaktiboak

Denboran zehar atmosferaren konposizioa aldakorra izan da. Lurrean bizia hasi zeneko lehen atmosfera gehienbat N_2 eta CO_2 -z osatua zegoela uste da. Hala, azaldu ziren lehen organismoak ez zeuden ia O_2 -ra ezarriak, hots, organismo anaerobikoak ziren eta ez zuten O_2 -rik erabiltzen bizirauteko. Are gehiago, halako organismoak oso sentikorrek ziren O_2 -ra, izan ere ez zuten inongo defentsa mekanismorik.

Hala ere, atmosferako konposizioan bat-bateko aldaketa gertatu zen CO_2 kopuru handi bat O_2 -ra bihurtuz [1, 2]. Honela, organismoek eboluzionatu egin zuten O_2 kontzentrazio handiagoko inguruetan bizirauteko. Gauzak horrela, organismoak O_2 -a hasi ziren erabiltzen energia iturri gisa. Erabilpen honen funtsa O_2 -ak duen izaera oxidatzailean datza, zeinak elektroiak onartzen dituen, bere burua erreduzituz eta beste espeziea oxidatuz. Egun, ez-inbestekoa da organismo aerobikoetan, elektroi garraio prozesuan parte hartzen baitu. O_2 -ak elektroiak hartzeko duen gaitasuna Orbital Molekularren diagramaren bidez ikus daiteke, Irudia 1.1. Erdi beteta dauden azken bi orbitalak energetikoki degeneratuak daude, ondorioz, O_2 -ak elektroiak har ditzake.

Organismo aerobikoen helburu nagusia adenosin trifosfatoa (ATP), txanpon energetikoa, sortzea da. Mitokondria da ATP-aren ekoizle nagusia, organismoko ATP osoaren %80 organela honetan eratzen dela estimatu da [3], albo produktu gisa H_2O eratuz [4]. Aitzitik, batzuetan beste albo produktu batzuk eratzen dira, mekanismo orokorretik ihes egindako elektroien ondorioz, *espezie erreaktiboak* [4, 5].

Figure 1.1: O₂ Orbital Molekular diagrama.

1.1.1 Espezie errektiboen klasifikazioa

Espezie errektibo terminoa oso zabala da eta maiz anbigua gerta daiteke. Izenak aditzera ematen duen moduan, *espezie errektiboak* konposatu kimiko ezegonkorak dira zeinak beste entitate kimikoekin erraz erreakziona dezaketen [6]. Izaera kimikoaren arabera sailkatu ditzakegu, hau da, erradikalak eta ez-erradikalak [1]. Hala, “erradikal askea” hitzak erradikal izaeradun molekula adierazten du, hots, elektroiz ez-parekatu bat duena. “Askea” hitzak bestalde, biziraupen independenteari deritzo [1, 3]. *Espezie errektiboak*, osaturik dauden atomo zentralaren arabera defini daitezke. Honela, ondorengo sailkapena genuke, Oxigeno Espezie Erreaktiboak (OEE), Nitrogeno Espezie Erreaktiboak (NEE), Sufre Espezie Erreaktiboak (SEE) etab [3, 7].

- OEE: H_2O_2 , $\bullet O_2^-$, $\bullet OH$, $\bullet OOH$
- NEE: $ONOO^-$, $\bullet NO$
- SEE: $RSSR^{\bullet-}$, $RSOH$, RS^{\bullet}

1.1.2 Espezie errektiboen produkzioa

Espezie errektiboen produkzioari dagonkionez, endogenoa edo exogenoa izan daiteke. Produkzio endogenoa organismoaren behar edo akatsagatik sor daiteke [3]. Prozesu ugartan sortzen dira *espezie errektiboak*: NADPH oxidasa entzima (NOX), zeina neutrofiloetan dauden patogenoei aurre egiteko [4, 5, 8], lotura lekutik ihes egindako trantsizio metalek katalizaturik, arnasketa mitokondrialeko prozesuan. Adibide hauek produkzio endogenoari dagozkie, produkzio exogenoaren kasua dugu erradiazioaren bidez eratuak direnak.

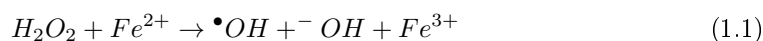
Elektroi garraio prozesuaren bitartean ATP-a eratzen du mitokondriak. Elektroiak erredukzio potentzial ezberdina duten konplexuetatik zehar garraiatuak dira, H^+ gradiente bat sortuz eta O₂-a H₂O-an bilakatuz. OEE-ak esaterako O₂-a bezalako elektroiz onartzaile



Figure 1.2: Erdoilaren eraketa errebox erreakzioen adibide gisa.

bat erreduzitzerakoan sor daitezke, espezie erreduzitzailea NADH edo FADH izan daitezke [4]. Mitokondrian OEE-aren %90 sortzen da zelula eukariotetan [9], non elektroi garraioan parte hartzen duen O_2 -aren %1-4 OEE-an bilakatzen den [8, 10-14]. Elektroi garraioko katean jakina da I eta III Konplexuak direla OEE gehien produzitzen dutenak, izan ere aldaketa handia gertatzen da energia potentzialean oxigenoaren erreduzioarekiko [11, 15-18]. Espezie hauek eratzearen arrazoi nagusia elektroi garraio kateko elektroi isuria da, zeinak O_2 -aren bidez harrapatuak diren, $O_2^{\bullet-}$ -a sortuz [15, 19].

*Espezie errektibo*en produkzioa erradiazioaren ondorioz ere gerta daiteke, hala adibide batzuk azaltzen dira. UM erradiazioak H_2O_2 produzitu dezake Trp eta O_2 -aren presentzian, karga transferentzia mekanismoaz [5]. Hidroxilo erradikala ($\bullet OH$) erradiolisiz eratu daiteke, ur molekula ionizatuz edo uraren egoera kitzikatu batetik beraren disozioaz [20]. H_2O_2 -a UM-en bitartez homolitikoki disozia daiteke $\bullet OH$ -a produzituz [1]. Azkenik, Fenton erreakzioan [1, 21-25], H_2O_2 -a eta trantsizio metal bat (maiz Cu^+ edo Fe^{2+}) $\bullet OH$ -a produzitzen da (1.1 erreakzioa).



1.1.3 Espezie errektiboak eta estres oxidatiboa

Redox erreakzioak, erreakzio garrantzitsuak dira biologian. Erreakzio hauetan molekula bat oxidatu egiten da, beste molekula bat erreduzituz. Definizioz, oxidazio prozesua elektroia galtzea da, eta erreduzioa berriz, elektroiak hartzea. Oxidatzen diren molekulei erreduzitzaile deitzen zaie eta erreduzitzen direnei oxidatzaile. Kontutan hartu beharrekoa da halako prozesuak batera gertatzen direla, hots, ez da erreduziorik oxidaziorik gabe. Hortaz, garbi geratzen da mekanismoaren izenez tapena nondik datorren Red (erreduzioa) Ox (oxidazioa). Azkenik, redox erreakzio batean bi molekula bera badira oxidatu eta erreduzitzen direnak, disproporzio edo dismutazio bezala ezagutzen da. Erdoila eratzearen mekanismoa errebox erreakzioaren adibide aparta dugu (Irduia 1.2). Errebox erreakzioak berebiziko garrantzia dute biokimikan eta bizitzan, baina gaixotasunekin ere erlazionatu da.

Espezie errektiboek eragiten duten kaltea normalean oxidazio gisa ezagutzen da. Haatik, beste espezie kimiko bat erreduzitu dezakete elektroia(k) emanaz. Superoxido anioia ($O_2^{\bullet-}$) da adibidea, zeinak elektroia eman dezaken oxigeno molekularra eratuz, Habber-Weiss erreazioaren lehen urratsean, esaterako [26]. Beraz, nabaria da *oxidatzaileak* soilik direla esatea ez dela oso egokia. Nabarmendu beharra dago espezie hauek ezinbestekoak direla organismoaren funtzionamendu apropos baterako. Are gehiago, OEE-ek prozesu garrantzitsu ugarian parte hartzen dute proteinen fosforilazioko redox erregulazioan, ioi ubidetan, transkripzio faktoretan, tiroide hormona produkzioan, matrize extrazelularreko sareatzean, apoptosian, hazkuntzan, defentsan edo seinaleztapenean [4, 12, 27 29].

Bestalde, halako espezien kontzentrazio balantza egokia mantentzeak garrantzi handia du. Izan ere, *espezie errektiboek* superabitak edo defizitak kalteak eragiten ditu [4]. OEE kontzentrazio baxua immunoeskasiarekin lotua izan da, makrofago eta neutrofiloentzat ezinbestekoak bait dira fagozitosi prozesuan [4]. Hala, *espezie errektiboek* kontzentrazioaren balantzearen haustura estres oxidatibo gisa ezaguna da [1].

Zentzu honetan, OEE eta zahartze prozesuaren arteko korrelazioa ikusi ostean, Harmanen hipotesiak *erradikal askeak* zahartzearekin uztartu zituen. Ikerketa honek erakutsi zuen hainbat antioxidatzailek biziraupena luza zezaketela [30 32]. Hipotesiaren zuntza, adinarekin galtzen den mitokondrien funtzionalitatea da. Jakina da mitokondriek OEE gehiago produzitzen dutela inhibiturik daudenean. Paradoxikoki, estres oxidatibo handiko hainbat mutantek biziraupen luzea erakutsi dute. Beraz, OEE produkzio altua adinaren epifenomenotzat hartu da [33].

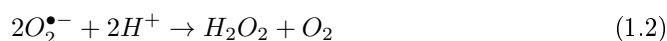
Espezie errektiboak gaixotasun neurodegeneratibo ugariarekin lotuak izan dira, hala nola Alzheimer-arekin [34]. Gaixotasun hauen karakteristika nagusia *estres oxidatibo* altua da [35 39]. Hala ere, ez dago garbi *espezie errektiboak* gaixotasunaren kausa edo ondorio direnez.

Erradikal aske eta beste molekulen arteko erreazioaren espezifikitatea, erreaktibitatearen araberakoa da. Zenbat eta errektiboagoa molekula orduan eta zehaztasun gutxiago izango du erasoak. Errektiboek diren espezien artean, peroxinitroa, oxigeno singletea [4] eta $\bullet OH$ -a [18, 40, 41] aurki ditzakegu. $\bullet OH$ -a da *erradikal askeetan* errektiboena, jomuga ezberdinetarako erreazio konstanteak gutxi aldatzen direla ikusi da, eta beraz erreazio tasa jomuga den molekularen kontzentrazioaren araberakoa dela esan da [40].

1.2 Antioxidatzaileak

Espezie errektiboak neutralizatu, produkzioa ekidin edo sortutako kalteak konpontzen dituzten konposatuak, antioxidanteak deritze [1, 42]. Sinplistegia da antioxidatzaileak onak eta *espezie errektiboak* kaltegarriak direla esatea. *Espezi errektiboek* betetzen dituzten hainbat funtzio aipatu dira lehenago eta kalteak kontzentrazioaren oreka apurtzen denean gertatzen direla esan da. Are gehiago, argumentu honen alde, ikusi da estres oxidatiboak melanomaren metastasia eskiditen duela eta antioxidatzaileek lagundu egiten dutela [43]. Dena den, *espezie errektibo* gehiegiaen aurka entzima asko aurki daitezke organismoetan. Hiru taldetan banatuak daude:

1. **Entzima antioxidatzaileak:** Aktibitate antioxidatzailea duen entzima ugari dago. Adibide gisa, superoxido dismutasak (SOD) katalitikoki neutralizatzen ditu superoxido ($\bullet O_2$) espezieak [1]. Erreazio osoa honakoa izanik:



Bestalde, katalasak, peroxidasak eta glutatona entzimek H_2O_2 neutralizatzen dute.

2. **Metal-ioi bahiketa:** Mekanismo hau organismoan libreki mugitzen diren eta prooxidatzaile izaera duten metal ioien atzematean datza.
3. **Pisu molekular baxuko antioxidatzaileak:** Endogenoak edo exogenoak izan daitezke. Lehenaren adibide moduan bilirrubina edo Q koenzima aurki ditzakegu, organismoak produzituak. Bigarren kasuan aldiz, C edo E bitaminak ditugu, dietaren bidez hartuak [1, 18, 44–46].

Dena den, kontutan hartu behar da antioxidatzaileek ezin dutela *espezie erreaktibo* oro neutralizatu eta hau dela eta organismoek errekupeazio mekanismoak garatu dituzte, kaltetutakoak berreskuratzeko [3, 34, 47–50]. Metionina sulfoxido erreduktasak adibide egokiak ditugu, zeinak metionina sulfoxidoa erreduzitu eta metionina berreskuratzen duten [3, 34, 47–50].

1.3 Osagai zelularren oxidazioa

Estres oxidatibo egoeran *espezie erreaktiboek* zelulako osagaiak, ADN, lipido eta proteinak kaltetu ditzakete [3, 9, 40]. Denboran zehar gertatzen den espezie oxidatuen metaketak jatorri ezberdinak izan ditzake, *espezie erreaktiboen* produkzioaren hazkuntza, antioxidatzaile kontzentrazio baxua edo berreskuraketa mekanismoen efizientzia galtzea, esaterako [51]. Era berean, espezie oxidatuen metaketak *espezie erreaktibo* gehiago produzitzea ekar lezake [34].

ADN. Mitokondriaren ADN-a da *espezie erreaktiboen* erasoari zaugarrien [4, 11]. Era berean, erasoturiko ADN mitokondrialak organelaren lau polipeptido konplexuetako baten kodifikazio informazioa badu, elektroio garraio katean eragina izan lezake, OEE gehiago sortuaz [10].

Lipidoak. Jakietan, lipidoen oxidazioa gustu minduarekin lotua izan da. Lipidoen oxidazio produktu arruntenak malondialdehidoa (MDA) eta 4-hidroxi-2-nonenala (HNE) dira. Jakina da bi produktu hauek proteinen amino taldeekin erreakziona dezaketela Schiff baseak eratuz [9]. Dena den, ez dira oxidazio produktu bakarrak, peroxi eta alkoxi erradikalak, H_2O_2 eta epoxidoak ere eratzen dira. Oro har, organismoen barnean ematen den lipidoen oxidazioak zelulako gainerako osagaien oxidazioa dakar [52, 53].

1.3.1 Proteinak

Amino azidoak (Irudia 1.3) proteinak osatzen dituzten molekulak dira. Karbono atomo zentral bat dute (C_α), zeina estereozentroa den. Atomo honi lotuta H atomo bat, azido karboxiliko talde bat (COOH), C terminal gisa ezaguna, amino talde bat (NH₂), N terminal gisa ezaguna, eta amino azido bakoitzak bereizgarritzat duen albo katea aurki ditzakegu. Amino azidoak maiz beren albo katearen polaritatean arabera sailkatuak aurki ditzakegu.

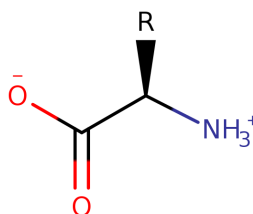


Figure 1.3: L-amino azido baten forma zwiterionikoa. R taldeak albo katea adierazten du.

Amino azidoak bata besteari lotzen zaizkio, amida loturak eratuz. Amida lotura hauek azido karboxiliko eta amina taldearen arteko erreakzioaren ondorioz sortzen dira. Amida lotura hau da, hain zuzen, lotura peptidiko bezala ezaguna dena. Konbentzioz, 30 amino azido baino gutxiagoz eraturiko molekulak peptido gisa ezagutzen dira eta hauek baino gehiago dutenei proteinak deritze. Hortaz, proteinak biomolekula handiak dira, zeinak funtzio ugari betetzen dituzten organismoaren barnean: erreakzio metabolikoen katalisia, ADN errepikazioa, molekulen garraioa etab. Zentzu honetan, proteinek duten egitura garrantzi handiko gaia da beren bete beharrak modu egokian egin ditzaten. Proteina baten egitura lau taldetan banatua dago [54]:

- **Egitura primarioa:** amino azido sekuentzia.
- **Egitura sekundarioa:** egitura lokalak hidrogeno loturaz egonkortuak, alfa helize eta beta xafak esaterako.
- **Egitura tertziarioak:** proteinen azken hiru dimentsioko forma, interakzio ez-kobalentez eratua.
- **Egitura koaternarioa:** polypeptidoen interakzio ez-kobalentez lorturiko proteina. Gizakion hemoglobina dugu hemen adibide, lau azpiunitatez eratutako proteina zeinak interakzio ez-kobalentez lotzen diren.

Proteinen desnaturalizazio prozesua hauen egitura sekundarioa, tertziarioa edo koaternarioa galtzea da, kanpo estresak eraginda, tenperatura altuak edo pH aldaketak, esaterako. Tesi lan hau proteinek jasaten duten oxidazioa ikastera bideratua dago, aurrerago aurkeztu den bezala.

1.3.2 Proteinen oxidazioa

Proteinak dira *espezie erreaktibo*en helburu nagusietako bat, organismoetan duten kontzentrazio altua dela eta [40, 53]. Proteinen oxidazioak makromolekula hauen inaktibazioa ekar lezake eta beraz ikasketa gai interesgarria da. Are gehiago, halako prozesuek produktu egonkorak eman ohi dituzte eta hauek dira, hain zuzen, experimentalki neurtuak direnak, *estres oxidatiboaren* intentsitatea kuantifikatzeko [55]. Maiz, amino azidoen (Lys, Arg, His, Pro, Thr, Glu eta Asp) oxidazioak karbonilo taldeak sortzen ditu [9], zeinak neurtuak diren [1, 56–58]. Bestalde, jakina da oxidazio prozesuak mekanismo konplexuak direla eta

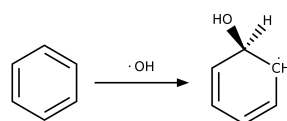
produktu anitz sor daitezke [56]. Karboniloen neurketa soilak oxidazio prozesu osoaren zati bat bakarrik adierazten du [58]. Hauen neurketa ordea, lagungarria da kuantifikazioan, osaturiko karbonilo taldeak ezin bait dira berriz hasierako formara erreduzitu. Hortaz, jasandako oxidazio mailaren adierazle gisa erabil daitezke [47, 56].

Alabaina, bete beharreko zeregina ez da dirudien bezain erraza. Oxidaturiko proteinen metaketa proteasen aktibitate baxuaren ondorio izan bait daiteke. Proteasa hauen funtsa kaltetutako egituren degradazioa da eta hauen aktibitatea mugatua edo inhibitua gerta daiteke, oxidazioaren ondorioz [9, 19, 59]. Hortaz, proteinen efizientzia galera neurgarria den beste faktore bat da, zeinak proteinen oxidazioaren informazioa ematen duen. Bai zahartzeak eta gaixotasun neurodegeneratiboek proteinen oxidazioarekin lotura erakutsi dute [60-62].

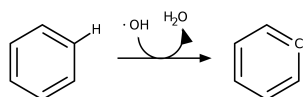
Berreskuratze mekanismo gutxi daude proteinentzat eta gehienetan kaltetutako proteinak degradatu egiten dira. Berreskuratze mekanismoen artean metionina erreduktasa, isoaspartilaren konbertsioa eta frutosaminari loturiko proteinen fosforilazioa aurkitzen ditugu [47]. Oxidaturiko egiturak berreskuratu edo ezabatu ezean, proteina oxidatuak proteinen metaketara gidatu gaitzake [4, 47]. Izan ere, proteina oxidatuak sareatu edo konformazio aldaketak eragiten dituzte, zeinak azkenik proteina metaketara eramaten gaituen [47]. Ildo hontatik, oso oxidatuak dauden proteinek ihes egiten dute proteasoma prozesutik [47] eta hauen pilatzea eragotzi ezin daiteken prozesua da. Ondoren, proteinen oxidazioko hainbat ezaugarri garrantzitsu azaltzen dira.

Erreakzio motak. Oxidazio mekanismoak elektroi bakarrekoak edo bikoak izan daitezke. $\bullet\text{OH}$ -ak elektroi bakarreko mekanismoaren bidez oxidatzen du eta posibleak diren erreakzioak erakusten dira segidan

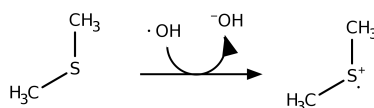
1. Erradikal adizioa

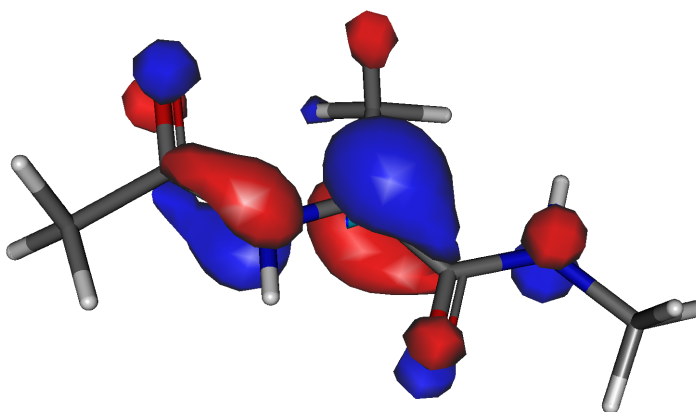


2. H abstrakzioa



3. Elektroi abstrakzioa



Figure 1.4: Alanina C_α erradikalaren SOMO orbitala.

Azken erreakzio hau oxidazio eta erredukzioan banatu daiteke eta zati bakoitzaren erredukzio potentziala Nerst ekuazioaren bidez adierazi:

$$E^0 = \frac{-\Delta G^0(X)}{F} - E_{SHE}^0$$

E_{SHE}^0 hidrogen estandar elektrodoa izanik, zeina 4.47 V den IEFPCM erabiliz [63], F Faraday-en konstantea ($F=96.485$ C/mol) eta $\Delta G^0(X)$ X espezieariaren erredukziori dagokion gibbs energia librea:



Azaldu diren hiru erreakzioetan sortzen da erradikal bat eta elektroik bakarra da oxidazioaren eragile. Bestalde, bi elektroiko oxidazioaren adibide dugu H_2O_2 , non bi elektroik hartzen duten parte mekanismoan [64].

Erradikalen erreaktibitatea. Argi dago erradikal guztiek ez dutela egonkortasun erlatibo bera. Labur esana, elektroik ez-parekatua duen orbitalaren eta energetikoki eta espazialki gertu dagoen orbitalaren arteko interakzioak erradikalak egonkortzen ditu. Hiperkonjokazio efektua elektroik ez-parekatua σ eta σ^* orbitalekin interakzionatzerakoan ematen da sistema saturatuetan, eta π eta π^* orbitalekin sistema ez-saturatuetan. Hiru zentro hiru elektroik interakzioak dira. Elektroik ez-parekatuak elektroik ez-lotzaile parearekin duen interakzioari bi zentro hiru elektroik lotura deritzo. Erradikalak alboan ordezkatzaille ez-saturatu bat eta elektroik ez-lotzailea parearekin baditu efektu kaptodotibo gertatzen dela diogu [65]. Kasu partikular honetan aurretik aurkeztutako bi efektuak gertatzen dira batera. Adibide gisa C_α zentroko amino azido eta proteina erradikaletan dugu, zeinetan amino eta karbonilo taldeak dituen alboan (Irudia 1.4), egonkortasun erlatibo handia erakutsiz.

Erreakzioaren kokapena. Eraso proteinan edo kofaktorean (zati ez-proteikoa) gerta daiteke. Zentzu honetan, hemoglobina, ezinbestekoa dugun proteina, hemo talde kofak-

toreaz osatua dago, zeinetan burdin atomoa aurkitzen dugun. Burdina erraz oxidatu eta erreduzitzen den atomoa da eta *espezie erreaktiboak* produzitzen dituela jakina da. Beraz, argi dago atomo hau organismoetan aske ez ibiltzearen arrazoia. Burdin ioiak zelulen sistema espezifikoaren bitartez antzemanak dira. Egoera patologikoetan burdina askatu daiteke eta honek zelularen hondamendia dakar, espezie erreaktiboak produzitzen baititu [3, 9]. Oxidazioko helburu nagusi bezala aurkitzen ditugu Pro, His, Arg eta Lys, metal ioiei lotzen baitzaizkie [5, 9, 66, 67], zeina modu zehatzean gertatzen den [57, 68]. Eraturiko *espezie erreaktiboak* metal ioiari loturiko amino azidoen albo katearekin erreakzionatzen dute. Prozesu honi *Metal ioi bidez katalizaturiko oxidazioa* deritzo.

Glutamina sintasa (GS) proteinen oxidazioa ikasia izan den sistema da. *Escherichia coli*ri dagokion GS entzimaren inaktibazioa His269, Asn-n eta Arg344, glutamiko semialdehidoan bihurtzean gertatzen da, prozesuaren espezifikitatea argi erakutsiaz [68]. Oxidaturiko forma hau hidrofilikoa da, inaktiboa baina ez degradagarria. Degradagarria izan dadin gehiago oxidatu behar da proteina (His209 edo His210), entzima hidrofobikoago bilakatuz [9, 68-70].

Oro har, amino azido bakoitzaren kokapena kontutan hartzeko faktore bat da oxidazioan zehar. Amino azidoa oxidatzaileetatik urrun badago ez da oxidatuko, nahiz eta oxidatzeko joera izan [71]. Zentzu honetan, proteinen disolbatzailearen eskuragarritasuna handitzeak proteinen antioxidatzaile izaera handitzea dakarrela ikusi da [71].

1.4 Lanaren helburua

Azken hamarkadan proteinen oxidazioak interes handia jaso du, prozesuaren ondorio eta aplikazio posibleak direla eta. Honela, proteina oxidatuaren produktuen identifikazioak beraien kuantifikazioan lagun dezake. Egun, karboniloak dira neurtzen diren produktu oxidatu nagusiak, nahiz eta beste alternatibak existitu. Beraz, egonkortasun termodinamikoaren azterketak eta bitartekariaren karakterizazio elektronikoa informazio baliagarri asko ekar dezake proteinen oxidazio prozesuari.

Tesi lan hau onartuak eta berriak diren oxidazio prozesuaren karakterizazioa bideratua dago. Zentzu honetan, experimentalki ikusi diren produktuak arrazionalizatu nahi dira. Oxidazio prozesu anitz kontsideratu ditugu eta beraien egonkortasun erlatiboan zentratu gara, hala bitartekari nola produktuentzat. Hala, experimentalki ikusiak diren oxidazio produktuen alternatibak proposatu ditugu, zeinak etorkizunean baliagarriak izan daitezken.

1.5 Metodoak

Atal honetan tesian zehar erabilitako metodoak laburbilduko dira.

1.5.1 Dentsitate Funtzionalaren Teoria

Dentsitate Funtzionalaren Teoria, N elektroien uhin funtzioa eta dagokion Schrödingeren ekuazioaren orde, $\rho(\mathbf{r})$ elektroien dentsitatea darabil. $\rho(\mathbf{r})$ hiru koordenatu espazialen funtzioa besterik ez da eta beraz uhin funtzioa baino simpleago da. Egoera elektronikoa, energia eta edozein sistemaren propietate elektronikoa, $\rho(\mathbf{r})$ honen funtzioan deskribatzen dira.

Hohenberg eta Kohn-ek [72] degeneratua ez den oinarrizko egoera duen sistema baten propietate elektronikoak $\rho(\mathbf{r})$ elektroi dentsitateak determinatzen dituela demostratu zuten. Beraz, E_0 oinarrizko egoeraren energia $\rho(\mathbf{r})$ -ren funtzionala da. Orokortuz, oinarrizko egoeraren elektroi-dentsitatea jakinez gero, oinarrizko egoeraren propietate elektroniko guztiak kalkulatzeko posible da, funtzional dependentziak finkatu ostean. Energi funtzionala aurkitzeko energiaren bariazio-printzipio bat finkatu zuten. Horrela, $E[\rho]$ funtzionalaren forma zehatza jakinik oinarrizko egoeraren dentsitatea bilatu genezake. Zoritxarrez, funtzionalaren forma zehatza ezezaguna dugu.

Kohn eta Sham-ek [73] funtzional honen hurbilketa ez-zuzen bat garatu zuten. Ondorioz, DFT kalkulu zehatzak egiteko tresna erabilgarria bihurtu zen. Haiek N elektroiz osaturiko eta ρ oinarrizko egoeraren elektroi dentsitatea duen molekula baten E_0 oinarrizko egoeraren energia elektronikoa ondorengoa dela erakutsi zuten:

$$E_0 = -\frac{1}{2} \sum_{i=1}^N \langle \psi_i(1) | \nabla_1^2 | \psi_i(1) \rangle + \int \nu(r) \rho(1) d\vec{r}_1 + \frac{1}{2} \int \int \frac{\rho(1)\rho(2)}{r_{12}} d\vec{r}_1 d\vec{r}_2 + E_{xc}[\rho] \quad (1.4)$$

$\nu(r) = -\sum_{\alpha} \frac{Z_{\alpha}}{r_{1\alpha}}$ nukleoaren eragriez dagoen konpo potentziala da, ψ_i Kohn-Sham orbitalak eta $E_{xc}[\rho]$ truke-korrelazio energia.

Kohn-Sham prozeduran oinarrizko egoeraren ρ zehatza, Kohn-Sham orbitaletatik lor daiteke,

$$\rho = \sum_{i=1}^N |\psi_i|^2 \quad (1.5)$$

eta Kohn-Sham orbitalak

$$\hat{F}_{KS}(1) \psi_i(1) = \varepsilon_i \psi_i(1) \quad (1.6)$$

elektroi bakarreko ekuazioak ebatziz lortzen dira, \hat{F}_{KS} Kohn-Sham operadorea

$$\hat{F}_{KS} = -\frac{1}{2} \nabla_1^2 + \nu(1) + \sum_{j=1}^n \hat{J}_j(1) + V_{xc}(1) \quad (1.7)$$

delarik. \hat{J} Coulomb operadorea da, eta V_{xc} truke-korrelazio potentziala. \hat{F}_{KS} HF ekuazioetan agertzen den Fock operadorea bezalakoa da, gauza batean izan ezik. Truke operadorearen orde, truke eta korrelazioa kontuan hartzen dituen V_{xc} jartzen da.

Ekuazio hauek iteratiboki ebazten dira. Hasierako dentsitate batetik hasita \hat{F}_{KS} eraikitzen da, eta (1.5) ekuazioa ebazten da. Emaitza \hat{F}_{KS} berri bat eratzeko erabiltzen da. Prozedura hau konbergentzia lortu arte errepikatzen da.

Kohn-Sham orbitalen esan nahi fisikoa eztabaidan dago oraindik. Autore batzuen iritziz ez dute inolako zentzurik, eta ρ zehatzaren kalkuan dira erabilgarri soilik. Era beran, Kohn-Sham orbitalen energiak molekula orbitalen energiekin ez lirakeke nahastu behar. Beste batzuk ordea, HOMO-aren Kohn-Sham energia ionizazio potentzialaren negatiboa dela kontuan harturik, eta honetaz gain Kohn-Sham ekuazioak, HF kasuaren antzera partikula askeen eredu gogora ekartzen duela kontuan harturik, Kohn-Sham orbitalei HF orbital kanonikoek duten antzeko esan nahi fisikoa egokitzen diete.

Dena den, $E_{xc}[\rho]$ truke-korrelazio funtzionala eta beraz, $\nu_{xc}[\rho; \mathbf{r}]$ truke-korrelazio potentziala elektroien gas uniformearen kasurako baino ez da ezagutzen. Zorionez, funtzional hurbilduak garatu dira. Horietako bat, dentsitate lokalaren hurbilketa (DLH) da. Honen ideia, $\rho(\mathbf{r})$ dentsitate lokala duen bolumen elementu bakoitza elektroien gas homogeneoa bezala kontsideratzea da. Ikuspuntu honetatik hurbilketa hau dentsitate espazioan zehar mantso aldatzekotan zehatza da. $E_{xc}[\rho]$ ondorengo espresioak emana dator:

$$E_{xc}^{DLH}[\rho] = \int \rho(\mathbf{r}) \varepsilon_{xc}(\rho) d\mathbf{r} \quad (1.8)$$

$\varepsilon_{xc}(\rho)$, ρ elektroien dentsitatea duen elektroien gas homogeneoaren truke-korrelazio energia da, elektroien bakoitzeko. Espresio hau aplikatuta dentsitate lokalaren hurbilketa (DLH) edo spin dentsitate lokalaren hurbilketa (SDLH) lortzen dira. Azken honen kasuan spin ezberdina duten elektroientzat orbital eta ρ^α eta ρ^β dentsitate ezberdinak erabiltzen dira. Noski, molekulen kasuan hauek funtzional zehatzaren hurbilketa dira, ρ homogeneoa ez delako. Hurbilketa, dentsitate gradientearen espansio bat eginez hobetu liteke, aurretikoa Taylor seriearen lehen terminotzat hartuz. Metodo hauek generalizaturiko gradientearen hurbilketa (GGA) dira, eta molekulen azterketan garrantzi handia dute, elektroien dentsitatea homogeneoa dela ezin baita kontsideratu.

Hohenberg-Kohn-en teorematik, jakina da E_{xc} zehatza existitzen dela. Hala ere, ezezaguna da eta beraz zehazki mintzatuz, esan liteke DFT kalkuluak ez direla *abinitio* kalkuluak. Dena den, datu esperimenteralaren doitzeko parametririk erabiltzen ez dutenez, *abinitio* direla esan liteke. Metodo honen abantaila handienetakoa HF metodoaren koste konputazional antzekoa izanik elektroien korrelazioa kontuan hartzen dutela da. Dena den, korrelazio efektu hauek ezin dira zehazki sailkatu, hastapenetik ez korrelaturiko emaitzarekin nahasturik daudelako. Honetaz gain, sofistikazio gehiago aplikatuz, kalkuluak hobetzeko bide sistematikorik ez dago, eta honen ondorioz emaitzak diren bezala onartu behar dira. Arazo hauek izan arren, DFT-k sistema kimiko batzuen oinarritzko egoeraren propietateentzat emaitza onak eman ditu. Kostu konputazional baxua dela eta, sistema handien kasurako DFT aukeratzeko den metodoa da, elektroien korrelazioa MP edo CI metodoen bidez kontsideratzea oso garestia delako.

Funtzional asko daude gaur egun merkatuan eta dugun problema kimiko zehatzerako balioko duen funtzionala erabili behar da. Bestalde, DFT kalkuluak ez dira hain zehatzak interakzio ez lotuetarako [74]. Elkar banatu gabeko bi elektroien distribuzioak ez dute energia jaitsieran partizipatzen, zeinak elektroien dentsitate lokalean duen bakarrik dependentzia. London interakzioak errepresentatzeko funtzional ez lokala behar da eta dentsitate lokaleko funtzionalek ez dituzte, printzipioz, halako efektuak deskribatzen. Beraz, halako efektuak kontuan harturik, meta-GGA funtzional bat erabili dugu gure lanean zehar, hots, MPWB1K.

Lotura hautura eta eraketa fenomenoak arruntak dira tesian zehar. Jakina da, funtzional puruek ezin dituztela ondo deskribatu halako jokaerak [75, 76]. Zentzu honetan, aukeraturiko geure funtzionalak %44 HF trukea du. Are gehiago, funtzional honek ondo ematen ditu erradikal estabilizazio energiak [77].

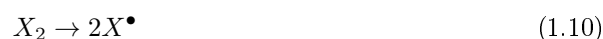
Azkenik, aukeratu den funtzionalak jokaera ona du termokimikan eta zinetikan [78]. Zehazki, ikerketa batean ikusi da zein funtzionalak duten jokaera egokiena $\bullet\text{OH}$ eta $\bullet\text{OOH}$ -aren bidez gertatzen diren adizio eta H abstrakzio mekanismoetan, 3-metilpirroletik eta bentzenotik. Hemen ikusten da aukeraturiko funtzionalak balio egokiak ematen dituela $\bullet\text{OH}$ -aren kasuan.

Beraz esan daiteke, ikusitako proben ostean eta funtzionalak berez duen diseinuaren arabera MPWB1K funtzionala egokia dela ikerketa lan honetarako, non $\bullet\text{OH}$ -aren bidez oxidatuko diren proteinak.

1.6 Erabilitako modeloa eta protokoloa

Egitura optimizazioak gas fasean eginak daude, 6-31+G(d,p) oinarritzko funtzioak erabiliz. Bibrazio frekuentzia harmonikoak kalkulatu dira gradienteen diferentziazio analitikoaz, karakterizaturiko egiturak minimoa edo trantsizio egoerak diren jakite aldera. Bestalde, entalpiari egindako zuzenketa termalak ($T = 298 \text{ K}$) osziladore harmonikoaren hurbilketaren bitartez lortu dira. Kalkulu puntualak egin dira 6-311++G(2df,2p) oinarritzko basea erabiliz eta dielektriko ezberdinak erabiliaz, IEFPCM formalismoan. Bi konstante dielektriko erabili dira i) $\varepsilon = 4$ proteina barruko inguru giroa simulatzeko eta ii) $\varepsilon = 80$ proteina gainazaleko ingurak simulatzeko. Kontutan hartzekoa da lan honetan infinituki separaturiko erreaktibo eta produktuak hartu direla, hortaz, efektu entropikoak ez daude orekatuak eta beraz, entalpia balio erlatiboak erabili dira diskusioan zehar. Balio hauek gas fasean lorturiko entalpia kontribuzioak, disoluzioko energiei batuaz lortuak dira, ΔH_4^{298} eta ΔH_{aq}^{298} lortuaz. Lan osoa GAUSSIAN09 software programa erabiliaz burutu da [79].

Proposaturiko protokoloa probatzeko hainbat proba egin dira ondorengo erreakzioekin, zeinentzat kalkulaturiko D_e balioak experimentalekin konparatu diren:



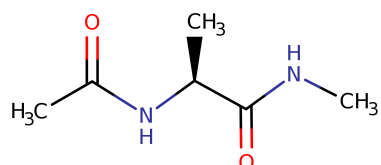


Figure 1.5: Erabilitako modeloa, Ala ageri da adibide gisa.

	D_e (kcal/mol)		
	MPWB1K	expt	diferentziak
$CH_4 \rightarrow H^\bullet + CH_3^\bullet$	112.4	113.0	-0.6
$C_2H_6 \rightarrow H^\bullet + C_2H_5^\bullet$	107.9	109.4	-1.5
$H_2O_2 \rightarrow H^\bullet + HO_2^\bullet$	89.1	92.7	-3.6
$H_2O \rightarrow H^\bullet + HO^\bullet$	122.3	126.0	-3.7
$NH_3 \rightarrow H^\bullet + NH_2^\bullet$	114.2	115.9	-1.7
$C_2H_6 \rightarrow CH_3^\bullet$	98.7	96.6	2.1
$H_2O_2 \rightarrow 2HO^\bullet$	49.4	55.1	-5.7
MAD			2.7
$CH_4 + HO^\bullet \rightarrow CH_3^\bullet + H_2O$	-9.9	-13.0	3.1
$NH_3 + HO^\bullet \rightarrow NH_2^\bullet + H_2O$	-8.2	-10.1	1.9
$C_2H_6 + HO^\bullet \rightarrow C_2H_5^\bullet + H_2O$	-14.4	-16.6	2.2
$H_2O_2 + HO^\bullet \rightarrow HO_2^\bullet + H_2O$	-33.3	-33.3	0.0
MAD			1.8

Table 1.1: Kalkulatoriko eta experimentalak diren D_e balioak.

Ikusi diren disozioazio eta H abstrakzio mekanismoentzat diferentziak txikiak dira, Taula 1.1. Hortaz, esan genezake proposaturiko protokoloa onargarria dela.

1.6.1 Modeloa

Tesian zehar erabili den modeloa Irudia 1.5-ean ageri da. Hemen, bi lotura peptidiko dituen amino azidoa ikus daiteke. Angelu dihedroak orientatuak izan dira, α -helize-antzeko eta β -xafila egiturak erreproduzitzeko. Alboko N- eta O-terminalak diren amino azidoak C_α atomoan daude moztuak, azken hauek metil talde batez ordezkatuak.

1.7 Amino azidoen oxidatzeko joera

Amino azido guztiek ez dute oxidatzeko joera bera. Erreakzioaren izaerak amino azidoen albo katean du dependentzia, zeinak maizen erreakzionatzen duen oxidatzailearekin, bera baita agerian geratzen den zatia. 1.2 Taulan ageri dira amino azidoen produktu oxidatu ezagunenak.

Cys	Zistina, tiol erradikalak[9, 41]
Met	Sulfoxidoa, Sulfona [9, 41]
Phe	Hidroxifenilalanina[41, 80]
Tyr	Sareaturiko tirosinak[5, 9, 41, 47, 71, 81, 82], DOPA[1, 41, 47, 66, 71, 80, 81], Ortho-tirosina[1]
Trp	Formil-kinureina[5, 9, 66], Kinurenina[1, 47, 83], 3-hidroxi-kinurenina[5, 9, 41, 47, 83]
Asp	Azido pirubikoa [9, 41]
Glu	Azido pirubikoa [9, 41]
Arg	Glutamato semialdehidoa[1, 9, 41, 47, 67, 84]
Lys	Adipiko semialdehidoa[1, 9, 41, 47, 67, 84]
His	2-oxohistidina[1, 9, 41, 47]
Pro	Glutamato semialdehidoa[1, 9, 41, 47, 67, 84]
Val	Hidoxidoak[1, 47]
Leu	Hidoxidoak[1, 47]
Thr	Azido 2-amino-3-zetobutirikoa [9, 41, 47]

Table 1.2: Amino azidoen produktu oxidatu ezagunenak.

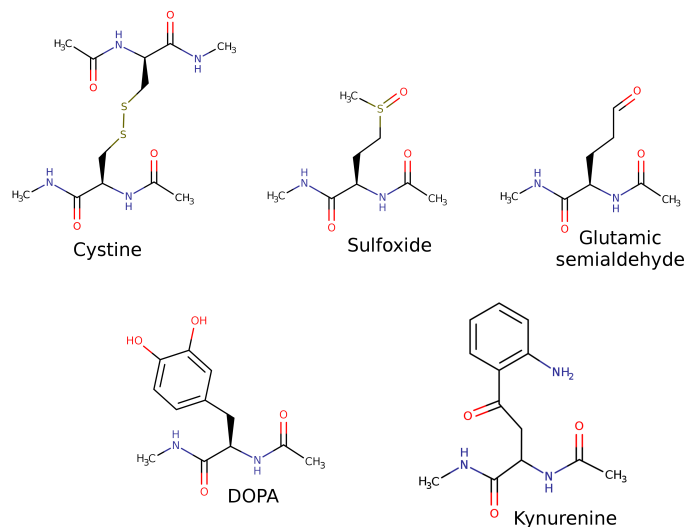


Figure 1.6: Amino azidoen produktu oxidatu batzuk.

Ondoren azaltzen dira tesi lan honetan aztertutako amino azidoen oxidazio mekanismoak albo katearen izaeraren arabera sailkatuak. Erabilitako oxidazio mekanismoan bi $\bullet\text{OH}$ -k hartzen dute parte. Lehenak bitartekaria eratzen du eta bigarrenaren erasoaren ostean amaierako produktuak sortzen dira.

1.7.1 Sufrea duten amino azidoen oxidazioa

Oxidazio prozesuetan, zisteina eta metionina amino azidoak izaten dira helburu nagusiak [56, 85–88], hauen oxidazioa itzulgarria delako. Amino azido hauen oxidazioa kontrol biologiko mekanismoen parte izan daiteke [85]. Hau ez da beti hala izaten, zentzu honetan, metioninaren oxidazioa Alzheimer gaixotasunarekin erlazionatua dagoela ikusi da [36]. Amino azido hauen oxidazio mekanismoa H edo elektroi abstrakzioaren ondorioz ematen da.

Zisteinaren oxidazioak azido sulfenikoa, sulfinikoa, deribatu sulfonikoa edo zistina eratu ditzake. Azido sulfenikoa gehiago oxidatu daiteke azido sulfinikoa emanaz edo zisteinara erreduzitu daiteke. $\bullet\text{OH}$ -ak eragiten duen zisteinaren oxidazioan S atomoko H abstrakzio mekanismo esanguratsua dela ikusi da, sufre erradikala osatuz [89]. Halako bi erradikalek elkarrekin erreakzionatu ezker lotura eratzen dute eta sorturiko produktua zistina da. Interakzio honek egonkortasuna ematen dio proteinaren egiturari, zeina galdu egiten den hau apurtu ezker. Hala, aktibitate entzimatikoa galdu egin daiteke proteinaren egitura galtzerakoan [90].

Metionina oxidatzerakoan sulfoxidoa edo sulfona eratzen da, lehena berriro erreduzitu daiteke metioninara [9, 85, 91, 92]. Ez da ikusi metioninarentzat funtzio espezifikorik eta normalean zati aktibotik at aurkitzen da [9]. Hau dela eta, *espezie erreaktiboak* neutralizatzeko gaitasuna atxikitu zaio amino azido honi [66, 92]. Honela, gainazaleko metioninei inguru giroko *espezie erreaktiboak* neutralizatzeko eta zentro aktibotik gertu daudenei berriz auto-oxidazioa ekiditeko funtzioa atxiki zaie [92]. Horrela, proteinetan daukaten posizioaren arabera metionina amino azidoak bereizi daitezke bi taldetan: gainazalekoak eta barnekoak. Lehenak inguru giroan aurkitzen diren *espezie erreaktiboak* neutralizatzen dituzte eta bigarrenak zati aktibotik gertu aurkitu daitezke, autooxidazioa ekidinez [92].

Oxidazio erreakzio hauetan eratzen diren produktuen egonkortasun erlatiboa oso garrantzitsua da. Molekula ezegonkorak eratzen badira alboko molekulekin erreakzioak gerta daitezke, azken hauetan aldaketak sortuz [71]. Metioninak bi elektroi edo bakarreko oxidazioa eman dezake. Lehenak sulfoxidoaren eraketa dakar eta azkenak sufre erradikal katioia [91]. $\bullet\text{OH}$ erasoaren bidez osatzen den sufre erradikal katioia, hydroxysulfuranil aduktu ezegonkorren bitartez eratzen da [91, 93, 94]. Bitartekari hau protoi bat hartu ostean disoziatzen da, sufre erradikal katioia eta ur molekula bat sortuz, Irudia 1.7. Beraz, $\bullet\text{OH}$ -ak S atomoko elektroi bat hartzen du, ^-OH eta aipaturiko sufre erradikal katioia emanaz. Sufre erradikal katioi hau disproporzionatzen den espeziea dela pentsatu da, metionina bat eta sulfoxido bat emanaz [95].

Sufre erradikal katioia biziraupen baxuko espeziea da, mikrosegundu batzuk baino ez [96]. Bestalde, aipaturiko erradikal katioi hau aldameneko molekula edo taldeek egonkortua izan daiteke [96–99], amina bateko N atomoak esaterako [100]. Sufre eta nitrogeno atomoaren artean eraturiko lotura pH-aren arabera da eta nahiz eta egonkorra izan ez da eratu daitekeen bakarra. Are gehiago, sufre oxigeno lotura ere ikusi da [91]. Oro har, sufre erradikal katioia ezegonkorra da eta elektroia hartzeko joera du, tirocina batetik [94] edo deskarboxilazio mekanismoa bultzatzen du [101–103].

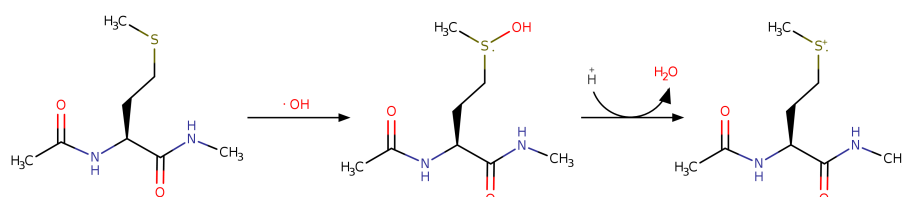


Figure 1.7: Metioninaren elektroi bakarreko oxidazioa, hydroxisulfuranil bitartekaria eratzuz eta azkenik sulfre erradikal katioa osatuz.

Esan dena kontuan harturik, zisteina eta metionaren kasuak lehen $\bullet\text{OH}$ -aren erasoak H edo elektroi abstrakzioa eman ditzake, erradikal bitartekari bat eratzuz. Bigarren $\bullet\text{OH}$ baten erasoja jasango du bitartekari honek, adizioa edo H abstrakzioa gertatuz eta amaierako produktuak emanez.

Elektroi abstrakzioaren bitartez eratzten den sulfre erradikal katioiak egonkortua behar du izan elektroia emalea den talde baten bidez [100]. Horrela, bizkarrezurreko O eta N atomoekin eratu ditzaketen interakzioak kontsideratu dira lan honetan. Metioninaren kasuan bost edo sei atomotako eratzunak eratu daitezke eta zisteinaren kasuan berriz lau edo bost atomotakoak. Kontutan hartu behar da halako interakzioak metioninarentzako soilik aurkitu direla, amino azidoa terminala denean. Irudia 1.8-ean ageri dira kalkulaturiko metionina eratzun horietako batzuk. Ikasi diren kasu guztiak B.4 Taulan azaltzen dira. Bestalde, zisteinaren kasuan, elektroia abstrakzioa baino hobetsiago dago H abstrakzioa [88].

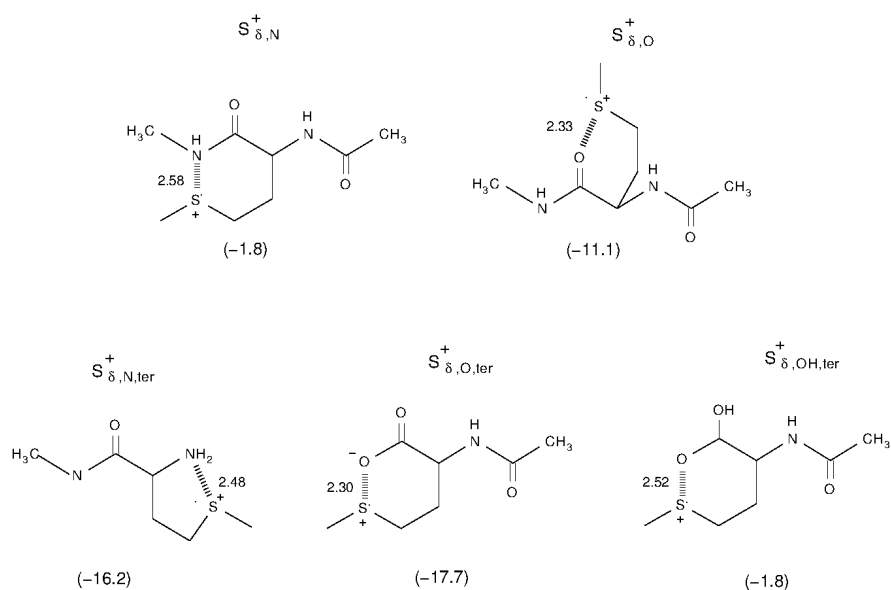


Figure 1.8: $\bullet\text{S}^+$ -aren bost errepresentazio eskematiko. Parentesi artean ageri dira ΔH_{aq}^{Int} balioak, kcal/mol-etan. 3 e -2 c (S eta X) lotura distantziak aldamenen daude Å-etan.

Elektroi abstrakzioaz gain, H abstrakzio erreakzioak ere gerta daitezke, zeinak erreakzio lehiakorrek izatea ikusi diren [104]. Zentzu honetan, lehen $\bullet\text{OH}$ -ak zisteinako C_β edo S_γ posiziotan eragin dezake H abstrakzioa.

Zisteinan gerta daitezken aukera guztiak aztertuak agertzen dira Irudia 1.9-ean. Garbi geratzen da, elektroi abstrakzio mekanismoak bitartekari ezegonkorrera garamatzala eta hortaz H abstrakzio erreakzioa hobetsia dago, aurreko lanetan ikusi den bezala [89]. Bi aukeren artean, S_γ -tik H abstrakzioa gertatzeak, $\text{C-Int}^{\text{S}\gamma}_1$ baino 6 kcal/mol egonkorragoa den $\text{C-Int}^{\text{S}\gamma}_1$ bitartekaria eratzea dakar. Esterikoki ere S_γ atomoa ageriago dago C_β baino eta beraz errazagoa da lehenean gertatzea eraso.

Bi bitartekari hauetatik bost amaierako produktu karakterizatu dira. Egonkorrena den $\text{C-Int}^{\text{S}\gamma}_1$ bitartekaritik abiatuta, tiozetonan ($\text{C}=\text{S}$) C-Prod_4 eratu liteke, C_β atomotik H abstrakzioa gertatu ezker. $\bullet\text{OH}$ -a sufre erradikalari gehitu dakioke C-Prod_3 eratuz, bere tautomeroa ere estimatu da (C-Prod_5). Bestalde, bi zisteina erradikal espazialki gertu aurkitu ezker, lotura eratu lezakete, zistina osatuz (C-Prod_1). Azkenik, C-Prod_2 eratu liteke, $\bullet\text{OH}$ -a $\text{C-Int}^{\text{C}\beta}_2$ -ra gehituko balitzaio.

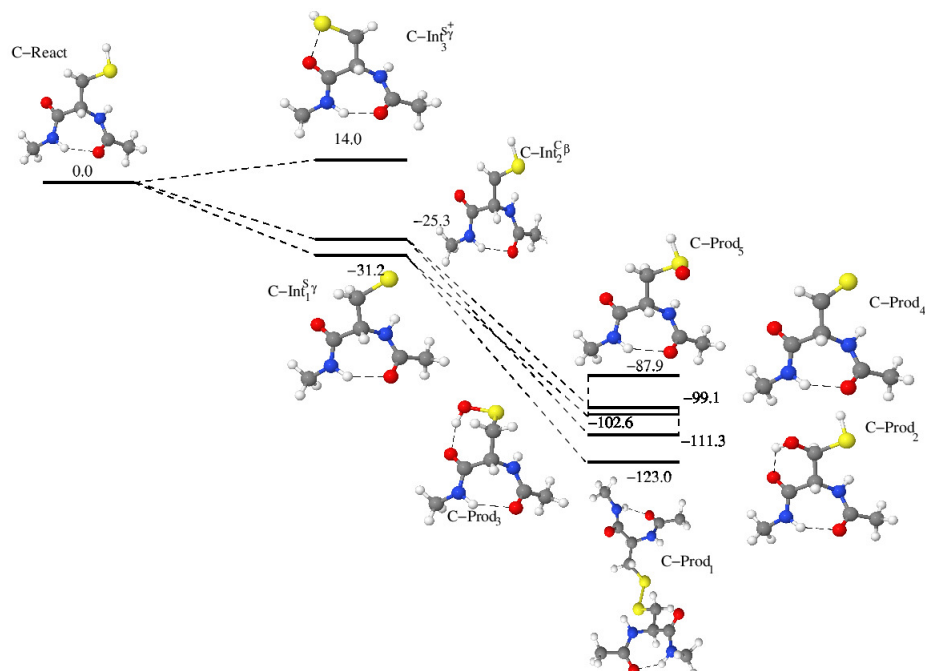


Figure 1.9: Zisteinaren albo katean bi $\bullet\text{OH}$ -ren erasoaren bidez gerta daitezken erreakzio bide osoak. ΔH_{aq} balioak kcal/mol-etan emanak daude. Erreakzio barrerak ez dira ematen ez bait dira esanguratsuak, 11 Kapituluaren aurkitu daitezke balio hauek.

Zistina disulfuro zubi baten bidez eratua dago eta proteinetan agertzen da egiturari egonkortasuna emanaz. Hori dela eta, gerta daitezken $\bullet\text{OH}$ erasoak ere ikasi dira, Irudia 1.10.

Lehen $\bullet\text{OH}$ -aren erasoak konplexu baten eraketa dakar zeina erreaktiboak baino 9.7

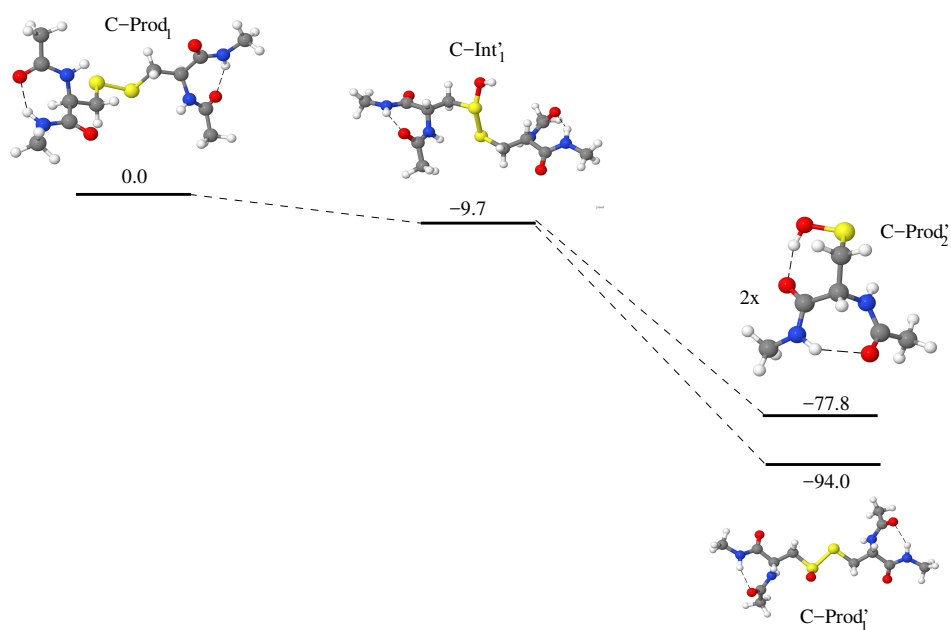


Figure 1.10: Bi $\bullet\text{OH}$ -ren bidez gerta daiteken zistinaren oxidazio erreakzio bide osoa. Barrerak ez dira eman ez bait dira esanguratsuak.

kcal/mol egonkorragoa den. Erradikal izaera bi S atomoen artean banatua dago, 3 elektroi bi zentro lotura batean. Hortaz, S-S lotura ahuldu egiten da, eta erraz banatu daiteke.

Bigarren $\bullet\text{OH}$ -ak eratutako konplexuko (C-Int₁) OH-ari eraso dakioko, H atomo bat kenduz. Honela, C-Prod₁ eratzen da, zeina errektiboak baino 94 kcal/mol egonkorragoa den. Bestalde, bigarren $\bullet\text{OH}$ -aren eraso ondoko S atomoan gertatzen bada, disulfuro zubia apurtu eta C-Prod₂ eratzen da (C-Prod₃ zisteinaren kasuan). Hala ere, termodinamikoki ez da C-Prod₁ bezain egonkorra (-77.8 kcal/mol), beraz lehen produktua dago hobetsia.

Metioninaren oxidazio erreakziori dagokion lehen $\bullet\text{OH}$ -aren erasoak H edo elektroi abstrakzioa dakar, Irudia 1.11. H abstrakzioie dagokienez, C_γ atomoan gertatzen den H abstrakzioa da egonkorrena, errektiboak baino 29.0 kcal/mol egonkorragoa den bitartekaria lortuz (M-Int^{C_γ}₁). Gainerako H abstrakzio bidez lortutako bitartekariak 6 eta 10 kcal/mol ezegonkorragoak dira. Sufre erradikal katioia M-Int^{C_γ}₁ baino 18 kcal/mol ezegonkorragoa da. Dena den, azken honen egonkortasunak inguru giroan du dependentzia, lehenago azaldu den bezala.

Ikusi dugu, sufre erradikal katioia egonkortua dela metionina terminala denean, karboxilato edo amina taldeen bidez (Irudia 1.8) eta hau bat dator experimentalki ikusi diren emaitzekin [95]. Bestalde, emaitzek adierazten dute elektroi transferentzia prozesua hobetsia dagoela ur dielektrikoan, logikoki, kargadun espezieak egonkortuak bait dira inguru giro polarretan, B.4 Taulan ikus daiteken bezala.

Bigarren $\bullet\text{OH}$ -aren erasoaren ostean, lortzen diren produktuei begira, M-Prod₁ da egonkorrena, zeina M-Int^{C_ε}₃-ri adizionatuz lortzen den. M-Prod₂ eta M-Prod₃ oso gertu daude energetikoki, lehenak tiozetona talde bat du eta bigarrenak C_γ-C_β lotura bikoitz bat. Azken

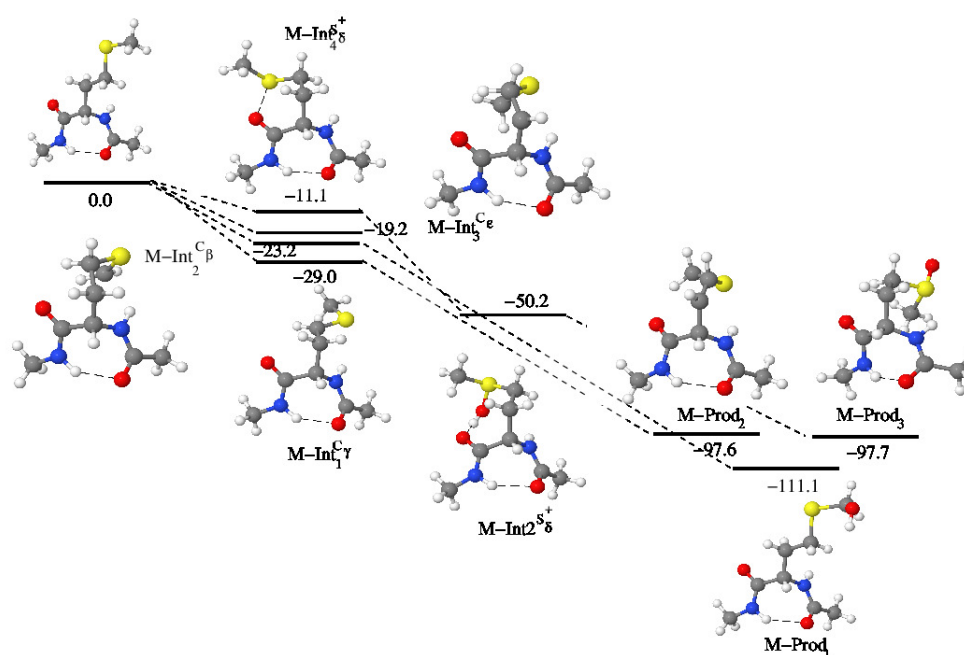


Figure 1.11: Bi $\bullet OH$ -ren bidez gerta daiteken metionina albo katearen oxidazioa. ΔH_{aq} balioak kcal/mol-etan ageri dira.

bi hauek dira experimentalki detektatzen diren produktuak, eta ez lehen aipatzen dena. Arrazoa, bitartekarien egonkortasunean aurki dezakegu. M-Prod₁ produktua 10 kcal/mol ezegonkorragoa den bitartekari batetik sortzen da eta beraz, zentzuzkoa da beste bi produktuak detektatzea.

M-Prod₂ bi H abstrakzioaren ondorioz lortzen da eta M-Prod₃ berriz, elektroi transferentzia eta $\bullet OH$ adizio baten ostean. Azken honen eraketarako lehen $\bullet OH$ -ak elektroi abstrakzioa eragiten du S atomoan, sulfre erradikal katioia eta ^-OH osatuz. Sufre erradikal katioia egonkortua egongo da elektroi emalea den talde baten bidez, aipatu bezala. Orduan, bigarren $\bullet OH$ -a adizionatuko zaio. Azkenik, OH-ari protoia kenduko dio aurretik eratu den ^-OH -ak, sulfoxidoa eta ur molekula bat emanaz.

1.7.2 Alkohola duten amino azidoak

Amino azido hauetan gertatzen diren $\bullet\text{OH}$ erasoek H abstrakzio mekanismo bidez gauzaten dute oxidazioa. Serinaren kasuan lehen $\bullet\text{OH}$ -ak C_β edo O_γ posizioetan eman dezake H abstrakzioa, Irudia 1.12. Osatzen diren bitartekarietatik, $\text{S-Int}_1^{C_\beta}$ da egonkorrena, 10 kcal/mol inguru. Treoninaren kasuan, metil talde bat gehiago dugu albo katean, baina emaitzak ez dira gehiegi aldatzen. Izan ere, C_β posizioan gertatzen den H abstrakzioak ematen du bitartekari egonkorrena, $\text{T-Int}_1^{C_\beta}$. Hala ere, ikusi daiteke (Irudia 1.13), metil taldeak gertatzen den H abstrakzioa, O atomotik gertatzen dena baino 5 kcal/mol egonkorragoa dela.

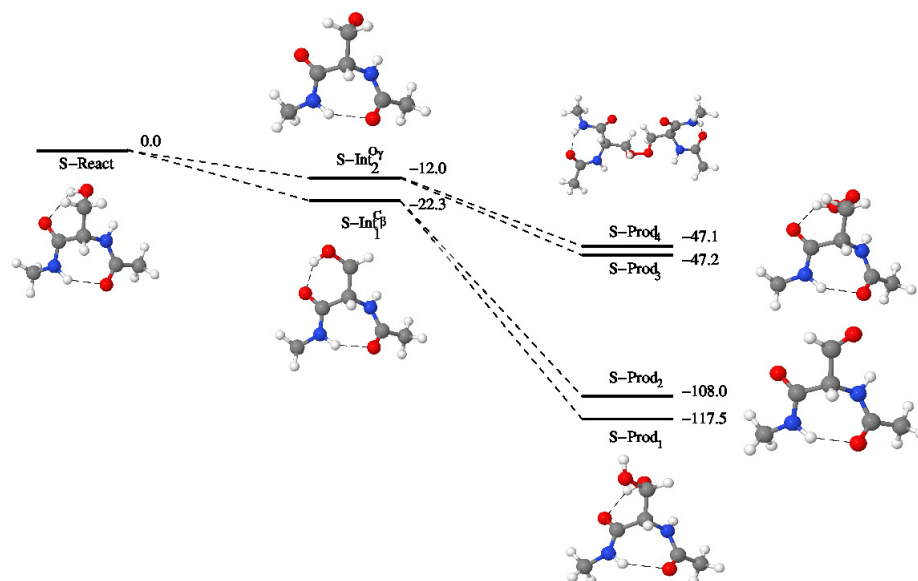


Figure 1.12: Bi $\bullet\text{OH}$ -k serinaren albo katean eragiten duten oxidazio erreakzio bide osoa. ΔH_{aq} balioak kcal/mol-etan emanak daude.

Bigarren $\bullet\text{OH}$ -aren erasoak adizio edo H abstrakzio mekanismoen bidez ematen da. Bi kasuetan, serina eta treonina, C_β posizioan gertatzen diren adizioak ematen dituzte produktu egonkorrenak, dialkoholak. Bestalde, aldehido edo zetonen eraketa eman daiteke, H abstrakzio baten ostean, zeinak produktu nahiko egonkorrak diren. Aipaturiko dialkoholak eta karboniloa duten konposatuak erlazionatuak daude beraien artean: dialkoholak ur molekula bat galduaz karbonilo konposatuak eratzen bait dituzte.

1.7.3 Amino azido aromatikoak

Kasu hauetan eratzen diren erradikalak, eraztun aromatikoan ematen diren delokalizazio efektuen bidez egonkortuak izan daitezke. Hortaz, nabaria da oxidazio prozesuan duten interes handia. Oxidazio mekanismoa H abstrakzio edo adizio bidez ematen da. Oro har, azken hauek azkarragoak dira, lehenak baino beren trantsizio barrerak baxuagoak direlako [105]. Oxidazio mekanismoak maiz produktu hidroxilatuak ematen dituzte [1, 41, 66, 71, 80, 81]

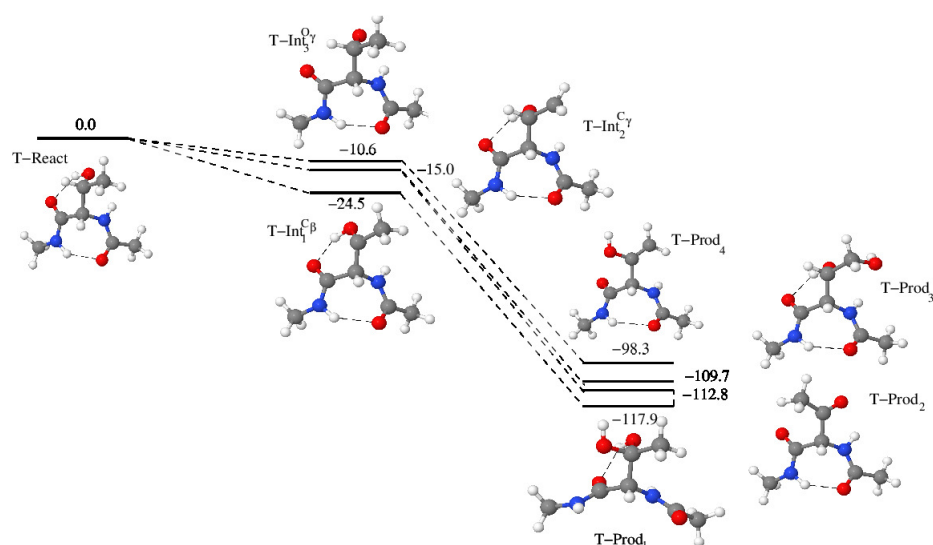


Figure 1.13: Bi $\bullet OH$ -k treoninaren albo katean eragiten duten oxidazio erreakzio bide osoa. ΔH_{aq} balioak kcal/mol-etan emanak daude.

eta zehazki triptofanoaren kasuan indol eraztunaren zatikatzea ekar dezake, kinureina eratuz [5, 9, 41, 47, 83]. Tirosinak produktu sareatuak eman ditzake zeinak bi tirosina erradikalen elkarrekintzaren ostean sortzen diren [82, 106]. Tirosina erradikal hauek entzimek katalizatzen dituzten erreakzio bitartekari bezala aurki ditzakegu [107].

Buruturiko lanean, oxidazio mekanismoa bi $\bullet OH$ -ren erasoaz gertatzen da. Azterturiko prozesuak, adizioa eta H abstrakzioa dira, ordenak garrantzi gutxi izanik. Izan ere, adizioa lehenik eta H abstrakzioa ondoren edo alderantziz gertatu, produktu bera lortzen da. Orokorri, erreakzio osoa H atomo bat OH batez ordezkatzeari bezala kontsidera daiteke. Erabilitako nomenklatura Irudia 1.14-en erakusten da eta erreakzioaren adibidea Irudia 1.15-ean.

Fenilalaninaren kasuan, lehen $\bullet OH$ -aren erasoan, zinetikoki hobetsiak daude adizio erreakzioak (Taula 1.3). Hala ere, C7 posiziotik gertatzen den H abstrakzioa mekanismo kompetitiboa da. Izan ere, azken honentzat aurkituriko trantsizio barrera adizioen antzekoa da. Termodinamikoki, C7-ko H abstrakzioak bitartekari egonkorragoak ematen ditu, adizioek baino, 14 kcal/mol egonkorragoa gutxi gora-behera.

Bigarren $\bullet OH$ -a, osatu den bitartekari erradikalariora adizionatuko da. Hortaz, eraztun aromatikoan edo C7-an adizionatuko dira, OH taldea sartuz. Eraztun aromatikoan sorturiko OH produktuak oso antzekoak dira, energetikoki (Taula 1.4) eta C7 posizioan gertatzen den OH adizioak produktu ezegonkorragoak dakar. Esan behar da, C7 bitartekaria eratzean, bigarren H abstrakzio bat gerta daitekela, C $_{\alpha}$ posiziotik hain zuzen ere. Hala lorturiko amaiera produktuak lotura bikoitza du C7-C $_{\alpha}$.

Tirosinaren kasuan, fenilalaninarenean bezala, H abstrakzioek trantsizio barrera handiagoak erakusten dituzte adizioek baino, Taula 1.5. C7 eta O8 posiziotan gertatzen diren H abstrakzioek trantsizio barrera baxua erakusten dute, adizioen antzekoa. Hala ere, abstrakzio hauetatik sortzen diren bitartekariak, adiziotik sortzen direanak baino egonkorragoak dira, energetikoki. Azkenik, kontutan hartu beharra dago O8 posizioako H abstrakzioa

·OH Addition										
	r_{CO}^{TS}	ΔH_4^{TS}	ΔH_{aq}^{TS}	ρ_s^O	ρ_s^C	r_{CO}^{Int}	ΔH_4^{Int}	ΔH_{aq}^{Int}	ρ_s^O	ρ_s^C
C1	1.985	-0.4	1.1	0.65	-0.15	1.425	-18.0	-17.2	0.02	-0.16
C2	1.969	1.0	1.7	0.65	-0.16	1.423	-16.3	-16.0	0.02	-0.15
C3	1.974	0.4	1.0	0.65	-0.15	1.423	-18.0	-17.0	0.02	-0.09
C4	1.965	1.0	1.7	0.64	-0.17	1.419	-16.5	-15.5	0.02	-0.18
C5	2.011	-4.5	-1.3	0.62	-0.13	1.434	-17.7	-15.1	0.02	-0.23
C6	1.999	-0.5	0.6	0.64	-0.11	1.442	-18.6	-14.9	-0.03	-0.09
H Abstraction										
	r_{CH}^{TS}	r_{OH}^{TS}	ΔH_4^{TS}	ΔH_{aq}^{TS}	ρ_s^O	ρ_s^C	ΔH_4^{Int}	ΔH_{aq}^{Int}		
C1	1.236	1.240	4.1	4.9	0.58	0.41	-4.6	-4.9		
C2	1.241	1.228	3.7	4.1	0.58	0.42	-4.7	-5.5		
C3	1.240	1.229	4.1	4.7	0.58	0.42	-4.2	-4.9		
C4	1.248	1.219	5.3	6.7	0.57	0.48	-5.4	-6.2		
C5	1.259	1.208	2.2	5.4	0.56	0.46	-4.9	-5.4		
C7	1.149	1.524	0.1	3.2	0.78	0.32	-29.7	-29.1		

Table 1.3: Fenilaminarentzat kalkulaturiko entalpia balioak (kcal/mol) bi konstante dielektrikotan 4 eta 80, trantsizio egoera eta erradikal bitartekariarentzat. Bi mekanismo kontsideratu dira: adizioa eta H abstrakzioa. Adizio C-O lotura distantzia eta H abstrakzio C-H eta O-H distantziak (Å-etan) erakusten dira. O atomo erradikaleko (ρ_s^O) eta C atomoko (ρ_s^C) spin dentsitateak ere aurkezten dira.

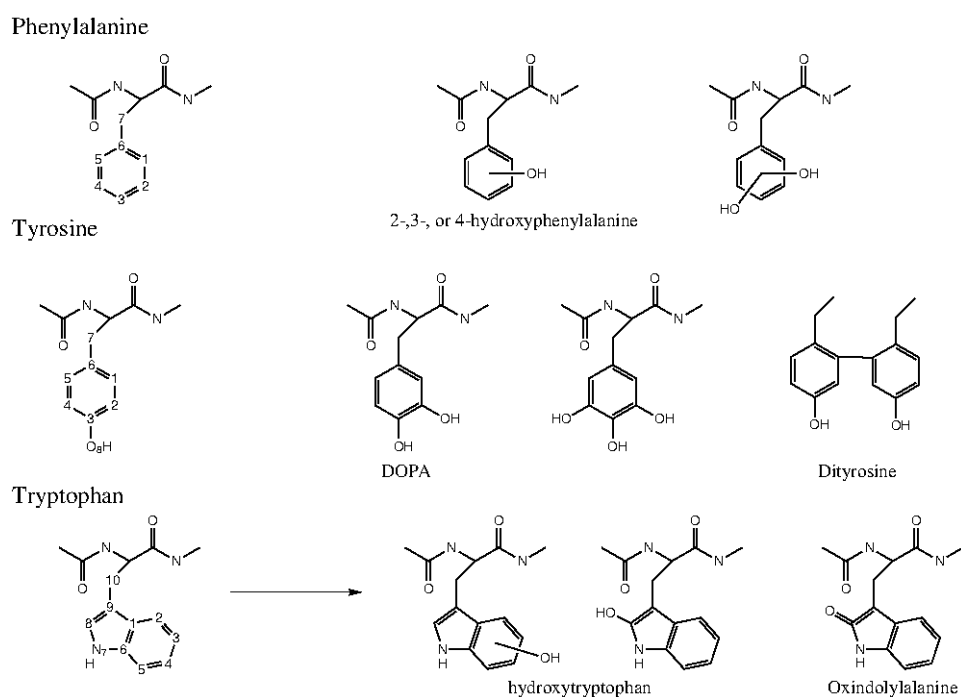


Figure 1.14: Hiru amino azido aromatikoen zat (fenilalanina, tirosina eta triptofanoa) erabili den numerazioa.

hobetsia legokela esterikoki, C7-koarekin alderatuz, azken posizio hau zailagoa baita er-radikalek ikusten.

Bigarren \bullet OH-aren erasoaren ostean, hainbat produktu eratu daitezke. Egonkorrenak eraztun aromatikoa OH talde bat sartzen denean gertatzen dira. C7 posizioan, OH talde bat sar daiteke, baina ez da lehenak aipatu diren produktuak bezain egonkorra. Bestalde, C7-C α lotura bikoitza eratzea termodinamikoki hain egonkorra ez den beste produktu batera garamatza. Azkenik, bi-tirosinak aztertu dira: C2 edo O8 posiziotik lotu daitezke bi tirosil erradikal. Honela lorturiko produktuen egonkortasuna erlatiboki baxua da, ikusi Taula 1.6, eta beraz, esan daiteke, eraztun aromatikoa gertatzen diren ordezkapenak direla produktu egonkorrenak ematen dituztenak.

Triptofanoaren kasuan ere \bullet OH-aren adizio mekanismoak trantsizio barrera baxuak ditu. Dena den, C8 eta C2 posizioetan ematen diren adizioak ohi baino egonkorragoak diren bitartekariak ematen dituzte, hurrenez hurren, 10 eta 5 kcal/mol egonkorragoak diren bitartekariak dira.

Sei atomoko eraztun aromatikoa gertatzen diren H abstrakzioek, adizioek baino trantsizio barrera handiagoa erakusten dute, fenilalanina eta tirosinaren kasuan bezala. Hala ere, eraztun honetatik kanpo dauden N7 eta C10 posizioetan gertatzen diren H abstrakzioek trantsizio barrera baxua dute. Are gehiago, hemen lortzen diren bitartekariak egonkortasun handia erakusten dute eta C8 eta C2 posizioetan gertatzen diren adizioekin konpetitzen dutela ikus daiteke, Taula 1.7.

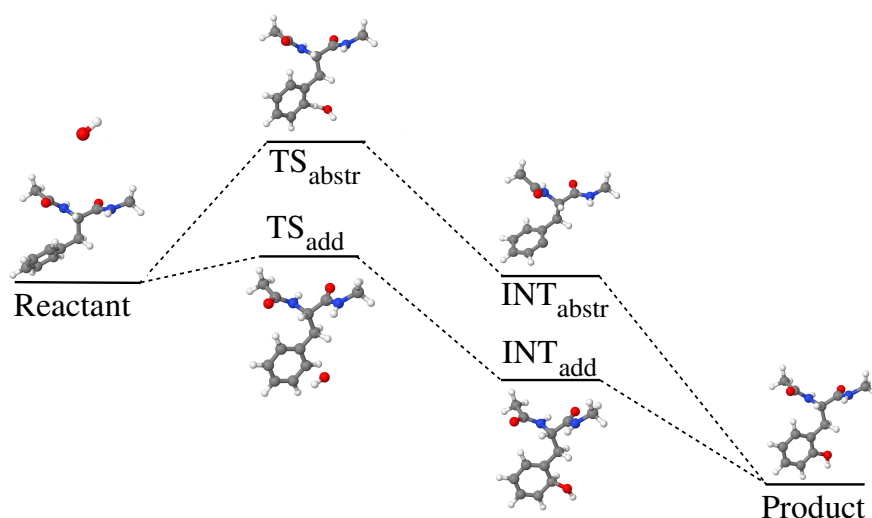


Figure 1.15: Fenilalaninaren C1 atomoan eman daitezken erreakzioak: i) adizioa eta ii) H abstrakzioa. Erakusten diren energia mailak ez daude eskalan jarrita.

	ΔH_4^{298}	ΔH_{aq}^{298}
Prod _{Phe} ^{C1}	-117.1	-116.6
Prod _{Phe} ^{C2}	-116.9	-116.7
Prod _{Phe} ^{C3}	-116.5	-116.2
Prod _{Phe} ^{C4}	-116.4	-115.1
Prod _{Phe} ^{C5}	-115.9	-114.5
Prod _{Phe} ^{C7}	-111.0	-108.4
Prod _{Phe} ^{C7α}	-102.5	-100.6

Table 1.4: Fenilalaninaren erreaktiboekiko kalkulaturiko entalpia balioak (kcal/mol) bi konstante dielektrikotan 4 eta 80.

Bigarren $\bullet\text{OH}$ -aren erasoak sortzen dituen produktu hidroxilatuak energetikoki oso antzekoak dira. Produktu egonkorrena C8 posizioan gertaturiko adizioari dagokio eta eze-gonkorrena berriz N7 posizioko adizioari. Int_{Trp}^{C10}-tik abiatuz C α posizioan H abstrakzioa ematen bada, C10-C α lotura bikoitza duen produktua lortzen da. Produktu hau, egonkorrenak baino 10 kcal/mol eze-gonkorragoa da. Bestalde, OH taldea adizionatzeak 5 kcal/mol eze-gonkorragoa den produktua dakar, Taula 1.8.

Oro har, adizio erreakzioek trantsizio barrera baxuagoak erakusten dituzte. C β -ko H abstrakzioa da salbuespena, hemen kalkulaturiko trantsizio barrerak adizioen oso antzekoak dira eta eskuratzen den bitartekaria, orokorrean, adizioak baino egonkorragoa da. Argi geratzen da beraz, amino azido aromatikoetan C β dela leku aproposa halako oxidazio mekanismoak gertatzeko. Salbuespen moduan agertzen zaigu triptofanoko indol eraztuneko C8 posizioan gertatzen den adizioa, zeinak bitartekari egonkorra ematen duen Irudia 1.16. Bestalde, nahiz eta adizio mekanismoak amaieran produktu egonkorrenetara eramaten, osaturiko bitartekariak ez dira C β posiziotik gertatzen den H abstrakzioz lorturikoak bezain

·OH Addition										
	r_{CO}^{TS}	ΔH_4^{TS}	ΔH_{aq}^{TS}	ρ_s^O	ρ_s^C	r_{CO}^{Int}	ΔH_4^{Int}	ΔH_{aq}^{Int}	ρ_s^O	ρ_s^C
C1	1.981	0.9	2.3	0.64	-0.17	1.426	-16.7	-15.7	0.02	-0.13
C2	1.996	0.6	0.8	0.66	-0.11	1.418	-18.1	-17.2	0.02	-0.09
C3	2.005	2.5	4.3	0.63	-0.12	1.420	-18.9	-17.8	0.03	-0.10
C4	2.000	1.1	3.2	0.57	-0.04	1.425	-18.2	-15.9	0.01	-0.27
C5	2.036	-3.4	-0.3	0.62	-0.12	1.438	-17.0	-14.4	0.02	-0.19
C6	2.034	-1.8	-1.1	0.64	-0.11	1.446	-19.5	-15.9	0.02	-0.09
H Abstraction										
	r_{XH}^{TS}	r_{OH}^{TS}	ΔH_4^{TS}	ΔH_{aq}^{TS}	ρ_s^O	ρ_s^C	ΔH_4^{Int}	ΔH_{aq}^{Int}		
C1	1.236	1.239	5.2	5.9	0.59	0.39	-3.7	-3.6		
C2	1.264	1.194	6.2	6.9	0.57	0.35	-2.2	-2.6		
C4	1.245	1.236	5.8	8.8	0.54	0.38	-2.6	-2.5		
C5	1.260	1.205	3.0	6.2	0.56	0.46	-3.8	-4.2		
C7	1.141	1.575	0.9	4.1	0.79	0.29	-29.6	-29.1		
O8	0.988	1.456	2.4	4.8	0.68	0.20	-29.3	-28.8		

Table 1.5: Tirosinarentzat kalkulaturiko entalpia balioak (kcal/mol) bi konstante dielektrikotan 4 eta 80, trantsizio egoera eta erradikal bitartekariarentzat. Adizkioko C-O lotura distantzia eta H abstrakziooko C-H eta O-H distantziak (Å-etan) ere ematen dira. Azkenik, O atomo erradikalaren (ρ_s^O) eta jomuga den C atomoaren (ρ_s^C) spin dentsitateak ematen dira.

	ΔH_4^{298}	ΔH_{aq}^{298}
Prod $_{Tyr}^{C1}$	-116.5	-115.9
Prod $_{Tyr}^{C2}$	-114.9	-113.4
Prod $_{Tyr}^{C4}$	-114.1	-111.6
Prod $_{Tyr}^{C5}$	-116.4	-113.6
Prod $_{Tyr}^{C7}$	-111.0	-108.5
Prod $_{Tyr}^{C7\alpha}$	-101.3	-99.6
Prod $_{Tyr-Tyr}^{OO}$	-37.3	-30.9
Prod $_{Tyr-Tyr}^{22}$	-107.7	-104.5

Table 1.6: Tirosina errektiboekiko kalkulaturiko entalpia balioak (kcal/mol) bi konstante dielektrikotan 4 eta 80.

egonkorrak eta beraz, ez lirateke hain maiz gertatuko, faktore energetikoak kontsideratuz. Hala ere, termodinamika ez da kontuan hartu beharreko faktore bakarra. Efektu esterikoek bere biziko garrantzia dute eta hortaz, aipaturiko C_β posizioak ez dira horren eskuragarriak.

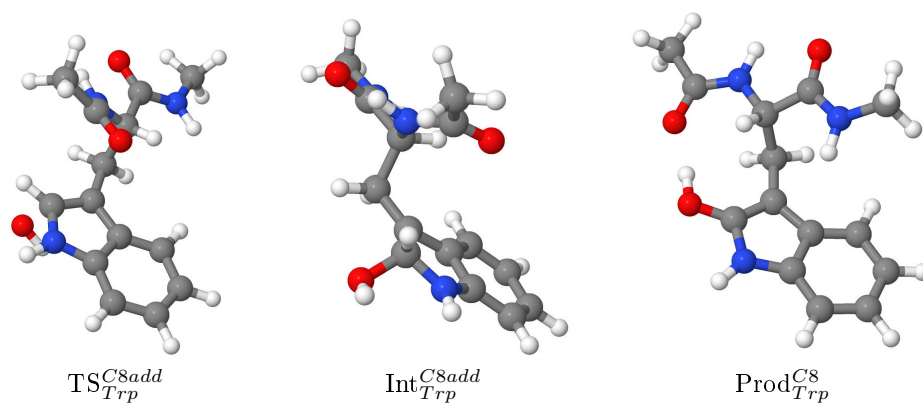


Figure 1.16: Triptofano C8 adizioari dagozkion egoera estazionario egonkorrenak erakusten dira.

·OH Addition										
	r_{CO}^{TS}	ΔH_4^{TS}	ΔH_{aq}^{TS}	ρ_s^O	ρ_s^C	r_{CO}^{Int}	ΔH_4^{Int}	ΔH_{aq}^{Int}	ρ_s^O	ρ_s^C
C2	2.107	0.1	2.0	0.69	-0.12	1.431	-24.4	-21.2	0.00	-0.15
C3	1.975	0.7	1.2	0.62	-0.11	1.429	-15.3	-14.8	0.01	-0.13
C4	2.002	-0.4	0.0	0.64	-0.14	1.427	-17.7	-17.4	0.02	-0.14
C5	2.043	-0.8	-0.1	0.67	-0.11	1.423	-19.8	-19.0	0.02	-0.16
C8	2.125	-5.7	-4.8	0.66	-0.08	1.405	-28.6	-27.4	0.00	-0.01
H Abstraction										
	r_{XH}^{TS}	r_{OH}^{TS}	ΔH_4^{TS}	ΔH_{aq}^{TS}	ρ_s^O	ρ_s^C	ΔH_4^{Int}	ΔH_{aq}^{Int}		
C2	1.209	1.296	1.7	4.4	0.60	0.37	-4.4	-4.2		
C3	1.238	1.234	4.7	5.3	0.58	0.41	-3.1	-3.4		
C4	1.239	1.231	4.9	5.3	0.59	0.44	-3.3	-3.8		
C5	1.243	1.232	5.8	7.0	0.56	0.36	-2.1	-2.2		
N7	1.071	1.416	2.2	5.0	0.57	0.24(N)	-24.5	-24.6		
C8							3.3	3.1		
C10	1.145	1.530	-1.6	0.1	0.78	0.25	-28.7	-27.7		

Table 1.7: Triptofanoarentzat kalkulaturiko entalpia balioak (kcal/mol) bi konstante dielektrikotan 4 eta 80, trantsizio egoera eta erradikal bitartekariarentzat. Adizioko C-O lotura distantzia eta H abstrakzioa C-H eta O-H distantziak (Å-etan) ere ematen dira. Azkenik, O atomo erradikalaren (ρ_s^O) eta jomuga den C atomoaren (ρ_s^C) spin dentsitateak ematen dira.

	ΔH_4^{298}	ΔH_{aq}^{298}
Prod $_{Trp}^{C2}$	-116.2	-114.4
Prod $_{Trp}^{C3}$	-113.9	-113.7
Prod $_{Trp}^{C4}$	-114.6	-114.6
Prod $_{Trp}^{C5}$	-114.6	-114.0
Prod $_{Trp}^{N7}$	-74.7	-71.4
Prod $_{Trp}^{C8}$	-123.5	-118.2
Prod $_{Trp}^{C10}$	-111.6	-109.3
Prod $_{Trp}^{C10\alpha}$	-104.6	-105.6

Table 1.8: Triptofano errektiboekiko kalkulaturiko entalpia balioak (kcal/mol) bi konstante dielektrikotan 4 eta 80.

1.7.4 Amino azido azido eta basikoak

Azidoak diren amino azidoen kasuan, oxidazio mekanismoa H edo elektroi abstrakzioaren ondorioz ematen da. Azido formikoarekin antzekotasuna badute halako erreazioek eta konpara genezake bertako H abstrakzio mekanismoarekin [108]. Ikerketa honetan ikusten da $\bullet\text{OH}$ -ak nagusiki O atomoari loturiko H atomoa hartzen duela. Bestalde, azido karboxilikoaren pKa 3.9 inguruan dabil. Hau dela eta, pH altu eta fisiologikoetan deprotonatua aurkituko dugu. Hala ere, azido aspartiko eta glutamikoentzat bi protonazio egoerak kontsideratu ditugu. Honela, lehen $\bullet\text{OH}$ -ak H abstrakzioaren bitartez gauzatzen du oxidazio mekanismoa. Elektroi abstrakzio mekanismoa ere posible da, karboxilatoa dugun kasuetarako.

Albo katean gertatzen den oxidazioa aztertzea dugu helburu, haatik, aspartatoan gerta daiteken dexkarboxilazio mekanismoa aztertzeko, C_α posizioan gerta daiteken H abstrakzioa ere azertu behar da. Azken honek ematen du bitartekari egonkorrena, Irudia 1.17. C_β posizioan ere gerta daiteke H abstrakzioa eta O_δ posizioan elektroi abstrakzioa, baina lortzen diren bitartekarien egonkortasuna txikituz doa. $\text{Int}_{Asp}^{C_\beta}$ erradikal sekundarioa da eta $\text{Int}_{Asp}^{O_\delta}$ berriz, erradikal primarioa, hortaz hiperkonjokazioa efektu garrantzitsua da hauen egonkortasuna arrazionalizatzerakoan. Protonaturiko azido aspartikoak joera bera erakusten du, Irudia 1.18.

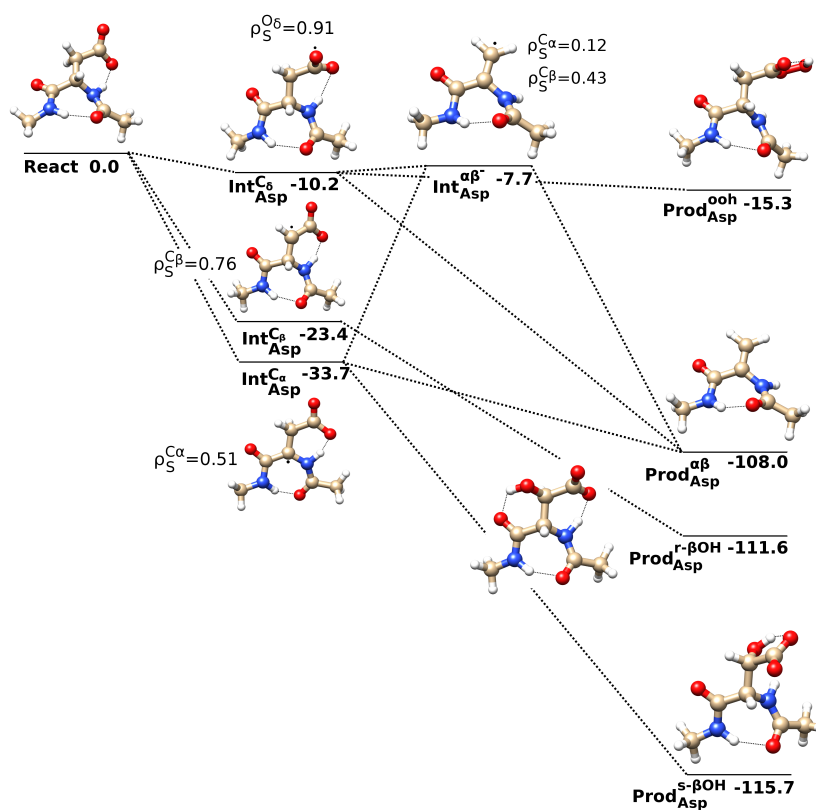


Figure 1.17: Aspartatoaren erreazio bidearen errepresentazio eskematikoa. Erreaktibo (React), bitartekari (Int) eta produktuek (Prod) oxidazioa gertatzen den posizioaren arabera dute labela. Entalpia balio erlatiboak kcal/mol-etan emanak daude. Azkenik, TFVC spin dentsitateak daude jarrita bitartekari guztientzat.

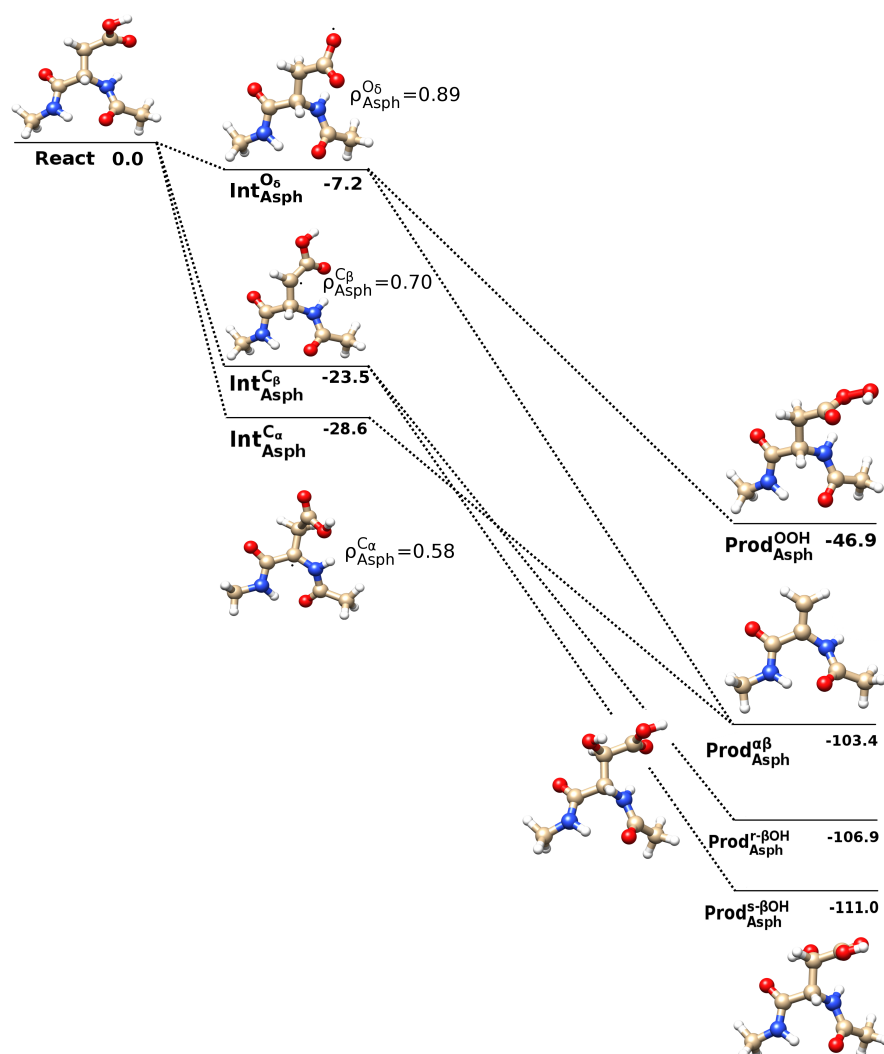


Figure 1.18: Azido Aspartikoaren erreazio bidearen errepresentazio eskematikoa. Erreaktibo (React), bitartekari (Int) eta produktuek (Prod) oxidazioa gertatzen den posizioaren arabera dute labela. Entalpia balio erlatiboak kcal/mol-etan emanak daude. Azkenik, TFVC spin dentsitateak daude jarrita bitartekari guztientzat.

Lorturiko Int^{C α} _{Asp}-k albo kateko karboxilatoaren apurketa heterolitikoa ekar lezake. Honela gertatuz gero, erradikala eta karga dituen beste bitartekari bat sortuko litzateke, Int^{- $\alpha\beta$} _{Asp},

CO₂-a askatuz. Aspartikoaren kasuan, bitartekari honen eratzeak protoi bat askatzea dakar. Dena den, energetikoki ezegonkorragoa da eta ez da gertatzen erreazio erraza.

Bigarren •OH-aren erasoak, beste H abstrakzio bat edo adizioa eman ditzake. C_β posizioan emandako adiziotik sorturiko produktuak dira egonkorrenak. Bestalde, peroxidoaren eraketa ez dago hobetsia, hau da ikusiriko produktu ezegonkorrena. Azkenik, bigarren eraso honek, albo katearen apurketa ekar lezake. Int^{C_α}_{Asp}-tik abiatuz, bigarren •OH-ak, O_δ posizioeko elektroio abstrakzioa ekarri ezker, albo katea apurtu eta CO₂ eta lotura bikoitza duen produktua (Prod^{αβ}_{Asp}) sor daitezke. Prozedura berdina posiblea da azido aspartikoarentzat.

Ildo beretik, azido glutamiko eta glutamatoaren oxidazio mekanismoak ditugu. Hemen, -CH₂- talde bat gehiago dugu albo katean eta aukera gehiago daude oxidaziorako. Hala ere, mekanismoa aurretik aipatutakoaren berdina da.

Lehen •OH-ak, C_β, C_γ edo O_ε posizioetan eraso dezake. Lorturiko erradikal bitartekari egonkorrena C_γ posizioan erasotzean osatzen da. Erradikal sekundarioa dugu, zeinak aldameneko karboxilo/karboxilato taldeari esker elektroio ez-parekatua apur bat gehiago delokalizatu dezaken. Ezegonkorrena berriz, O_ε posizioan osatzen den erradikal primarioari dagokio, Irudia 1.19 eta 1.20.

Bigarren •OH-ak, aipatu bezala, adizioa edo beste H abstrakzio bat eman ditzake. Produktu egonkorrenak, adizioaren bitartez eratzen dira, bi H abstrakzioz eratutako produktuak 20 kcal/mol inguru ezegonkorragoak dira, C.4 Taulan agertzen dira balioak. Azkenik, hemen ere albo katearen haustura gerta daiteke. Int^{C_β}_{Glu}-tik abiatuz, bigarren •OH-ak O_ε-ko elektroioari erasotzen badio, CO₂ eta Prod^{βγ}_{Glu} eratuz. Azken produktu hau, adiziotik sortzen direnak baino 10 kcal/mol inguru ezegonkorragoa da eta beraz adizioak izango dira nagusiki eratzen direnak. Mekanismo berdina posiblea da azido glutamikoarentzat.

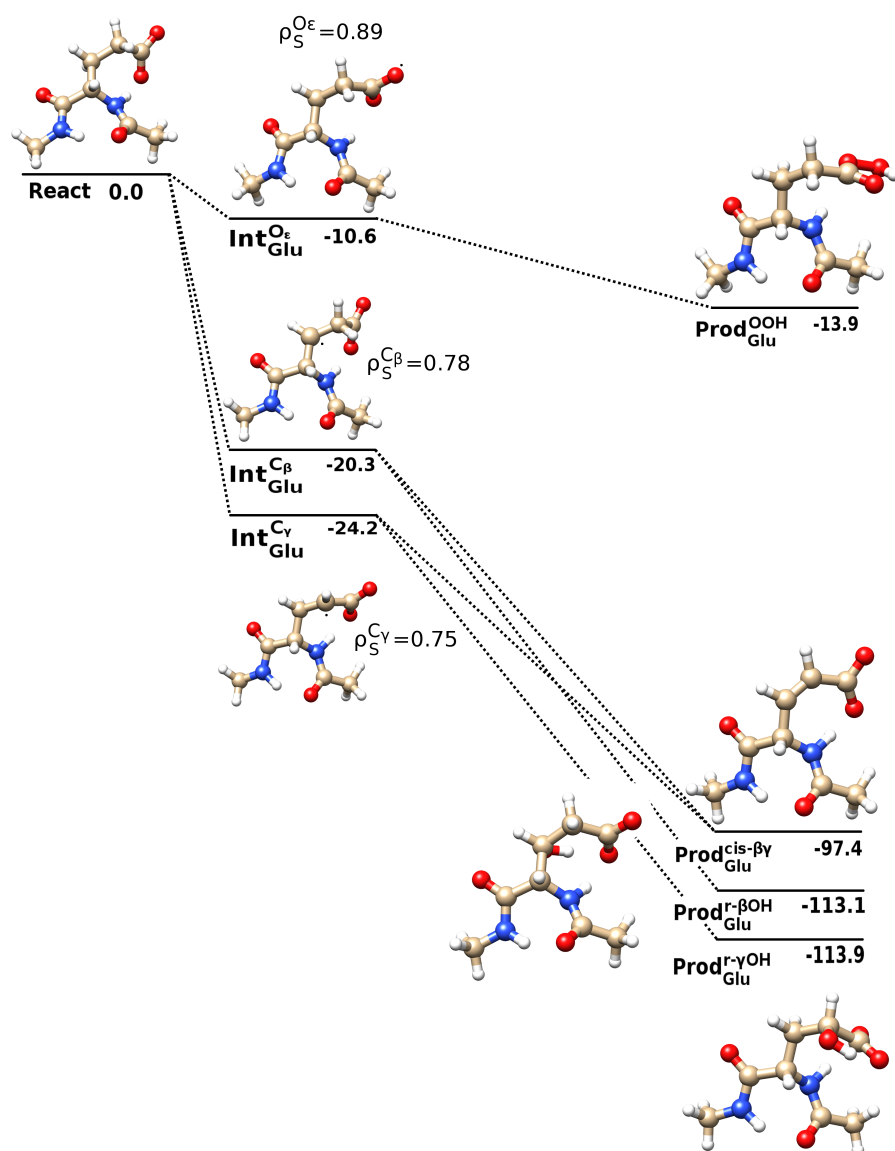


Figure 1.19: Glutamatoaren erreazio bidearen errepresentazio eskematikoa. Erreaktibo (React), bitartekari (Int) eta produktuek (Prod) oxidazioa gertatzen den posizioaren arabera dute labela. Entalpia balio erlatiboak kcal/mol-etan emanak daude. Azkenik, TFVC spin dentsitateak daude jarrita bitartekari guztientzat.

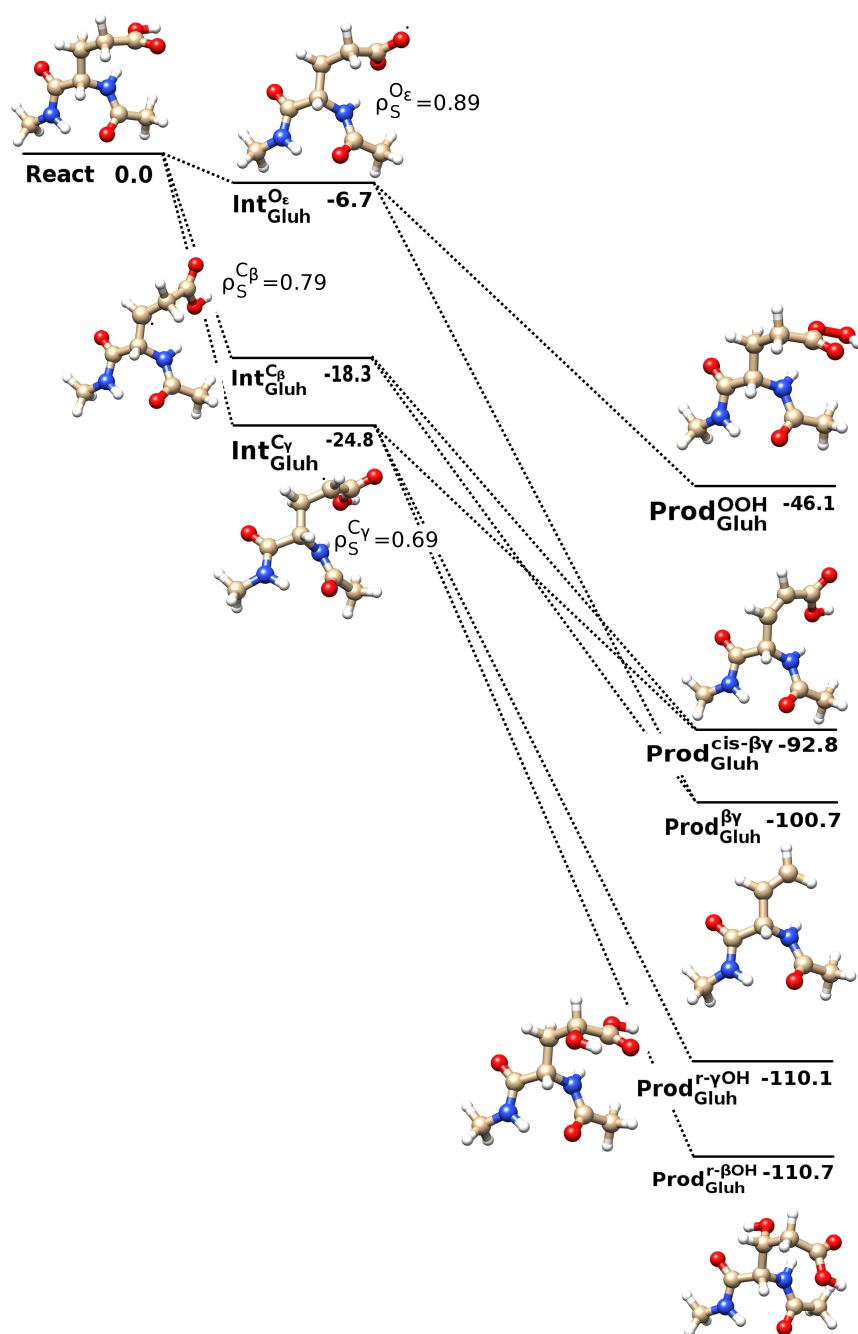


Figure 1.20: Azido glutamikoaren erreakzio bidearen errepresentazio eskematikoa. Erreaktibo (React), bitartekari (Int) eta produktuek (Prod) oxidazioa gertatzen den posizioaren arabera dute labela. Entalpia balio erlatiboak kcal/mol-etan emanak daude. Azkenik, TFVC spin dentsitateak daude jarrita bitartekari guztientzat.

Amino azido basikok bezala ditugu arginina, lisina eta histidina, zeinak nagusiki oxidatuak diren metalei lotuak daudenean. Halako amino azidoak maiz aurkitzen ditugu *espezie erreaktiboak* produzitu ditzaketen metalei lotuta, eta amino azido hauek oxida daitezketekete. Histidinak, imidazol talde bat du albo katean eta beraz amino azido aromatikoek bezalako erreakzio bideak erakutsiko ditu. Hemen, arginina eta lisinaren oxidazio erreakzio bidea aztertzen dugu.

Arginina eta lisinaren kasuan eman daitezken oxidazio mekanismoetan, H abstrakzio bat gertatzen da lehen $\bullet\text{OH}$ -aren eraginez, Irudiak 1.21 eta 1.22. Bi amino azidoen kasuan, C atomoetatik gertatzen diren H abstrakzioen ondorioz eratutako bitartekariak dira egonkorren. N atomoetatik gertatzen den H abstrakzioak ez ditu hain bitartekari egonkorak ematen, aurrekoak baino 10 kcal/mol ezegonkorragoak dira hauek. Bestalde, argininan C_ζ posizioan adizioa gerta daiteke, $\text{Int}_{Arg}^{C_\zeta}$ osatuz. Hala eratzen den bitartekaria da aurkitu den ezegonkorrena, endotermikoa da erreakzioa +1.2 kcal/mol. Bitartekari honek albo katearen apurketa ekar dezake, experimentalki aurkitu diren produktuak emanez: zitulina eta ornitina (Irdudia 1.23). Beraz, kontutan izan behar da erradikal baten erasoarekin soilik lortzen direla produktu hauek.

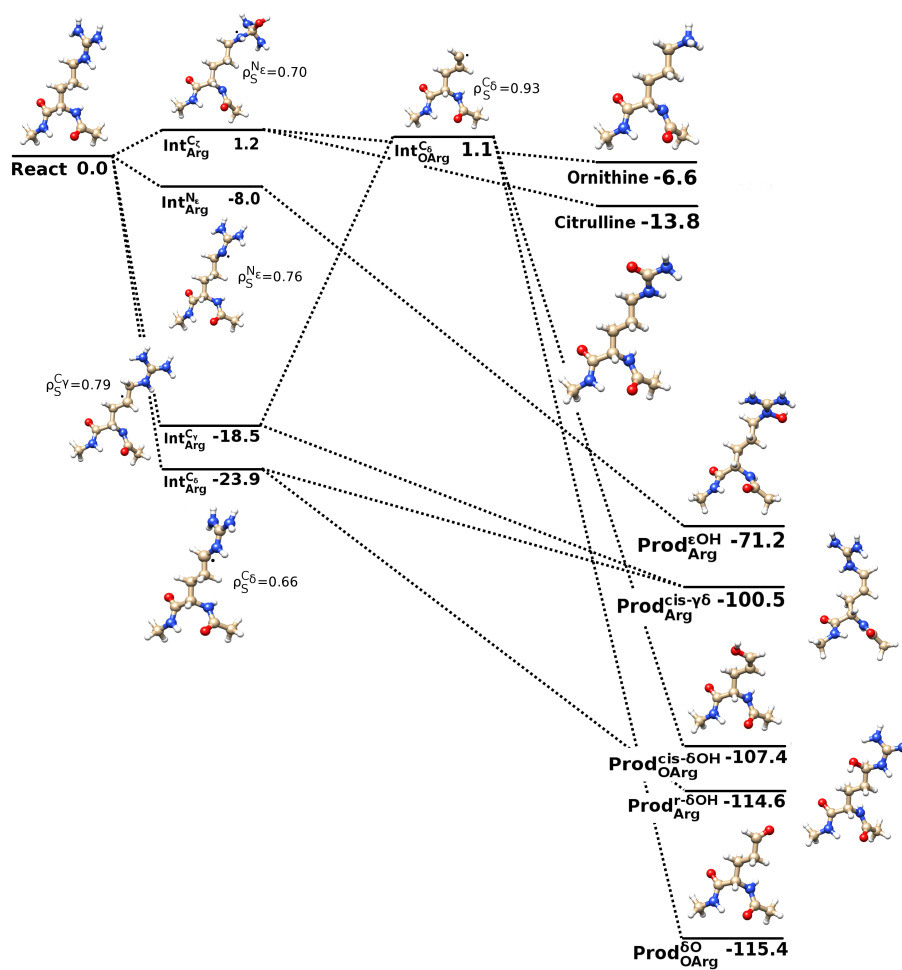


Figure 1.21: Argininaren erreakzio bidearen errepresentazio eskematikoa. Erreaktibo (React), bitartekari (Int) eta produktuek (Prod) oxidazioa gertatzen den posizioaren arabera dute labela. Entalpia balio erlatiboak kcal/mol-etan emanak daude. Azkenik, TFVC spin dentsitateak daude jarrita bitartekari guztientzat.

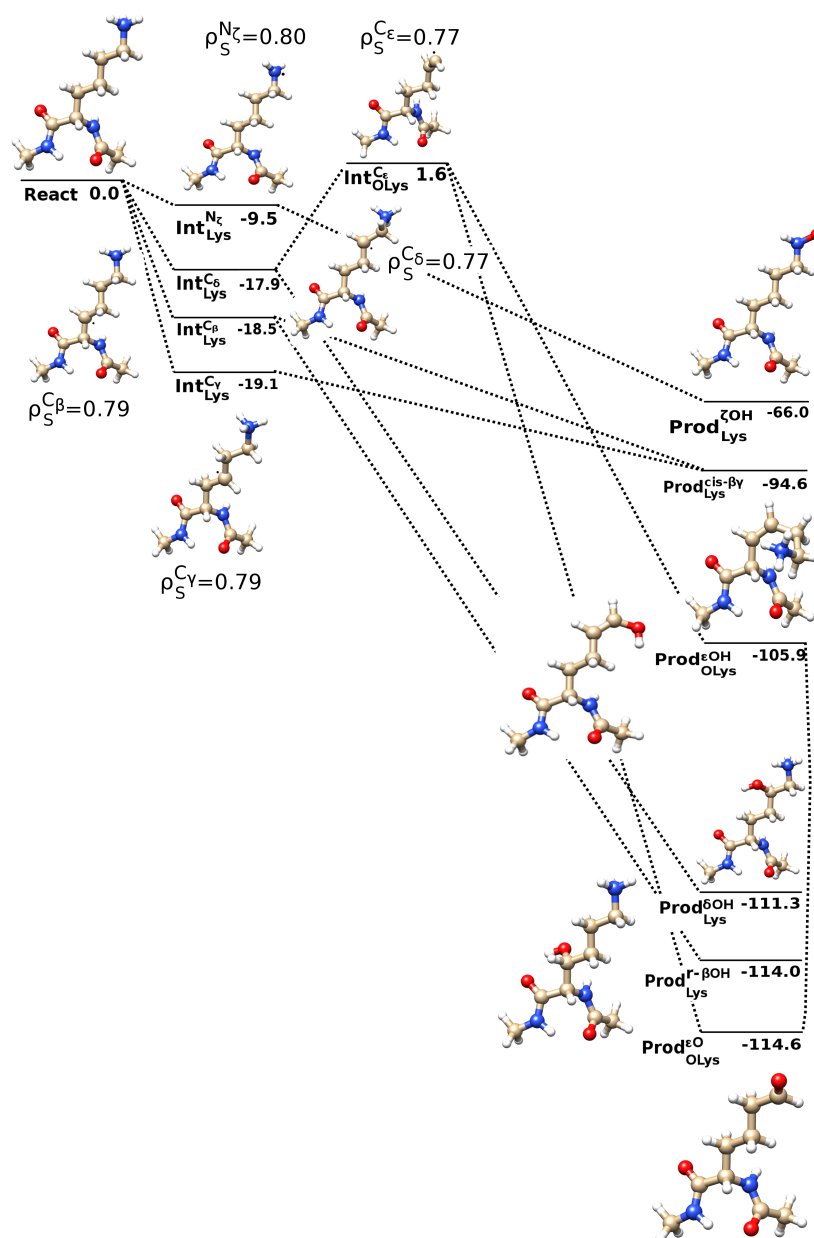
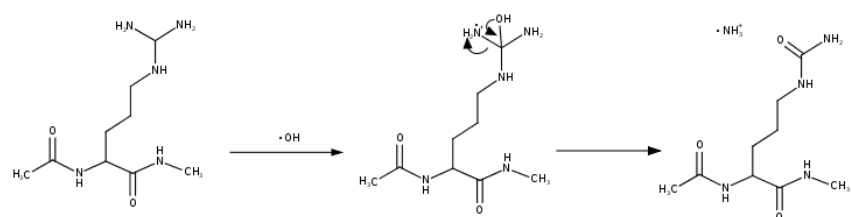
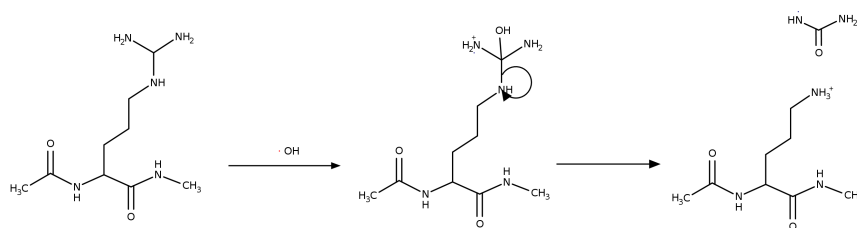


Figure 1.22: Lisinaren erreakzio bidearen errepresentazio eskematikoa. Erreaktibo (React), bitartekari (Int) eta produktuek (Prod) oxidazioa gertatzen den posizioaren arabera dute labela. Entalpia balio erlatiboak kcal/mol-etan emanak daude. Azkenik, TFVC spin dentsitateak daude jarrita bitartekari guztientzat.



(a)



(b)

Figure 1.23: a) Zitrulina produktua eratzeke erreakzio bidea. b) Ornitina produktua eratzeke erreakzio bidea.

Bestalde, bigarren $\cdot\text{OH}$ -aren erasoak beste H abstrakzio bat edo adizioa eman ditzake. Bi kasutan, produktu egonkorrenak lortzen dira adizioaren bitartez: bigarren H abstrakzio bat baino 15 kcal/mol egonkorragoak, gutxi gora-behera.

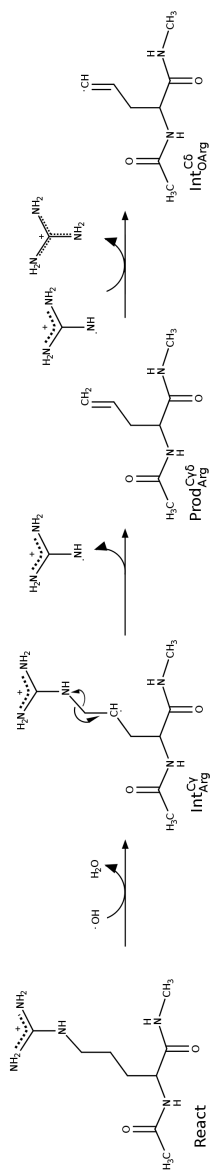


Figure 1.24: $Int_{C_{\gamma}Arg}$ -aren disoziazio homolitiko lotura bikoitzeko produktua ($Prod_{C_{\gamma}\delta}$) eta guanidinio erradikala eratu. $Int_{C_{\delta}Arg}$ bitartekaria eraten da, guanidinio erradikalak eragindako H abstrakzioaren ondoren.

1.7.5 Beste amino azidoak

Geratzen diren amino azidoak errektibitate baxuenekoak dira: alifatikoak eta amida dutenak. Halakoetan, H abstrakzio mekanismoa gertatzen da eta bitartekari egonkorrena C_α posizioan sortzen denari dagokio [20, 66, 109-111]. Azaldu den bezala, posizio honetan efektu kaptodatiboa ematen da, bitartekari erradikala egonkortuz [112-114]. Dena den, posizio honetan gertatzen den erasoa glizinan eta alaninan ikusi izan da, kasu hauetan esterikoki ez baitago horren zaildua [20]. Lehenak H atomo bat du albo kate bezala eta ondorengoak, metil talde bat. Bestalde, osaturiko C_α erradikalek, O_2 -rekin erreakzionatu edo amino azidoen sareatzea bultzatzen dute, aldaketak ekarriz proteinari.

Aipatu bezala, amino azido hauek H abstrakzio erreakzioa ematen dute. Asparaginaren kasuan, N_δ posizioan gertatzen den H abstrakzioak dakar bitartekari ezegonkorrena. C_α posizioan gertatzen dena berriz da egonkorren, $Int_{Asn}^{C_\alpha}$. Bitartekari honek, albo katearen apurketa ekar dezake, $\bullet CONH_2$ eta C_α - C_β atomoen artean lotura bikoitza duen produktua eratuz ($Prod_{Asn}^{\alpha\beta}$). Era beran, osaturiko erradikal produktu honek H abstrakzioa eragin dezake $Prod_{Asn}^{\alpha\beta}$ -aren C_β posizioan, $Int_{OAsn}^{C_\beta}$ bitartekaria osatuz. Bitartekariaren eraketa endotermikoa dela ikusi da eta beraz erreakzio bide hau ez dago hobetsia, Irudia 1.25.

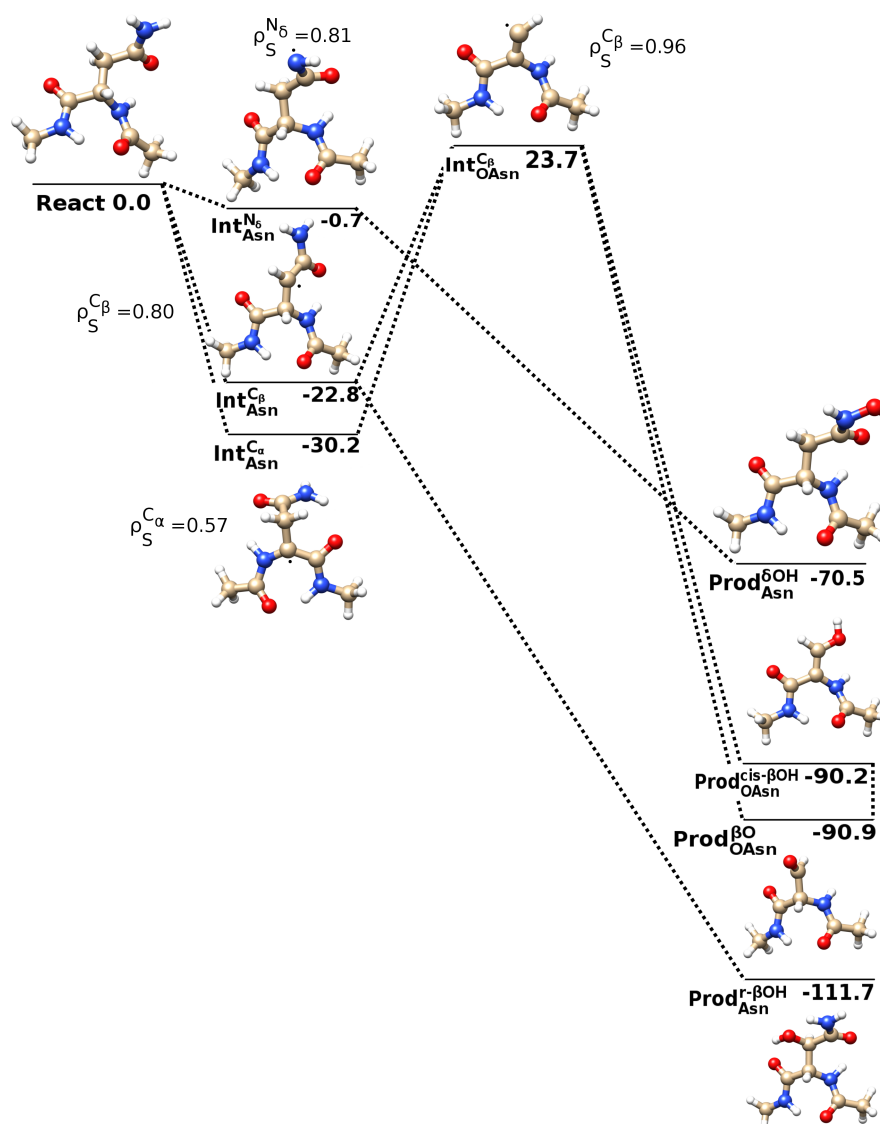


Figure 1.25: Asparaginaren erreazio bidearen errepresentazio eskematikoa. Erreaktibo (React), bitartekari (Int) eta produktuek (Prod) oxidazioa gertatzen den posizioaren arabera dute labela. Entalpia balio erlatiboak kcal/mol-etan emanak daude. Azkenik, TFVC spin dentsitateak daude jarrita bitartekari guztientzat.

Bigarren $\bullet\text{OH}$ -aren erasoak, beste H abstrakzio bat ekar lezake edo osaturiko erradikal bitarterari gehitu dakiok. Asparagin, produktu egonkorrena C_β posizioan gertatzen den adizioaren ostean sortzen den alkohola da.

Mekanismo bera dugu glutaminan, non aurreko kasuan baino $-\text{CH}_2-$ talde bat gehiago

dugun orain. Lehen $\bullet\text{OH}$ -aren erasoak C_γ posizioan eragiten duen H abstrakzioaren ondorioz eratzen da bitartekari egonkorrena. C_β posizioan gertatzen dena ($\text{Int}_{\text{Gln}}^{\text{C}_\beta}$ sortuz) 6 kcal/mol inguru ezegonkorragoa da, lehenak karbonilo talde bat baitu alboan, erradikala gehiago delokalizatuz. $\text{Int}_{\text{Gln}}^{\text{C}_\beta}$ bitartekariak albo katearen haustura ekar dezake, $\bullet\text{CONH}_2$ eta C_β - C_γ lotura bikoitza duen produktua eratuz, $\text{Prod}_{\text{Gln}}^{\beta\gamma}$. Era berean, $\bullet\text{CONH}_2$ -aren erasoagatik H abstrakzio bat gerta daiteke $\text{Prod}_{\text{Gln}}^{\beta\gamma}$ -aren C_γ posizioan, $\text{Int}_{\text{OGln}}^{\text{C}_\gamma}$ eratuz. Bitartekari honen eraketa endotermikoa dela ikusi da eta hortaz ez dago hobetsia, Irudia 1.26.

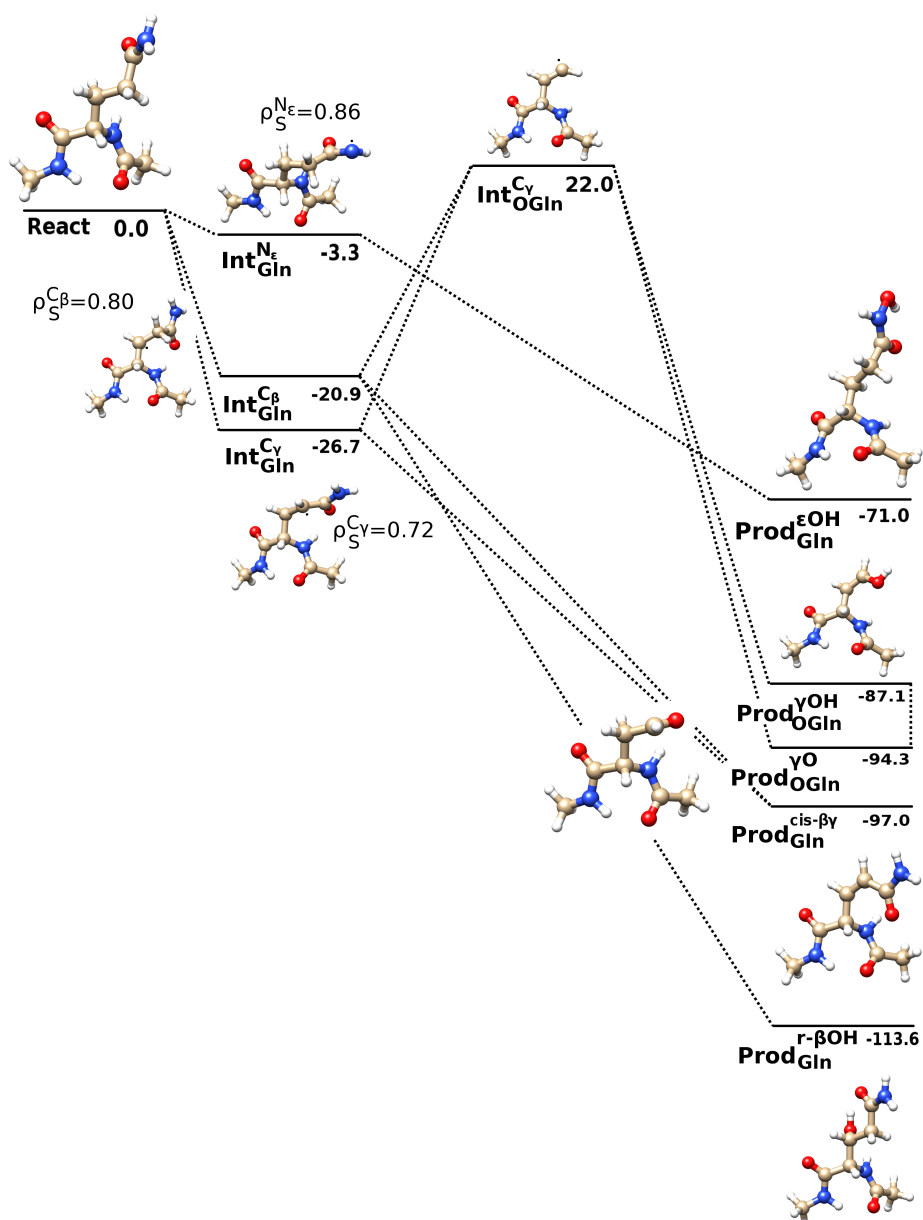


Figure 1.26: Glutaminaren erreazio bidearen errepresentazio eskematikoa. Erreaktibo (React), bitartekari (Int) eta produktuek (Prod) oxidazioa gertatzen den posizioaren arabera dute labela. Entalpia balio erlatiboak kcal/mol-etan emanak daude. Azkenik, TFVC spin dentsitateak daude jarrita bitartekari guztientzat.

Bigarren $\bullet\text{OH}$ -aren erasoak, beste H abstrakzio bat ekar lezake edo osaturiko erradikal bitarterari gehitu dakioko. Produktu egonkorrenak C_{β} eta C_{γ} posizioetan OH-a adizion-

atzeak ematen ditu. Bi H abstrakzio bidez eratzen diren lotura bikoitzeko produktuak 15 kcal/mol inguru ezegonkorragoak dira. Azkenik, aipatu behar da N atomoa ez dela leku aproposa erradikalen erasorako eratzen diren bitartekari eta produktuak ez baitira horren egonkorrak.

1.7.6 Amino azidoen bizkarrezurra

Orain arte azalduko erreakzio guztiek, amino azidoen albo katea zuten helburu. Dena den, amino azidoen bizkarrezurra eraso gerta daiteken beste eskualde bat da. Alderdi hau garrantzitsua da amino azido, peptido edo proteinen egiturarako, bere orientazioak baldintzatua bait dator. Esan bezala, C_α posizioan gertaturiko H abstrakzioek bitartekari oso egonkorak ematen dituzte, efektu kaptodatiiboaren ondorioz. Bestalde, bada beste posiziorik oxidazioa gertatzeko, N atomoa, hain zuzen. Bertan gertatzen diren H abstrakzioak ordea erradikal ezegonkorragoak eratzten ditu. Era berean, prozesuarentzako ikusitako trantsizio barrerak ere altuagoak dira eta hortaz ez da oxidazioa gertatzeko leku aproposena [115, 116].

Eskualde honen ikerketa interesgarria gertatzen da badirelako teknika experimentalak bizkarrezurraren apurtzea bultzatzen dutenak: zatien ondorengo identifikazio eta polipeptidoen sekuentziazioa helburu izanik. Zentzu honetan, Elektroi Transferentziako Disoziazioa (ETD) [117], Elektroi Atzematearen Disoziazioa (EAD) [118] eta Erradikal Askeek Hasiriko Peptido Sekuentziatzea (EAHPS) aurki ditzakegu [119-121].

Azkenik, bizkarrezurrean erradikalak eratzeak, proteina eta peptidoen egitura aldaketa ekar dezake. Behin erradikala osatua, lotura distantzia eta dihedroen aldaketak atzeman daitezke. Beraz, zentzuzkoa da proteina edo peptidoaren egitura sekundarioan aldaketak ikustea [122, 123]. Are gehiago, halako espezieak proteinen α -helizeen hedaketan parte har dezaketela ikusi da [116]. Honela, erradikalek hasiriko hedaketa fenomeno garrantzitsua dela azpimarratua izan da, amiloide plaken eraketan parte har bait dezakete.

Buruturiko lan honetan sistematikoki aztertu dira amino azido guztietan eman daitezken C_α eta C_β posizioetako H abstrakzioak. Izan ere, C_β gertatzen diren H abstrakzioek lotura peptidikoaren apurketa ekartzen dutela ikusi da, EAHPS teknikan gertatzen dena hain zuzen [121]. Honela, apurketa gehin bat C_α -C loturen artean gertatzen da. Ser eta Thr ditugu salbuespenak, non C_α -N lotura peptidikoaren apurketa ere atzeman den. Hortaz, lana bi zatitan banatua azaltzen da: lehen zatian H abstrakzioa aztertzeko da eta bigarrenean berriz gerta daitezken lotura peptidikoaren apurketa.

Lehen pausoko H abstrakzioak erradikal bitartekariaren eraketa dakar, eraso gertatzen den lekuaren arabera INT_{C_α} edo INT_{C_β} osatuz. Bigarren pausuan, INT_{C_β} bitartekariaren disoziazioa aztertzeko da, zeina aipaturiko bi lotura peptidikoetan gerta daiteken. Erreakzio hauen errepresentazio eskematikoa ikus daiteke Irudia 1.27.

C_α posizioan gertatzen diren lehen pausoko trantsizio puntuak aztertu dira, eta ikusi da energetikoki oso baxuak direla Kapitulu 10-eko Taula 10.5-ean aurkezten dira. Beraz, kontsideratuz barrera guztiak antzekoak eta baxuak direla, lan honetan termodinamikan zentratu gara. Bestalde, bi dielektrikoaren artean ezberdintasun gutxi nabaritu dugu, hori dela eta diskusio osoa uretako dielektrikoarekin egina dago.

Bitartekari guztientzat kalkulaturiko ΔH balioak -14/-39 kcal/mol tartean daude, beraz H abstrakzioa prozesu exotermikoa da. Oro har, INT_{C_α} bitartekariak egonkorragoak dira INT_{C_β} bitartekariak baino, Irudia 1.28. Lehenak -25/-34 kcal/mol tartean aurkitzen dira, eta ikusten da amino azido kargatuak direla bitartekari egonkorrenak ematen dituztenak, hots, Asp, Lys, Arg eta Glu. Bestalde, INT_{C_β} bitartekariak egonkortasun baxuagoa erakusten dute, hauen artean, amino azido aromatikokoak dira egonkorren, Trp, Tyr eta Phe.

Bestalde, konformazioei dagokienez, Taula A.1-ean ikus daiteke INT_{C_α} bitartekaria eratzeko nabarmen eragiten duela konformazioak eta β -xaffa konformazioan agertzen diren bitartekariak egonkorragoak direla. Taula A.2-n ordea INT_{C_β} bitartekariarentzako tartekak

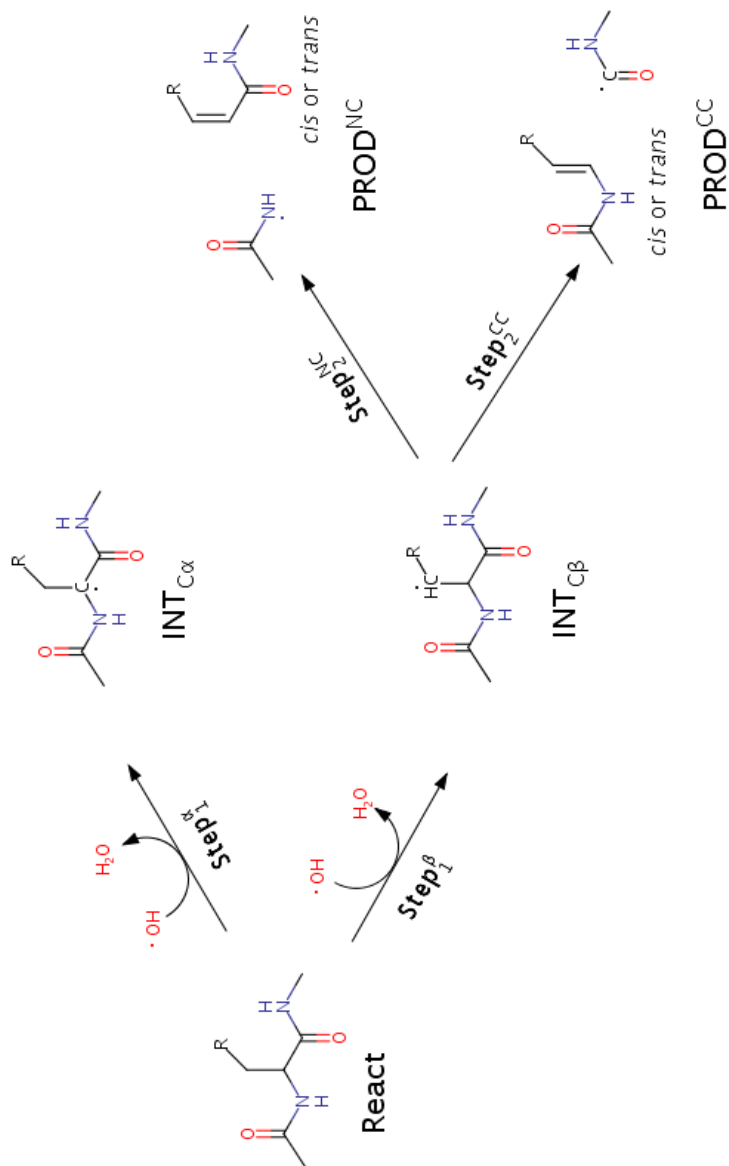


Figure 1.27: Azterturiko amino azidoen bizkarrezurreko erreakzioak: 1) ·OH-aren bitartez gertatzen den C_α edo C_β posizioetako H abstrakzioa INT^{C_α} edo INT^{C_β} erradikal bitartekaria eta ur molekula bat eratzeko, eta 2) bizkarrezurreko lotura peptidikoaren disoziazio homolitikoa (C-N edo C-C) PROD^{NC} edo PROD^{CC} eratzeko. Erreakzio bide hauek amino azido natural guzientzat aztertzen da, bi dielektriko (4 eta 78) eta konformazio (α-helize eta β-xafla) kontuan hartuta.

aztertzen dira eta ikus daiteke ez dagoela hain eragin handia. Are gehiago, Taula A.3-n ikus daitekeen bezala $INT_{C\alpha}$ bitartekarien ondorioz dago hobetsia β -xafla konformazioa.

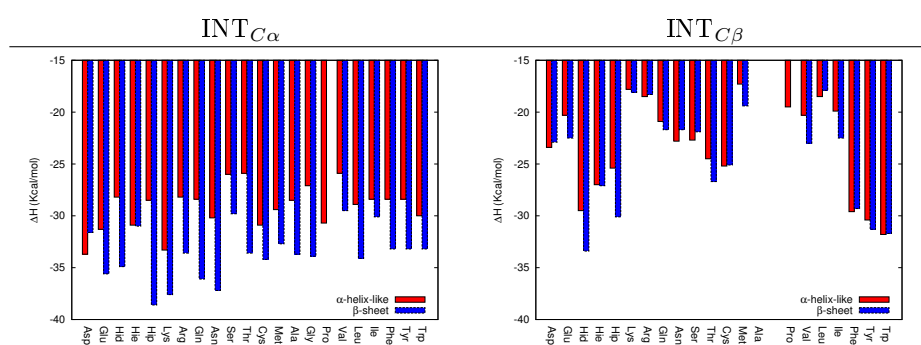


Figure 1.28: Bitartekariei dagokien entalpia balio erlatiboak, ezkerrean $INT_{C\alpha}$ eta eskubitan $INT_{C\beta}$ bitartekariei dagozkienak, ur dielektrikotan kalkulatuak. Bi konformazioak ageri dira α -helize (bloke gorriak) eta β -xafla (bloke urdinak).

Bi joera nagusi ikus ditzakegu beraz: i) $C\alpha$ posizioan gertatzen den $\cdot\text{OH}$ -aren erasoak bitartekari egonkorrenak eratzten ditu eta ii) β -xafla konformazioan gertatzen diren $C\alpha$ -ko erasoak egonkorragoak dira, $C\beta$ -ri dagokionez ordea ez da konformazioen artean ezberdintasunik igerri (Taulak A.1, A.2 eta A.3).

Arrazoi nagusia konformazio bakoitzak bitartekaria egonkortzeko duen posibilitatean dago. Hala, errektibo eta bitartekari ororentzat ψ eta φ dihedroak neurtu ditugu, Irudia 1.29. Hemen argi ikus daiteke, $INT_{C\beta}$ bitartekaria eratzean aldaketarik ez dela somatzen. Ez da ordea berdina gertatzen $INT_{C\alpha}$ bitartekariarentzat, kasu honetan, α -helize konformazioa ere planarra dela ikus daiteke. Planartasun honi esker, efektu kaptodatiboa maximizatzen da. Efektu hau, lehenago aipatu bezala, talde emale eta hartzaileak alboan izanda gertatzen da. Ondorioz, ez parekatuik dagoen elektroia delokalizatzen da eta bitartekaria egonkortu [112]. Hala, bitartekari molekula bakoitzaren spin dentsitatea kalkulatu dugu, erradikala delokalizatzeko duten joera kuantifikatzeko, Irudia 1.30. Argi ikusten da $INT_{C\alpha}$ bitartekariak $INT_{C\beta}$ baino spin dentsitate baxuagoak dituela, efektu kaptodatiboa dela eta. Efektu hau lehenengo bitartekarietan soilik gertatzen da, $INT_{C\beta}$ kasuan hurrunez bait daude talde emale eta hartzaileak. Dena den, azken bitartekari hauen kasuan, spin dentsitate baxua igertzen da amino azido aromatikoentzat, hemen, erradikala talde aromatikora delokalizatu bait daiteke.

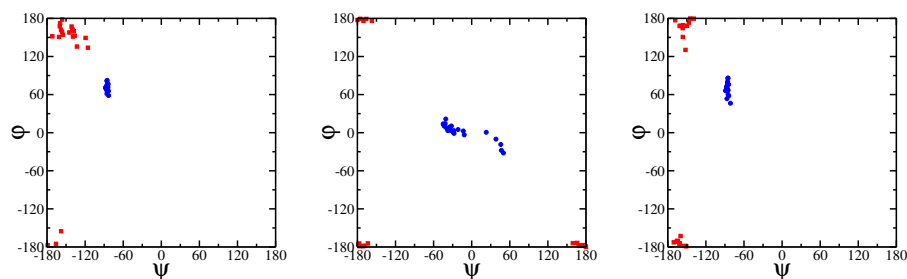


Figure 1.29: Ramachandran grafikoak errektibo (ezkerretan), $INT_{C\alpha}$ (erdian) eta $INT_{C\beta}$ (esku-bikoan) espezi-entzat, α -helize (urdinez) eta β -xafla (gorriz) konformazioentzat.

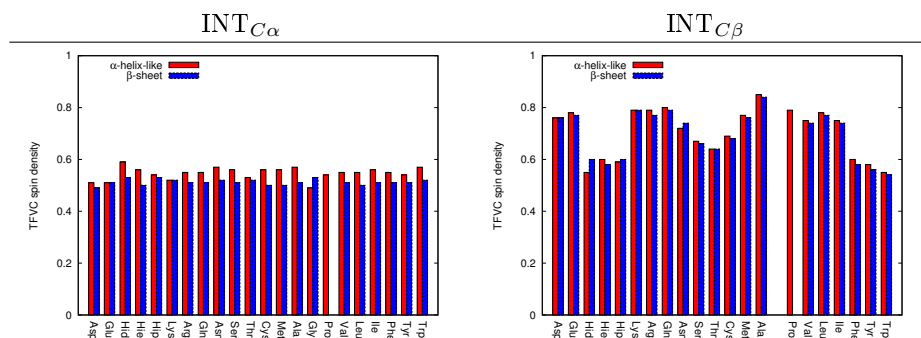


Figure 1.30: Topological Fuzzy Voronoi Cell spin densities computed at the $C\alpha$ and $C\beta$ atoms of $INT_{C\alpha}$ and $INT_{C\beta}$ species, respectively.

Hortaz, ondoriozta daiteke spin dentsitatea zenbat eta baxuagoa izan orduan eta bitartekari egonkorragoa dugula. Are gehiago, β -xafla konformazioan aurkitzen ditugun $INT_{C\alpha}$ bitartekariak apur bat egonkorragoak dira. Honen arrazoia, egituraren planartasunean dugu. β -xafla konformazioak erabat planarrak ditugu, ez ordea α -helize egiturako bitartekariak, zeinak ez diren erabat planoak eta beraz efektu kaptodotiboa ez dago maximizatua azken kasu honetan.

Azkenik, ikus dezakegu amino azidoen albo kateak ez duela gehiegi eragiten $INT_{C\alpha}$ -ren egonkortasunean, izan ere, balio guztiak dira antzekoak. Beraz, pentsa genezake efektu esterikoak direla erreakzioa gidatuko dutenak.

Behin $INT_{C\beta}$ bitartekaria eratuta, erreakzioak aurrera jarrai dezake, lotura peptidikoaren apurketa gertatuz (Irudia 1.27). Hala, bi aukera posible daude, N- $C\alpha$ edo C- $C\alpha$ loturak apurtu daitezke. $INT_{C\alpha}$ -ren kasuan halako hausturak ezin gerta daitezke, efektu kaptodotiboak lotura hauek sendotzen bait ditu (lotura orden sendoagoak ikus daitezke, Taula A.9). Hortaz, $INT_{C\beta}$ bitartekarian gerta daitezken bizkarrezur hausturei dagozkien ΔH_{aq} balioak azaltzen dira Irudia 1.31 eta Taula A.6-ean. Hemen ere bi konformazioak kontsideratu dira, nahiz eta ezberdintasunak esanguratsuak ez diren (Taula A.7). Gauzak laburtze aldera, β -xafla konformazioari dagozkien balioak diskutatuko dira. Bestalde, kontutan izan behar da ere produktuetan bi isomero direla posible: cis eta trans.

Emaitzek garbi erakusten dute, oro har, C-C_α loturaren hausturak ematen dituela produktu egonkorrenak. N-C_α loturaren apurketa endotermikoa da kasu gehienetan, 10-18 kcal/mol gorago aurkitzen dira azken honentzako balioak, salbuespena dira Ser eta Thr. C-C_α loturaren apurketa hobetsia dago batez ere amino azido aromatikoentzat, zeinentzat balio negatiboak aurkitu diren. Isomeroen artean, trans-ek ematen dute orokorki apur bat egonkorrago, 0-6 kcal/mol.

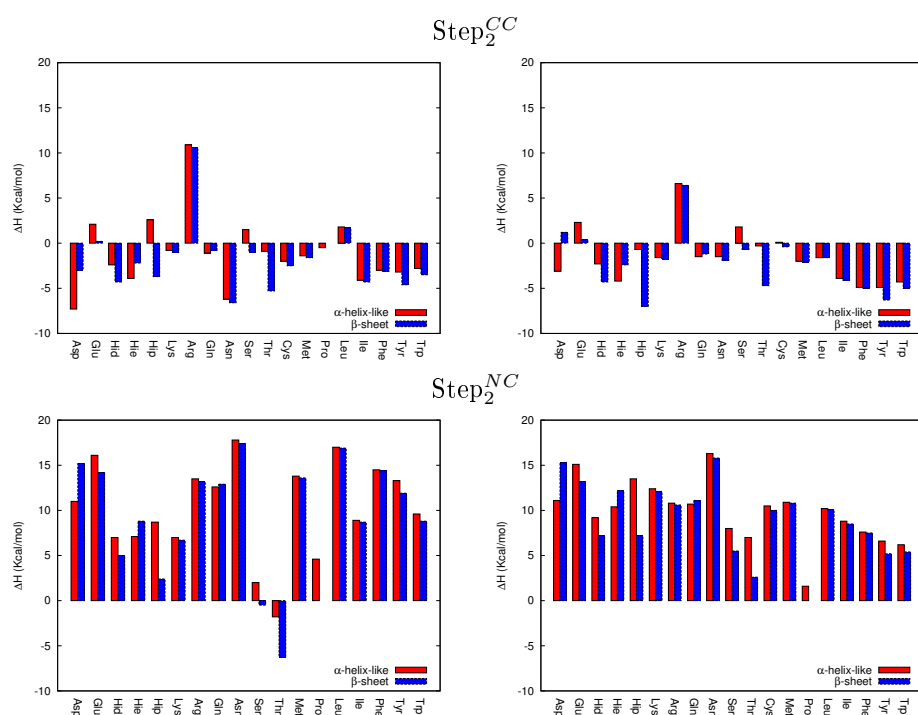


Figure 1.31: ΔH_{aq} balioak (kcal/mol) INT_β bitartekaritik abiatuta haustura homolitikoaren bidez lortutako produktuentzat (Step2, Irudia 1.27). Gohian dauden balioak C_α – C loturaren apurketari dagozkie; eta behekoak ordea, C_α – N loturaren apurketari. Produktu ez-erradikalaren bi isomeroak ageri dira: *cis* (ezkerretan) eta *trans* (eskubitan).

Aipatu bezala Ser eta Thr dira bi erreakzioak exotermikoak diren kasu bakarrak. Thr-n kalkulaturiko ΔH_{aq} balioak -5.3 eta -6.3 kcal/mol dira, C-C_α eta N-C_α loturen apurketentzat, hurrenez hurren. Ser-n kasuan ordea -1.0 eta -0.5 kcal/mol dira kalkulaturiko balioak. Beraz, nahiz eta C-C_α loturaren apurketa exotermikoa izan, bi kasu hauetan N-C_α loturen apurketa ere gerta litekela ikus daiteke, aurreko ikerketekin bat etorriaz [121]. Ikerketa honetan, Ser eta Thr-an N-C_α lotura ahulketa gertatzen dela adierazten dute, hidrogeno loturen ondorioz. Dena den, lan honetan kalkulaturiko lotura ordenek ez dute halakorik adierazten, Taula A.9.

Irudia 1.27-ean ikus daiteken bezala produktu ez erradikalarioak isomeroak dira C-C_α edo N-C_α lotura apurtu, eta beraz konparagarriak dira. Hortaz, amino azido bakoitzarentzat lau isomero konpara ditzakegu. Honela, Thr-aren lau produktu ez erradikalarioak daude jarrita

Irudia 1.32-n. Gauza bera egin da Ser-n kasuan. Hala, ikusten da hidrogeno loturak *cis* isomeroen kasuan bakarrik gerta daitezkeela. Bestalde, N-C $_{\alpha}$ loturaren apurketatik eratzen da produkturik egonkorrena, lotura honen apurketa azalduaz.

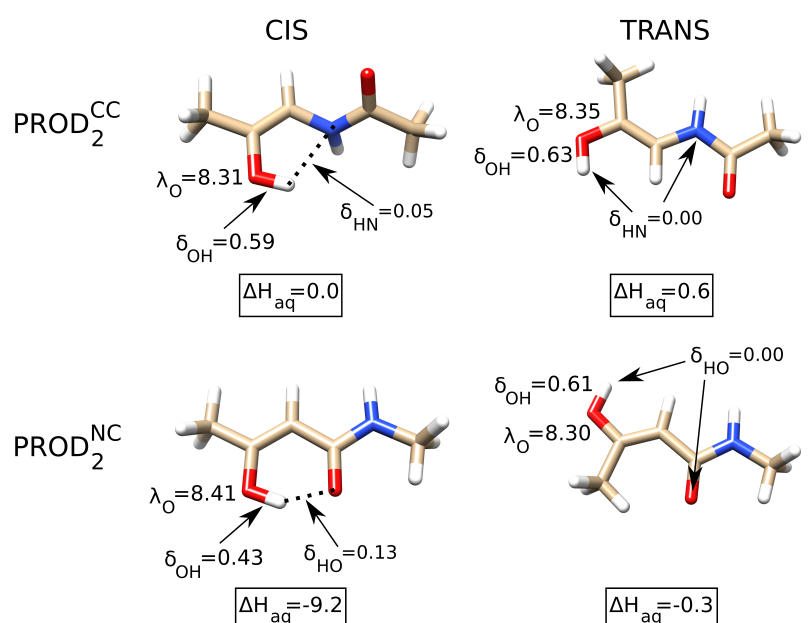


Figure 1.32: Produktu ez-erradikalen *cis* eta *trans* isomeroak, Step2 $_2^{CC}$ eta Step2 $_2^{NC}$ pausuentzako Thr amino azidoarentzat. Beren entalpia erlatiboak *cis* C $_{\alpha}$ - C produktu-arekiko daude (ΔH_{aq} , kcal/mol). Gainera, hiru parametro elektroniko ageri dira: i) elektroilokalizazio indizea alkoholeko oxigenoan (λ_O), ii) elektroidelokalizazio indizea O-H alkohol taldearen loturari dagokiona (δ_{OH}) eta iii) elektroidelokalizazio indizea, alkoholaren H eta aldameneko karboniloko O (δ_{HO}) edo aminaren N-ren artean (δ_{HN}).

Azken produktu honen egonkortasuna arrazionalizatzeko elektroilokalizazio (λ) eta elektroidelokalizazio (δ) indizeei begiratu diegu. Indize hauek elektroipareen lokalizazio eta elektroidelokalizazioa adierazten dute, Lewis egituren antzera. *cis*-PROD $_2^{NC}$ da alkohol eta bizkarrezurraren artean elektroidelokalizazioa baimentzen duen bakarra: $\delta_{HO} = 0.13$. Bestalde, *cis*-PROD $_2^{CC}$ produktuan gertatzen den hidrogeno lotura ez da hain sendoa $\delta_{HN} = 0.05$. *trans* isomeria duten produktuek ordea ez dute halako hidrogeno loturarik eta beraz azalpen bat dugu lorturiko balio energetikoentzat. Hidrogeno loturaren bidez osatzen den sei atomoko eraztunak egonkortasuna dakarkio produktu ez erradikalarioei.

Beraz, Ser eta Thr-n gerta daitekeen N-C $_{\alpha}$ loturaren apurketa produktu ez erradikalarioek daukaten egonkortasunagatik dela adierazten dute gure kalkuluek eta ez bitartekarien ondorioz, aurreko ikerketak adierazten zuen bezala.

1.8 Ondorioak

Tesi lan honek proteinen oxidazio mekanismoari buruzko alderdi berriak aztertzen ditu. Oxidazio prozesua ekidin ezin daiteken gertaera da, zeinak proteinen estruktura aldaketa bultzatzen duen. *Espezie errektiboak* dira oxidazio prozesua gertatzearen erantzule nagusiak. Lan honetan hiru erreazio mekanismo aztertu dira: i) H abstrakzioa, ii) elektro transferentzia eta iii) $\bullet\text{OH}$ -aren adizioa. Gauzak sinplifikatu aldera, oxidazio mekanismoa bi pausutan dago banatua, eta horietako bakoitzean $\bullet\text{OH}$ baten eraso aztertzen da. Oro har, aztertutako erreazio langak baxuak dira, eta hortaz termodinamika kontsideratu dugu erreazioa gidatzen duen faktore nagusia. Are gehiago, aztertutako erreazio langak ez dira oso ezberdinak beraien artean bai ordea bitartekarien energia erlatiboak. Beraz, diferentzia honek eragingo du gehien erreazioaren norabidean. Azkenik, bigarren $\bullet\text{OH}$ -aren eraso bi erradikalen arteko erreazioa da eta beraz langa gabeko prozesua dela kontsideratu dugu.

Inguru giroaren eragina kontutan hartu da konstante dielektrikoa aldatuaz. Hortaz, konstante dielektriko baxu eta urarena erabili dira proteina barneko eta gainazaleko inguruak simulatzeko. Oro har, ikusi diren ezberdintasunak txikiak dira eta esanenezake erreazioak ez direla inguruaren arabera aldatuko. Dena den, kontutan hartu behar dira hemen efektu esterikoak, honela, barneratuak dauden amino azidoak zailago izango dira oxidatzen. Bestalde, jakina da bizkarrezurra zati malgua dela eta konformazio ezberdinak sor daitezke bere angelu dihedroak aldatuaz. Lan honetan bi konformazio posible kontsideratu dira: α -helizea eta β -xaffa. Orokorki, konformazioen artean ez da lehentasunik igerri, salbuespena dugu C_α posizioiko H abstrakzioaren bitartez eratzen den bitartekaria, zeinak β -xaffa konformazioan dauden erradikalak egonkorragoak diren.

Oro har, H abstrakzioaren ostean eratzen den bitartekaririk egonkorrena C_α posizioan eratzen denari dagokio. Amino azido aromatikoaren alboko taldeetatik gertatzen den H abstrakzioak ere bitartekari egonkorak eman ohi ditu. Are gehiago, bitartekariak sortzeko energia erlatiboa eta azken hauen spin dentsitatearen arteko korrelazioa antzeman da, Irudia 1.33. Beraz, spin dentsitatea zenbat eta delokalizatuago egon orduan eta entalpia balio erlatibo baxuagoa ikusi da.

Triptofanoaren eratzun aromatikoko N atomotik gertatzen den H abstrakzioak bitartekari egonkorra eratzen du, eta spin dentsitatea baxua da. Era beran, tirosinaren alboko O atomotik gertatzen den H abstrakzioa. Arrazoia, eratu ditzaketen egitura erresonanteetan dago, zeinak eratu ezin ditzaketen bitartekariak baina gehiago egonkortzen dituzten, spin dentsitatea jaitsiaz. Era berean, H abstrakzioa gertatzen den posizioa zenbat eta ordezkatuago egon orduan eta egonkorragoa izango da bitartekaria. Salbuespena, zisteinako S atomotik gertatzen den H abstrakzioa da, zeina egonkortua dagoen SH lotura ahula dela eta. Aipaturiko hiru kasu hauek markaturik ageri dira Irudia 1.33-n.

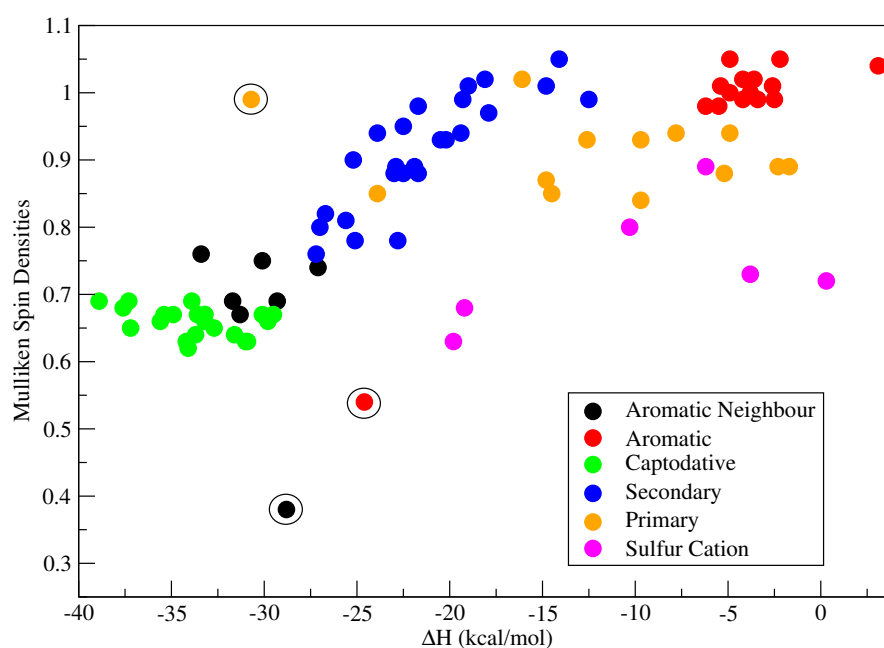


Figure 1.33: Mullikenen spin dentsitateak, entalpia erlatiboarekiko (kcal/mol), aztertuturiko H abstrakzio bitartekari ororentzat, β -xafla konformazioan eta uraren dielektrikoan.

Erastun aromatikoean gertatzen den \bullet OH-aren adizioak bitartekari egonkorak eratzen ditu, nahiz eta aromatizitateari eragin. Arrazoi honen ondorioz, adiziotik sorturiko bitartekariak, H abstrakziotik sorturiko bitartekari egonkorrenak baino ezegonkorragoak direla ikusi da. Dena den, salbuespena ere aurkitu dugu kasu honetan, triptofanoan gerta daiteken C8 posizioako adizioa, zeinak aromatizitatea galtzen duen, baina egonkortua dagoen egitura erresonanteen bidez. Azkenik, zistinan gerta daiteken \bullet OH-aren adizioak, S-S lotura ahultzen duela ikusi dugu, hortaz, oxidazioaren bidez lotura honen apurketa gerta daiteke.

Elektroi transferentzia mekanismoa, zisteina eta metionina amino azidoetako S atomotik elektroi bat ateratzean kontsideratu dugu. Prozesu honek inguru giroarekiko dependentzia erakusten du. Honela, terminalak diren amino azidoek bitartekari egonkorrenak ematen dituzte, karboxilatoaren bidez egonkortuz sorturiko S erradikal katioia. Metioninak ematen du bi amino azidoen artean bitartekari egonkorrena, bitartekariak eratu ditzaken erastun luzeagoen ondorioz. Hala ere, azpimarratu beharra dago zisteinan eta metioninan gerta daitezkeen H abstrakzioak hobetsiak daudela, bitartekari egonkorragoak eratzen bait dituzte.

Albo katearen oxidazio produktuei dagokienez, alkoholen eraketa hobetsia dagoela ikusi dugu. Oro har, buruturiko lan osoan ikusi den produkturik egonkorrena zistina da. Zentzuzko emaitza da, produktu hau erabiltzen baitu naturak egitura egonkortasuna emateko proteinei. Bestalde, arginina eta lisinaren kasuan albo katearen hausturaren ostean eraturiko produktuak egonkorak direla ikusi da. Halako apurketa ere aspartatoan eta glutamatoan gerta daitezke, baina ez dira hain egonkorak.

Azkenik, bizkarrezurreko aldaketei dagokienez, C_{α} erradikal bitartekariak C_{α} -C eta C_{α} -N loturen sendotzea erakusten dute, beraien haustura ekidinez. Bestalde, C_{β} erradikal

bitartekariak aipaturiko loturen apurketa ekar dezakete, nagusiki C_{α} -C loturarena. C_{α} -N loturaren haustura serina eta treonina amino azidoentzat gerta daitekela ikusi da, hausturatik eratzen diren produktuak hidrogeno loturen bidez egonkortuak bait daude.

Chapter 2

Introduction

2.1 Cellular respiration and Reactive species

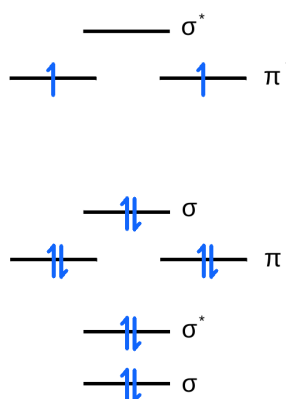
The composition of the atmosphere has not maintained constant, it has changed throughout the centuries. At the beginning of life in Earth, it was mainly formed by N_2 and CO_2 and the first organisms in the Earth were barely exposed to O_2 . They were anaerobe organisms that did not use O_2 to survive. Moreover, these organisms were very susceptible to oxygen exposure as they lack a defense system to this chemical.

However, there was a sudden change in the composition of the atmosphere as most of the CO_2 was converted to O_2 in the so called Great Oxidation Event [1, 2]. The organisms evolved in order to be able to survive in an environment with high O_2 levels. Furthermore, the evolution made these organisms to use O_2 as a source to obtain energy in a more efficient way. O_2 is an oxidant species which accepts electrons reducing itself and oxidizing other molecules. The chemical interpretation for the ability of O_2 to accept electrons demonstrated by the Molecular Orbital diagram shown in Figure 2.1. The last two singly occupied orbitals are degenerate, as a consequence O_2 can accept electrons.

Organisms have evolved in such a way that O_2 is now vital for aerobes as it plays an essential role in the so called electron transport chain. The main goal of this process is the formation of adenosine triphosphate (ATP) [4]. Mitochondria is the major responsible for the production of ATP, indeed, it has been estimated that around 80% of ATP is produced in this organelle [3]. However, from time to time alternative products, these are *reactive species*, are created due to the electron leak [4, 5]. This is a possible formation mechanism for such species but not the unique one, in the following sections the production of these chemicals is explained in more detail.

2.1.1 Classification of reactive species

The terminology involving *reactive species* is very extense and can sometimes be ambiguous. As their name indicates, *reactive species* are unstable chemicals that can easily react with other chemical entities [6]. The term groups a wide variety of molecules with variant reactivity. They can be classified by their chemical nature, this is, radical or non-radical [1]. The word “free radical” involves the species with a radical character, where radical refers to

Figure 2.1: Molecular orbital diagram of O_2 .

species containing at least an unpaired electron, whereas “free” refers to the capability of independent existence [1, 3]. *Reactive species* can also be described by the central atom that forms them. Therefore, we can identify Reactive Oxygen Species (ROS), Reactive Nitrogen Species (RNS), Reactive Sulphur Species (RSS) and so on [3, 7].

- ROS: H_2O_2 , $\bullet O_2^-$, $\bullet OH$, $\bullet OOH$
- RNS: $ONOO^-$, $\bullet NO$
- RSS: $RSSR^{\bullet-}$, $RSOH$, RS^{\bullet}

2.1.2 Production of reactive species

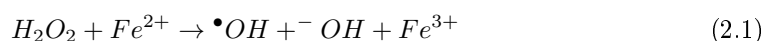
The production of *reactive species* can be endogenous or exogenous. Endogenous production occurs due to a necessity or failure in the organism [3]. There are a wide variety of processes that produce *reactive species*: NADPH oxidase enzymes (NOX), which are present in neutrophils in order to fight against external pathogens [4, 5, 8], transition metals that have escaped from their common binding sites, mitochondrial respiratory process (as examples of endogenous production) or radiation (exogenous production).

The electron transport chain, as introduced, is the process by which mitochondria produces ATP. Electrons are driven through complexes (named from I to IV) of different reduction potentials in order to generate a H^+ gradient while O_2 is converted into H_2O . For instance, ROS can be produced when an electron acceptor, like O_2 , is reduced by molecules like NADH or FADH [4]. Indeed, mitochondria produces 90% of ROS in eukaryotic cells [9], where, 1-4% of O_2 participating in the electron transport chain is converted into ROS [8, 10–14]. Complex I and III are known to be a source for the production of ROS due to the fact that large potential energy change occurs relative to the reduction of O_2 [11, 15–18]. The main cause for the production of such species is the electron leak which reacts with O_2 to form $O_2^{\bullet-}$ [15, 19].



Figure 2.2: The formation of rust is a well known redox process.

Radiation is another source for the production of *reactive species*. UV radiation can produce H_2O_2 in the presence of Trp and O_2 , via charge transfer [5]. In the same way, hydroxyl radical ($\bullet\text{OH}$) can be produced by radiolysis, ionizing the water molecule or through an excited water molecule which is able to dissociate [20]. UV can also lead to homolytic dissociation of H_2O_2 producing $\bullet\text{OH}$ [1]. Another source for the production of $\bullet\text{OH}$ is the Fenton reaction [1, 21–25], reaction (1.1), which requires a reduced transition metal, usually Cu^+ or Fe^{2+} .



2.1.3 Reactive species and oxidative stress

Redox type reactions are utterly important in biology. Redox reaction is the process where a species gets oxidized and the other one is reduced. The oxidation process is known as the loss of electron, while the reduction process is just the opposite. The species which gets oxidized is known as reductant whereas the species that gets reduced is recognized as oxidant. These events do not never take place independently but together. Therefore, one could imagine the reason of the naming: Red(uction) Ox(idation). In case where the redox reaction takes place by two of the same molecules, where one gets reduced and the other one is oxidized, the reaction is known as disproportion or dismutation. The formation of rust is a good example of the redox reaction Figure 2.2. Redox reactions are essential in biochemistry and of course for life, but as we will discuss later, they may be the cause of a number of diseases.

In this manner, the damage caused by *reactive species* is usually associated with oxidation. However, they can reduce another chemical by donating electron(s). The superoxide anion ($\text{O}_2^{\bullet-}$) is an example of this case, whose electron can be donated reducing a molecule and forming molecular oxygen, which is the first step in the Haber-Weiss reaction [26]. Therefore, it is obvious that calling them *oxidants* is not a very suitable name. It has to be remarked that the presence of these chemicals is essential for the adequate function of the organism.

Indeed, ROS are involved in essential tasks inside an organism such as redox regulation of protein phosphorylation, ion channels, and transcription factors. They are also required in thyroid hormone production, crosslinking of extracellular matrix, apoptosis, growth, defence and other signalling [4, 12, 27–29].

Nevertheless, a careful balance is utterly important in the concentration of these species. The disruption of this balance in the concentration of *reactive species* is known as oxidative stress or redox imbalance [1]. In this sense, a surplus of *reactive species* causes damage as it is the case for an excessively low concentration of them [4]. Low concentration of ROS is related to immunodeficiency as they are essential for macrophages and neutrophils in order to perform phagocytosis [4].

Due to the observed correlation between age and ROS generation, Harman hypothesized that the aging might be associated to the *free radicals*. The investigation showed that some antioxidants may help increasing the life span [30–32]. Indeed, mitochondrial function is lost during aging and it is known that the mitochondrion produces more ROS when inhibited. Paradoxically, in some cases mutants with high level of oxidative stress have shown a prolonged lifespan. Therefore, the high production of ROS has been speculated to be an epiphenomena of the aging [33].

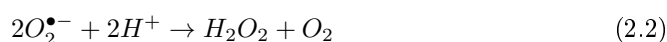
Interestingly, *reactive species* have been linked to a wide variety of neurodegenerative diseases such as Alzheimer [34], characterized by an increase in *oxidative stress* [35–39]. However, it is not clear whether reactive species are the cause or the consequence of these diseases.

The specificity of the reaction between *free radicals* and other entities depends on their reactivity. The most reactive the chemical is, the less specific the attack will be. Among the most reactive species we can find peroxyxynitrite, singlet oxygen [4] and $\bullet\text{OH}$ [18, 40, 41]. $\bullet\text{OH}$ is one of the most reactive free radicals, the observed rate constants for different targets vary in a relatively small amount and therefore the concentration of the target molecule is crucial for the overall reaction rate constant [40].

2.2 Antioxidants

Antioxidants are species that quench *reactive species*, prevent their formation or repair damaged structures even at low concentration [1, 42]. It is rather simplistic to state that antioxidants are good and that *reactive species* play a harmful role. It has previously been remarked that *reactive species* fulfill a wide range of tasks and that the damage occurs when an imbalance of these species happen. Indeed, it has been observed that oxidative stress limits the metastasis of melanoma, whereas antioxidants promote them [43]. There are lots of enzymes in organisms whose task is to remove these *reactive species*. They are classified in three different groups:

1. **Antioxidant enzymes:** There are several enzymes with an antioxidant activity. For instance, superoxide dismutase (SOD) catalytically removes superoxide ($\bullet\text{O}_2^-$) species [1]. The overall reaction is as follows:



On the other hand, catalases, peroxidases and glutathione are enzymes that remove H_2O_2 .

2. **Metal-ion sequestration:** This strategy consists in capturing free metal ions as Cu^{2+} or Fe^{3+} , which have a pro-oxidant activity.
3. **Low-molecular-mass antioxidants:** They can be endogenous or exogenous. In the first case we can find bilirubin or coenzyme Q and are produced by the organism. While in the second type we find vitamin C or E and are introduced in the diet [1, 18, 44–46].

However, it has to be taken into account that antioxidants cannot scavenge every single *reactive species* and therefore the organisms have also developed some recovery strategies in order to restore some of the created damages. Methionine sulfoxide reductases are a good example, these enzymes reduce methionine sulfoxide rendering back the Met residue [3, 34, 47–50].

2.3 Oxidation of cell constituents

Under oxidative stress conditions *reactive species* damage cell constituents such as DNA, lipids and proteins [3, 9, 40]. The accumulation of oxidized species may happen due to different reasons such as increase of *reactive species*, low concentration of antioxidants or loss of efficiency of the reparation mechanisms [51]. The accumulation of oxidized cell constituents may boost the generation of *reactive species*, entering a vicious cycle [34].

DNA. Mitochondrial DNA is the most vulnerable to the attack of those species [4, 11]. Interestingly, the attack towards mitochondrial DNA could induce coding of polypeptides which would affect to the four complexes of mitochondria responsible for the electron transport chain and therefore promote ROS production [10].

Lipids. In foods, the lipid oxidation process is associated with rancidity. The most common products of this process are malondialdehyde (MDA) and 4-hydroxy-2-nonenal (HNE). These examples of lipid oxidation products are known to react with protein amino groups forming Schiff bases [9]. However, they are not the unique oxidation products, peroxy and alkoxy radicals, H_2O_2 and epoxides are also generated. Overall, lipid oxidation promotes the oxidation of other cell constituents [52, 53].

2.3.1 Proteins

Amino acids (Figure 2.3) are the molecules that compose proteins. They have a central carbon (C_α) atom, which is a stereocenter. Bound to this atom, we find the following: an H atom, a carboxylic acid group (COOH) (known as the C terminal), an amino group (NH_2) (known as the N terminal) and a variable group which defines each amino acid. This last variable group is called the side chain and all the rest form the backbone. Amino acids are usually classified by the polarity of the group present at the side chain.

Amino acids bind one to another by an amide bond, formed by the reaction between the carboxylic acid and the amine group. This amide bond is known as the peptidic bond

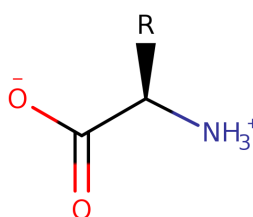


Figure 2.3: Zwitterionic form of a L-amino acid. R represents the side chain group.

in peptides and proteins. The molecules formed by less than 30 amino acids are considered peptides, while those with a higher number of amino acids are known as proteins. Proteins are therefore large biomolecules that perform a wide variety of functions inside an organism, catalysis of metabolic reactions, DNA replication, molecule transporting and so on. The structure that the protein adopts is crucial for the specific task they fulfill. The protein structure is divided into four groups [54]:

- **Primary structure:** the amino acid sequence.
- **Secondary structure:** local structures stabilized by hydrogen bonds i.e. alpha-helix, beta-sheet.
- **Tertiary structure:** the final three dimensional shape of a protein obtained by non-covalent interactions.
- **Quaternary structure:** a protein yield by non-covalent interaction between other polypeptides. Human hemoglobin is an example of quaternary structure, a protein formed by four subunits bound to each other by non-covalent interactions.

The application of external stress such as high temperature, radiation, acidic or basic pH, may induce the so called desnaturalization of a protein which makes the protein lose its secondary, tertiary and quaternary structure and could lead to its disfunction. This thesis is devoted to the oxidation that proteins suffer and is introduced below.

Protein oxidation. Proteins are one of the main target of *reactive species* due to their high concentration in organisms [40, 53]. The protein oxidation can render its inactivation and therefore it is an interesting topic to study. Moreover, such process leads to stable products which are employed as markers to measure the intensity of the *oxidative stress* [55]. Typically, the oxidation of certain amino acids (Lys, Arg, His, Pro, Thr, Glu and Asp) leads to cabonyl derivatives [9] which are the ones usually measured [1, 56–58]. However, it is known that oxidation mechanisms are complex and can lead to several other products [56]. The unique measurement of carbonyls is just a fraction of the oxidized chemicals [58]. These carbonyl groups cannot be reduced back to its initial form and therefore, they could be used as markers for the oxidation degree that has been caused [47, 56, 84].

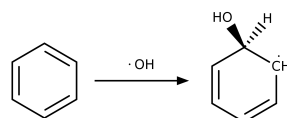
Nevertheless, such a task is not as simple as it might look at first glance. The accumulation of oxidized proteins can also be associated with a lowering activity of proteases

whose aim is to degrade those damaged structures. The activity of these proteases may be limited or inhibited, in the same way, due to the oxidation [9, 19, 59]. Therefore, the loss of efficacy of the proteins is something measurable that could provide valuable clues to the protein oxidation. Both aging and neurodegenerative diseases show to be linked to protein oxidation [60–62].

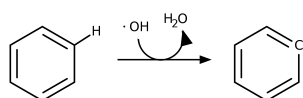
Only few recovery mechanisms are available for proteins and the majority of the damaged macromolecules get degraded. Some examples of the recovery mechanisms are methionine reductases, conversion of isoaspartyl and phosphorylation of protein-bound fructosamine [47]. In the case where the oxidized entities are not repaired or eliminated, protein oxidation may lead to protein aggregates [4, 47]. Cross linking and missfolding are phenomena observed in the protein oxidation which at the end of the day render protein aggregates [47]. It has to be noted that heavily oxidized proteins escape from the proteasomes [47]. Below, several important features of the protein oxidation reactions are given.

Reaction types. The oxidation mechanisms can be one-electron or two-electron. $\bullet\text{OH}$ is a reactive species that acts as a one-electron oxidant, the possible reaction mechanisms considered in this thesis are shown below

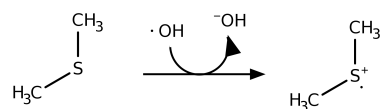
1. Radical addition



2. H abstraction



3. Electron abstraction



In all three mechanisms a radical is formed and a single electron is the responsible for the oxidation process. On the other hand, as an example of two-electron oxidants we find H_2O_2 , where two electrons take part in the mechanism [64].

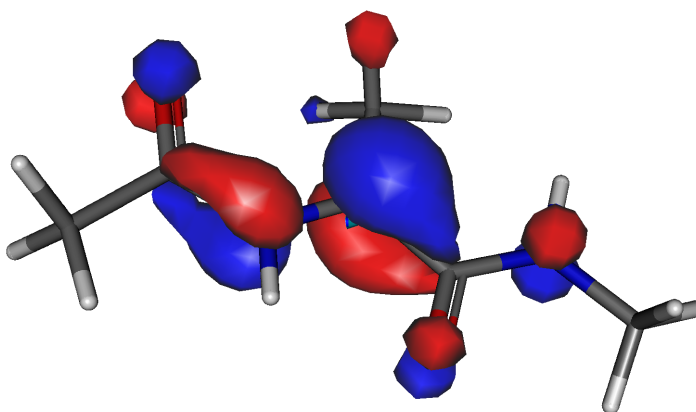


Figure 2.4: Alanine C_α radical's SOMO orbital.

Reactivity of radicals. Not all the radicals display the same relative stability. Briefly, the radicals are stabilised by the interaction between the orbital containing the unpaired electron and energetically and spatially adjacent orbital. The hyperconjugation effect is the interaction of the unpaired electron with σ and σ^* , in a saturated system, or π and π^* , in an unsaturated system. They are three center three electron interactions. In case that the unpaired electron interacts with the lone pair present at the non-bonding orbitals, the stabilisation effect is known as two-center three-electron bond. The particular case where the radical is flanked by both an unsaturated substituent and a lone pair containing group is said to be stabilised by the captodative effect [65]. In this case both effects participate in the stabilisation of the radical. This is typical for C_α centered radicals in amino acids and proteins that are flanked by a carbonyl and an amino group (Figure 2.4), showing higher stabilities.

Reaction location. The attack can occur at the protein or at a cofactor (a non-proteinic site). In this sense, hemoglobin, a vital protein to human beings, is formed by a heme cofactor, where an iron atom is present. This metal is easy to reduce and oxidize and it is known to promote the production of *reactive species*. Therefore, it is logical for it not to be freely moving in an organism. Indeed, most of the iron ions are captured by special systems of the cell. Under pathological conditions iron can be released [9, 85] and this can have catastrophic consequences to the cell as they could enhance the production of *reactive species* [3, 9]. In this sense, Pro, His, Arg, Lys are usual targets for oxidation as they bind to the metal [5, 9, 66, 67]. Such attacks occur in a specific way and little fragmentation has been observed in such cases [57, 68] they are known as *Metal ion-catalyzed oxidation*.

In Glutamine synthase (GS) from *escherichia coli* the enzyme inactivation occurs due to the conversion of His269 to Asn and Arg344 to glutamic semialdehyde, which resembles the specificity of the process [68]. This oxidized form is a hydrophylic enzyme which is inactive but not degradable by proteases. Further oxidation (at position His209 or His210) renders a hydrophobic enzyme that can be degraded [9, 68 70].

Cys	Cystine, thiol radicals[9, 41]
Met	Sulfoxide, Sulfone [9, 41]
Phe	Hydroxyphenylalanine[41, 80]
Tyr	Tyr cross-link[5, 9, 41, 47, 71, 81, 82], DOPA[1, 41, 47, 66, 71, 80, 81], Ortho-Tyr[1]
Trp	Formyl-kynureine[5, 9, 66], Kynurenines[1, 47, 83], 3-hydroxy-kynurenine[5, 9, 41, 47, 83]
Asp	Pyruvic acid [9, 41]
Glu	Pyruvic acid [9, 41]
Arg	Glutamate semialdehyde[1, 9, 41, 47, 67, 84]
Lys	Adipic semialdehyde[1, 9, 41, 47, 67, 84]
His	2-oxohistidine[1, 9, 41, 47]
Pro	Glutamate semialdehyde[1, 9, 41, 47, 67, 84]
Val	Hydroxides[1, 47]
Leu	Hydroxides[1, 47]
Thr	2-amino-3-ketobutyric acid [9, 41, 47]

Table 2.1: Most common oxidation products for different amino acids.

Overall, the location of each amino acid is a factor to be taken into account for the oxidation process. In case an amino acid is found far away from oxidants it will not get oxidized, no matter its propensity [71]. Increasing the solvent accessibility of a protein has been observed to also increase the antioxidant ability [71].

Amino acid propensity to oxidation. Not all amino acids display the same propensity to react with oxidants. The nature of the reaction usually depends on the side chain which tends to be the main site of the reaction, as it usually is the most exposed part. In Table 2.1 the most common measured experimental oxidation products are shown, and some of them are shown in Figure 2.5.

In the following paragraphs different oxidation events are examined for amino acids which are grouped depending on the nature of their side chains.

Sulphur containing amino acid oxidation. Cys and Met are the main oxidation targets [56, 85–88], due to the fact that their oxidation is reversible. The oxidation of these residues may be part of a biological control mechanism [85]. However, this is not always the case and Met oxidation has been observed to be associated with Alzheimer’s diseases [36]. The possible oxidation reactions for these amino acids are H atom or electron abstraction.

The oxidation products of Cys are sulfenic, sulfinic and sulfonic acid derivatives and cystine. The attack of the $\bullet\text{OH}$ towards Cys H atom bound to S is observed to be an important mechanism in the oxidation of this amino acid, leading to a sulphur radical [89]. In case that two of these radicals find each other, a bond between both atoms can be formed rendering cystine. Such interaction provides structural stability to the protein that is lost

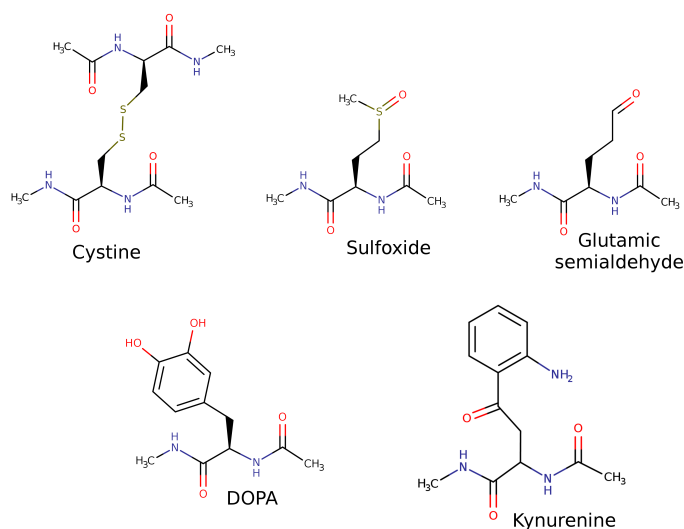


Figure 2.5: Some of the most popular oxidized products.

upon scission. Notice that the loss of structural stability can lead to loss of enzymatic activity [90].

Met can get oxidized leading to Met sulfoxide or sulfone, the former oxidized form can be reduced back to Met [9, 85, 91, 92]. Met does not have a specific function and is commonly located outside the active site [9]. Therefore, it has been hypothesized that it can act as a *reactive species* scavenger [66, 92]. Moreover, depending on the position of Met residues one can make the distinction between the ones located at the surface, that may have a protective role against environmental oxidants, and Met residues close to the active site, which may avoid autoxidation [92]. Interestingly, the case study of GS from *escherichia coli* did not show increase in hydrophobicity or protease susceptibility until six Met residues were oxidized. These results would point out the antioxidant character of Met in the protein.

In all this kind of reactions, the relative stability of the formed oxidized amino acid is crucial. In case where an unstable molecule is obtained the reaction may follow and modify the neighbouring side chains [71]. Met can lead to one-electron or two-electron oxidation. The former leads to sulphur radical cation while the latter renders sulfoxide [91]. The formation of these sulphur radical cations by the attack of a $\bullet\text{OH}$ toward the S atom is driven by the formation of an unstable adduct (hydroxysulfuranyl) [91, 93, 94]. This intermediate is dissociated by a proton, forming the sulphur radical cation and a water molecule, Figure 2.6. This sulphur radical cation has been speculated to disproportionate rendering a methionine and a sulfoxide [95].

The sulphur radical cation is a short living species, only few microseconds [96]. It has to be taken into account that the neighbouring side chains or the backbone may also stabilise the formed radical [96–99]. An amine from a N terminal or a Lys residue could stabilise the sulphur radical cation and decrease the reduction potential of the radical cation [100]. The results also indicate that the sulphur radical cation tends to dissociate in water solution from

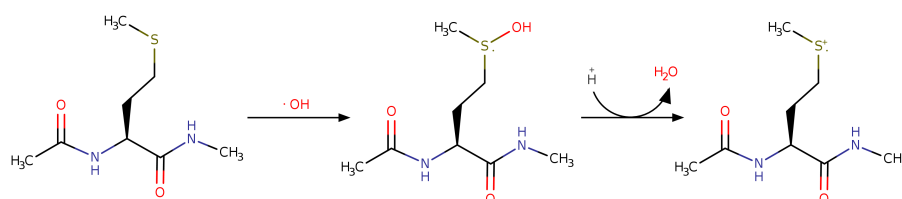


Figure 2.6: One electron oxidation of Met, rendering sulphur radical cation through hydroxysulfuranyl intermediate.

the formed complexes with the exception of amine containing complex. The bond formed between sulphur and nitrogen atoms is pH dependent and even though it is a favorable bond it is not the unique possibility. Indeed, sulphur oxygen bond has been observed when the radical cation is formed [91]. Overall, the sulphur radical cation is an unstable chemical and may abstract an electron from another molecule as Tyr [94] or produce a decarboxylation in the C terminal [101–103].

However, the sulphur atom is not the unique place at which the attack can occur. The Met H abstraction reactions have been investigated and observed that all three reactions compete [104].

Aromatic amino acids. The aromatic amino acids offer a radical scavenging activity. The very interest for the oxidation of these amino acids remain in the aromaticity of the side chains. The formed radicals at the rings or in the neighbouring atoms of the ring are stabilised by the delocalisation effects. In this case the H abstraction and addition mechanisms are typical, the latter reactions have lower barriers and are in consequence faster than the H abstraction reactions [105]. The overall oxidation of these amino acids usually leads to hydroxylated [1, 41, 66, 71, 80, 81] forms and in the case of Trp the process may split the indole, forming a kynureine [5, 9, 41, 47, 83]. Tyr can also lead to cross linked products that are formed in the case that two Tyr side chain radicals find each other [82, 106]. Tyr radicals can be found in reactions that are catalysed by enzymes as intermediates [107].

Acid and base amino acids. The possible oxidation mechanism in this case is the H or electron abstraction. The former mechanism has been studied for the formic acid [108] which remarks that the dominant H abstraction is that from the O atom of the carboxylic group.

Arg, Lys and His are majorly oxidized when bound to metal. The reason is that these metals could act as *reactive species* producers, as explained ahead. The H abstraction reaction is plausible for any of these amino acids. However, the aromatic moiety of His is adequate for the radical addition process to take place.

Other amino acids. We are left with the least reactive amino acids. This category groups aliphatic, alcohol and amide side chain containing amino acids. The oxidation mechanism involves the H abstraction, which showed to be most favored to occur at C $_{\alpha}$ position [20, 66, 109–111]. The reason for such selectivity lies on the further stabilisation that the radical

achieves at this position due to the mentioned captodative effect [112–114]. However, the H abstraction from C_α majorly takes place in Gly and Ala where there is no side chain or it only consists of a methyl group [20]. Consequently, one can say that the steric effects are a key factor in such reactions.

On the other hand, it is known that these radicals formed at C_α can promote cross-linking [9] or react with molecular oxygen and leading to several modifications of the protein that could end in the backbone cleavage [9, 66]. Cross-linked proteins are known not to be degradable by proteases and/or proteasomes [9] and it is common in aliphatic amino acids [20, 66].

Backbone. Through the introduction the attack at the side chain has been explained but little is said about the backbone. The backbone is an important site at any amino acid, peptide or protein whose orientation conditions the structure. As pointed out before, C_α atoms are a clear target due to the high stabilization of the oxidized intermediate owing to the captodative effect. However, there are other sites that may experience the attack, as the N atom. The H abstraction from the N atom of the backbone leads to less stable radicals and proceeds from a higher transition state barrier [115, 116] compared to the attack occurring at C_α , hence one could expect that such process will not have as much chances to take place.

There are experimental techniques such as Electron Transfer Dissociation (ETD) [117], Electron Capture Dissociation (ECD) [118] and Free Radical Initiated Peptide Sequencing (FRIPS) which employ radicals in order to sequence peptides and proteins [119–121]. The main goal of such methods is to provoke the backbone fragmentation and later identify the pieces for the final sequencing of the polypeptide.

Finally, the formation of radicals at the backbone has been observed to cause structural alterations in peptides and proteins. Once the species are created the changes in the bond distances and dihedrals occur, so that the radical species is as stable as possible. Therefore, it is logical that the secondary structure of the protein or peptide will be affected [122, 123]. Moreover, such species are involved in the unfolding of the helical structures [116]. The radical initiated protein unfolding is an extremely important event as it has been hypothesized as the first step towards the amyloid plaque formation.

2.4 Scope of the work

During the last decades, protein oxidation has experienced incremental progress triggered by its consequences and possible applications. In this sense, the identification of the protein oxidation products would help developing the scenario for their quantification. At present, carbonyls are the main measured oxidized products, even though it is known that other alternatives exist. Therefore, the analysis of the relative thermodynamic stability as well as the characterization of the electronic state of the intermediates would shed light into the protein oxidation process.

This thesis work is devoted to the characterization of the established and novel oxidation routes, in order to rationalise the experimentally observed oxidized products. Bearing this in mind, we have considered broad range of possible oxidation mechanisms and focus on their relative stability, for both the intermediates and products. In this way, we have pro-

vided with alternative oxidized products, inspired in the mechanisms of the experimentally observed ones. Therefore, this work presents possible oxidation mechanisms and products and pinpoints alternative stable ones which could be handy to consider in the future, as a prevailing mechanism.

The work has been organized as follows: in Chapter 3, the theoretical background is described. Then, from Chapters 4 to 7 the results are given and discussed. Concretly, Chapter 4 is meant to address the protein backbone oxidation mechanism. All natural amino acids are systematically studied for the H abstraction mechanism from C_α and C_β sites. The latter is then considered for a homolytic backbone dissociation.

Chapters 5, 6 and 7 are dedicated to the side chain oxidation mechanisms. Possible side chain oxidation mechanisms of different amino acids are considered. Interestingly, depending on the chemistry of these side chains different reactions are depicted.

Finally, conclusions are detailed in Chapter 8.

Chapter 3

Methods

Chemistry is the science that studies the structures, properties and reactivity of substances. Historically, it has been an experimental science, but due to the development of robust physical theories and computers, a new branch of chemistry is in development since the 1960s, computational chemistry. It is a very useful tool in order to explain experimental data, but also to predict the possible synthesis of new compounds with interesting properties. In this way, it can anticipate molecules with promising properties or can be looked as an utterly handy and robust tool in order to study mechanisms or molecules that are risky to manipulate or expensive to carry on in a lab. In this field molecules are designed and simulated employing computer facilities and previously codified theories.

This chapter is devoted to describe the methods employed during this thesis work. The objective is not to provide a detailed view and the further interested reader is referred to the references.

3.1 Historical perspective

Before any quantum theory was developed, classical physics were failing on the attempts to describe microscopic world. In 1900, Max Planck introduced the idea that the energy is *quantized* for the first time in order to explain the energy irradiated by the black body. Different models were proposed, based on the idea of the energy quantization, in order to understand how electrons move in an atom i.e. Bohr-Sommerfeld model.

This discovery enhanced the development of the quantum mechanics [124–128], which is settled in the postulates. The information of a system under study is in the wave function and the time independent Schrödinger's equation (3.1) has to be solved.

$$\hat{H}\psi = E\psi \tag{3.1}$$

The Hamiltonian is the energy operator and is represented as \hat{H} . This operator contains the interactions between the particles of the system

$$\hat{H} = \hat{T}_N + \hat{T}_e + \hat{V}_{ee} + \hat{V}_{Ne} + \hat{V}_{NN} \tag{3.2}$$

\hat{T}_N and \hat{T}_e are the kinetic energy of the nuclei and electrons respectively. \hat{V}_{ee} is the interaction between electrons, \hat{V}_{Ne} is the interaction between nuclei and electrons and \hat{V}_{NN} is the interaction between nuclei.

It is a second order differential equation which is not in general analytically solvable. The equation is only solvable for mono-electronic systems, that is, hydrogen atom-like systems. In this sense, the Born-Oppenheimer approximation can be employed, where the motion of electrons and nuclei are separated, considering the nuclei to be fixed [129]. This approximation leads to *Potential Energy Surface* (PES), which basically represents the change in the potential energy occurring after nuclei position change. In 1927, Hartree introduced self-consistent theory [130] and later, Slater and Fock point out the requirement of an antisymmetrized determinant [131, 132], giving birth to the Hartree-Fock (HF) method in 1930.

The main feature of the HF technique is the *mean field* approach. Here, each electron moves in an average potential created by the rest of electrons. In this sense, the problematic pairwise term of the Hamiltonian, \hat{V}_{ee} , is converted into one electron additive term. The direct consequence is that the Hamiltonian can be splitted into each electron term of the system and so is the case for the wave function:

$$|\Psi\rangle = |\phi_1\phi_2 \cdots \phi_n\rangle \quad (3.3)$$

here, ϕ_i is a mono-electronic wave function, usually called orbital [133]. The term orbital was first employed in 1932 by Mulliken, which indicates the region where the electron is calculated to be present.

The first attempt to rationalise the chemical bonding was done by Lewis in 1916, proposing that the chemical bond is formed from the sharing of electrons. Later on, more sophisticated wave function based methods were developed. In this sense, two of the most popular ones are Valence Bond (VB) and Molecular Orbital (MO) theories. The former came first, on the hands of Heitler and London [134], and Pauling developed some key concepts such as hybridisation and resonance [135]. On the other hand, MO theory was obtained by several contributions [136-138], and opposite to VB the electrons are not assigned to individual bonds. Moreover, another difference that must be highlighted between both methods is that VB employs non orthogonal orbitals, whereas in MO the employed orbitals are orthogonal. Overall, MO has become popular due to its lower computational cost compared to VB. In any case, a non orthonormal atomic orbitals basis set is employed for convenience which was independently proposed by Roothaan and Hall [139, 140].

However, the HF method did not experienced much use due to the increase computational cost. This problem was overcome in 1956 in MIT where the first ab initio calculation was performed [141]. The increase in computational capacities has become crucial for computational chemistry to grow and it has evolved as a robust and consolidated branch of chemistry, playing a relevant role in the understanding of chemical processes.

There are a wide variety of techniques available to the user depending on the complexity and the chemical nature of the problem. Beyond the HF methods, post-HF methods were developed. This type of methodologies in essence try to fix the lack of electron correlation in HF. In this way, Møller-Plesset perturbational theory was developed [142], where the remaining electron correlation is treated as a perturbation.

In the Configuration Interaction (CI) method [143, 144], the wave function is expressed as a linear combination of configurations. Alternative methodologies are available in the

market such as Coupled Cluster [145–147], Multi-Reference Configuration Interaction (MR-CI) or Complete-Active-Space (CAS) [148, 149].

3.2 Density functional theory

Density functional theory (DFT) has experienced great use within the last 30 years. Its main advantage is the low computational cost for solving problems of theoretical chemistry. Herein a brief introduction to the theory is given. The theory is based on the electron density $\rho(\mathbf{r})$, a function of the three coordinates of the vector \mathbf{r} and therefore much simpler, in principle, than the wave function that depends on the $3N$ coordinates of the vectors $\mathbf{r}_1, \mathbf{r}_2, \dots$. In essence, the method advocates the use of electron density as the variable of a functional, i.e. a function of other function. In particular, the energy of the system is described by $E[\rho(\mathbf{r})]$, the energy functional of electron density.

Density functional theory is customarily worked out within the Born-Oppenheimer approximation. Namely, the nuclei are fixed and therefore electrons move in the potential created by fixed nuclei. The potential set by those fixed nuclei is known as the *external potential*.

3.2.1 Hohenberg-Kohn

Hohenberg-Kohn theorems [72] laid the theoretical foundations of the methodology. The first theorem demonstrates that non-degenerate ground states can be determined by a functional of the electron density inasmuch as it proves that there exists a one-to-one mapping between the external potential and the electron density, which fully specifies the Hamiltonian operator of the system as,

$$\hat{H} = \hat{T} + \hat{U} + \hat{V}_{ext} \quad (3.4)$$

Notice that \hat{T} , the kinetic energy operator and \hat{U} , the electron repulsion operator depend solely on the number of the electrons of the system. Consequently, by virtue of the above mentioned mapping, given $\rho(\mathbf{r})$ one can obtain its associated \hat{V}_{ext} and, using Eq 3.4, \hat{H} . Then, by solving the Schrödinger equation

$$\hat{H}\psi = E\psi \quad (3.5)$$

one obtains the energy, E , of the state described by the wavefunction ψ . Consequently, we have associated an energy E to a given $\rho(\mathbf{r})$ i.e. the energy is a functional of the electron density, $E[\rho(\mathbf{r})]$. The first Hohenberg and Kohn theorem demonstrates that this $E[\rho(\mathbf{r})]$ is a well-behaved functional for nondegenerated states within the domain of v -representable functionals, namely the set of those $\rho(\mathbf{r})$ associated with the antisymmetric ground-state wavefunction of a Hamiltonian of the (3.4) with some external potential $v(\mathbf{r})$ (not necessarily a Coulomb potential).

Furthermore, Hohenberg and Kohn demonstrated that $E[\rho(\mathbf{r})]$ delivers the exact ground state energy for the exact electron density, i.e. $E_{g.s.} = E[\rho_{g.s.}(\mathbf{r})]$.

The second Hohenberg and Kohn theorem demonstrates that this functional satisfies the variational principle for the ground state energy

$$E[\rho(\mathbf{r})] \geq E[\rho_{g.s.}(\mathbf{r})] = E_{g.s.} \quad (3.6)$$

The Hohenberg-Kohn theorem requires non-degenerate ground states with v -representable electron densities.

Later, it was shown by the constrained search formulation of Levy [150] that neither the non-degeneracy nor the v -representability of $\rho(\mathbf{r})$ are necessary.

Levy introduced the following functional

$$Q[\rho] = \min_{\Psi \rightarrow \rho} \langle \Psi | \hat{T} + \hat{U} | \Psi \rangle \quad (3.7)$$

where the subscript $\Psi \rightarrow \rho$ means that the search has to be carried out within the domain of electron densities ρ that come from antisymmetric, square integrable, wavefunctions ψ . This domain is called the N-representable domain of electron densities.

Given an electron density $\rho(\mathbf{r})$, the functional $Q[\rho]$ searches all the wavefunctions ψ that yield $\rho(\mathbf{r})$ and for each of these wavefunctions evaluates the quantity $\langle \psi | \hat{T} + \hat{U} | \psi \rangle$, then selects the minimum of them all and delivers this value, namely $Q[\rho]$.

Levy demonstrates that $Q[\rho]$ exists, is well defined and is universal in the sense that it does not depend on the external potential, V_{ext} . Furthermore, Levy demonstrated that

$$Q[\rho_{g.s.}] + \int \rho_{g.s.}(\mathbf{r}) V_{ext}(\mathbf{r}) d\mathbf{r} = E_{g.s.} \quad (3.8)$$

This lifts the requirements of the non-degeneracy of the ground state and the v -representability of the electron density required by the Hohenberg and Kohn, by replacing them from the N-representability of the electron density. The latter is an easy condition to impose. Namely for a density $\rho(\mathbf{r})$ to be N-representable it must satisfy:

$$N = \int \rho(\mathbf{r}) d\mathbf{r} \quad (3.9)$$

$$\int |\nabla \rho^{1/2}(\mathbf{r})|^2 d\mathbf{r} < \infty \quad (3.10)$$

This last condition, equation (3.10), was introduced by Lieb [151] in order to keep the kinetic energy finite.

3.2.2 Kohn-Sham (KS)

In practice Kohn-Sham formulation [152] is the most popular among DFT due to its affordable computational cost. This theory relies on an assistant system which has the same density as the real system, but the particles do not interact, their motion is dependent on an effective one-particle potential. This term consists of the external potential, Coulomb interaction between electrons and the exchange and correlation. Once that the effective potential is known Kohn-Sham method is solved in a self consistent way [73, 153].

One could construct the Slater determinant corresponding to the non-interacting system by approximating that the ground state wave function can be adequately represented by a single Slater determinant. Therefore, the wave function is built from N spin orbitals χ_i . The Hamiltonian for such system is

$$\hat{H}_S = \frac{1}{2} \sum_i^N \nabla_i^2 + \sum_i^N V_S(r_i) \quad (3.11)$$

where $V_S(r)$ denotes for the effective potential. The Slater determinant associated to the system

$$\Psi_S(x_1, x_2, \dots, x_N) = \frac{1}{\sqrt{N!}} \begin{vmatrix} \varphi_1(x_1) & \varphi_2(x_1) & \cdots & \varphi_N(x_1) \\ \varphi_1(x_2) & \varphi_2(x_2) & \cdots & \varphi_N(x_2) \\ \vdots & \vdots & & \vdots \\ \varphi_1(x_N) & \varphi_2(x_N) & \cdots & \varphi_N(x_N) \end{vmatrix} \quad (3.12)$$

and solving by the variational principle

$$\hat{f}^{KS} \varphi_i = \varepsilon_i \varphi_i \quad (3.13)$$

\hat{f}^{KS} being the one-electron Kohn-Sham operator defined as

$$\hat{f}^{KS} = -\frac{1}{2} \nabla^2 + V_S(r) \quad (3.14)$$

The key factor here is to choose wisely the effective potential $V_S(r)$ so that the density obtained from the Kohn-Sham orbitals (φ_i) of the assistant non-interacting system is the same as the real system,

$$\rho_S(r) = \sum_i^N \sum_s |\varphi_i(r, s)|^2 = \rho_0(r) \quad (3.15)$$

The density functional is therefore written as

$$F[\rho(\mathbf{r})] = T_S[\rho(\mathbf{r})] + J[\rho(\mathbf{r})] + E_{xc}[\rho(\mathbf{r})] \quad (3.16)$$

where T_S denotes for the kinetic energy of the non-interacting system, which is different from the real system. Thereby, the *exchange correlation energy* is defined as

$$E_{xc}[\rho(\mathbf{r})] = (T[\rho(\mathbf{r})] - T_S[\rho(\mathbf{r})]) + (E_{ee}[\rho(\mathbf{r})] - J[\rho(\mathbf{r})]) = T_C[\rho(\mathbf{r})] + E_{ncl}[\rho(\mathbf{r})] \quad (3.17)$$

here, T_C is the residual part of the kinetic energy between the real and assistant systems and E_{ncl} is the non-classical electrostatic contribution. Therefore, every unknown term is plugged into the *exchange correlation* term. Rewriting equation (3.17) in terms of the orbitals (3.15) we have that

$$E[\rho(\mathbf{r})] = T_S[\rho(\mathbf{r})] + J[\rho(\mathbf{r})] + E_{xc}[\rho(\mathbf{r})] + E_{Ne}[\rho(\mathbf{r})] =$$

$$T_S[\rho(\mathbf{r})] + \frac{1}{2} \int \int \frac{\rho(\mathbf{r}_1)\rho(\mathbf{r}_2)}{r_{12}} d\mathbf{r}_1 d\mathbf{r}_2 + E_{xc}[\rho(\mathbf{r})] + \int V_{Ne}\rho(\mathbf{r}) d\mathbf{r} \quad (3.18)$$

$$- \frac{1}{2} \sum_i^N \langle \varphi_i | \nabla^2 | \varphi_i \rangle + \frac{1}{2} \sum_i^N \sum_j^N \int \int |\varphi_i(\mathbf{r}_1)|^2 \frac{1}{r_{12}} |\varphi_j(\mathbf{r}_2)|^2 d\mathbf{r}_1 d\mathbf{r}_2 +$$

$$E_{xc}[\rho(\mathbf{r})] - \sum_i^N \int \sum_A^M \frac{Z_A}{r_{1A}} |\varphi_i(\mathbf{r}_1)|^2 d\mathbf{r}_1 \quad (3.19)$$

Applying the variational principle employing the constraint of $\langle \varphi_i | \varphi_j \rangle = \delta_{ij}$, leads to the following set mono-electronic equations, known as Kohn-Sham equations

$$\left(-\frac{1}{2} \sum_i^N \nabla^2 + \left[\int \frac{\rho(\mathbf{r}_2)}{r_{12}} d\mathbf{r}_2 + V_{xc}(\mathbf{r}_1) - \sum_A^M \frac{Z_A}{r_{1A}} \right] \right) \varphi_i =$$

$$\left(-\frac{1}{2} \sum_i^N \nabla^2 + V_{eff}(\mathbf{r}_1) \right) \varphi_i = \varepsilon_i \varphi_i \quad (3.20)$$

Comparing (3.19) with (3.11) we have that V_{eff} is identical to V_S

$$V_S(\mathbf{r}) \equiv V_{eff}(\mathbf{r}) = \int \frac{\rho(\mathbf{r}_2)}{r_{12}} d\mathbf{r}_2 + V_{xc}(\mathbf{r}_1) - \sum_A^M \frac{Z_A}{r_{1A}} \quad (3.21)$$

here V_{xc} is the potential due to the *exchange correlation* energy E_{xc} . This term is unknown and so is the potential for which we have no clue to its explicit form. Hence, V_{xc} is simply defined as the functional derivative of E_{xc} with respect to ρ

$$V_{xc} \equiv \frac{\delta E_{xc}}{\delta \rho} \quad (3.22)$$

Unlike HF model, the Kohn-Sham approach is in principle exact. One should *just* need to know the form of E_{xc} and V_{xc} . Unfortunately this is not an easy job and it is approximated. Note that the non-interacting assistant system is represented as a single reference Slater determinant, not the real one. Therefore, employing the exact E_{xc} the real system can be represented.

The physical meaning of the Kohn-Sham orbitals is a reason of debate. It is argued that the Kohn-Sham orbitals correspond to the assistant system and not to the real one and therefore the only connection between the KS orbitals and the real system is that the sum of their squares add up to the exact density. However, due to the fact that KS orbitals are associated with the one-electron potential, which include all non-classical effects, might be legitimate for these orbitals to have physical meaning. Indeed, HF orbitals are farther away from the real system as the correlation effects are not taken into account and the density does not correspond to the real system.

3.2.3 Approximations to exchange-correlation energy

The true E_{xc} is a universal functional but as stated before it is not known. There exist a wide variety of functionals in the market which try to approximate the E_{xc} . Herein some concepts concerning different approaches are given.

3.2.3.1 Local Density Approximation (LDA)

The Local Density Approximation (LDA) considers each volume element with a local density $\rho(\mathbf{r})$. The model represents properly systems with slowly varying density. Nevertheless, this is not the general case for molecules where density varies rapidly. The E_{xc} is given by

$$E_{xc}^{LDA}[\rho] = \int \rho(\mathbf{r}) \varepsilon_{xc}[\rho] d\mathbf{r} \quad (3.23)$$

here, $\varepsilon_{xc}[\rho]$ is the exchange-correlation energy per electron in an homogeneous gas with electron density ρ .

3.2.3.2 Generalized Gradient Approximation (GGA)

In order to account for the non-homogeneity of the true electron density the logical step is to consider the gradient of the density, $\nabla\rho(\mathbf{r})$, apart from the density $\rho(\mathbf{r})$. Therefore, LDA can be thought to be the first term of a Taylor expansion of the exchange-correlation functional E_{xc} in terms of the density

$$E_{xc}^{GEA}[\rho_\alpha, \rho_\beta] = \int \rho \varepsilon_{xc}(\rho_\alpha, \rho_\beta) d\mathbf{r} + \sum_{\sigma, \sigma'} \int C_{xc}^{\sigma, \sigma'}(\rho_\alpha, \rho_\beta) \frac{\nabla\rho_\sigma}{(\rho_\sigma)^{2/3}} \frac{\nabla\rho_{\sigma'}}{(\rho_{\sigma'})^{2/3}} d\mathbf{r} + \dots \quad (3.24)$$

where σ and σ' stands for α and β spin. This form of the functional is termed the Gradient Expansion Approximation (GEA) and it can be shown that it applies to a model system with not uniform density but slowly varying. However, if employed in order to solve a real molecular problem does not perform as expected. This is due to the fact that the exchange-correlation hole associated with a functional has lost many of the properties which made LDA hole physically meaningful. This is solved employing the restrictions valid for the true LDA holes. These functionals are known as Generalized Gradient Approximations (GGA). They are written as

$$E_{xc}^{GGA}[\rho_\alpha, \rho_\beta] = \int f[\rho_\alpha, \rho_\beta, \nabla\rho_\alpha, \nabla\rho_\beta] d\mathbf{r} \quad (3.25)$$

3.2.3.3 Meta Generalized Gradient Approximation (mGGA)

These functionals include the laplacian of the density and kinetic energy

$$E_{xc}^{mGGA}[\rho] = \int f[\rho_\alpha, \nabla\rho_\sigma, \nabla^2\rho_\sigma, \tau_\sigma] d\mathbf{r} \quad (3.26)$$

with $\sigma = \alpha, \beta$ and

$$\tau_\sigma(\mathbf{r}) = \sum_{i=1} |\vec{\nabla}\varphi_i(\mathbf{r})|^2 \quad (3.27)$$

is the Kohn-Sham orbital kinetic energy density for electron of spin σ .

3.2.3.4 Hybrid functionals

The functionals introduced before are rigorously established by DFT. Becke [154, 155] proposed a different approach for the exchange-correlation, where HF and DFT are combined, leading to hybrid functionals. HF provides exact description of the exchange but lacks electron correlation. Meanwhile, DFT methods include correlation effects, in a much easier way than post-HF, but often fail in the description of the exchange. The exchange-correlation proposed by Becke is based on the adiabatic connection,

$$E_{xc} = \int_0^1 E_{ncl}^\lambda d\lambda \quad (3.28)$$

E_{ncl}^λ is the non-classical term. At $\lambda = 0$ it represents the non-interacting system and the non-classical term corresponds to the exchange due to the fact that electrons are fermions. This exchange contribution can be computed exactly. When $\lambda = 1$, it represents the interacting system and the non-classical term corresponds to both exchange and correlation. Unfortunately, such exchange-correlation energy is unknown and the E_{xc} has to be approximated. Both the non-interacting and interacting systems are connected through a continuum of partially interacting systems, which share the same density, the density of the fully interacting system. However, the evaluation of equation 3.27 is not possible as E_{ncl}^λ is not known for intermediate values of λ . Alternatively, E_{ncl}^λ is considered to be a linear function of λ

$$E_{xc} = \int_0^1 E_{ncl}^\lambda d\lambda = \frac{1}{2}E_{ncl}^{\lambda=0} + \frac{1}{2}E_{ncl}^{\lambda=1} \quad (3.29)$$

employing the LDA exchange-correlation functional for $E_{ncl}^{\lambda=1}$ in equation 3.28 represents the *half-and-half* combination of exact exchange and density functional exchange correlation. Later on, a generalization of equation 3.28 was proposed, where two adjustable parameters were introduced.

$$E_{xc} = c_0 E_{xc}^{\lambda=0} + c_1 E_{xc}^{\lambda=1} \quad (3.30)$$

There exist a wide variety of combinations and inclusion of semiempirical coefficients in order to reproduce the properties of interest. However, if certain amount of the exact exchange is present all these functionals belong to hybrid functional group.

Another type of functionals can be found in the market. Hybrid meta-GGA functionals combine a meta-GGA functional with the HF exchange. The double-hybrid functionals, in turn, are constructed adding a non-local electron correlation to a hybrid functional. The range-separated hybrid functionals split the Coulomb operator into its long-range and short-range compounds, which are treated differently.

3.2.4 Final remarks on DFT

From the Hohenberg-Kohn theorem it is known that the exact E_{xc} exists. However, it remains unknown and therefore it can be said that DFT is not strictly *ab initio*. There are a bunge of functionals available in the market and one has to be wise enough to select a functional that works acceptably for its certain chemical problem. The main advantage of DFT is that it has similar computational cost to HF method with the inclusion of some kind of electron correlation. However, one has to be aware that approximate exchange-correlation functionals fail to exactly cancel the self-interaction, present at the Coulomb energy [77].

Besides, "DFT has been observed to be less accurate for nonbonded interactions than for bonded ones" [74]. Two unshared electron distributions do not contribute by any means to an energy lowering in functional forms which depend only on a local electron density. In order to describe London interactions, a fully nonlocal functional must be applied and a local density functional is in principle not capable of describing this long-range, nonlocal correlation effects. Therefore, in order to account for such effects we employ a hybrid meta-GGA functional (MPWB1K), which has previously been tested for these type of interactions [74].

Moreover, the breaking and creation of chemical bonds is a common event throught this thesis. It is known that pure functionals (those that do not include any HF exchange) overestimate bond energies and underestimate barrier heights [75, 76] and therefore, for our case a hybrid functional is required. In this sense, the selected MPWB1K functional has %44 of HF exchange. Furthermore, this functional has been observed to behave properly for radical stabilisation energies [77].

Finally, the selection of the density functional is based on its good performance in thermochemistry and thermochemical kinetics [78]. More preciesly, a benchmark study has been carried in order to stablish which functional performs best for $\bullet OH$ and $\bullet OOH$ addition and H abstraction from 3-methylpyrrole and benzene. These case studies are very similar to the ones that are shown herein and therefore they should be inspected with severe consideration. It is shown that the obtained results with this functional for the $\bullet OH$ addition

and H abstraction are acceptable. However, the error increases when the attack of $\bullet OOH$ is considered [156]. Overall, as a result of the design of the functional and its behaviour in similar cases, we expect MPWB1K to be a suitable density functional to study the chemical oxidation processes by the $\bullet OH$ in proteins.

3.3 Basis sets

The Schrödinger equation can only be analytically solved for hydrogen-like atoms, that is for mono-electronic cases. In other cases, the Schrödinger equation has to be solved approximately and it is customary to use a set of basis functions to construct the corresponding wavefunction. Namely, the wavefunction uses a set of molecular orbital, that result from the combination of these basis functions. The basis functions are typically hydrogen-like orbitals that consist of a radial $R_{n,l}$ and spherical harmonic angular part $Y_{l,m}$

$$\phi(\mathbf{r}; \alpha, R) = R_{n,l} Y_{l,m} \quad (3.31)$$

where the radial part, $R_{n,l}$, is of Slater type. Slater Type Functions (STF) are

$$\phi^{STF}(\mathbf{r}; \alpha, R) = A r^l e^{-\alpha(r-R)} \quad (3.32)$$

where r is the electron position, R refers to the position of the nucleus, α is a charge dependent constant, l an integer number accounting for the angular momentum and A the normalization constant so that $\int |\phi^{STF}|^2 d\mathbf{r} = 1$. These kind of Slater type functions describe the electron and are said to describe an orbital. Therefore, they are also known as Slater Type Orbitals (STO).

In the case of polyelectronic atoms or molecules the HF approach considered the *mean field*. Hence, the wave function can be divided into orbitals, as mentioned ahead. An orbital, is a mono-electronic wave function, whose combination gives rise to a good approximation of the actual wave function.

However, the three- and four-centre two-electron integrals involving STO can not be performed analytically. Instead, Gaussian Type Orbitals (GTO) or Gaussian Type Functions (GTF) are employed which are easier to integrate.

$$\phi^{GTF}(\mathbf{r}; \alpha, R) = A r^l e^{-\alpha(r-R)^2} \quad (3.33)$$

The GTOs has problems representing the cusp of STOs near the nucleus and decay too rapidly far from the nucleus. Therefore, the solution is to represent the STO by a linear combination of GTOs

$$\phi^{STO} \approx \sum_{i=1}^L c_{i\mu} \phi^{GTO} \quad (3.34)$$

In this thesis work GTOs are employed, in particular, Pople's basis set.

3.3.1 Basis set superposition error (BSSE)

The BSSE is a technical problem, specially notorious in dimers. The issue arises as a consequence of the sharing of basis set corresponding to each monomer, whenever they form a bigger system. Originally introduced by Liu and McLean in 1973 [157] it was firstly reported by Kestner in 1969 [158], it occurs as a result of the basis set incompleteness. Having a dimer (AB) formed from monomers A and B, each monomer is further stabilised at the dimer due to the fact that the B donates basis functions to A and vice versa. This is a phenomena that cannot occur in the separated monomers and therefore the dimer is overstabilised. The counterpoise correction include the neighbour monomer's orbitals in order to have same basis set as in the dimer. However, the mere inclusion of virtual or both, occupied and virtual orbitals is under debate. Another important fact related to this problem is the definition of fragments, specially when having open shell systems.

Several different cases were thoroughly studied by Alvarez-Idaboy and Galano [159] and it was concluded that the best solution is not to include the counter poise correction and employ as largest basis set as possible in order to minimize the BSSE problem.

For the particular case of this work we perform the optimizations with a double zeta basis set and increased the basis set in the single points employing a triple zeta basis set with the purpose of minimizing the BSSE.

3.4 Molecular Space Partitions

Even though it may seem intuitive to define an atom inside a molecule, the task represents a real challenge in the quantum chemistry field, as there is not a unique way of doing this. There are a wide variety of methods in order to perform such job being the Mulliken partition [160] the most popular one.

3.4.1 Mulliken

The charge density is expressed in terms of atomic orbitals

$$\rho(\mathbf{r}) = \sum_{\mu} \sum_{\nu} P_{\mu\nu} \phi_{\mu}(\mathbf{r}) \phi_{\nu}^*(\mathbf{r}) \quad (3.35)$$

The molecular orbitals are expressed as a linear combination of atomic orbitals,

$$\psi_a = \sum_{\mu=1}^K c_{\mu a} \phi_{\mu} \quad (3.36)$$

in this sense, the population matrix P is,

$$P_{\mu\nu} = 2 \sum_i c_{\mu i} c_{\nu i}^* S_{\mu\nu} \quad (3.37)$$

and we have that the sum of the integrals of the molecular orbitals is

$$N = 2 \sum_a^{N/2} \int d\mathbf{r} |\psi_a(\mathbf{r})|^2 \quad (3.38)$$

In a single-determinant wavefunction, the total number of electrons is divided into two electrons per molecular orbital, by substituting the basis expansion of ψ_a into 2.43

$$N = \sum_{\mu} \sum_{\nu} P_{\mu\nu} S_{\nu\mu} = \sum_{\mu} (PS)_{\mu\mu} \quad (3.39)$$

and it is possible to interpret $(PS)_{\mu\mu}$ as the number of electrons to be associated with ϕ_{μ} . One of the main drawbacks of Mulliken population analysis is its basis set dependence.

3.4.2 Fuzzy Atom Scheme

The fuzzy atom partition is based on weight functions $w_A(\mathbf{r})$ defined for each atom of the molecule, A, in a point of the Cartesian space, \mathbf{r} [161]. Each atom is associated with a weight factor and has to obey the condition of rendering unity when summing over all the atoms

$$\sum_A w_A(\mathbf{r}) = 1 \quad (3.40)$$

The weight factors are obtained from promolecular densities

$$w_A(\mathbf{r}) = \frac{\rho_A^0(\mathbf{r})}{\sum_A \rho_A^0(\mathbf{r})} \quad (3.41)$$

ρ_A^0 is the density of the isolated A atom. Therefore the atomic populations in this case are given as

$$N_A = \int \rho_A(\mathbf{r}) d\mathbf{r} = \int w_A(\mathbf{r}) \rho(\mathbf{r}) d\mathbf{r} \quad (3.42)$$

The computed fuzzy atom partition were done employing APOST-3D program [162], using topological fuzzy Voronoi cells (TFVC) [163] to define the atomic boundaries within the molecule. TFVC are three-dimensional atomic partitions based on a modified partition of the fuzzy atomic Voronoi cells introduced by Becke [164, 165].

3.5 Solvation

Most of the chemical reactions occur in a solvent and therefore it is important to mimic its behaviour in order to understand its effects. Conceptually, a solvated molecule can be thought as a process in which first a cavity has to be created in the solvent in order to place the solute molecule. Then, the cavity is polarized due to the electric field created by the solvent. The produced cavity's polarization generates an electric field at the solvent molecule. It is this last effect that can be modelled as a perturbation operator which is added to the Hamiltonian of the solute in the gas phase.

The solute is embedded in a polarizable continuum of dielectric ε . First a cavity is created in order to accommodate the solute. The free energy variation for this step is called the *cavitation energy*. When the molecule of the gas phase geometry and electronic structure is placed inside the cavity, the electric field created by the molecule, polarizes the continuum and an electrostatic potential arises in the cavity. Such electrostatic potential is called *reaction potential* and interacts with the molecule and generates a total free energy change. The free energy change arising from the solute-solvent, solvent-solvent and internal solute electrostatic interactions is called the *electrostatic* contribution. Finally, the solute-solvent dispersion energy gives rise to the *dispersion* term.

The solvation free energy i.e. the free energy change to transfer a molecule from vacuum to solvent is

$$\Delta G_{sol} = \Delta G_{elec} + \Delta G_{disp} + \Delta G_{cav} \quad (3.43)$$

When the solvent is treated as a continuum the Laplacian of the *reaction potential*, $\phi(\mathbf{r})$, is related to the free charge density, $\rho(\mathbf{r})$, by the Poisson's equation [166]

$$\nabla \varepsilon(\mathbf{r}) [\nabla \phi(\mathbf{r})] = -4\pi \rho(\mathbf{r}) \quad (3.44)$$

where ε is the homogeneous dielectric constant.

The polarizable continuum model (PCM) solves the electrostatic problem by introducing a charge distribution spread on the cavity surface [167, 168]. The cavity volume is obtained by adding up the van der Waals spheres of the atoms of the solute. The surfaces of these resulting volumes are rather irregular and in general no analytic functions can fit them. As a consequence, ΔG_{elec} is calculated numerically. The cavity surface is divided into a large number of small surface elements, tesserae, and a point charge is associated with each surface element.

The reaction potential is then added to the solute hamiltonian and solved iteratively by SCF

$$\hat{H} = \hat{H}_0 + \phi(\mathbf{r}) \quad (3.45)$$

After each SCF iteration new values of the surface charges are calculated from the current wave function to update the *reaction potential*, which is used in the next iteration until the solute wave function and the surface charges are self-consistent [169].

The dispersion and cavitation components are usually considered proportional to the surface defined by the van der Waals spheres and the solvent accessible surface is used to calculate dispersion contribution.

3.6 Employed method and protocol

As introduced before, all this thesis work was carried out using the meta-GGA functional MPWB1K, developed by Truhlar and coworkers [78, 170–172] within density functional theory [72, 73]. Structure optimizations were carried out in gas phase, using the 6-31+G(d,p) basis set. Harmonic vibrational frequencies were obtained by analytical differentiation of gradients, in order to determine whether the structures found are minima or transition states, and to evaluate the thermal ($T = 298$ K) corrections to the enthalpy in the harmonic oscillator approximation. Single point calculations using the 6-311++G(2df,2p) basis set and the integral equation formalism of the polarized continuum model (IEFPCM) of Tomasi and coworkers [173, 174] were performed on the optimized structures to estimate the effects of bulk solvent. Two dielectric constant were employed to carry out these calculations: i) $\epsilon = 4$ to consider a low solvent accessible area inside a protein and ii) $\epsilon = 80$ in bulk aqueous solution. It should be noted that the reactions studied in this work consider infinitely separated reactants and products, which leads to unbalanced entropic effects and therefore the enthalpy values (ΔH^{298}) have been considered for discussion along the work. These values were determined adding the enthalpic contributions in the gas-phase to the electronic energy in solution to give the final enthalpies, ΔH_4^{298} and ΔH_{aq}^{298} . The GAUSSIAN09 package [79] was used throughout the study.

In order to test the proposed protocol we have considered several different reactions and compared the obtained D_e values with the experimental ones in the same way as shown in the work performed by Lopez et. al [175], Table 3.1.



The difference for the studied dissociations and H abstractions is observed to be encouragingly small, and therefore we are playing safe.

3.6.1 The model

The model structure employed through this thesis is shown in Figure 3.1. The picture presents two peptide bonds flanking the side chain of the amino acid. The dihedral angles are oriented to simulate α -helix-like and β -sheet. The protein chain is expected to alter very

	D_e (kcal/mol)		
	MPWB1K	expt	difference
$CH_4 \rightarrow H^\bullet + CH_3^\bullet$	112.4	113.0	-0.6
$C_2H_6 \rightarrow H^\bullet + C_2H_5^\bullet$	107.9	109.4	-1.5
$H_2O_2 \rightarrow H^\bullet + HO_2^\bullet$	89.1	92.7	-3.6
$H_2O \rightarrow H^\bullet + HO^\bullet$	122.3	126.0	-3.7
$NH_3 \rightarrow H^\bullet + NH_2^\bullet$	114.2	115.9	-1.7
$C_2H_6 \rightarrow CH_3^\bullet$	98.7	96.6	2.1
$H_2O_2 \rightarrow 2HO^\bullet$	49.4	55.1	-5.7
MAD			2.7
$CH_4 + HO^\bullet \rightarrow CH_3^\bullet + H_2O$	-9.9	-13.0	3.1
$NH_3 + HO^\bullet \rightarrow NH_2^\bullet + H_2O$	-8.2	-10.1	1.9
$C_2H_6 + HO^\bullet \rightarrow C_2H_5^\bullet + H_2O$	-14.4	-16.6	2.2
$H_2O_2 + HO^\bullet \rightarrow HO_2^\bullet + H_2O$	-33.3	-33.3	0.0
MAD			1.8

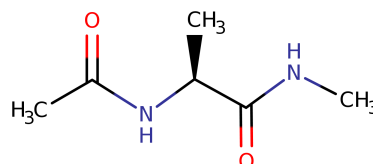
Table 3.1: Calculated and experimental D_e values.

Figure 3.1: The employed model for Ala as an example.

slightly the kinetics and the thermodynamics of the studied reactions. Nevertheless, one should take in mind that steric effects could be different for other protein folding. The N- and O-terminals of these two peptide bonds are capped by a methyl group, simulating the C_α of the lateral amino acids.

The reaction pathways described in the following chapters imply that the concentration of $\bullet OH$ is high enough to allow the rapid attack of the second $\bullet OH$ onto the radical intermediate. We should bear in mind that, in biological systems, the amino acid side chains (or the radical intermediates) might be exposed not only to $\bullet OH$ but also to a large range of other radical species. Thus, many other reaction mechanisms may also occur. However, the simplest reaction pathway that can explain the formation of many of the experimentally characterized oxidized products is the sequential attack of two $\bullet OH$ and, consequently, this pathway has been characterized in this study. The kinetics and thermodynamics of the reaction mechanisms were analyzed, in order to determine the most probable reaction pathway.

Chapter 4

Protein Backbone Homolytic Dissociation By $\bullet OH$

In this work the hydrogen abstraction by $\bullet OH$ from C_α and C_β atoms of all amino acids is studied, in the framework of density functional theory, as this is the most favorable reaction mechanism when this kind of radical attacks a protein. From the myriad routes that the oxydation of a protein by a $\bullet OH$ may follow, fragmentation of the protein is one of the most damaging ones, as it hampers the normal function of the protein. Therefore, the cleavages of the C_α -C and C_α -N backbone bonds have been investigated as the second step of the mechanism. To the best of our knowledge, this is the first time that this reaction pathway is systematically studied for all natural amino acids. The study includes the effects that the solvent dielectrics or the conformation of the peptide model employed has on the reaction. Interestingly, the results indicate that the nature of the side chain has little effect on the H abstraction reaction, and that for most of amino acids the attack at the C_α atom is favored over the attack at the C_β atom. The origin of this preference relies on the larger capability of the formed radical intermediate to delocalize the unpair electron, thus maximizing the captodative effect. Moreover, the reaction is more favorable when the reactant presents a β -sheet conformation, where the peptide backbone is completely planar. With respect to the homolytic splitting of the C_α -C and C_α -N bonds, the former is favorable for almost all amino acids whereas Ser and Thr are the only amino acids favoring the later. These evidences agree with previous investigations but the accurate description of the electronic density analysis performed indicates that the origin of the different reaction pathway preferences relies on a large stabilization of the product rather than in the bond weakening at the radical intermediate.

4.1 Introduction

Sometimes the backbone splitting is triggered in purpose in techniques such as electron-capture dissociation (ECD), electron-transfer dissociation (ETD) or free radical initiated peptide sequencing (FRIPS) in order to sequencing a peptide or a protein, as it was already introduced in Chapter 1. In these cases, first the radical specie abstracts a hydrogen from

the C_β atom, and then either the C_α -C bond or C_α -N bond is cleaved. Recently, Thomas et al. combined FRIPS experiments with computational calculations to investigate the homolytic splitting of backbone peptide bonds [121]. Once a radical intermediate is formed by the radical attack at the C_β atom, the results indicate that most of the amino acids show preference for the cleavage at C_α -C bond, but nevertheless the C_α -N bond cleavage is favored for Ser and Thr. The authors suggested that this difference is due to the capability of Ser and Thr to form hydrogen bonds that weakens the electronic stability of the C_α -N bond at the radical intermediate, not possible with the remaining amino acids.

Herein we present a systematic study of the H abstraction reaction on all amino acids. This large set of calculations allow us to provide a complete overview of the reaction and determine the influence that the side chain has on the H abstraction reaction. Moreover, the effects of the peptide conformation or the dielectric constant are taken into account, along with the capability of each radical intermediate to stabilize the unpaired electron. The reaction pathway characterized (represented in Figure 4.1) involves two steps: i) H abstraction from the amino acid C_α or C_β atom, producing a water molecule and a radical intermediate, refers to INT_{C_α} or INT_{C_β} depending on the target C atom in the protein and ii) either of the two homolytic splitting of a backbone peptide (C_α -C or C_α -N) to form $PROD^{NC}$ or $PROD^{CC}$ (see Figure 4.1). The study therefore also investigates the backbone dissociation on all amino acids radical intermediates and provides with a new explanation of why Ser and Thr deviate in the general pattern of the C_α -C backbone bond cleavage.

4.2 Results and discussion

The reaction pathway was characterized for all natural amino acids, allowing a rational analysis of the effects that the side chains might have on the different reactions. Moreover, other effects, such as peptide backbone conformation, dielectric, or alternative isomers are taken into account.

4.2.1 Step 1: H abstraction

4.2.1.1 Energies of the intermediate species.

The first step involves the abstraction of the hydrogen to form a radical intermediate, namely INT_{C_α} or INT_{C_β} . The transition states for the formation of INT_{C_α} were characterized for all amino acids and the two conformations stated above. However, due to the high reactivity of the $\bullet OH$ the energy barriers are very small and therefore thermodynamics rather than kinetics drives the reaction. In any case, the energy barriers are included in the Appendix (Table A.5) and we focus on the relative thermodynamic stability of the different species. Furthermore, the relative enthalpy values computed at low dielectric constant (Tables A.1 and A.2) show not significant differences and the energy profiles are equivalent. Thus, for the sake of clarity, only the ΔH_{aq} values will be presented through the text. The relative enthalpies computed for the two intermediate species characterized for all amino acids are shown in Figure 4.2 and Tables A.1 and A.2. Even that due to the large set of data and the heterogeneity of the amino acids studied, several clear trends can be observed when the data is analyzed.

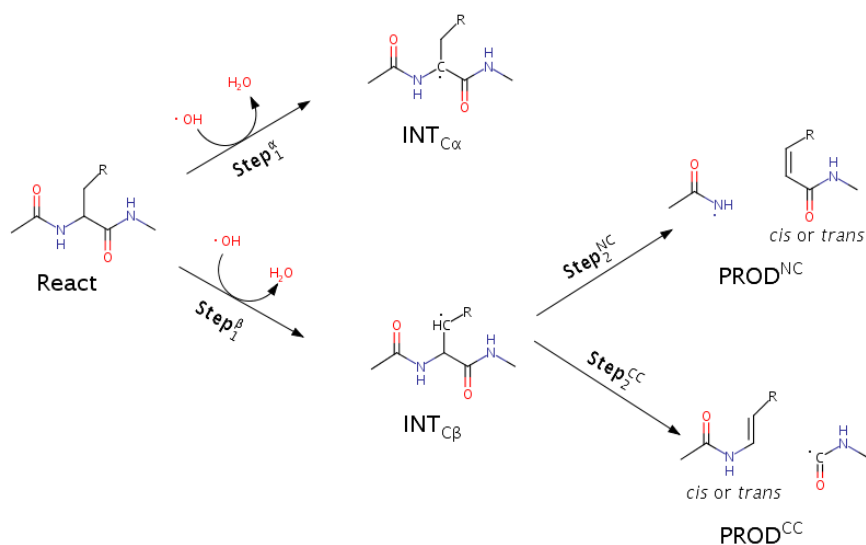


Figure 4.1: The reaction mechanism studied herein that involves two steps: 1) hydrogen abstraction by the $\bullet\text{OH}$ radical from the C_α or C_β atoms to form INT_{C_α} or INT_{C_β} radical species, respectively and a water molecule, and 2) homolytic splitting of either the C-N or C-C backbone bonds to form PROD^{NC} or PROD^{CC} . The reaction pathway was characterized for all natural amino acids and considering two alternative conformations of the amino acid backbone: α -helix-like and β -sheet

All the ΔH_{aq} values of the intermediates computed are negative, indicating that the abstraction of a H by the $\bullet\text{OH}$ is favorable for all amino acids. The values are spread in the -14/-39 kcal/mol range, so the different effects studied influence the final stability of the intermediates. Therefore, we will analyze each of these effects individually. The ΔH_{aq} values corresponding to the α -helix-like conformation of INT_{C_α} (red blocks on the left plot), are in the -25/-34 kcal/mol range. Three amino acids show the less stable intermediates (Ser, Thr and Val), with ΔH_{aq} values of -26 kcal/mol. On the other hand, Asp, Lys, Arg and Glu show the most favorable intermediates, suggesting that the charged amino acids may tend to stabilize better the radical intermediate. However, the values show not remarkable differences and no clear trend can be depicted between the ΔH_{aq} values and the amino acid type.

The difference between the ΔH_{aq} values computed with the α -helix-like and β -sheet conformations ($\Delta H_{aq}^{\alpha-\beta}$) at each stationary point are presented in Table A.3. Interestingly, the attack of the $\bullet\text{OH}$ on the amino acids with β -sheet conformation lead in many cases to stabilize the INT_{C_α} in about 5-8 kcal/mol more than their counterparts with α -helix-like conformation, with an average $\Delta H_{aq}^{\alpha-\beta}$ of 3.9 (see Table A.3). As a consequence, the most stable INT_{C_α} species with β -sheet conformation presents a ΔH_{aq} value of about -39

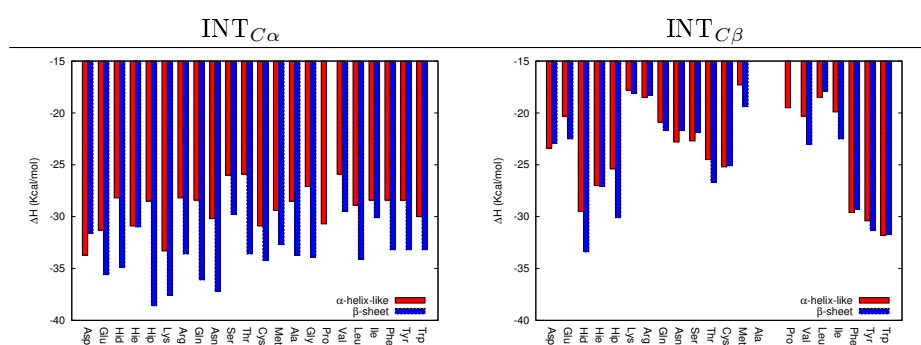


Figure 4.2: Relative enthalpy values corresponding to the $INT_{C\alpha}$ (left) and $INT_{C\beta}$ (right) stationary points computed in solution (ΔH_{aq} , in kcal/mol) for all natural amino acids and two backbone conformations: α - like (red blocks) and β -sheet (blue blocks).

kcal/mol, while the less stable ones are around -30 kcal/mol. Therefore, the ΔH_{aq} values of all $INT_{C\alpha}$ with β -sheet conformation differ in less than 9 kcal/mol among them but there is not any clear relationship between the side chain character of the amino acids and their stability. However, the results confirm that the β -sheet conformation favor rather than the α -helix-like conformation the attack of the $\bullet OH$ at the C_α atom (Table A.1), in agreement with previous studies [176].

The ΔH_{aq} values computed for the $INT_{C\beta}$, that is, when the $\bullet OH$ attacks at the C_β atom, are in general less favorable than their $INT_{C\alpha}$ counterparts, as all their ΔH_{aq} values are in the -14/-33 kcal/mol range. When the amino acids adopt the α -helix like conformation, the ΔH_{aq} values are in the -15/-32 kcal/mol range, remarkably less stable than when the radical attacks at the C_α atom. It is noteworthy that the differences between the amino acids are more significant than with $INT_{C\alpha}$. The most stable $INT_{C\beta}$ are formed by the three amino acids with aromatic rings, i. e., Trp, Tyr, and Phe (ΔH_{aq} values of around -31 kcal/mol) due to a higher delocalisation of the radical (Figure 4.5). On the other hand, amino acids with hydrophobic side chains, such as Ala, Ile and Leu are among the less stable ones, together with Lys, Met and Arg. Unlike with the attack at C_α reactions, the β -sheet conformation does not significantly stabilise the process and in fact with many amino acids the reaction is slightly less favored (see Figure 4.2). The difference ($\Delta H_{aq}^{\alpha-\beta}$) is in most cases less than 3 kcal/mol and the obtained average ($\bar{\chi}=0.2$) and MAD values point out no significant effect of the conformations (Table A.3).

4.2.1.2 Rationalizing intermediate's stability

The relative enthalpy values presented in the previous section show two clear trends: i) the attack of the $\bullet OH$ at C_α formes more stable intermediates than the attack at the C_β atom, and ii) the attack at C_α is slightly favored in β -sheet conformation, while the conformation does not influence the attack at C_β and forming $INT_{C\beta}$ (Tables A.1, A.2 and A.3).

The main reason for these results lies on the capability that each conformation has to stabilize the radical intermediate. The ψ and φ angles are measured on all reactant and

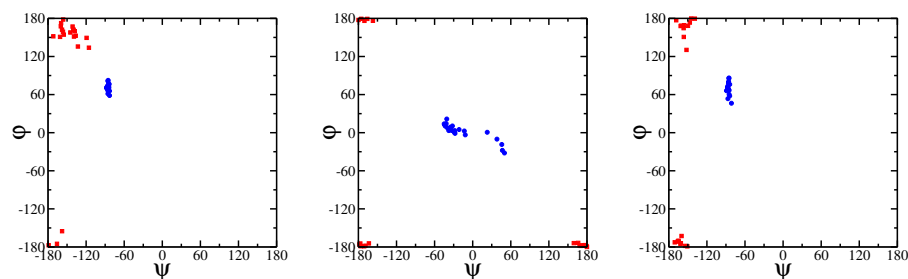


Figure 4.3: Ramachandran plot of reactants (left panel), $INT_{C\alpha}$ (middle panel) and $INT_{C\beta}$ (right panel) species computed with the α -helix like (blue points) and β -sheet (red points) conformations.

intermediate species in order to built their Ramachandran plot (shown in Figure 4.3). The angles computed on the reactants confirm that the two conformations considered herein are indeed the α -helix like and β -sheet, as the ψ and φ angles are ca -60 and 60 for the former conformation and close to 180 for the later. Note that the values computed for Gly and Ala correspond to the β_L and γ_L conformations reported by Owen et al [122]. The angles computed on the $INT_{C\beta}$ species show similar values, indicating that the abstraction of a H atom from the C_β atom to form a radical specie does not modify substantially the geometry of the amino acids. However, this is not the case for the $INT_{C\alpha}$ species. The dihedral angles keep their values close to 180 degrees with the β -sheet conformation, whereas with the α -helix-like conformation the values of the two angles have approached to 0 degrees, even that this conformation prevents a completely planar backbone arrangement (see Figure 4.4).

These differences on the planarity of the backbone determine the final stability of each radical intermediate, which depends on the capability of the structure to delocalize the unpaired electron, also known as captodative effect. This phenomena occurs when a captor and dative groups are close to the radical, as the amino and carbonyl groups in an amino acid. As a consequence the unpaired electron of the radical is delocalized towards the captor and dative groups, providing further stabilization to the radical specie [112]. In order to quantify the capability of each species to delocalized the unpaired electron, the spin densities were computed at the C_α and C_β atoms of $INT_{C\alpha}$ and $INT_{C\beta}$, respectively (see Figure 4.5). The values indicate that the radical is slightly more delocalized in the former species (spin densities in the 0.5-0.6 range) than in the later (densities close to 0.8). Therefore, the captodative effect significantly lowers the spin density at $INT_{C\alpha}$ species. This cannot take place in the $INT_{C\beta}$, where the radical located at the C_β atom is too far away from the captor and dative groups present at the backbone. Interestingly, the spin density values are lower than 0.6 for the the $INT_{C\beta}$ species of the three protonation states of His, Phe, Tyr, and Trp. In these cases, therefore, it seems that the aromatic side chain may partially contribute to delocalize the radical located at the C_β atom and in fact these amino acids are among the most stable $INT_{C\beta}$ species.

The lower spin densities computed on the $INT_{C\alpha}$ species therefore explain why these stationary points are more stable than the $INT_{C\beta}$ ones. Furthermore, these values also show a clear tendency of a better delocalization of the radical (lower spin densities) on the $INT_{C\alpha}$ intermediates with β -sheet conformation than with α -helix-like conformation (see

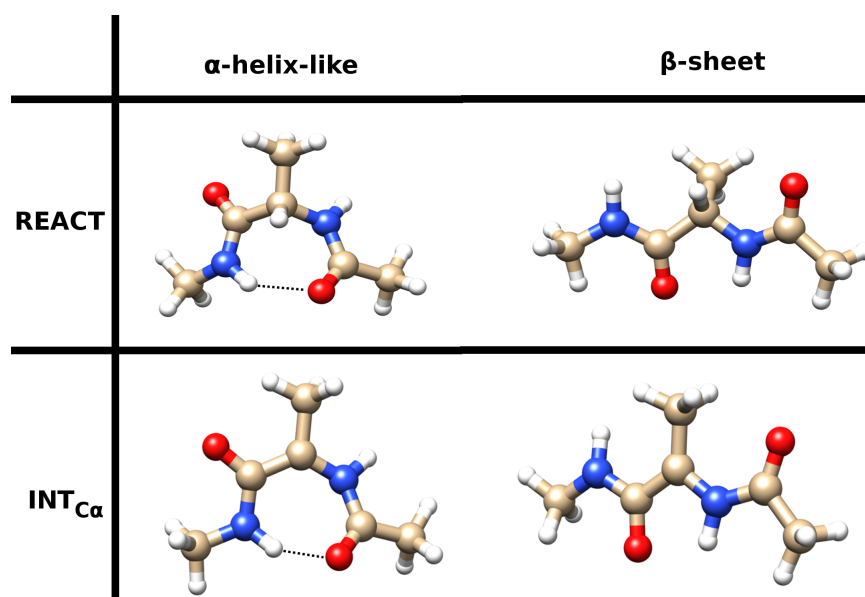


Figure 4.4: As illustrative example, the reactant (above) and $\text{INT}_{C\alpha}$ (below) species characterized for alanine with the two conformations considered: α -helix-like (left) and β -sheet (right).

Figure 4.5). This is not surprising as the completely planar arrangements of the former conformation maximizes the captodative effect. By contrast, the effect is not so optimum in the slightly out-of-plane backbone conformation adopted by the $\text{INT}_{C\alpha}$ intermediates with the α -helix-like conformation, what explains why the $\text{INT}_{C\alpha}$ species with this conformation are about 5-8 kcal/mol less stable than their planar counterparts.

Finally, the spin densities also indicate that the side chain has little effect in altering the captodative effect that occurs at the backbone, as the values are very similar for all amino acids. This may explain why there is not any clear correlation between the nature of the side chain and the ΔH_{aq} values of $\text{INT}_{C\alpha}$ species. Thus, based on these results, we hypothesize that steric effects rather than the electronic stability of the radical species formed determine ultimately the target of the radical attack.

4.2.2 Step 2: homolytic bond dissociation.

Once that the $\text{INT}_{C\beta}$ is formed the mechanism could proceed through a homolytic bond splitting of the backbone at $\text{N}-\text{C}_\alpha$ (Step_2^{NC}) or $\text{C}-\text{C}_\alpha$ (Step_2^{CC}) (see Figure 4.1). Note that these pathways are unlikely to occur departing from the $\text{INT}_{C\alpha}$ stationary points, due to the high stability of these bonds as a consequence of the captodative effect (higher bond orders are observed at both $\text{N}-\text{C}_\alpha$ and $\text{C}-\text{C}_\alpha$ bonds, see Table A.9) and only the reactions departing from $\text{INT}_{C\beta}$ will be presented. The ΔH_{aq} of the two reaction pathways computed for all amino acids are shown in Figure 4.6 and Table A.6. As in the first step, the two conformations of the peptide backbone were taken into account. However, the effect of the

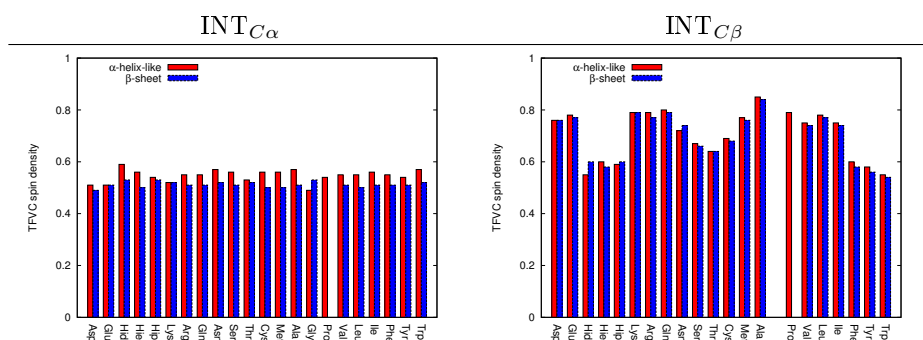


Figure 4.5: Topological Fuzzy Voronoi Cell spin densities computed at the C_α and C_β atoms of INT_{C_α} and INT_{C_β} species, respectively.

conformation is small in this reaction step (see Table A.7) and for the sake of simplicity, only the ΔH_{aq} corresponding to the β -sheet conformation will be discussed. Moreover, note that both the *cis* and *trans* isomers were considered for the non-radical products of all amino acids.

The results clearly shows that the $Step_2^{CC}$ is thermodynamically more favorable than $Step_2^{NC}$ for most of the studied amino acids (see Figure 4.6). With most of the amino acids the ΔH_{aq} of $PROD^{CC}$ is 10-18 kcal/mol more stable than the ΔH_{aq} of $PROD^{NC}$. The difference is even larger for Asn, while the difference is slightly smaller for Lys, Hid, Arg and Hip. The only exceptions with this trend are shown by Ser and Thr (see below). Thus, the ΔH_{aq} of $PROD^{CC}$ are in overall exothermic, specially with the *trans* isomer, which are in the 0/-4 kcal/mol range and about 0 to 4 kcal/mol more stable than the *cis*-products. The only four amino acids with positive ΔH_{aq} values are Ala (+2.4), Asp (+1.2), Glu (+0.4) and Arg(+6.4), while the amino acids with aromatic side chains present the most favorable reactivity: Hip (-7.8), Tyr (-6.3), Phe (-5.0) and Trp (-5.0). On the other hand, the $Step_2^{NC}$ step is clearly endothermic for all amino acids, except with the *cis* isomers of Ser and Thr (see below). Again, the *trans* isomer is in overall slightly more stable, in the 0-6 kcal/mol range. Noteworthy the difference of 8.9 kcal/mol with Thr due to a hydrogen bond, which is further discussed below.

As a result, Ser and Thr are the only amino acids for which both reactions are exothermic. In the case of Thr, the ΔH_{aq} values with the most stable isomer of the product are -5.3 and -6.3 kcal/mol for $Step_2^{CC}$ and $Step_2^{NC}$ steps, respectively. In the case of Ser, the ΔH_{aq} values are -1.0 and -0.5 kcal/mol for $Step_2^{CC}$ and $Step_2^{NC}$ steps, respectively. Therefore, even that the $Step_2^{CC}$ pathway is favorable, in line with most of the other amino acids, the alternative $Step_2^{NC}$ pathway is also favorable. This results are in agreement with the work of Thomas et al [121]. They attribute this change in the preferred cleavage pathway to the ability of the Ser and Thr side chain in forming stable hydrogen bonds at INT_β that weakens the C_α -N bond. Nevertheless, we computed the bond orders on all radical intermediates (see Table A.9) and in spite of the hydrogen bond interaction, not any relevant decrease of this parameter was observed for the C_α -N bonds of Ser and Thr, what should be expected if the bond is weakened due to the hydrogen bond interaction.

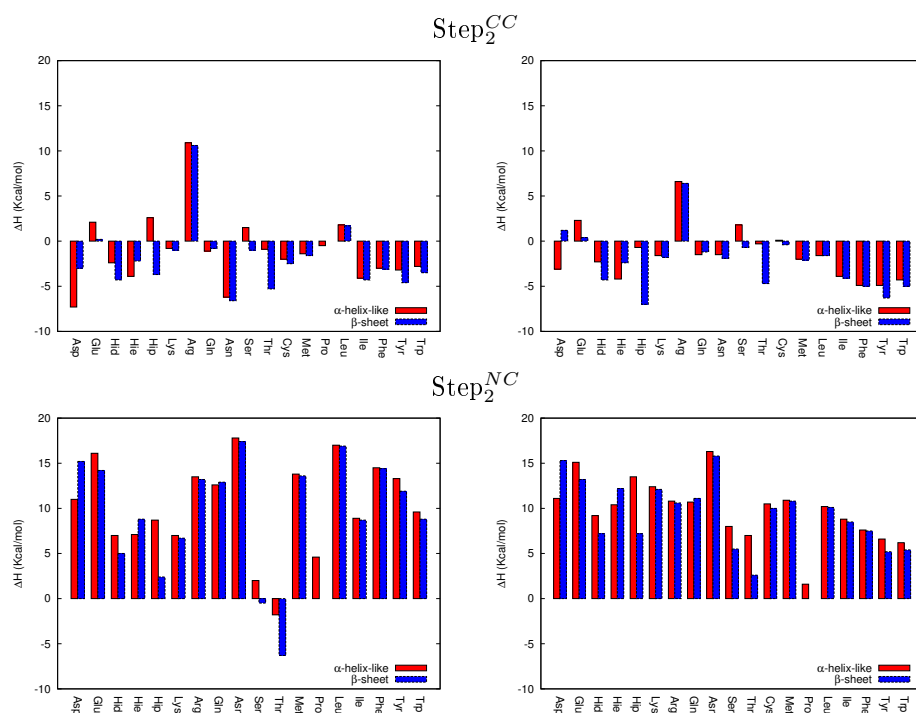


Figure 4.6: ΔH_{aq} values (in kcal/mol) of the homolytic splitting products (Step2 in Figure 4.1) obtained departing from the INT_{β} radical intermediate. Above, the values for the $C_{\alpha} - C$ bond cleavage; below, the values for the $C_{\alpha} - N$ bond cleavage. Two isomers were characterized for the non-radical product of each mechanism: *cis* (on the left) and *trans* (on the right).

4.2.2.1 Origin of the Ser and Thr preference for the $Step_2^{NC}$ step

As it can be seen in Figure 4.1, the non-radical product obtained from either of the two $Step_2$ pathways are analogous for each amino acid and therefore their stability can be directly compared. Thus, for each amino acid, four different isomers can be compared, corresponding to the *cis* and *trans* conformations of the $Step_2^{CC}$ and $Step_2^{NC}$ steps. The four products characterized for Thr, their relative ΔH_{aq} values (taking the *cis* product of $Step_2^{CC}$ as reference) and some additional electronic parameters are shown in Figure 4.7. Equivalent structures were obtained with Ser (data not shown). As it can be seen, the side chain alcohol group forms a hydrogen bond interaction only at the two *cis* products. However, the *cis* product of $Step_2^{NC}$ step is clearly more stable, about 9 kcal/mol more stable than the other three products, what may explain the preference for the $Step_2^{NC}$ step shown by the two amino acid.

In order to understand the origin of the different stabilities of the four products, we computed the electron localization at the alcohol oxygen of Thr side chain (λ_O) and delocalization indexes at the O-H alcohol bond (δ_{OH}) and between the alcohol H atom and either

carbonyl O (δ_{HO}) or peptide bond N atom (δ_{HN}) (data shown in Figure 4.7). The localization (λ) and delocalization (δ) indexes are physically unambiguous parameters that estimate the electron pairs localized on an atom or delocalized between two atoms, respectively, similar to the electron pairing described by a Lewis structure. *cis*-PROD^{NC} is the only structure that allows an electron delocalization between the alcohol group and the backbone, namely with the carbonyl oxygen: $\delta_{HO}=0.13$. By contrast, the equivalent delocalization values are very low in the other three structures: $\delta_{HO}=0.05$ in *cis*-PROD^{CC} and $\delta_{HN}=0.0$ in the two *trans* products. As a consequence of this electron delocalization, the $\delta_{OH}=0.43$ value is smaller and $\lambda_O = 8.41$ larger in *cis*-PROD^{NC} than in the other three product. Looking at the geometry of *cis*-PROD^{NC}, it can be observed that a six member ring is formed between the side chain and the backbone, what favors certain electron delocalization along the ring, not possible in the other products. This special arrangement thus provides an extra stabilization to the product, what explain why this product is significantly more stable than the other three.

In summary, the data presented agree with previous studies determining *cis*-PROD^{NC} as the most favorable product for Ser and Thr. However, our results indicate that the origin of this reaction mechanism is not due to a weakening of the bond at the intermediate, but rather to a particular structure of *cis*-PROD^{NC} with a six-member ring that allows a further electronic stabilization, not possible in the products of the Step₂^{CC}.

4.3 Conclusion

In this work the attack of $\bullet OH$ toward all natural amino acids have been investigated, considering different conformations and dielectrics. The work focuses on the H abstraction reaction at the C_α and C_β atoms of the amino acids, as they are the most likely target sites for the attack. The study also analyzes the homolytic dissociation of the C_α-C or C_α-N bonds, which are observed in the fragmentation of proteins upon their oxidation by $\bullet OH$, but also in experimental techniques such as FRIPS.

The results allow for the first time a complete analysis of the effect that the side chain may play in the reaction. Nevertheless, quite unexpectedly, the side chain has little effect on the stability of the radical intermediates and not any clear trend between the nature of the amino acid side chain and the reaction selectivity can be discerned. A negligible effect of the dielectric constant was determined as well. However, it must be taken into account that the model employed is not large enough to include other effects such as steric effects, the solvent accessible area of the target amino acid or the secondary structure of the protein, what may influence significantly the reaction preferences.

A clear effect of the peptide bond conformation was observed. Based on the two conformations of the amino acid considered herein, a preference of the β -sheet conformation over the α -helix-like conformation was distinguished when the radical attacks at the C_α atom to form INT_{C_α}. This preference on the β -sheet conformation is due to the completely planar intermediates formed, maximizing the captodative effect. By contrast, the analogous intermediates are slightly less planar with the α -helix-like conformation, decreasing the captodative effect and making them less stable.

The results clearly indicate that the H abstraction from the C_α atom is more favorable than the attack at the C_β atoms, certainly because the captodative effect can not take

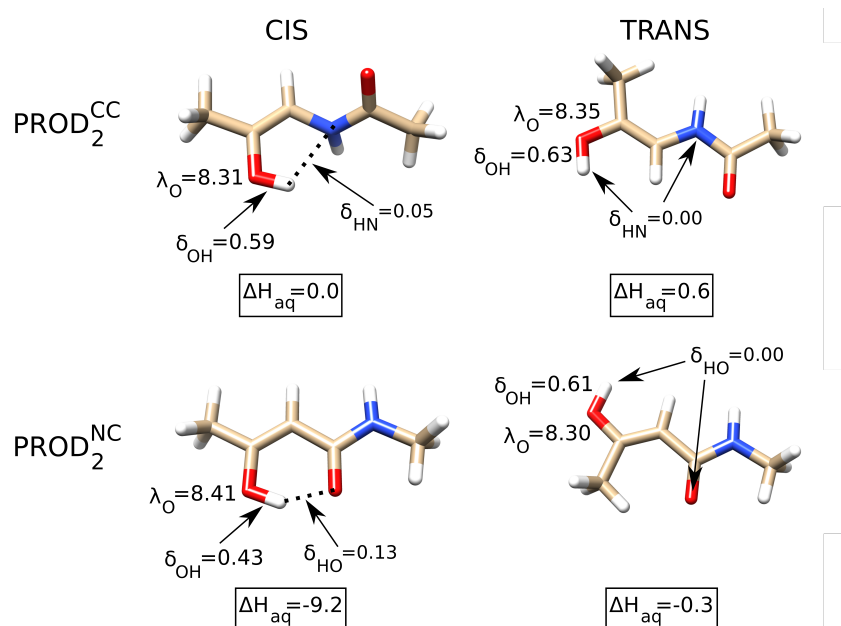


Figure 4.7: The *cis* and *trans* non-radical products characterized for the Step2^{CC} and Step2^{NC} steps of the Thr amino acid. Their relative enthalpies with respect to *cis* $C_\alpha - C$ product (ΔH_{aq} , in kcal/mol) are shown. In addition, three electronic parameters are shown: i) electron localization index at the alcohol oxygen (λ_O), ii) electron delocalization index at the O-H alcohol group bond (δ_{OH}) and iii) electron delocalization index at bond between the alcohol H and carbonyl oxygen (δ_{HO}) or peptide bond nitrogen (δ_{HN}).

place in $INT_{C\beta}$. Moreover, this radical intermediate does not show any preference for conformation and no significant variation is observed at the backbone atoms or the bond orders. The lowest spin densities are obtained for the aromatic amino acid $INT_{C\beta}$, where the aromatic ring allows the delocalization of the unpaired electron, stabilizing the $INT_{C\beta}$ structure.

Therefore, the study predicts that the formation of the $INT_{C\alpha}$ radical intermediate is energetically more favorable, which is prompted to undergo other reactions due its high reactivity. However, the experimental evidences indicate that the $INT_{C\beta}$ can also be formed, what may lead to a backbone bond cleavage and trigger the fragmentation of the protein. The computed ΔH_{aq} values indicate that the scission of the C-C $_{\alpha}$ bond is the most favorable splitting mechanism for the vast majority of the amino acids. Thr and Ser are the only two amino acids in which both the C-C $_{\alpha}$ and C $_{\alpha}$ -N bonds cleavage are competitive. The reason for this difference lies on the higher stability achieved by the non-radical products of these two amino acids when they present the *cis* conformation. On these structures, a stable six-member ring is formed between the side chain and the backbone, allowing a strong hydrogen bond interaction between the alcohol group and the peptide bond carbonyl oxygen, not possible in any other product or with any other amino acid. Thus, the results confirm that the cleavage of the C $_{\alpha}$ -N bond is favored with Ser and Thr due to a higher stability of the products formed.

Chapter 5

The Attack Of $\bullet OH$ Onto Aromatic Amino Acids

The attack of $\bullet OH$ to aromatic amino acid side chains, namely, phenylalanine, tyrosine and tryptophan, have been studied. Two reaction mechanisms have been considered: i) addition reactions to the aromatic ring atoms, and ii) hydrogen abstraction from all possible atoms of the side chains. The thermodynamics and kinetics of the attack of a maximum of two $\bullet OH$ have been studied, considering the effect of different protein environments at two different dielectric values, 4 and 80. The obtained theoretical results explain how the radical attacks take place and provide new insight into the reasons for the preferential mechanism. The results indicate that even that the attack of the first $\bullet OH$ at an aliphatic C atom is energetically favored, the larger delocalization and concomitant stabilization obtained by attacking the aromatic side chain prevail. Thus, the obtained theoretical results are in agreement with the experimental evidences that the aromatic side chain is one of the main target for the radical attack and show that first the $\bullet OH$ is added to the aromatic ring while a second radical abstracts a proton at the same position to get the oxidized product. Moreover, the results indicate that the reaction can be favored in buried region of the protein.

5.1 Introduction

Herein the reaction paths concerning the sequential attack of two $\bullet OH$ onto phenylalanine, tyrosine and tryptophan amino acid side chains is presented. Two type of reactions have been considered: i) $\bullet OH$ addition to the aromatic ring, with the formation of adduct radicals, and ii) H abstraction, in which a hydrogen abstracted from all possible side chain atoms by the radical to yield a radical intermediate and a water molecule (see Figure 5.1B). In both cases, the transition states, which determine the kinetics of the reactions, and intermediates were characterized. Then, the attack of a second radical onto the radical intermediate was analyzed. Since this step involves the reaction between two radical species, no stable transition state is expected, and therefore, only the final products were characterized. Thus, the kinetics of the reactions are determined by the energy barrier of the first step. Note that the final products are the result of a sequential attack of two hydroxyl radicals onto the

amino acid by an abstraction and an addition reaction, regardless the order in which they take place. Therefore, the entire reaction pathway can be considered as a substitution of a hydrogen by the hydroxyl group, and it can only take place in those C atoms with at least one hydrogen atom.

Two type of reactions have been considered (see Figure 5.1B), the hydrogen abstraction by the radical, and the addition of this species to the aromatic rings of the amino acid side chains. In the three cases, the attack of $\bullet OH$ onto all possible positions in the amino acid side chains were considered. The obtained results provide valuable data in elucidating which are the most favored oxidized products, both thermodynamically and kinetically, along with the favored mechanisms of these reactions.

5.2 Results

The results are given for each amino acid, dividing the reaction at two stages where a single $\bullet OH$ is introduced at each stage.

5.2.1 Phenylalanine

Reaction paths for the attack by two $\bullet OH$ to the side chain of phenylalanine are described in this subsection. As mention above, two reaction mechanisms have been considered: i) addition to the double-bonded ring carbon atoms and ii) hydrogen abstraction. The entire process involves a two-step pathway in which the two mechanisms are combined sequentially, i.e, addition/abstraction or abstraction/addition.

Attack of a first $\bullet OH$. The addition of a $\bullet OH$ onto each of the six C atoms forming the aromatic ring, and the hydrogen abstraction from each of the six C atoms of the side chain (atoms of the aromatic ring and the C_β atom, C7 in Figure 5.1A) of the amino acid side chain residue have been calculated. The main geometrical parameters, spin densities at radical O atom and attacked C atom, and enthalpies of all these reaction mechanisms at two different dielectrics (4 and aq) are given in Table 5.1. The optimized stationary points of the attack of $\bullet OH$, both for addition and abstraction, onto C1 are illustrated in Figure 5.2 as example.

The enthalpy barriers of all the addition reactions are very low, and in some cases they show negative values. Note that these values are calculated compared to infinitively separated reactants. We have characterized one of the possible reactant complex formed by the phenylalanine and hydroxyl radical (see Figure 5.2). This complex is energetically slightly below all the transition states. Note that, considering all the reaction mechanisms involved, a large number of reactant complexes and reactant products are expected, without significantly altering the conclusions of this work. Therefore, hereafter no reactant complexes or product complexes will be considered. In five of the six addition reaction pathways the enthalpy barriers are in the -1.0/1.0 kcal/mol with $\epsilon = 4$ and in the 1-2 kcal/mol

·OH Addition										
	r_{CO}^{TS}	ΔH_4^{TS}	ΔH_{aq}^{TS}	ρ_s^O	ρ_s^C	r_{CO}^{int}	ΔH_4^{int}	ΔH_{aq}^{int}	ρ_s^O	ρ_s^C
C1	1.985	-0.4	1.1	0.65	-0.15	1.425	-18.0	-17.2	0.02	-0.16
C2	1.969	1.0	1.7	0.65	-0.16	1.423	-16.3	-16.0	0.02	-0.15
C3	1.974	0.4	1.0	0.65	-0.15	1.423	-18.0	-17.0	0.02	-0.09
C4	1.965	1.0	1.7	0.64	-0.17	1.419	-16.5	-15.5	0.02	-0.18
C5	2.011	-4.5	-1.3	0.62	-0.13	1.434	-17.7	-15.1	0.02	-0.23
C6	1.999	-0.5	0.6	0.64	-0.11	1.442	-18.6	-14.9	-0.03	-0.09
H Abstraction										
	r_{OH}^{TS}	ΔH_4^{TS}	ΔH_{aq}^{TS}	ρ_s^O	ρ_s^C	ΔH_4^{int}	ΔH_{aq}^{int}			
C1	1.236	1.240	4.1	4.9	0.58	0.41	-4.6	-4.9		
C2	1.241	1.228	3.7	4.1	0.58	0.42	-4.7	-5.5		
C3	1.240	1.229	4.1	4.7	0.58	0.42	-4.2	-4.9		
C4	1.248	1.219	5.3	6.7	0.57	0.48	-5.4	-6.2		
C5	1.259	1.208	2.2	5.4	0.56	0.46	-4.9	-5.4		
C7	1.149	1.524	0.1	3.2	0.78	0.32	-29.7	-29.1		

Table 5.1: Enthalpy values (in kcal/mol) computed in a dielectric constant of 4 and 80 (aqueous solution) at the transition states and radical intermediates for the attack of the first OH radical onto phenylalanine, considering two reaction mechanisms: addition and abstraction. The C-O distance in addition and C-H and O-H in abstraction (in Å) are also shown. The spin densities at the radical O atom (ρ_s^O) and target C atom (ρ_s^C) are also presented.

range with $\epsilon = 80$. The exception is the addition on C5 atom, since the hydrogen bond interaction between the oxygen atom of the hydroxyl radical and the proton of an amide group has decreased the ΔH_4^{298} and ΔH_{aq}^{298} values to -4.5 and -1.3 kcal/mol, respectively. On the other hand, the energy barriers for H abstraction from the aromatic ring atoms are significantly larger, with values ranging 3.7-5.3 kcal/mol for ΔH_4^{298} and 4.1-6.7 kcal/mol for ΔH_{aq}^{298} . Clearly, the attack of a radical to the aromatic ring atoms favors the formation of the adduct intermediates, as could be expected. However, the energy barrier for the H abstraction from the aliphatic C7 atom is similar to those of addition reactions. Therefore, from a kinetic point of view, the addition to aromatic ring and H abstraction from C7 are competitive processes. Thermodynamically, however, the abstraction from C7 is clearly favored. ΔH_4^{298} and ΔH_{aq}^{298} values are close to -29 kcal/mol, about 14 kcal/mol more stable than the intermediates formed by the addition of the hydroxyl radical.

Let us focus now on the geometrical parameters of these reactions. In the addition reactions, the $\bullet OH$ approaches the attacked C atom perpendicular to the aromatic ring, resulting in a similar $O_{OH}C$ distance at all transition states characterized, in the range of 1.97-2.01 Å. The longest distance is found at the transition state corresponding to the attack at C5 carbon (2.011 Å), due to a hydrogen bond interaction between O_{OH} and the H_{NH} atom of the backbone (O_{OH} -HN distance of 1.913 Å). Once the attack takes place, a radical intermediate is formed. The $O_{OH}C$ distances are similar in all characterized intermediates, ranging between 1.42-1.44 Å. Again, the proximity of the backbone determines the length of this distance and the hydrogen bond interaction between O_{OH} and H_{NH} lengthens the O_{OH} -C distance to 1.434 and 1.442 Å in Int_{Phe}^{C5Add} and Int_{Phe}^{C6Add} , respectively. In the abstraction reaction from the aromatic ring, the hydroxyl radical approaches in the same plane as the ring, leading to very similar geometrical features in all reaction pathways characterized. In the transition state, the finally abstracted hydrogen is shared by the hydroxyl O atom and the ring C atom, being both distances ca 1.2 Å. For the hydrogen abstraction from the aliphatic C7 atom, however, the transition state occurs at an earlier stage, being the hydrogen atom closer to the C atom (1.149 Å) than to the oxygen atom (1.524 Å). This is in agreement with the calculated smaller reaction barriers.

Finally, we analyze the spin density at the O_{OH} atom (ρ_s^O) and at the target C atom (ρ_s^C), which indicates the evolution of the location of the radical character along the reaction coordinates. In the case of addition reactions, the trend is similar for all aromatic carbon atoms. For infinitely separated atoms, the radical character is fully localized at the O atom of the hydroxyl radical. Then, in TS structures, ρ_s^O reduces to ~ 0.65 . Note that ρ_s^C is ~ -0.15 , denoting a delocalization of the remaining radical character (~ -0.20) along the aromatic ring. In the adducts, the radical character is fully delocalized at the aromatic ring, as one may deduce from the values of ~ 0.02 and ~ -0.15 for ρ_s^O and ρ_s^C , respectively. The behavior of the spin density is different for H abstraction reaction.

For the abstraction from the aromatic ring, the radical character is roughly 60% at the O atom, and 40% at the C atom. Hence, the radical character is completely localized at the O_{OH} and attacked C atoms. On the other hand, the radical character at O_{OH} is enlarged to 78% in the attack to the aliphatic C7 atom, which is in agreement with the fact that there is an earlier TS in this case, and, as a consequence, the radical character is less transferred to C7.

Attack of a second $\bullet OH$ Due to its high reactivity, the radical intermediate formed after the reaction of phenylalanine with a first hydroxyl radical is prompted to react with a second hydroxyl radical to form a non-radical product. As it was pointed out previously, the reaction can take place only in those C atoms with at least one hydrogen atom. This fact reduces the possibilities to five C atoms in the aromatic ring and the C7 atom. In addition, note that H abstraction from the C_α would lead to the formation of a double bond between these carbons close to the aromatic ring. This process could be favored thermodynamically due to the formation of an extra conjugated double bond near the aromatic ring. Therefore, in this special case abstraction from the backbone has been considered. The reaction enthalpies of all these products are presented in Table 5.2.

	ΔH_4^{298}	ΔH_{aq}^{298}
Prod $_{Phe}^{C1}$	-117.1	-116.6
Prod $_{Phe}^{C2}$	-116.9	-116.7
Prod $_{Phe}^{C3}$	-116.5	-116.2
Prod $_{Phe}^{C4}$	-116.4	-115.1
Prod $_{Phe}^{C5}$	-115.9	-114.5
Prod $_{Phe}^{C7}$	-111.0	-108.4
Prod $_{Phe}^{C7\alpha}$	-102.5	-100.6

Table 5.2: Enthalpy values (in kcal/mol) computed in a dielectric constant of 4 and 80 (in aqueous solution) and calculated with respect to the initial reactants of the products formed by the attack of a second hydroxyl radical onto phenylalanine.

The oxidation of a C atom located in the aromatic ring is a very favorable reaction. The enthalpy values are very similar for the five products, with ΔH_{aq}^{298} values in the -114/-117 kcal/mol range. In all cases, the ΔH_4^{298} values are very similar. In spite of the small differences between them, a deeper analysis of the ΔH_{aq}^{298} values indicate that the oxidation reaction at C1 and C2 atoms shows the most favorable enthalpies with a ΔH_{aq}^{298} of -117 kcal/mol, followed by a value of -116 when the oxidation take place at C3, while at the C4 and C5 the values are -115 and -114. These values suggest that there is not any preference on the ring position and that the attacks of the hydroxyl radical are equally likely at ortho-, metha- or para- positions, but instead the position of the ring with respect to the backbone may influence the final stability of the product, without considering steric effects.

Departing from the radical intermediate formed by the abstraction of a hydrogen atom from the aliphatic C7 carbon (Int $_{Phe}^{C7ab}$), two alternative products can be formed: addition of the second hydroxyl group at C7 (Prod $_{Phe}^{C7}$) or abstraction of the hydrogen from the C_α atom (Prod $_{Phe}^{C7\alpha}$). The ΔH_{aq}^{298} values for these stationary points show that the Prod $_{Phe}^{C7}$ is more stable, with a value of -108.4 kcal/mol. However, even that Int $_{Phe}^{C7ab}$ is clearly the most stable radical intermediate, the oxidation at C7 is ca. 8 kcal/mol less stable than the oxidation at any of the aromatic C atom. Therefore, if the radical concentration is large enough to allow for two hydroxyl molecules reaching the phenylalanine side chain, the oxidation of any of the aromatic ring atoms would be the most favored products, due to thermodynamical, kinetic and steric reasons.

5.2.2 Tyrosine

Reaction paths for the attack by two $\bullet OH$ to the double-bonded ring carbon atoms and hydrogen abstractions from all possible atoms of the amino acid side chain of tyrosine are described in this subsection.

Attack of a first $\bullet OH$ The difference between phenylalanine and tyrosine side chains is a hydroxyl group at para position in the aromatic ring, at C3. Therefore, the studied addition reactions are in tyrosine similar to previously studied processes in phenylalanine, but H abstraction now takes place from O8 instead of from C3. The main geometrical parameters, spin densities at radical O atom and at the target atom, and enthalpies of all these reaction mechanisms at two different dielectrics (4 and aq) are given in Table 5.3. The optimized stationary points are not depicted for the sake of brevity, since they resemble those of phenylalanine.

The potential energy surfaces of the addition of the first hydroxyl radical onto the aromatic C atoms of tyrosine resemble those computed for phenylalanine. Therefore, the hydroxyl group present in tyrosine has little effect on the hydroxyl radical's addition. The calculated energy barriers, ΔH_4^{298} in the -3.4/2.5 kcal/mol range, and the ΔH_{aq}^{298} values in the -1.1/-4.3 kcal/mol range, are similar to those obtained for phenylalanine, although with larger differences. The highest barrier found in the radical attack onto the C3 atom can be due to the influence of the hydroxyl group located at this C atom. On the other hand, the attacks onto the C5 and C6 atoms show the lowest barriers, due certainly to the influence of the backbone. The enthalpy of the radical intermediate adducts are close in energy, as it was for phenylalanine. At $\epsilon = 4$, the most stable structure is Int_{Tyr}^{C6} with a value of -19.5 kcal/mol, and Int_{Tyr}^{C1} is the less stable one with a relative enthalpy of -16.7 kcal/mol. On the other hand, in aqueous solution Int_{Tyr}^{C3} is the most stable intermediate with a ΔH_{aq}^{298} value of -17.8 kcal/mol, and Int_{Tyr}^{C1} the less stable one with a value of -14.4 kcal/mol.

As in the case of phenylalanine, energy barriers for the hydrogen abstraction from the aromatic ring are slightly larger than for addition reactions, with enthalpy barriers ca. 6-7 kcal/mol. Note that thermodynamically, these processes are also less favorable. However, H abstraction from both C7 and O8 show similar energy barriers as addition processes, but thermodynamically both processes are favored by around 12 kcal/mol. Sterically, abstraction from O8 would be favorable compared to C7, and, therefore, these results suggest that the attack of a first hydroxyl radical would eventually abstract a hydrogen atom from O8 position, rather than other abstraction or addition processes. In this concrete case, the hydroxyl O atom approaches to 1.456 Å to the abstracted H, while the O8-H distance is very slightly enlarged to 0.988 Å. This early TS geometry is in agreement with the calculated small barrier. Note that the spin density located at the hydroxyl O is larger than in the cases of the abstraction from the aromatic carbon atoms. Note that the geometrical and spin density analysis for the remaining cases is very similar to those of phenylalanine.

Attack of a second $\bullet OH$ The radical intermediate formed after the reaction of tyrosine with a first hydroxyl radical is prompted to react with a second hydroxyl radical to form a non-radical product. The reaction enthalpies of all the products characterized are presented in Table 5.4.

$\bullet\text{OH}$ Addition										
	r_{CO}^{TS}	ΔH_4^{TS}	ΔH_{aq}^{TS}	ρ_s^O	ρ_s^C	r_{CO}^{Int}	ΔH_4^{Int}	ΔH_{aq}^{Int}	ρ_s^O	ρ_s^C
C1	1.981	0.9	2.3	0.64	-0.17	1.426	-16.7	-15.7	0.02	-0.13
C2	1.996	0.6	0.8	0.66	-0.11	1.418	-18.1	-17.2	0.02	-0.09
C3	2.005	2.5	4.3	0.63	-0.12	1.420	-18.9	-17.8	0.03	-0.10
C4	2.000	1.1	3.2	0.57	-0.04	1.425	-18.2	-15.9	0.01	-0.27
C5	2.036	-3.4	-0.3	0.62	-0.12	1.438	-17.0	-14.4	0.02	-0.19
C6	2.034	-1.8	-1.1	0.64	-0.11	1.446	-19.5	-15.9	0.02	-0.09
H Abstraction										
	r_{XH}^{TS}	r_{OH}^{TS}	ΔH_4^{TS}	ΔH_{aq}^{TS}	ρ_s^O	ρ_s^C	ΔH_4^{Int}	ΔH_{aq}^{Int}		
C1	1.236	1.239	5.2	5.9	0.59	0.39	-3.7	-3.6		
C2	1.264	1.194	6.2	6.9	0.57	0.35	-2.2	-2.6		
C4	1.245	1.236	5.8	8.8	0.54	0.38	-2.6	-2.5		
C5	1.260	1.205	3.0	6.2	0.56	0.46	-3.8	-4.2		
C7	1.141	1.575	0.9	4.1	0.79	0.29	-29.6	-29.1		
O8	0.988	1.456	2.4	4.8	0.68	0.20	-29.3	-28.8		

Table 5.3: Enthalpy values (in kcal/mol) computed in a dielectric constant of 4 and 80 (aqueous solution) at the transition states and radical intermediates for the attack of the first OH radical onto tyrosine, considering two reaction mechanisms: addition and abstraction. The C-O distance in addition and C-H and O-H in abstraction (in Å) are also shown. The spin densities at the radical O atom (ρ_s^O) and target C atom (ρ_s^C) are also presented.

	ΔH_4^{298}	ΔH_{aq}^{298}
Prod $_{Tyr}^{C1}$	-116.5	-115.9
Prod $_{Tyr}^{C2}$	-114.9	-113.4
Prod $_{Tyr}^{C4}$	-114.1	-111.6
Prod $_{Tyr}^{C5}$	-116.4	-113.6
Prod $_{Tyr}^{C7}$	-111.0	-108.5
Prod $_{Tyr}^{C7\alpha}$	-101.3	-99.6
Prod $_{Tyr-Tyr}^{OO}$	-37.3	-30.9
Prod $_{Tyr-Tyr}^{22}$	-107.7	-104.5

Table 5.4: Enthalpy values (in kcal/mol) computed in a dielectric constant of 4 and 80 (in aqueous solution) and calculated with respect to the initial reactants of the products formed by the attack of a second hydroxyl radical onto tyrosine.

As in phenylalanine, the attack of a second radical onto the aromatic carbon atoms produces very stable oxidized products. The ΔH_{aq}^{298} of the four possible oxidized products (in orho- and meta- positions) are in the -111/-116 kcal/mol range. Among them, the most stable product corresponds to the oxidation at the C1 atom, with ΔH_4^{298} and ΔH_{aq}^{298} value \sim -116 kcal/mol. These thermodynamical data do not explain the experimental formation of 2,3- and 3,4-dihydroxyphenylalanine (DOPA), and not 1,3 or 3,5-dihydroxyphenylalanine. Even that the difference in the enthalpy values are small, the formation of the final DOPA products are driven by factors other than thermodynamics (see Discussion).

The most stable radical intermediates were formed by the hydrogen abstraction from the C7 and O8 atoms. From Int $_{Tyr}^{C7ab}$, two alternative products have been considered: addition of the radical to get the oxidized product (Prod $_{Tyr}^{C7}$) or a second abstraction from C $_{\alpha}$ to form a double bond between this atom and C7. The addition at C7 shows a ΔH_{aq}^{298} of -108.5 kcal/mol, 3/5 kcal/mol less stable than the attack onto an aromatic C atom; the abstraction from C $_{\alpha}$ is less favorable with an enthalpy of -99.6 kcal/mol. Therefore, as with phenylalanine, these two reactions are less favorable than the oxidation reaction at the aromatic ring.

Finally, the exposure of tyrosine to radicals may produce some bi-tyrosine cross-linked species (see Figure 5.1A) which are formed by the reaction of two tyrosine radical intermediates. In the present work, two bi-tyrosine molecules have been characterized departing from the Int $_{Tyr}^{C2}$ or Int $_{Tyr}^{O8}$ intermediates (shown in Figure 5.3), that is, the products of the cross-linked through the C2 and O8 atoms, respectively. The enthalpy values are negative for both bi-tyrosine species, and the cross-linked through the C2 atoms is much more stable than the linked through the O8 atoms, as they show ΔH_{aq}^{298} values of -104.5 and -30.9 kcal/mol respectively. These results are in agreement with the bi-tyrosine species characterized experimentally where they are linked by aromatic C atoms. However, the reaction is thermodynamically less favorable than the oxidation reaction what may suggest that the bi-tyrosine species are formed due to other factors (see Discussion).

5.2.3 Tryptophan

The side chain of tryptophan differs significantly from those of phenylalanine and tyrosine, since it is composed by a bicyclic indole group with a 6-member and 5-member rings. The exposure of tryptophan to $\bullet OH$ leads to several products, according to experimental evidence (see Figure 5.1A). Reaction paths for the attack by two $\bullet OH$ to the double-bonded ring atoms of tryptophan are studied in this subsection. Note that for H abstraction the C_β (C10) has also been considered, as for phenylalanine and tyrosine.

Attack of a first $\bullet OH$ Five addition reactions onto the two rings of tryptophan have been characterized, namely at the C2, C3, C4, C5 and C8 atoms. Notice that the addition of the radical onto the N7 atom does not lead to a stable stationary point, due to fact that it is not doubly bonded to any of the neighbour atoms. The considered H abstractions are from the above mentioned C atoms, along with from N7 and C10. The main geometrical parameters, spin densities at radical O atom and at the target atom, and enthalpies of all these reaction mechanisms at two different dielectrics (4 and aq) are given in Table 5.5

The enthalpy barriers of the addition processes, as in the previous cases of phenylalanine and tyrosine, are small. The addition to C8 atom is the most favorable one, as the ΔH_4^{TS} and ΔH_{aq}^{TS} values of -5.7 and -4.8 kcal/mol indicate. According to the intermediate radical formation enthalpies, Int_{Trp}^{C8ad} is also the most stable intermediate with a ΔH_{aq}^{298} value of -27.4 kcal/mol, followed by Int_{Trp}^{C2ad} (-21.2 kcal/mol); the ΔH_{aq}^{298} of the remaining intermediates are in the -15-19 kcal/mol range. Therefore, the enthalpies computed for the attacks onto the C2-5 atoms is comparable to the attacks onto the aromatic rings of phenylalanine and tyrosine, but the enthalpy of Int_{Trp}^{C8ad} is about 10 kcal/mol more stable, and that of Int_{Trp}^{C2ad} about 5 kcal/mol more stable. These results show that addition of the first $\bullet OH$ to these atoms are the most favored addition processes in all aromatic amino acid side chains.

Let us focus now on the enthalpies calculated for the H abstraction processes. According to enthalpy barriers and intermediate formation enthalpies, two separated cases are clearly distinguished. On one hand, the H abstraction from the C atoms of the six-member ring show enthalpy barriers of about 5 kcal/mol. The ΔH_{aq}^{298} values of the intermediates are -3/-4 kcal/mol, thus about 10 kcal/mol less stable than the radical addition at the same C atoms.

On the other hand, the most reactive positions for the H abstraction are those of N7 in the 5-member aromatic ring, and C10 position (as in tyrosine and phenylalanine). The enthalpy barriers for the abstraction from these two atoms are competitive with addition processes, but more importantly the ΔH_{aq}^{298} values of the intermediates are -24.6 for Int_{Trp}^{N7ab} and -27.7 kcal/mol for Int_{Trp}^{C10ab} . Finally, mention that all attempts to characterize the transition state for the abstraction from C8 failed, apparently due to the influence of the backbone. Nevertheless, the ΔH_{aq}^{298} for C8 is the only endothermic process and the energy barrier is therefore expected to be the largest one.

Let us focus now on the geometrical parameters of these reactions. In the addition reactions, the $\bullet OH$ approaches the attacked C atom perpendicular to the aromatic ring, resulting in a similar $O_{OH}C$ distance at all transition states characterized, in the range of 2.0-2.1 Å, with the exception of the attack to C8, which shows the longest distance at

·OH Addition										
	r_{CO}^{TS}	ΔH_4^{TS}	ΔH_{aq}^{TS}	ρ_s^O	ρ_s^C	r_{CO}^{Int}	ΔH_4^{Int}	ΔH_{aq}^{Int}	ρ_s^O	ρ_s^C
C2	2.107	0.1	2.0	0.69	-0.12	1.431	-24.4	-21.2	0.00	-0.15
C3	1.975	0.7	1.2	0.62	-0.11	1.429	-15.3	-14.8	0.01	-0.13
C4	2.002	-0.4	0.0	0.64	-0.14	1.427	-17.7	-17.4	0.02	-0.14
C5	2.043	-0.8	-0.1	0.67	-0.11	1.423	-19.8	-19.0	0.02	-0.16
C8	2.125	-5.7	-4.8	0.66	-0.08	1.405	-28.6	-27.4	0.00	-0.01
H Abstraction										
	r_{XH}^{TS}	r_{OH}^{TS}	ΔH_4^{TS}	ΔH_{aq}^{TS}	ρ_s^O	ρ_s^C	ΔH_4^{Int}	ΔH_{aq}^{Int}		
C2	1.209	1.296	1.7	4.4	0.60	0.37	-4.4	-4.2		
C3	1.238	1.234	4.7	5.3	0.58	0.41	-3.1	-3.4		
C4	1.239	1.231	4.9	5.3	0.59	0.44	-3.3	-3.8		
C5	1.243	1.232	5.8	7.0	0.56	0.36	-2.1	-2.2		
N7	1.071	1.416	2.2	5.0	0.57	0.24(N)	-24.5	-24.6		
C8							3.3	3.1		
C10	1.145	1.530	-1.6	0.1	0.78	0.25	-28.7	-27.7		

Table 5.5: Enthalpy values (in kcal/mol) computed in a dielectric constant of 4 and 80 (aqueous solution) at the transition states and radical intermediates for the attack of the first OH radical onto tryptophan, considering two reaction mechanisms: addition and abstraction. The C-O distance in addition and C-H and O-H in abstraction (in Å) are also shown. The spin densities at the radical O atom (ρ_s^O) and target C atom (ρ_s^C) are also presented.

the transition state (2.125 Å) and the shortest in the intermediate (1.405 Å). This is in agreement with calculated smaller barriers and larger stability of the intermediate radical. In the abstraction reaction, the most favored processes (abstraction from N7 and C10), show the longest distance between the O of the hydroxyl radical and the abstracted H, and the shortest distance between the atom of the aromatic ring and the abstracted reaction. These distances show that the TS occur in these cases at a much earlier stage, and therefore, they agree with the smaller barriers calculated for these processes.

We also analyze the spin density at the O_{OH} atom (ρ_s^O) and at the target C (or N) atom (ρ_s^C). In the case of addition reactions, the trend is analogous for all aromatic carbon atoms and similar to the trends observed with phenylalanine and tyrosine. Thus, in the infinitely separated reactants the radical character is fully localized at the O atom of the hydroxyl radical, in TS structures ρ_s^O reduces to ~ 0.65 and part of the radical character has begun to delocalize along the aromatic rings, while in the adducts is fully delocalized at the aromatic ring. On the other hand, at the transition states of the H abstraction reaction the radical character is not delocalized in the ring and instead is completely localized at the O_{OH} and attacked ring atom. The exception is the attack at the N atom, where there is around 20% of the radical character delocalized along the other ring atoms. The stability gained by this delocalization along the remaining ring atoms explains the calculated low enthalpic data. Finally, the radical character at O_{OH} is enlarged to 78% in the attack to C10 indicating that the radical character is less transferred to C10, which is in agreement with the earlier TS found for this reaction pathway. Recall that for other aromatic amino acid side chains, similar behavior at the C_β was observed.

Attack of a second $\bullet OH$ As with the other aromatic amino acids, the oxidation of the side chain atoms with a H atom have been considered, including the aliphatic C10 atom. As in phenylalanine and tyrosine, the product formed by the H abstraction from the C_α to form a double bond between itself and C_β has also been characterized. The reaction enthalpies of all the products characterized are presented in Table 5.6.

	ΔH_4^{298}	ΔH_{aq}^{298}
Prod $_{Trp}^{C2}$	-116.2	-114.4
Prod $_{Trp}^{C3}$	-113.9	-113.7
Prod $_{Trp}^{C4}$	-114.6	-114.6
Prod $_{Trp}^{C5}$	-114.6	-114.0
Prod $_{Trp}^{N7}$	-74.7	-71.4
Prod $_{Trp}^{C8}$	-123.5	-118.2
Prod $_{Trp}^{C10}$	-111.6	-109.3
Prod $_{Trp}^{C10\alpha}$	-104.6	-105.6

Table 5.6: Enthalpy values (in kcal/mol) computed in a dielectric constant of 4 and 80 (in aqueous solution) and calculated with respect to the initial reactants of the products formed by the attack of a second hydroxyl radical onto tryptophan.

The ΔH_{aq}^{298} values of the oxidized products formed when the second radical attacks the adduct radicals formed in the six-member aromatic ring are very similar, with values of ca -114 kcal/mol. These values are very close to the enthalpies computed for the attack onto the phenylalanine or tyrosine aromatic rings. Interestingly, the attack at the C8 atom present in the five-member ring is the most stable product, with ΔH_4^{298} and ΔH_{aq}^{298} values of -123.5 and -118.2 kcal/mol.

Even that Int_{Trp}^{N7ab} is the most stable adduct formed by the attack of the first $\bullet OH$ at the bicyclic group, Prod_{Trp}^{N7} is ca. 35 kcal/mol less stable. Similarly, the two products that can be formed from the intermediate formed by the H abstraction from the aliphatic C10 atom, Prod_{Trp}^{C10} and $\text{Prod}_{Trp}^{C10\alpha}$, are 10 kcal/mol less stable than Prod_{Trp}^{C8} .

5.3 Discussion

It is well known that the side chain of aromatic amino acids are the target of hydroxyl radicals to form a variety of products (see Fig 5.1A). However, information about kinetic and thermodynamics data about all possible reaction pathways is necessary in order to a better understanding of the process.

The data presented in this work indicate that the thermodynamics of the reaction is the main driving force and prevail over the kinetic of the reaction. The enthalpy barriers computed are in general low (the highest ΔH_{aq}^{298} value is 7.0 kcal/mol) and the difference in the energy barriers of the different reaction pathways characterized is small, in most of the cases within the method uncertainty. On the other hand, a larger difference is found between the relative enthalpies of the radical intermediates and products characterized for the same reaction mechanisms. Therefore, the thermodynamics data may help shedding light on the preferential targets and pathways followed by the radical when attacks an aromatic amino acid.

This work has considered that the oxidation of any of the aromatic amino acid involves the sequential attack of two $\bullet OH$ onto the amino acid going through a radical intermediate. The attack may take place by an addition of the radical or by the abstraction of a hydrogen from the amino acid. The thermodynamics results collected for all possible reaction pathways are analogous for the three aromatic amino acids considered. For phenylalanine and tyrosine, the radical intermediates formed after the addition of the radical at any of aromatic positions is roughly 12 kcal/mol more stable than the intermediates formed after a hydrogen abstraction. These data therefore predict that the first radical attack is added to form the radical intermediate, and that the second radical abstracts a hydrogen from the C atom to form the oxidized product.

This reaction pathway was consistent for all aromatic C atoms of Phe and Tyr. However, the most stable radical intermediates characterized with these two amino acids do not correspond to the addition at any of these atoms. Instead, the abstraction from the aliphatic C_β atom (C7 atom) produces an intermediate of about 11 kcal/mol more stable than the addition intermediates. The spin densities computed indicate that this difference may be due to the fact that when the radical is added to any of the aromatic C atom the aromaticity of the ring is broken, while the aromaticity is maintained when the attack occurs at the aliphatic part. In addition, the radical character is even more stabilized by its delocalization around the aromatic ring. However, when the second radical eliminates the hydrogen atom from the

adduct radical intermediate the aromaticity is recovered in the structure. As a consequence, the oxidation at any of the aromatic ring positions lead to products about 5 kcal/mol more stable than the oxidation of the aliphatic C carbon. These results are in agreement with the oxidized products characterized experimentally for Phe and Tyr [59].

The presence of the indole group in tryptophan makes more complex the reactions of hydroxyl radical with this amino acid side chain. On one hand, the attacks of two $\bullet OH$ at the benzene group show enthalpy values very similar to the reaction with phenylalanine. As with this amino acid, even that the H abstraction from the aliphatic C10 atom produces a more stable intermediate, the products formed from this intermediate are less favored. Consequently, the calculations predict that the reaction involves first the addition of the $\bullet OH$ to form the adduct, followed by the H abstraction. On the other hand, tryptophan has two additional atoms in the pyrrole ring liable to radicals attacks, the N7 and C8 atoms. The calculations demonstrate that the addition at the C8 atom and abstraction from N7 produce intermediates with very favorable ΔH_{aq}^{298} values, roughly 10 kcal/mol more stable than the ones formed by the additions at the six-member ring C atoms. These enthalpy values are therefore comparable to the intermediate formed after the hydrogen abstraction from the aliphatic C10 atom, but unlike this reaction pathway, the hydrogen abstraction at C8 produces the most stable product with a ΔH_{aq}^{298} value of -118.2 kcal/mol. These results therefore indicate that the C8 atom is the most preferred position for the attack of the radicals in tryptophan (entire reaction pathway depicted in Figure 5.4), and more favorable than the attack in phenylalanine or tyrosine.

Experimentally, it has been determined that the radicals can attack any of the phenylalanine ring positions [59], which is in agreement with our results. Nevertheless, the attack onto Tyr produces DOPA, which implies that the radical attacks Tyr at meta-positions. However, the enthalpies computed here show similar values for the attack at any ring position, with ortho-positions slightly more favorable than meta-positions. Moreover, even that the data indicate that the di-tyrosine species are thermodynamically less favorable than the oxidation of the ring, these species have been experimentally characterized [82]. All these data may suggest that in these reaction pathways other factors, such as steric effects, accessibility of the radical to the amino acid side chain positions or radical concentration predominates over thermodynamics. At this point, it is worthy to note that our calculations are carried out in an isolated model including a single amino acid side chain. This model is suitable to investigate the intrinsic chemistry governing the reaction, but does not include the influence of a large molecule such as a protein. It is expected that the access of the radical to the target amino acid is highly influenced by the bulk side of the protein. This may explain the preferences for the radical attack at meta position of tyrosine to form DOPA, as the ortho position are more hindered by the protein backbone. In this vein, it must be taken in mind that the experiments carried out by Stadtman et al.[66] indicate that the bulkier the amino acid, outer the regions of the amino acid in which the radical attack. Thus, the backbone is the target of the attack with small amino acids, while in larger residues the reaction occurs in the side chain. On the other hand, the di-tyrosine species can be produced when the radical concentration is sufficient to form the radical intermediates but nevertheless is insufficient to promote an immediate attack of a second radical onto the same side chain to produce the oxidation. In this way, the lifetime of these intermediates is long enough to allow the formation of the di-tyrosine species.

It is also worthy to note that the ΔH_4^{298} values of all the products characterized are in

general 2-3 kcal/mol lower than their ΔH_{aq}^{298} values. Interestingly the most stable product, (oxidation at the C8 atom of tryptophan) shows the largest difference with ΔH_4^{298} 5 kcal/mol more stable than ΔH_{aq}^{298} . This trend indicates that the radical attack can be thermodynamically favored in apolar areas of a protein, i.e. in buried regions.

5.4 Conclusions

The sequential attack of two $\bullet OH$ onto phenylalanine, tyrosine and tryptophan, the three aromatic amino acids have been investigated by DFT calculations. The low enthalpy values computed confirm that the side chains of the three aromatic amino acids can be the target of hydroxyl radicals. The results indicate that thermodynamics governs over the kinetics in the reaction, although other factors, such as radical concentration and steric effects may also be relevant in the mechanism. In the study, all possible attacks of the $\bullet OH$ onto the aromatic amino acid have been characterized, considering either the addition of the radical to the amino acid side chain or a hydrogen abstraction. For the three amino acids, the reaction goes through a two-step mechanism, in which the first $\bullet OH$ is added to the amino acid, and the second $\bullet OH$ abstracts a hydrogen to form the oxidized product. The oxidation of the phenylalanine and tyrosine rings, as well the six-member ring of tryptophan present very similar enthalpy values. Nevertheless, the most favorable product corresponds to the oxidation at the C8 atom of tryptophan, located in the five-member ring of this amino acid. Therefore, this atom is predicted as the weakest position for the radical attack among the three aromatic amino acids studied.

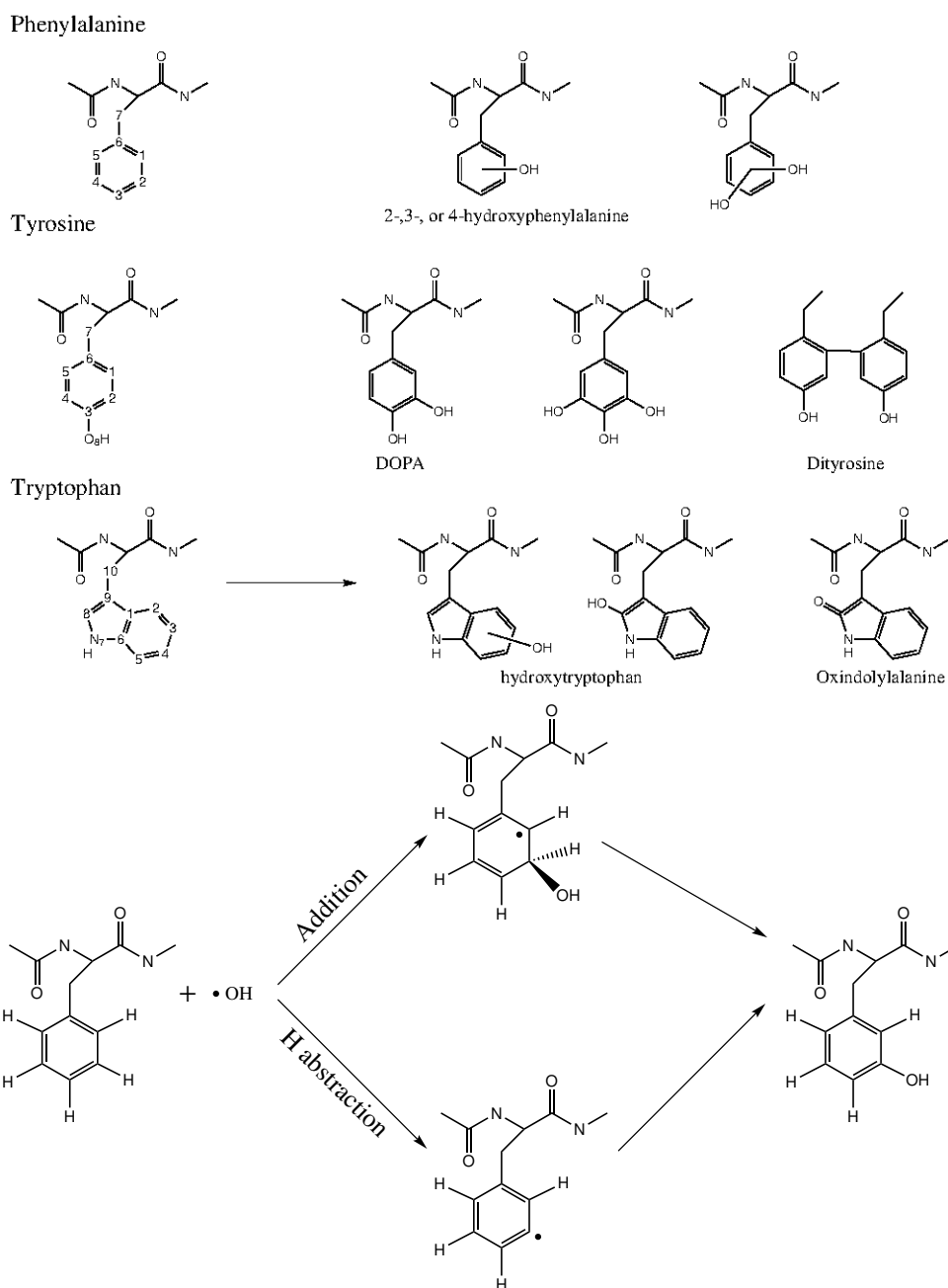


Figure 5.1: Above, atom labeling of the three aromatic amino acids studied: phenylalanine, tyrosine and tryptophan. The hydroxylation products characterized experimentally are also illustrated. Below, the two reaction mechanisms considered in this work: $\cdot\text{OH}$ addition and hydrogen abstraction.

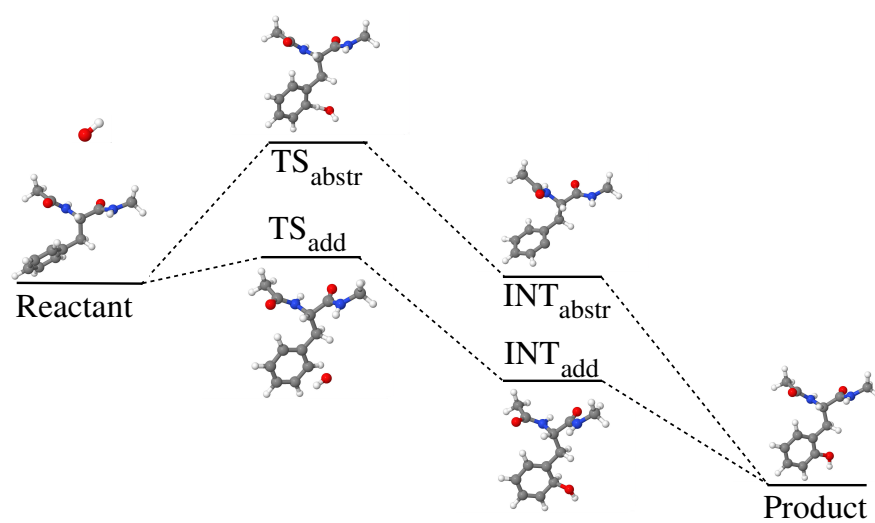


Figure 5.2: Stationary points along the reaction pathways characterized for the attack of two $\cdot OH$ radicals at the C1 atom of phenylalanine, following two mechanisms: i) addition and ii) hydrogen abstraction. Note that the energy levels depicted are not scaled to their values.

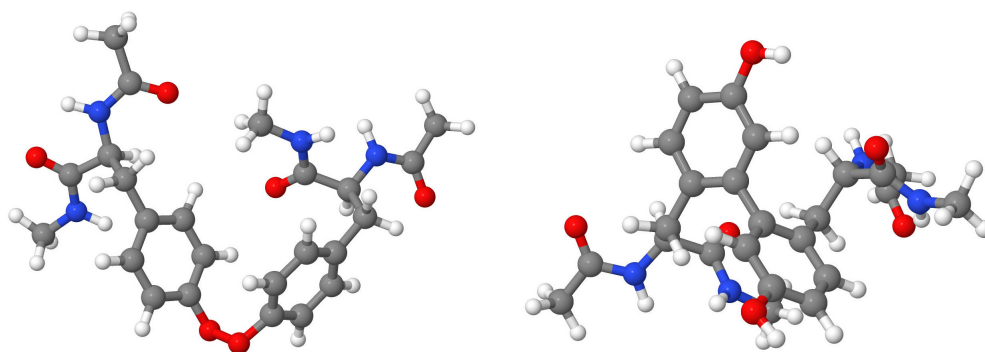


Figure 5.3: The two di-tyrosine cross-linked products characterized, linked through the O8 (on the left) and C2 (on the right) atoms.

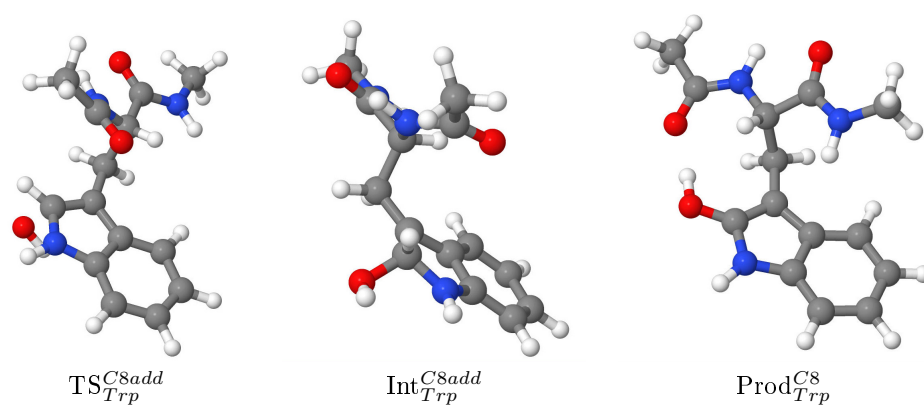


Figure 5.4: Stationary points along the most favorable reaction pathway: oxidation reaction at the C8 atom of tryptophan.

Chapter 6

•OH Oxidation Towards S- and OH- Containing Amino Acids

Herein, we present a theoretical study on the attack of hydroxyl radicals on hydroxyl- and sulfur-containing amino acid side chains. Several reaction mechanisms, such as hydrogen abstraction, electron transfer, or •OH addition have been considered to investigate several reaction mechanisms. Two different dielectric values (4 and 80) have been used to model the effect of different protein environments. In addition, different alternative conformations of the amino acid backbone have been considered. Overall, the results indicate that the thermodynamics is the main factor driving the reaction pathway preference, and in a great extent explain the formation of the experimental oxidized products. Sulfur containing amino acids would be oxidized more easily than OH containing amino acids, which confirms the experimental evidence. This is determined by the stability of the sulfur radical intermediates. These results are not dramatically affected by either different dielectrics or backbone conformations.

6.1 Introduction

In this work we focus on the oxidation of the two S-containing residues, cysteine (Cys) and methionine (Met), and the two alcohol group containing amino acids (Ser and Thr) due to their chemical similarity with Cys. The main oxidized products formed by Ser and Thr are aldehydes and ketones, respectively [9, 20, 177] (see Figure 6.1). However, under low •OH concentrations, the H abstraction from the C_β is favored, and this radical intermediate can facilitate the cleavage of the protein backbone as explained already in Chapter 3.

Sulfur containing amino acids (Met and Cys) show a more complex reactivity towards •OH (main oxidized products shown in Figure 6.1), since apart from the radical addition or H abstraction, they can also be involved in electron transfer to •OH [87, 180] (mechanisms shown in Figure ??). In the case of Met, the sulfoxide is the most abundant oxidized product, even that another product with a carbon-carbon double bond in the side chain was also identified [178]. The sulfoxide product can be formed through two alternative mechanisms that are dependent on the oxidant species: i) a direct two electron oxidation by

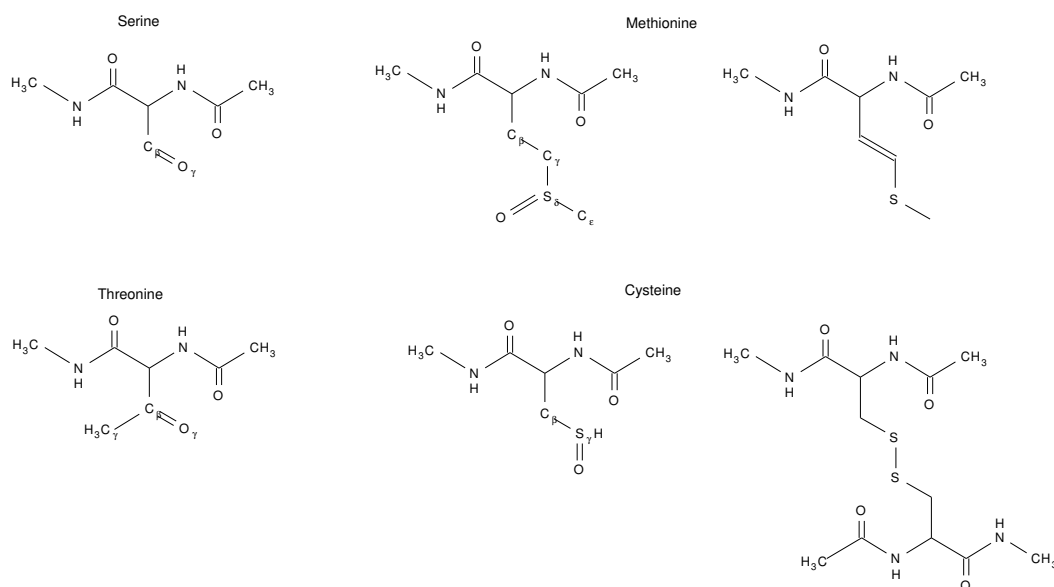


Figure 6.1: Most abundant oxidized products of alcohol containing[9, 20, 177] and sulfur containing[178, 179] amino acid side chains.

$HOCl$, H_2O_2 [181], or singlet O_2 or ii) one-electron oxidation by $\bullet OH$ or in presence of a metal ions [180], which takes place due to the large reduction potential of $\bullet OH$ (1.9 V) [182]. Electron transfer mechanism is accepted to be the first step in the oxidation of Met to reach the sulfoxide product. This mechanism is initiated when the $\bullet OH$ withdraws one electron from the sulfur atom to yield a radical cation ($\cdot S^+$), which must be stabilized by a Lewis base ($:X$) located in the protein, thus forming a three electron bond [91, 94, 95, 97, 98, 178, 183]. Such bonding phenomena has been carefully studied by Rauk et. al. using small Met side chain models [100] and Met containing dipeptides [95]. They concluded that the sulfur radical cation is not stabilized by itself and that an electron donor side chain is required to stabilize the radical cation intermediate formed by the electron transfer reaction.

In the case of Cys, the electron transfer phenomena is less frequent than the H abstraction from the thiol group [89]. The oxidation of this amino acid produces a variety of different products, including sulfenic acids, disulfides and under drastic conditions sulfinic or sulfonic acids (see Figure 6.1). Interestingly sulfenic acids and disulfides can be reversibly reduced back to thiols [88, 179]. In addition, in many protein Cys residues form Cystine, a disulfide structure where two Cys residues are linked by a disulfide bridge (S-S), a link that provides further stability to the protein. Thus, the cleavage of this bond may destabilize the protein conformation [90], and in fact disulfides can get further oxidized and yield thiosulfonates and thiosulfonates as products [86].

In summary, the possible oxidation products that may be obtained by the attack of $\bullet OH$ towards Ser, Thr, Met, Cys and Cystine are well established. However, the reaction mechanism by which these products are formed are unclear. Herein we investigate the entire route for the formation of these products considering three main reaction mechanisms (see

Chapter 2): hydrogen (H) abstraction, $\bullet OH$ addition or electron transfer [184]. The results are compared to previous experimental and theoretical results [20, 63, 103, 104, 121, 176, 185, 186], what allow us to put them in context and rationalize the mechanisms occurring in such oxidation processes.

6.2 Methodology for the electron transfer reactions

The already introduced methodology is suitable to describe properly both hydrogen abstraction and addition reactions. Nevertheless, besides these reaction mechanisms, $\bullet OH$ may also reduce to OH^- by electron transfer reactions. $\bullet OH$ is one of the species with higher reduction potential, i.e. $E^0 = 1.9$ V [182], and therefore it may oxidize other species by taking electrons. Methionine sulfur may be one of its targets, leading to the formation of radical cation intermediates.

In order to choose a proper methodology to study the electron transfer process, we have calculated the reduction potential of the $\bullet OH/OH^-$, $\bullet SCH_3/SCH_3^-$ and $CH_3CH_2S^+CH_3/CH_3CH_2SCH_3$ taking as reference the values obtained at the CCSD level of theory, as this level of theory is the most accurate one affordable for these type of systems. The reduction potentials have been calculated in solution, by means of the IEFPCM method at the MPWB1K/6-311++G(2df,2p) level. However, other functionals of different nature such as B3LYP, M06L, ω B97XD and CAM-B3LYP were also tested. In all cases, the effect of explicit water molecules was also studied by adding up to two water molecules. The obtained results are given in Table 6.1.

The reduction potential has been calculated according to the Nerst equation:

$$E^0 = \frac{-\Delta G^0(X)}{F} - E_{SHE}^0$$

being E_{SHE}^0 the standard hydrogen electrode, which is calculated to be 4.47 V using IEFPCM [63], F the Faraday constant ($F=96.485$ C/mol) and $\Delta G^0(X)$ the free energy corresponding to the reduction of group X :



Having a look to Table 6.1, clearly the MPWB1K functional is the one yielding closest values with respect to the reference CCSD values. Therefore, we may conclude that the methodology used for H abstraction and addition is also suitable to study electron transfer processes, and therefore will be used in this work. Moreover, it is noticeable the influence of including explicit water molecules, specially for the $\bullet OH$ and $\bullet SCH_3$ cases. In the case of $\bullet OH$, the calculated reduction potential increases from 0.37 V with no explicit water to 1.05 V with two explicit water molecules. The improvement is significant but the value is still far from its experimental reduction potential of 1.9 V [182]. The consideration of more explicit water molecules is clearly necessary. Thus, more explicit water molecules were added around $\bullet OH$ until an accurate reduction potential was calculated (See all values in Appendix). Finally, the addition of 23 water molecules (see Figure 6.2) was found necessary

for a proper description of the $\bullet OH$'s solvation sphere. The calculated reduction potential is now 1.8 V, very close to the experimental value. Therefore, 23 explicit water molecules were added both to the $\bullet OH$ and OH^- species (shown in Figure 6.2) when the electron transfer process presented below were determined.

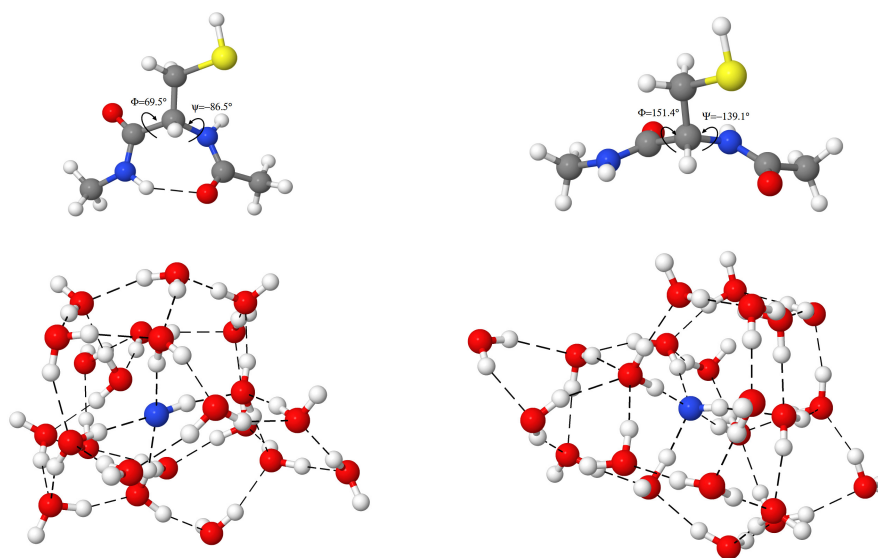


Figure 6.2: Above, illustrative example of the two conformations considered for cysteine: α -helix-like (left) and β -sheet (right). The values of Φ and Ψ dihedral angles are given in degrees. Notice that the values of these dihedral angles are given in the Appendix for the all the rest structures. Below, $\bullet OH - (H_2O)_{23}$ (left) and $OH^- - (H_2O)_{23}$ (right) complexes used to evaluate the electron transfer processes. In blue, the oxygen atom of the radical species is depicted.

6.3 Results and discussion

Herein the oxidation process on the alcohol-containing and sulfur-containing four amino acid side chains have been studied: serine (Ser), threonine (Thr), cysteine (Cys) and methionine (Met). Due to its relevance, the same process on cysteine has also been investigated. In all cases, the sequential attack of a maximum of two hydroxyl radicals were considered following one of these three mechanisms (see Figure ??): H abstraction, electron transfer or $\bullet OH$ addition. The attack of the first $\bullet OH$ may take place by H abstraction from different positions at the amino acid side chain (leading to a radical intermediate), or in the case of the sulfur containing amino acids side chain an electron transfer reaction (leading to a sulfur radical cation intermediate) can also take place. The second $\bullet OH$ reacts with a radical intermediate following either a second H abstraction or the addition of the hydroxyl radical to the radical intermediate. The intermediates and products characterized for the oxidation of each amino acid side chain are ordered numerically starting from the most stable one.

For the sake of clarity, the thermodynamics values evaluated in aqueous environment (ΔH_{aq}) for all intermediate and product stationary points will be presented in the body text, and the remaining data is included in the Appendix (Table B.3 and B.5).

First, the reaction pathways characterized for the alcohol containing side chains will be described and discussed. We will begin from serine (smallest one) and then will continue with threonine. Similar to this, the reactivity in sulfur containing side chains will be analyzed in this order: cysteine, cystine and methionine.

6.3.1 Alcohol containing amino acids

Ser has the smallest side chain, namely, $-CH_2OH$, while Thr has a methyl group linked to the C_β , and therefore presents more alternatives for the attack of the hydroxyl radicals. Concretely, in the case of Ser, the first $\bullet OH$ may abstract a H from C_β and O_γ . In addition to these two positions, in Thr hydrogens linked to C_γ may also be abstracted (see Figure 6.4). This C_γ was considered to be a free rotor, and hence, all H-s in there were considered topologically equal. The subsequent attack of a second $\bullet OH$ would attack the previously formed intermediate radical, via abstraction of a second H or addition towards the radical intermediate atom where the radical is located. All these possible reaction paths are depicted in Figure 6.3 and Figure 6.4, for the attack of two hydroxyl radicals towards Ser and Thr amino acid side chains respectively, considering α -helix-like conformation in solvent environment. The calculated values for α -helix-like conformation in protein environment, and for β -sheet conformation in protein and solvent environments are given in Tables 2, 3 and 4 of the Appendix, along with geometrical and other electronic data such as spin densities. As mentioned, the importance of kinetics is negligible due to their small barriers, and therefore, in Figure 6.3 and Figure 6.4 these barriers are not given. They are available in Table B.2 of the Appendix.

6.3.1.1 Serine

The reaction pathways corresponding to the oxidation of serine's side chain are shown in Figure 6.3. Due to the small size of its side chain, the first $\bullet OH$ may abstract a H from either C_β or O_γ . From a sterical point of view, both side chain atoms are similarly available for the attack of the radical, and therefore, the thermodynamics would prevail. According to the first step depicted in Figure 6.3, the abstraction from C_β is clearly favored. Compared to the intermediate radical obtained from the abstraction from the O_γ atom (S-Int $_2^{O_\gamma}$), S-Int $_1^{C_\beta}$ is about 10 kcal/mol more stable. These results are in agreement with those obtained by Thomas et. al. [121]. According to their calculations and experiments, the attack of a hydroxyl radical abstracts a hydrogen from the C_β atom. Then, the formed radical species may undergo different pathways, without the presence of any other species, leading to the breaking of the backbone. These processes has already been explained in Chapter 3 and in this Chapter the attack of a second radical has been studied.

Four different products have been characterized for the attack of a second $\bullet OH$: 1) addition to C_β , leading to $CH(OH)_2$ group (S-Prod $_1$). 2) Formation of an aldehyde (S-Prod $_2$). This product can be formed by a H abstraction from either the OH group of S-Int $_1^{C_\beta}$ or the C_β atom of S-Int $_2^{O_\gamma}$ 3) The addition of the hydroxyl radical to the O_γ atom, leading to a OOH group (S-Prod $_3$). 4) The $\bullet OH$ could attack a neighbour serine side chain to form

a second $S\text{-Int}_2^{O\gamma}$ radical intermediate, what ultimately would lead to the formation of a diserine product with an O-O bridge ($S\text{-Prod}_4$). Nevertheless, as it was pointed out above this product is unlikely to occur in a biological environment. All these possible products are depicted in Figure 6.3.

$S\text{-Prod}_1$ and $S\text{-Prod}_2$ are clearly the most stable products with a ΔH_{aq} value of -117.5 and -108.0 kcal/mol, respectively, while the ΔH_{aq} value of $S\text{-Prod}_3$ and $S\text{-Prod}_4$ are -47.2 and -47.1 kcal/mol. Notice that the aldehyde product ($S\text{-Prod}_2$) is the only product determined experimentally [20, 177]. Nevertheless, it must be taken into account that in solution the $\text{CH}(\text{OH})_2$ group present in $S\text{-Prod}_1$ loses a water molecule and end up on the aldehyde, so at the end $S\text{-Prod}_1$ and $S\text{-Prod}_2$ are equivalent. In summary, the results predict that the oxidation of Ser is initialized by a H abstraction from the C_β atom, followed by either a H abstraction from the alcohol group or the addition of the second $\bullet OH$ to C_β to form the $\text{CH}(\text{OH})_2$ group. In both cases, an aldehyde is the final product.

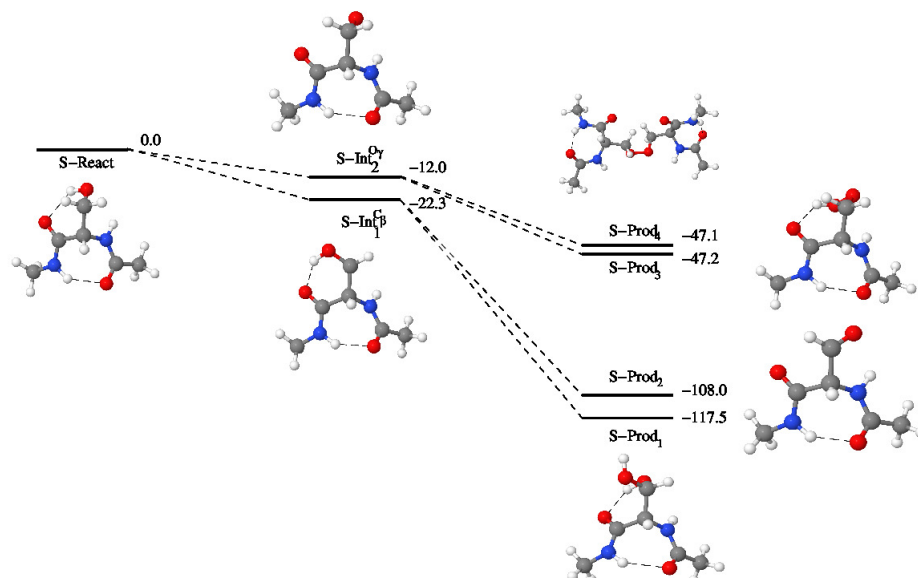


Figure 6.3: Full reaction path of the sequential attack of two $\bullet OH$ radicals towards Ser amino acid side chain. ΔH_{aq} values are given, in kcal/mol. The barriers for the first step are not given due to their low significance. These barriers, along with a model 2D-ChemDraw for each compound, are given in the Appendix.

6.3.1.2 Threonine

Compared to serine, the presence of the methyl group provides more alternatives to the oxidation of the threonine's side chain. Besides the H abstraction from the two atoms analyzed with Ser, a hydrogen linked to C_γ may also be abstracted in Thr. This C_γ was considered to be a free rotor, and hence, all H-s of this methyl group were considered topologically equivalent. All these possible abstractions have been studied and the results are given in Figure 6.4.

As with Ser, T-Int $_1^{C\beta}$ intermediate, which corresponds to the H abstraction from $C\beta$, is the most stable intermediate ($\Delta H_{aq} = -24.5$ kcal/mol). The abstraction of a hydrogen from $C\gamma$ is about 10 kcal/mol less stable ($\Delta H_{aq} = -15.0$ kcal/mol), while the abstraction from $O\gamma$ produces the less stable intermediate with a ΔH_{aq} value of -10.6 kcal/mol.

Four products have been characterized for the attack of the second $\bullet OH$. Three of them can be easily explained departing from the most stable intermediate (T-Int $_1^{C\beta}$): i) a $CH_3C(OH)_2$ group is formed by the addition of the second radical to $C\beta$ (T-Prod $_1$), ii) a ketone can be produced by a hydrogen abstraction from the alcohol group (T-Prod $_2$), iii) S-Prod $_4$ is produced when a second H is abstracted from $C\gamma$ (note that this product can also be reached from T-Int $_2^{C\gamma}$). Moreover, iv) the addition of the second radical to the $C\gamma$ atom in T-Int $_2^{C\gamma}$ can lead to S-Prod $_3$. Mention that more products can in principle be formed, but based on the results obtained for serine, the products with O-O bonds were assumed to be much less favorable.

The order in the stability of the products is similar to that obtained with Ser. The experimentally characterized ketone form is the second most stable product ($\Delta H_{aq} = -112.8$ kcal/mol), while the di-alcohol product (T-Prod $_1$) is the most stable one, with a ΔH_{aq} value of -117.9 kcal/mol. Nevertheless, as it was pointed out in the previous section, in solution these two products are equivalent, once T-Prod $_1$ loses a water molecule. The addition of the radical to the $C\gamma$ atom (T-Prod $_3$) is close in energy ($\Delta H_{aq} = -109.7$ kcal/mol) while the product with a double bond (T-Prod $_4$) is the less stable product characterized with a ΔH_{aq} value of -98.3 kcal/mol.

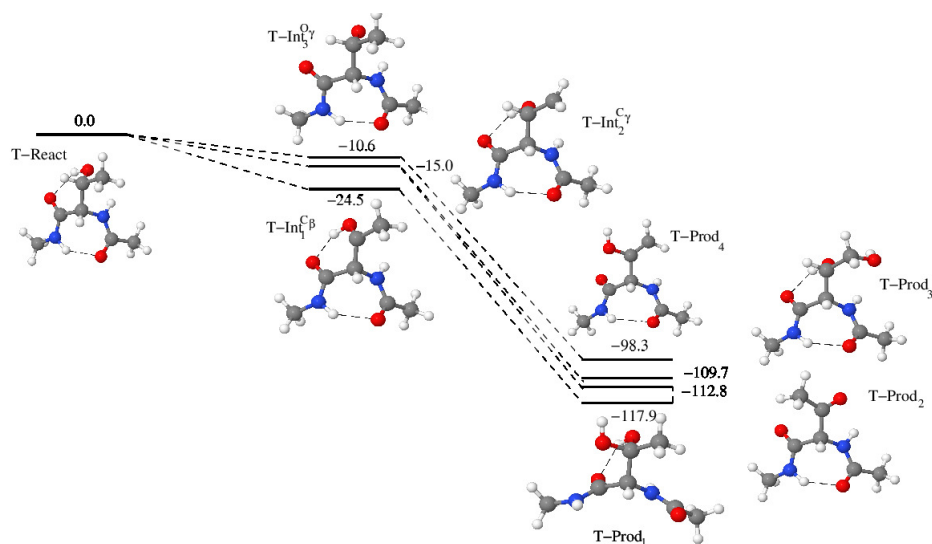


Figure 6.4: Full reaction path of the sequential attack of two $\bullet OH$ radicals towards Thr amino acid side chain. ΔH_{aq} values are given, in kcal/mol. The barriers for the first step are not given due to their low significance. These barriers, along with a model 2D-ChemDraw for each compound, are given in the Appendix.

6.3.2 Sulfur-containing amino acids

Met and Cys contain one sulfur atom at their side chains. In both cases, besides H abstraction from C or S atoms of the side chain, an electron transfer from a S lone-pair to $\bullet OH$ may occur, leading to the formation of OH^- and a sulfur radical cation intermediate ($\bullet S^+$). The electron transfer will only take place if such cation is sufficiently stabilized by the complexation of S with a electron donor acceptor, such as O or N. The N and O atoms of the backbone of each amino acid can be the source of electron donors, thus forming three electron bonds. With these type of interactions Met may form five- or six membered rings with the N or O atoms of its backbone, whereas four- or five- membered rings can be formed by Cys. Nevertheless, this radical cation stabilization has only been found in Met, mostly when the residue is a terminal amino acid, or when the $\bullet S^+$ is complexed with electron donor atoms of other side chains, like N of histidine, for instance. In this work, we have considered both electron transfer and H abstraction mechanisms for the attack of a first $\bullet OH$ towards Cys and Met, followed by $\bullet OH$ addition or a second H abstraction for the attack of a second $\bullet OH$.

6.3.2.1 Cysteine

Cys side chain is very similar to that of serine, the only difference being a S atom instead of an O atom. However, unlike O, S atom is able to form more than two covalent bonds, since its lone pairs are not so inner orbitals, which affects its reactivity. The attack of the first $\bullet OH$ could lead to the H abstraction from either C_β or S_γ atoms, or alternatively it could abstract an electron from one of the sulfur lone pairs. All these possibilities were analyzed and the calculated ΔH_{aq} values are shown in Figure 6.5. Interestingly, the electron transfer reaction is not thermodynamically favored, as the ΔH_{aq} value of $C-Int_3^{S^+}$ is +14.0 kcal/mol. This result was also found by Enescu et. al., [89] and is in concordance with the experimental evidence that the electron transfer process does not take place in Cys.

Therefore, the H abstraction reaction is predominant for the first attack of a hydroxyl radical on Cys side chain, with two target atoms: C_β or S_γ . Regardless the dielectric or the backbone configuration, abstraction from S_γ ($C-Int_1^{S_\gamma}$) is favored by 6 kcal/mol, with $\Delta H_{aq} = -31.2$ kcal/mol. This value is about 6 kcal/mol more stable than the attack onto the C_β atom ($C-Int_2^{C_\beta}$). The same difference is found with respect to the most stable intermediates characterized with Ser and Thr. In addition, this is the sterically more available site, so we can conclude that the most probable radical intermediate will be the one with the radical at the S atom.

Five different products (shown in Figure 6.5) have been characterized for the attack of the second $\bullet OH$ onto the two stable intermediates described above. Departing from the most stable $C-Int_1^{S_\gamma}$ intermediate, the abstraction of a H atom from C_β lead to a thioketone (C=S) group (C-Prod₄). The radical could be also added to the S radical, forming a sulfenic acid with a S-OH bond (C-Prod₃). The tautomer of this species (HS=O) has also been characterized (C-Prod₅). Alternatively, and if the concentration of $\bullet OH$ would be low enough, a second radical could abstract a H from another cysteine to form a second $C-Int_1^{S_\gamma}$ radical species. If these two radical species could find each other in space they would rapidly react to form a disulfide bond, known as cystine (C-Prod₁). On the other hand, a C(SH)(OH) group would be formed (C-Prod₂) if the second radical is added to $C-Int_2^{C_\beta}$.

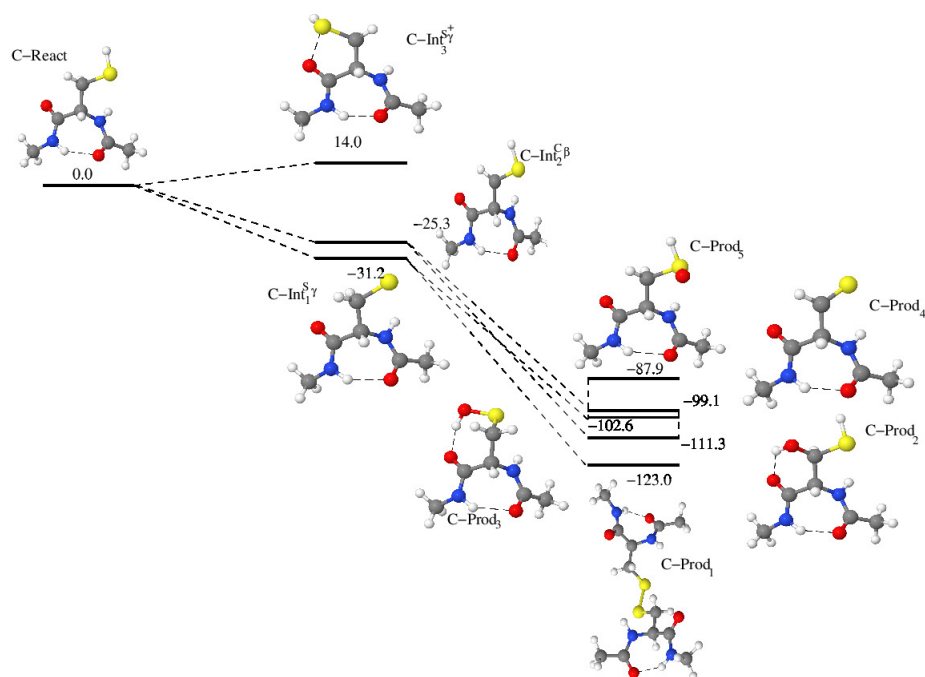


Figure 6.5: Full reaction path of the sequential attack of two $\bullet OH$ towards Cys amino acid side chain. ΔH_{aq} values are given, in kcal/mol. The barriers for the first step are not given due to their low significance. These barriers, along with a model 2D-ChemDraw for each compound, are given in the Appendix.

Cystine (C-Prod₁) is the most stable product, specially in the α -helix-like conformation, with a ΔH_{aq} value of -123.0 kcal/mol. Again, this product is ca 5 kcal/mol more stable than the most stable products found with Ser and Thr. Moreover, not only from a thermodynamic point of view cystine is favorable, but sterically the attack at the S atom seems to be favored. However, as pointed out before, the formation of this product would, in principle, occur only with a low concentration of $\bullet OH$. With higher radical concentrations, however, others product such as sulfenic acid (C-Prod₂ or C-Prod₃) may prevail and in fact these species have been observed experimentally.

6.3.2.2 Cystine

As pointed out before, cystine is not only a possible oxidation product of Cys, but the disulfide bridge is present in many proteins in order to provide further stabilization and function, like in the case of signaling, to the protein. Thereby, the reaction of $\bullet OH$ towards such structural motif is of relevant importance, since it might lead to a loose of the protein functionality. Herein, the attack of two $\bullet OH$ have been studied (reaction path shown in Figure 6.6), which would lead to two different kind of products, as explained below.

After the attack of the first $\bullet OH$, the sulfur radical complex species is formed, and is located -9.7 kcal/mol below the reactants. In this complex, even that the $\bullet OH$ has been

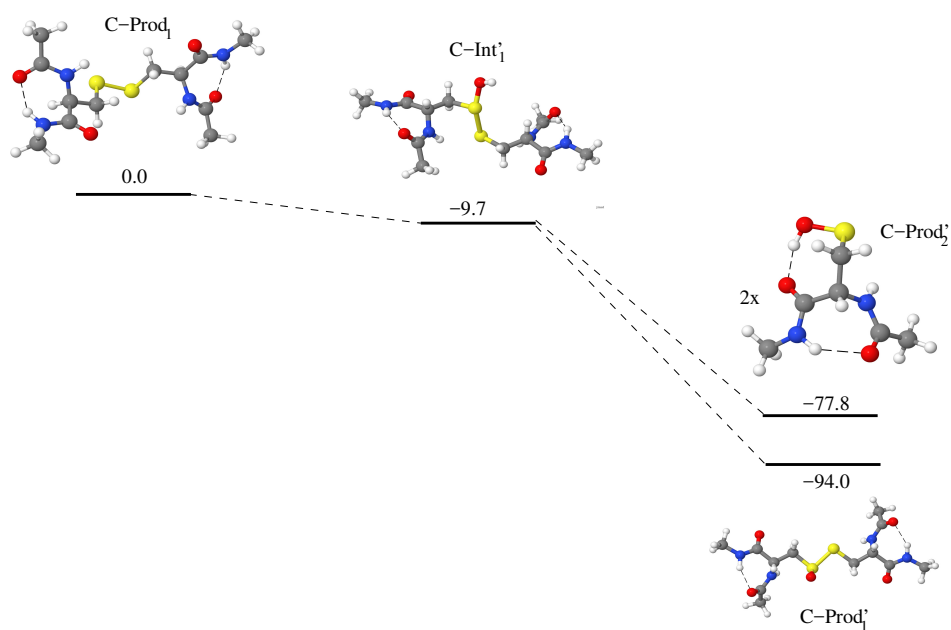


Figure 6.6: Full reaction path of the sequential attack of two $\bullet OH$ towards cysteine amino acid side chain. The barriers for the first step are not given due to their low significance. These barriers, along with a model 2D-ChemDraw for each compound, are given in the Appendix.

added to one of the S atoms, the radical character is shared between the two sulfur atoms, in a three electron two center bond. As a consequence, the disulfide bond is weakened and the S-S distance lengthened significantly from 2.05 Å to 2.48 Å. Due to the weak character of the S-S bond, it may easily be broken due to external or thermal influences. In other words, the sulfur bridge could be easily splitted with harmful effects for the structure and functionality of the protein.

The attack of a second $\bullet OH$ may produce a variety of products. For instance, the second hydroxyl radical may attack the OH group attached to one of the S atoms in $C-Int_1'$, abstracting the H atom from there and leading to a product with a sulfinyl group. This product lies -94.0 kcal/mol below the reactants. In this case, the disulfide bond length decreases to 2.18 Å, which is an indication that the bond strength has increased again. On the other hand, the $\bullet OH$ may attack the free sulfur in $C-Int_1'$, which eventually leads to the dissociation of the disulfide bond and the formation of two S-OH containing products ($C-Prod_3$ in the case of cysteine). These products lie -77.8 kcal/mol lower in energy than the reactants. Hence, breaking of disulfide bond due to the attack of hydroxyl radicals could occur, although thermodynamically the product containing the sulfinyl group is more likely to happen.

6.3.2.3 Methionine

In the case of Met, the first radical attack may occur via two different pathways. On one hand, H abstraction from one of the carbon atoms of the side chain, and on the other hand via electron transfer from the sulfur atom to the hydroxyl radical. The process includes two steps: first, an electron is transferred from a lone pair of the S atom to the $\bullet OH$, thus forming the radical cation intermediate species. Then, a second $\bullet OH$ is added to the radical cation, forming a non-radical intermediate. As it was explained in the Methodology section, the accurate prediction of the reduction potential (E^0) of the $\bullet OH$ requires the inclusion of 23 explicit water molecules, so $\bullet OH - 23 H_2O$ and ${}^{-}OH - 23 H_2O$ complexes have been used (shown in Figure 6.2) to study such reactions. It is worthy to mention that the inclusion of explicit water molecules in the radical cation species of Met and Cys should improve in more extend the results, but a systematic addition of them is not straightforward and therefore it would not necessarily guarantee better results. Moreover, due to the larger size of the system, the effect of explicit water molecules is less significant, but nevertheless it is important to keep in mind that the explicit water molecules could stabilize further the $\cdot S^+$ complex, what would give more exothermic ΔH values of this process. In this work, we have focused on both alternatives, H abstraction and electron transfer.

The reaction pathways characterized for the attack of two $\bullet OH$ onto Met side chain are shown in Figure 6.7. From the four target atoms for the first attack (C_β , C_γ , S_δ and C_ϵ), the H abstraction from the C_γ atom is the most favorable one, with a ΔH_{aq} value of -29.0 kcal/mol. The other carbon radical intermediates are less stable by roughly 6 and 10 kcal/mol. In Figure 6.7 the calculated more stable sulfur radical cation is depicted. Note that this radical cation is located roughly 18 kcal/mol above the most stable radical! Nevertheless, as pointed out above, the stabilization of the sulfur radical cations highly dependent on the environment, and hence other alternatives to central methionine, such as terminal methionine systems have been considered, as discussed below.

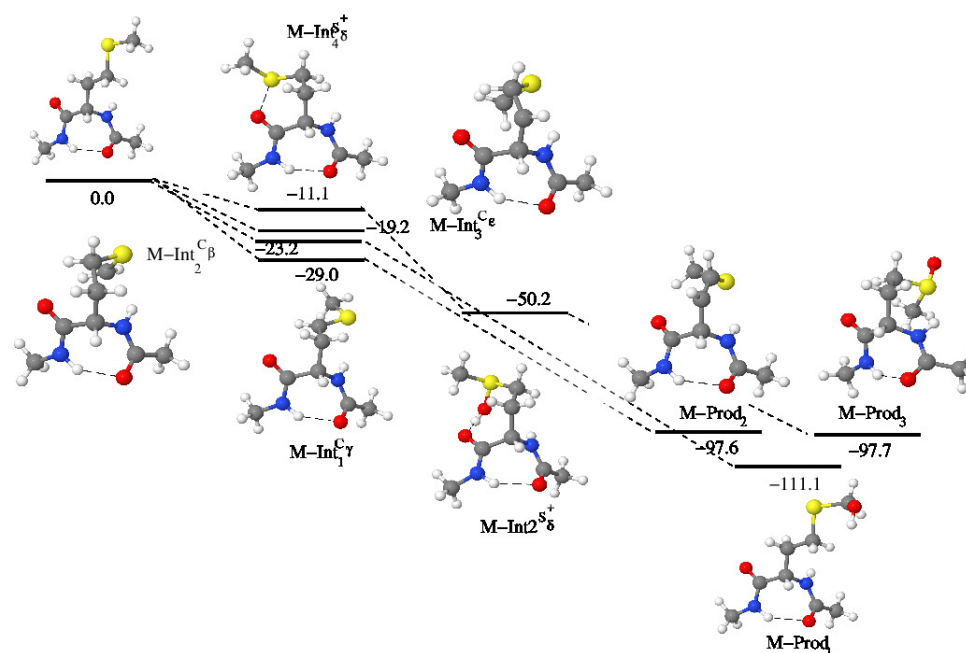


Figure 6.7: Full reaction path of the sequential attack of two $\bullet OH$ towards Met amino acid side chain. ΔH_{aq} values are given, in kcal/mol. The barriers for the first step are not given due to their low significance. These barriers, along with a model 2D-ChemDraw for each compound, are given in the Appendix.

The stabilization of the sulfur radical cation species in Met is due to electron donor atoms sited in its backbone, or other electron donor groups located in the side chains of other residues or species. In this work we have focused only on stabilization due to atoms of its backbone, but also considering the possibility of being a terminal methionine. In total, five interaction modes have been compared (presented in Figure 6.8). The nomenclature used for the labeling of such sulfur radical cation species appear obvious in Figure 6.8. Recall that the calculated reduction potentials, geometries and spin densities are given in the Appendix (Table B.4).

Comparing the stability of the different calculated sulfur radical cations and carbon radicals, it seems that the electron transfer process is less likely to occur, since all calculated sulfur radical intermediates lie higher in energy. However, there are two facts that should be taken into account before. On one hand, the lack of explicit water molecules in Met, which could further stabilize the sulfur radical cation. In principle, the effect of such water molecules would be smaller than in the $\bullet OH / ^-OH$ process, but it could stabilize sulfur radical cations some few kcal/mol, making the electron transfer process competitive with the H abstraction mechanism. On the other hand, there are other options to further stabilize the sulfur radical cations by the formation of complexes with other amino acid side chain residues, like Lys, that are not considered in the chapter. It is known experimentally that electron transfer process takes place in some cases (not in all Met) leading to the formation of S=O groups. Although according to our calculations electron transfer would not occur,

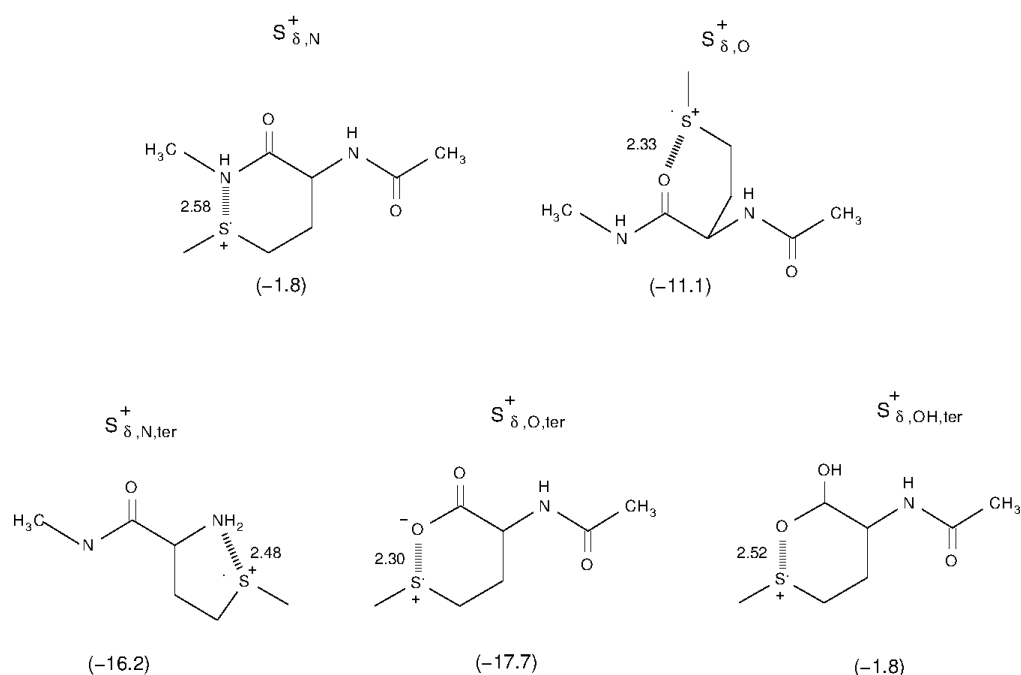


Figure 6.8: Schematic representation of the five patterns studied for the stabilization of the $\bullet\text{S}^+$ radical cation intermediate. In parenthesis, the ΔH_{aq}^{Int} values, in kcal/mol. The distance of the 3 e - 2 c bond (S and X), near the dashed bond, in Å.

we think that this is due to the reasons mentioned above. Therefore, the discussion hereafter related to the electron transfer mechanism should be considered qualitatively and not quantitatively.

According to the thermodynamic values given in Figure 6.8, electron transfer in Met is more likely to happen for terminal Met rather than intermediate Met. This is in agreement with the experimental results by Ignasiak et. al. [95], where they studied oxidation of methionine in dipeptides, observing that electron transfer mechanism may occur in these cases. This is due to the larger stabilization of the sulfur radical cation due to the terminal carboxylic or amine group. The S-X distances in such compounds are calculated to range between 2.3 and 2.6 Å, approximately. The calculated distances are typical of such S-X 3e⁻-2c interactions, as shown previously by other author [91, 94, 95, 97, 98, 178, 183]. Finally, it should be mentioned that electron transfer processes are more favorable at aqueous environment rather than at protein environments, as may be seen in the Appendix. This could be in principle expected, since charged species are further stabilized in polar environments.

For the attack of the second radical, all the intermediates, either carbon or sulfur radicals, have been considered. The products reached after the attack of a second $\bullet\text{OH}$ are similar to the ones reported before. The most stable one (M-Prod₁) forms by the addition of the radical to M-Int₃^{C_e}. The other two products characterized, M-Prod₂ and M-Prod₃, lie very close in energy (-97.7 and -97.6 kcal/mol), and they contain a thioketone group and a double

$C_\gamma - C_\beta$ bond, respectively. Notice that both M-Prod₂ and M-Prod₃ are the main products obtained experimentally [178], although M-Prod₁ is the thermodynamically most stable predicted product. So, why this product is not found experimentally? The reason for that appears clear having a look to the first step. In order to reach the final M-Prod₁ product, the reaction must go through M-Int₃^{C_δ} which lies roughly 10 kcal/mol above the most stable intermediate, and is by far the most unstable C radical intermediate. Hence, the probability of obtaining M-Prod₁ experimentally decreases dramatically. Nevertheless, in sufficiently high hydroxyl radical environments, M-Prod₁ should also be detected experimentally.

Focusing on M-Prod₂ and M-Prod₃, it is clear that the reaction mechanisms are different, since M-Prod₂ occurs after two H abstractions, and M-Prod₃ after one electron transfer, one OH addition and a proton transfer. The first mechanism to lead M-Prod₂ is obvious, henceforth we will describe the mechanism to get the thioketone product in more detail. The attack of a second $\bullet OH$ to the sulfur radical cation complex leads to a second cation intermediate. Notice that in this case, the radical character is cancelled. For each radical cation species, the second $\bullet OH$ may follow two different paths, breaking or not breaking the 3 electron bonds. Let us focus on the attack of a second $\bullet OH$ towards $S_{\delta,N,ter}^+$ species (see Figure 6.9). The second $\bullet OH$ may be added without breaking the 3 electron bond, labeled as -OH(R), and breaking it, labeled as -OH(S). In the first case, after the addition of the second radical, the S-N distance remains almost constant, being 2.51 Å. On the contrary, in the -OH(S) case, the S-N distance has enlarged to 3.46 Å. One would expect that OH(R)-type complexes, where 3 electron bonds are kept, were more stable than OH(S)-type complexes. However, one finds the opposite: -OH(S) complex lies -31.7 kcal/mol below the reference, while the -OH(R) complex lies -20.5 kcal/mol below (see Table B.4 in the appendix for the other cases). This is due to the fact that although this bond is broken, the charge is more stabilized in OH(S)-complexes. Such formed cation, $S - OH^+$ would finally react with the previously formed ^-OH and yield methionine sulfoxide, M-Prod₃.

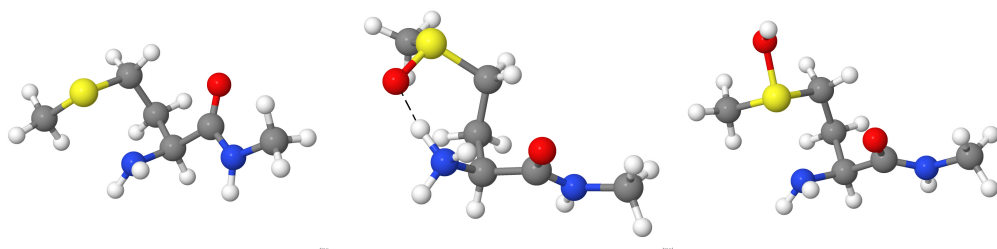


Figure 6.9: Radical Cation (left) and Cation intermediates (-OH(S) central and -(OH(R) right) for the $S_{\delta,N,ter}^+$ case.

Finally, let us discuss which amino acid side chain is the most prone to be oxidized by $\bullet OH$. In order to do so, we will focus on the ΔH_{aq}^{Int} values for the four amino acid side chains calculated in this work and the aromatic amino acid side chains calculated previously using the same tripeptide model and methodology [187]. According to the calculated theoretical data, sulfur containing amino acid side chains would be the easiest oxidized ones, with calculated lowest ΔH_{aq}^{Int} values of ~ -31 kcal/mol. Aromatic amino acid side chains would be the next ones in this scale, with $\Delta H_{aq}^{Int} \sim -28$ kcal/mol. However, it should be pointed out

that these values correspond to the attack towards C_β , which is sterically less favourable. For the case of Tyrosine, the attack to the OH group (sterically favored) also has a $\Delta H_{aq}^{Int} \sim -28$ kcal/mol, and therefore Tyr would be oxidized a bit easier than others. Finally, Ser and Thr are the ones with higher ΔH_{aq}^{Int} . The lowest lying intermediates are ~ -24 kcal/mol. It should be mentioned that experimentally there are also evidences that sulfur containing amino acids are the ones most prone to be oxidized [59, 92, 188, 189]. Also, the oxidation of Tyr via the abstraction of the hydrogen linked to oxygen in the side chain has been observed experimentally, which leads to the formation of Tyr-O-O-Tyr bridges. Hence, both calculated data and experimental evidence seem to indicate that S containing amino acids would be oxidized first, then aromatic amino acids such as Tyr, and finally -OH containing amino acid side chains like Ser and Thr.

6.4 Conclusions

The oxidation process by the attack of two $\bullet OH$ on the side chain of four amino acids i.e. Cys, Met, Ser and Thr, and cystine, was studied in this chapter. Three reaction mechanisms were considered for the study of their reaction pathways when possible, namely: H abstraction, $\bullet OH$ addition and electron transfer. The reaction barriers and energy differences for intermediate radicals and products were determined. It was observed that kinetically the H abstraction from different atoms located in the same side chain cannot be distinguished, since energy barriers do not differ in a significant way. However, larger differences were found between the enthalpic values of radical intermediates, what allow us to identify prevalence sites for the $\bullet OH$ attack on each amino acid. Thereby, it can be said that thermodynamics rule the first attack of $\bullet OH$ towards the side chain, in line with the previous study on aromatic amino acids, where small differences were encountered for the kinetic barriers (Chapter 4).

All in all, the stablest intermediate radicals are formed when the first $\bullet OH$ abstract a H from C_β atom in the case of Ser and Thr while C_γ and S_γ are the preferred sites for Met and Cys, respectively. The second $\bullet OH$ attack yields a wide range of products. In the case of Thr the most stable product is found to be a hydrated ketone. The same is true for Ser, where a hydrated aldehyde is found to be the stablest product. Indeed, this computational work provides with the flexibility to explain the relative stability of the products and which ones are the pronest to obtain by the mechanism presented herein.

On the other hand, the electron transfer reaction from Met and Cys to $\bullet OH$ was investigated. We found that up to 23 explicit water molecules must be add to $\bullet OH/OH^-$ for a proper description of the mechanism. Even that the process is barrierless, the radical intermediate must be stabilized by a electron donor atom. In our case, we investigated the capability of the protein backbone to stabilize the intermediate. Interestingly, the reaction is clearly exothermic with Met, but endothermic with Cys. We hypothesize that the main reason for this discrepancy comes from the capability of Met to form 5 or 6 member rings, while Cys can form 4 or 5 member ring, which are less stable. The results also indicate that the radical intermediate is further stabilized when Met is a terminal residue. However, the H abstraction from C_γ was found to lead to a more stable intermediate in Met than the sulfur radical cation intermediate formed with the electron transfer reaction. Therefore, the results predict that H abstraction would be dominant, even though the electron transfer reaction

CHAPTER 6. \bullet OH OXIDATION TOWARDS S- AND OH- CONTAINING AMINO ACIDS 129

is also a competitive process. In the case of Cys, the formation of cystine, which contains a disulfide bridge motif, was found as the most stable product. However, the formation of this product requires some specific conditions pointed out above.

In summary, the results presented herein provide a comprehensible explanation of how most of the oxidation products of Ser, Thr, Met and Cys found experimentally are reached, and give mechanistic details about the reaction pathways followed. However, the electron transfer mechanism in Met strongly depend on the surrounding environment and further work should be carried out in order to study all possible combinations.

Chapter 7

•OH Attack Towards Acid, Base And Amide Side Chains

Herein, the oxidation of acid (Asp and Glu), base (Arg and Lys) and amide (Asn and Gln) containing amino acids by the consecutive attack of two •OH is analysed. The oxidation mechanism is divided into two steps: 1) the first •OH can abstract an H atom or an electron, leading to a radical amino acid, which is the intermediate of the reaction 2) the second •OH can abstract another H atom or add itself to the formed radical, rendering the final oxidized products. This work includes solvent dielectric and conformational effects to the reaction, showing that both are negligible. Overall, the most favored intermediates at the side chain correspond to the secondary radicals stabilised by hyperconjugation. Intermediates show to be more stable in cases where the spin density of the unpaired electron is lowered. Alcohols formed at the side chains are the most favored products followed by the double bond containing ones. Interestingly, Arg and Lys side chain scission lead to the most favored carbonyl containing oxidation products, providing a clear clue for their experimental observation.

7.1 Introduction

The experimentally observed oxidation products of Asp, Glu, Lys and Arg are shown in Figure 7.1. Little is known about the oxidation products of amide containing Asn and Gln, but it has been reported that the -NH₂ group is suitable to suffer a H abstraction [47]. Therefore, the present study aims to shed light to the oxidation process and products for the already mentioned amino acids.

For proteins containing non aliphatic amino acids, the side chains are suitable sites to suffer the •OH attack; displaying more complex mechanisms. The H abstraction mechanism was thoroughly investigated by Anglada et al. where the •OH attack towards the formic acid was studied, it is observed that the preferential site of attack is to the acid H [108]. Lys and Arg are known to oxidize leading to aldehydes and ketones [9, 47]. However, they remain unstable and can get further oxidized; in the case of aldehydes to carboxylic acids [190], while ketones can react with amino groups present in the proteins and form Schiff bases [47, 190].

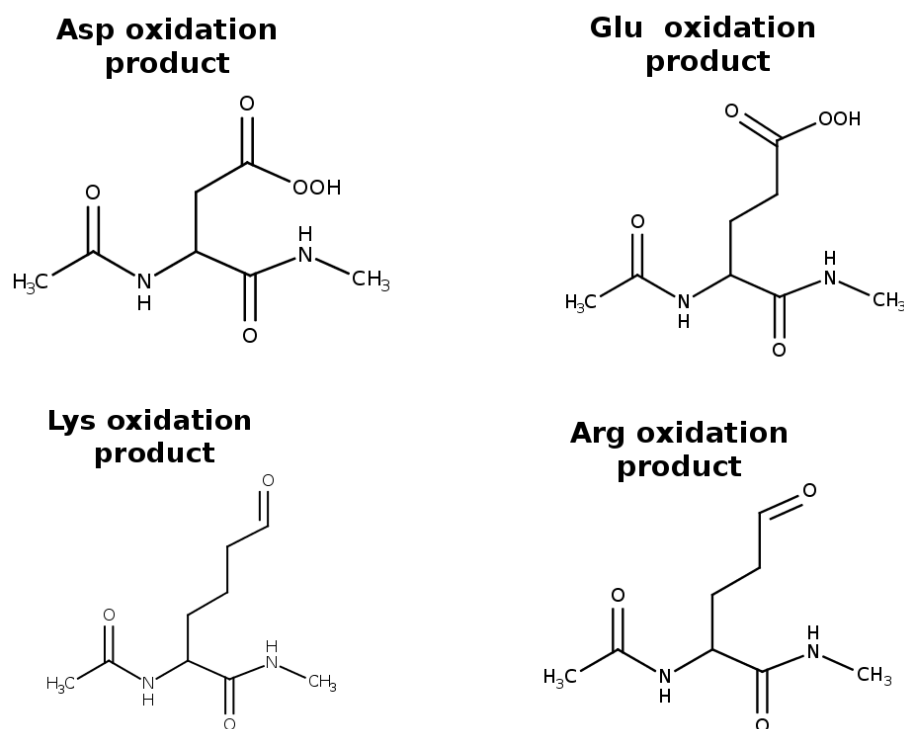


Figure 7.1: Asp, Glu, Lys and Arg experimentally observed oxidation products.

7.2 Results

The oxidation of the peptides containing an acid (Glu and Asp), a base (Lys, Arg) or amide (Gln, Asn) side chains is analysed. It must be said that during the protein oxidation not only they are exposed to the $\bullet OH$, but to many other reactive species and a myriad of possibilities exist for such process. The reaction pathway herein studied is a result of the consecutive attack of two $\bullet OH$. We divide the reaction by analysing the attack of a single $\bullet OH$ for each step. The attack of the first $\bullet OH$ can 1) abstract a H atom, converting the initial $\bullet OH$ into H_2O forming a radical intermediate or 2) abstract an electron from the carboxylate group present in Asp and Glu, transforming the $\bullet OH$ to ^-OH . In any case, an amino acid radical is created, which is presented as the intermediate in our reaction. The second $\bullet OH$ can 1) add itself to the radical, forming an alcohol or peroxide, depending on the intermediate, group at the side chain, or 2) abstract another H atom from the neighbouring atoms, leading to the formation of a double bond. Both steps are considered to be driven by thermodynamics, as similar reactions previously studied in other AA models. A schematic

representation of the overall reaction mechanism and the employed labelling is shown in Figure 7.2.

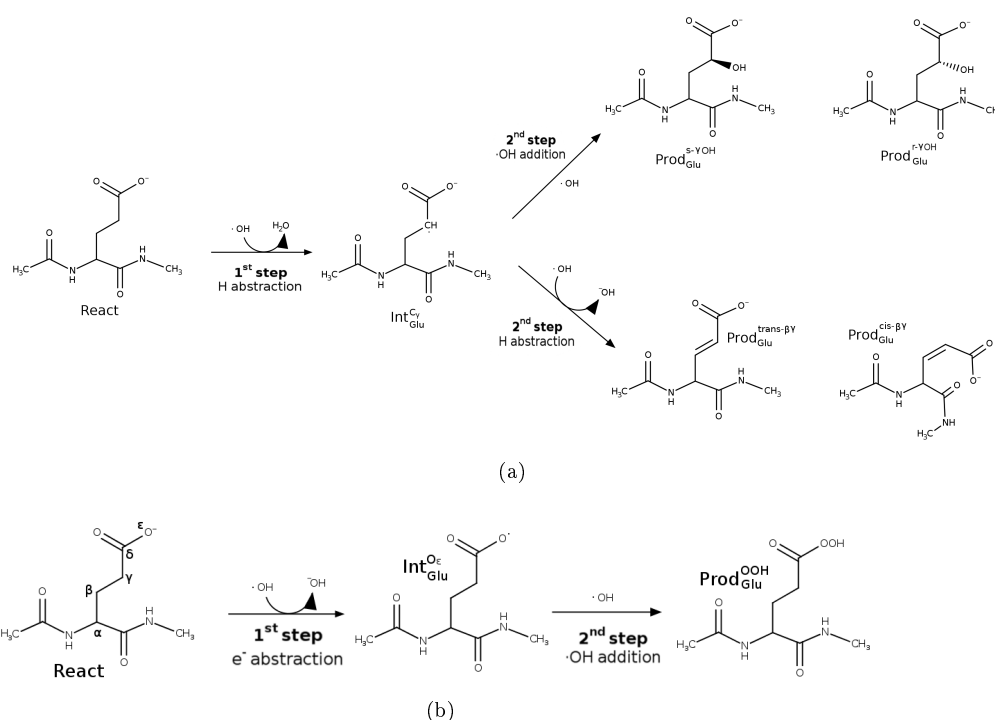


Figure 7.2: Schematic representation of the studied reaction mechanisms, for the attack on Glu. The overall oxidation reaction is splitted into two steps. a) first step considers a H abstraction and the second considers $\bullet OH$ addition or H abstraction b) first step considers an electron abstraction while the second consists on the $\bullet OH$ addition. The attack on Asp is the same as it is shown herein. The employed nomenclature is shown for the reactants in b).

As in the previous chapters, the effect of the backbone conformation is included. However, its effect on the attack at the side chain is neglectable. Indeed, the mean absolute difference for both conformations is 0.03 kcal/mol and 0.51 kcal/mol for intermediates and products respectively; while the mean absolute deviation (MAD) is of 1.75 kcal/mol for the former and 1.74 kcal/mol for the latter. Therefore, it can be said that no significant difference is found when changing the conformation and the discussion is done with the α – helix – like conformation. The calculated values for both conformations can be found in the appendix.

7.2.1 Acid containing amino acids

The carboxylic group has a pKa of 3.9 and in some proteins even higher. Asp and Glu show deprotonated state at both high and physiological pH values (carboxylate), while at low pH

values the protonated state of the functional group can be found (carboxylic acid). Hence, both protonation states are considered.

7.2.1.1 Aspartic acid

The deprotonated state aspartate (Asp) and the protonated state aspartic acid (Asph) are studied. Figure 7.3 displays the stages of the Asp reaction pathway. The attack of the first $\bullet OH$ produces the intermediates that are labelled as Int in Figure 7.3, whereas the second $\bullet OH$ attack renders the products labelled as Prod. In the same line, Figure 7.4 shows the reaction mechanism for Asph.

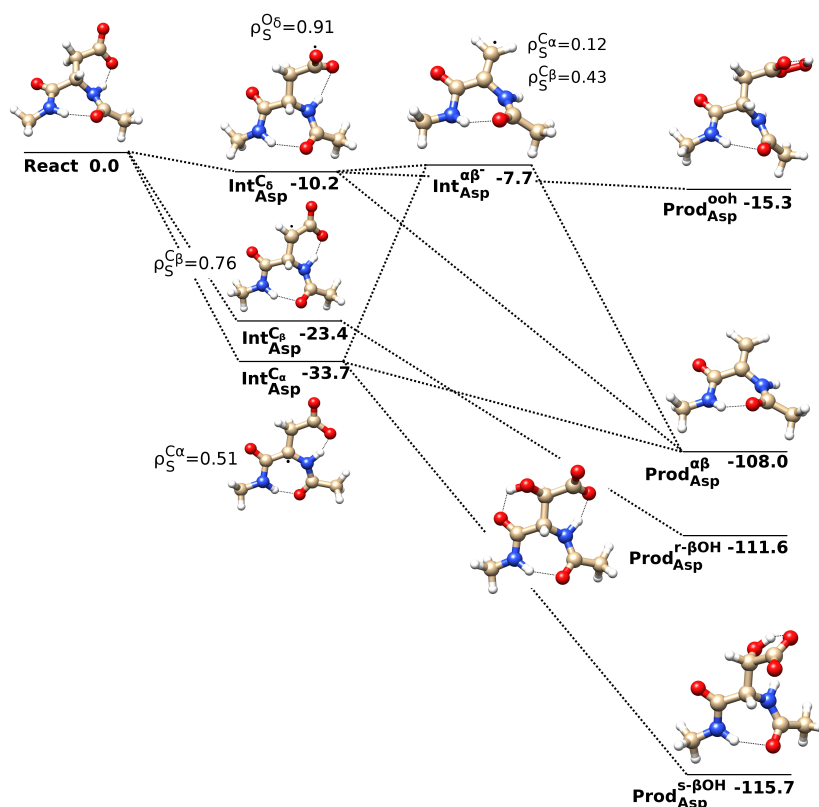


Figure 7.3: Schematic representation of Aspartate reaction pathway. Reactants (React), intermediates (Int) and products (Prod) are labelled depending on the attack site. Relative enthalpy values are given in kcal/mol. TFVC spin densities are shown for all Int.

1st $\bullet OH$ can abstract a H atom from C_{α} , C_{β} or an electron from the O atom of the carboxylate group (O_{δ}). In any case, a radical amino acid is obtained which is the intermediate

in the reaction, as was mentioned ahead. The relative enthalpies and TFVC spin densities are presented in Figure 7.3 and Table C.1. $Int_{Asp}^{C_\alpha}$ showed to be the most stable radical intermediate $\Delta H_{aq}^{298} = -33.7$ kcal/mol and lies about 10 kcal/mol lower than $Int_{Asp}^{C_\beta}$. Both intermediates have been studied in Chapter 1 and it is shown that any radical at C_α position is more favored than at C_β due to the captodative effect occurring at the former.

$Int_{Asp}^{O_\delta}$ represents the radical intermediate formed after the electron abstraction, which is about 13 kcal/mol higher than $Int_{Asp}^{C_\beta}$. Here, the •OH abstracts an electron from the O_δ atom of the carboxylate group to render the intermediate radical, $Int_{Asp}^{O_\delta}$. $Int_{Asp}^{C_\beta}$ is a secondary radical while $Int_{Asp}^{O_\delta}$ is a primary radical and the hyperconjugation effect further stabilises the secondary radical.

The spin densities indicate the localization of the unpaired electron, the more delocalized it is, the most stable the intermediate would be. $Int_{Asp}^{C_\alpha}$ has the lowest value, stabilised by the captodative effects, [112, 113] while $Int_{Asp}^{C_\beta}$ is a secondary radical that is stabilised due to hyperconjugation effects; and in the e^- abstraction intermediate $Int_{Asp}^{O_\delta}$, clearly the radical is localised in the O atom.

In the case of the carboxylic acid (Asph), energetically the same trend is obtained (Figure 7.4). That is, the most stable intermediate is the one corresponding to the H abstraction at C_α ($Int_{Asph}^{C_\alpha}$) $\Delta H_{aq}^{298} = -28.6$ kcal/mol, which is about 5 kcal/mol more favored than $Int_{Asph}^{C_\beta}$, while the H abstraction of the carboxylic group (O_δ) leads to an intermediate about 21 kcal/mol less stable than $Int_{Asph}^{C_\alpha}$.

Looking at the spin densities the lowest value is obtained for $Int_{Asph}^{C_\alpha}$, a tertiary radical stabilised by the captodative effect. $Int_{Asph}^{C_\beta}$ is a secondary radical stabilised by the hyperconjugation effect as mentioned, while the highest spin density is obtained for $Int_{Asph}^{O_\delta}$.

Side chain scission $Int_{Asp}^{C_\alpha}$ could drive to a side chain splitting through an heterolytic mechanism, where a CO_2 molecule is released and the radical remains on the amino acid. However, such intermediate, $Int_{Asp}^{-\alpha\beta}$ ($\Delta H_{aq}^{298} = -7.7$ kcal/mol), is about 27 kcal/mol higher than $Int_{Asp}^{C_\alpha}$, which remarks the energetic penalty that has to overcome in order to obtain such intermediate.

The spin density of the side chain scission intermediate $Int_{Asp}^{-\alpha\beta}$, is distributed along the backbone with a little preference by the C_α atom, and because of the heterolytic splitting the intermediate carries a negative charge.

The attack at C_α could lead to the side chain scission as in Asp ($Int_{Asph}^{-\alpha\beta}$). However, in this case, a proton is also released as a H atom is bound to the O_δ atom. In contrast with the deprotonated system, the reaction is now endothermic ($\Delta H_{aq}^{298} = 7.3$ kcal/mol) and so the chances to occur are greatly lowered (Table C.1).

$Int_{Asp}^{-\alpha\beta}$ and $Int_{Asph}^{-\alpha\beta}$ are the same chemical entities with different reactants as reference, and so the previous arguments are applicable for the spin density analysis.

2nd •OH can abstract another H atom from Asp, add itself to the already formed radical intermediate, or abstract an electron from either the carboxylate group or the formed negatively charged amino acid $Int_{Asp}^{-\alpha\beta}$. Note that the addition of the •OH toward the

formed $Int_{Asph}^{C_\alpha}$ is not considered as the purpose is to investigate the side chain oxidation mechanisms. This second attack yields the final products and herein we analyse their thermodynamical stability (Table C.2).

The most favored products correspond to the $\bullet OH$ addition to the formed $Int_{Asp}^{C_\beta}$, leading to $Prod_{Asp}^{r-\beta oh}$ ($\Delta H_{aq}^{298} = -111.6$ kcal/mol) and $Prod_{Asp}^{s-\beta oh}$ ($\Delta H_{aq}^{298} = -115.7$ kcal/mol), the latest is about 4 kcal/mol more stable than the former. Finally, the addition of the $\bullet OH$ to the formed O^δ radical to produce the peroxide group yields the least stable product, $Prod_{Asp}^{ooh}$, which lies 100 kcal/mol higher than $Prod_{Asp}^{s-\beta oh}$.

The same trend of products is observed for Asph (Table C.2). Interestingly, even though it is still the most unstable product, $Prod_{Asph}^{ooh}$ ($\Delta H_{aq}^{298} = -46.9$ kcal/mol) is greatly stabilised (by about 30 kcal/mol) when comparing to $Prod_{Asp}^{ooh}$. Once again, $Prod_{Asph}^{r-\beta oh}$ and $Prod_{Asph}^{s-\beta oh}$ are the most stable ones.

Side chain scission The plausible side chain dissociation is observed to occur after the consecutive attack of two $\bullet OH$. Departing from $Int_{Asp}^{C_\alpha}$ if the $\bullet OH$ abstracts an electron from the carboxylate, CO_2 is released by an homolytic splitting forming $Prod_{Asp}^{\alpha\beta}$ ($\Delta H_{aq}^{298} = -108.0$ kcal/mol). In the same way, $Int_{Asp}^{O^\delta}$ leads to the same product if the $\bullet OH$ abstracts an H atom from C_α . The same mechanism is observed for Asph and $Prod_{Asph}^{\alpha\beta}$ displays a $\Delta H_{aq}^{298} = -103.4$ kcal/mol.

7.2.1.2 Glutamic acid

As in the previous case, the H atom or e^- abstraction stages of the oxidation pathway of Glutamate (Glu) and Glutamic acid (Gluh) are analysed in two attacks of $\bullet OH$.

1st $\bullet OH$ The obtained results for Glu (Table C.3) point out that the most stable intermediate corresponds to the H abstraction at C_γ . $Int_{Glu}^{C_\beta}$ ($\Delta H_{aq}^{298} = -20.3$ kcal/mol) and $Int_{Glu}^{C_\gamma}$ ($\Delta H_{aq}^{298} = -24.2$ kcal/mol) are secondary radicals but the latter is about 4 kcal/mol more stable than the former owing to the neighbouring carboxylate group, which further stabilises the radical. $Int_{Glu}^{O_\epsilon}$ is a primary radical formed after the electron transfer from the O_ϵ of the carboxylate to the $\bullet OH$, forming the ^-OH and therefore it is about 14 kcal/mol higher than $Int_{Glu}^{C_\gamma}$.

For the intermediates of the H abstraction from Gluh, the same stability trend is observed, the $Int_{Gluh}^{C_\gamma}$ is more stable than the secondary radical $Int_{Gluh}^{C_\beta}$ due to the neighbouring carboxylic group that helps in the radical delocalisation, and the primary radical $Int_{Gluh}^{O_\epsilon}$ is the least stable one.

Regarding to the spin densities of the Glu and Gluh intermediates, as in the previous cases, the highest the value, the less stable the radical.

2nd •OH The final products are shown in Figure 7.5 (Table C.4). The most stable products correspond to the •OH additions to $Int_{Glu}^{C\beta}$ and $Int_{Glu}^{C\gamma}$ below 110 kcal/mol. The $Prod_{Glu}^{cis-\beta\gamma}$ and $Prod_{Glu}^{trans-\beta\gamma}$ that also contains a double bond in the side chain are about 8 kcal/mol less stable than $Prod_{Glu}^{s-\gamma^{oh}}$. Such products come from a second H atom abstraction at the neighbouring position at the $Int_{Glu}^{C\gamma}$ or $Int_{Glu}^{C\beta}$ radicals generating the respective isomers. And finally, the formation of the peroxide is the mechanism least favored, since the $Prod_{Glu}^{ooh}$ is about 100 kcal/mol above the most stable product.

The products for Gluh follow the same trend as already discussed for Glu, Figure 7.6 (Table C.4). The addition of •OH to the formed C radical intermediate yield the most favored products. $Prod_{Gluh}^{r-\beta^{oh}}$ is the most stable one ($\Delta H_{aq}^{298} = -110.7$ kcal/mol). Whereas, the isomer products are at 22.0 kcal/mol, and once again the peroxide product, $Prod_{Gluh}^{ooh}$, is the least favored, it lies about 55 kcal/mol higher than $Prod_{Gluh}^{\beta\gamma}$.

Side chain scission $Int_{Glu}^{C\beta}$ can lead to the side chain dissociation in case where the second •OH abstracts an electron from O_ϵ rendering $Prod_{Glu}^{\beta\gamma}$, which contains a double bond between C_β - C_γ and a CO_2 molecule ($\Delta H_{aq}^{298} = -104.6$ kcal/mol). $Int_{Glu}^{O_\epsilon}$ leads to the same product in case where a H atom is abstracted from C_β . The same mechanism is true for Gluh and $Prod_{Gluh}^{\beta\gamma}$ shows $\Delta H_{aq}^{298} = -100.7$ kcal/mol.

7.2.2 Base containing amino acids

Arg and Lys side chain's are formed by N atom containing groups. These groups are known to act as base and are often protonated. Indeed, the estimated pKa values are relatively high so herein we have just considered the protonated states of the amino acids.

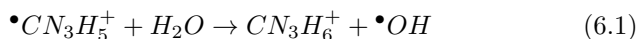
7.2.2.1 Arginine

The Arg mechanism oxidation occurs by a first H abstraction from the side chain atoms, and in the second step by a H abstraction or addition of the •OH to the formed radical amino acid.

1st •OH The intermediates that can be created from H abstractions are shown in Figure 7.7 and Table C.5. The most stable intermediate corresponds to $Int_{Arg}^{C\delta}$ ($\Delta H_4^{298} = -23.9$ kcal/mol), which is a secondary radical, where the lone pair of the neighbouring N_ϵ atom helps to stabilise the radical. The other two secondary radicals, $Int_{Arg}^{C\beta}$ and $Int_{Arg}^{C\gamma}$, are very close in energy and show to be about 5 kcal/mol higher than $Int_{Arg}^{C\delta}$. Finally the abstraction of H at N atoms have been investigated, such abstractions yield $Int_{Arg}^{N_\epsilon}$ (secondary radical) and $Int_{Arg}^{N_\eta}$ (primary radical). Both of them show to be the most unstable ones, but $Int_{Arg}^{N_\epsilon}$ is about 6 kcal/mol more favored than $Int_{Arg}^{N_\eta}$.

The TFVC spin densities show the lowest values for $Int_{Arg}^{C\delta}$ due to the delocalization to the neighbouring N_ϵ atom. The rest of the secondary radicals, $Int_{Arg}^{C\beta}$, $Int_{Arg}^{C\gamma}$ and $Int_{Arg}^{N_\epsilon}$ display higher spin densities, due to the lack of a neighbour N atom. The primary radical, $Int_{Arg}^{N_\eta}$ displayed the highest spin density (0.83).

Side chain scission $Int_{Arg}^{C_\gamma}$ could proceed through the side chain homolytic dissociation as it is shown in Figure 7.8, leading to a double bond between atoms C_γ and C_δ ($Prod_{Arg}^{\gamma\delta}$) and a guanidinium radical ($\bullet CN_3H_5^+$). The side chain scission reaction is observed to be $\Delta H_{aq}^{298} = 1.1$ kcal/mol.



Considering that the scission mechanism produces another radical, we evaluate its capacity to abstract a H atom through reaction (6.1). The estimated ΔH_{aq}^{298} is of -0.6 kcal/mol favoring slightly such process; therefore completing the mechanism of Figure 7.8, the H abstraction from C_δ of $Prod_{Arg}^{\gamma\delta}$ by the guanidinium radical leads to the formation of the isomers cis- and trans- $Int_{OArg}^{C_\delta}$. The subindex OArg indicates that the intermediate is formed from an already oxidized product of Arg, in this case from $Prod_{Arg}^{\gamma\delta}$. Their barely exothermic relative enthalpies suggest the possible formation at such intermediates once that the guanidinium radical is formed.

In the same way the production of Citrulline and Ornithine is possible via the side chain scission once the $\bullet OH$ is added at C_ζ (Figure 7.9). In this case the radical amino acid is $Int_{Arg}^{C_\zeta}$ and is observed to be slightly endothermic.

The spin density of the unpaired electron in the guanidinium radical is located in the NH group, according to the spin density analysis, with a value of 0.87 and in $Int_{OArg}^{C_\gamma}$ the radical is located in the C_δ with values of spin density of 0.98 in the trans isomer and 0.99 in the cis isomer.

2nd •OH The alcohol products of the addition of the $\bullet OH$ to the C radical, in the second attack, are more favored than those with a double bond products of a H atom abstraction. The energetic values for these chemicals range from -107.6 to -114.6 kcal/mol showing the narrow value at which they lie. The double bond containing products lie in a range between from -93.2 to -100.5 kcal/mol. Meanwhile, the hydroxylamine products formed after the addition to a N radical atom are observed to be about 40 kcal/mol less stable (Table C.6).

The products formed by a second $\bullet OH$ attack to $Int_{OArg}^{C_\delta}$, obtained via guanidinium radical are energetically very similar to the most stable products. Two conformers (cis and trans) of an alcohol product are obtained ($Prod_{OArg}^{\delta oh}$) and an aldehyde ($Prod_{OArg}^{\delta o}$), which is the keto form of $Prod_{OArg}^{\delta oh}$. Observe that among all the studied products the aldehyde is the most favorable one.

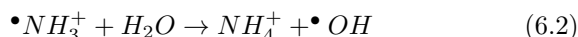
7.2.2.2 Lysine

The Lys oxidation takes place after a H abstraction from the side chain by the first $\bullet OH$; continuing with the addition of a second $\bullet OH$ to the formed radical or abstract another H atom from the neighbour atom.

1st •OH Once again, the formed secondary radicals are the most stable intermediates and the values spread in the -14.7/-19.1 kcal/mol range (Figure 7.10). A primary radical is formed after the abstraction from the N_ζ atom at the end of the side chain. $Int_{Lys}^{N_\zeta}$ lies about 10 kcal/mol higher than the most stable secondary radical intermediate, $Int_{Lys}^{C_\gamma}$ (Table C.5).

The spin densities are very similar for all of them. The lowest values are estimated for $Int_{Lys}^{C_\delta}$ and $Int_{Lys}^{C_\epsilon}$ with a value of 0.77. Meanwhile, the highest value is obtained for the primary radical, 0.80.

Side chain scission As in the Asp case, a homolytic dissociation mechanism may occur generating an ammonia radical ($\bullet NH_3^+$), however, the reaction to abstract a H atom from water is an endothermic process, $\Delta H_{aq}^{298} = 5.5$ kcal/mol according to the reaction (6.2).



The product from the side chain scission, $Prod_{Lys}^{\delta\epsilon}$, is very slightly favored ($\Delta H_{aq}^{298} = -0.1$ kcal/mol), but despite the fact that we considered the H abstraction from C_ϵ position in the $Prod_{Lys}^{\delta\epsilon}$ by the $\bullet NH_3^+$ to form the intermediate isomers, $Int_{Lys}^{C_\epsilon}$. The process is observed to be endothermic and therefore not a very favorable mechanism ($\Delta H_{aq}^{298} \approx 2$ kcal/mol).

2nd •OH The products where an alcohol group is formed are the most stable ones and are spread between -110 to -114 kcal/mol (Figure 7.10 and Table C.7). The products where a double bond is formed are about 15 to 20 kcal/mol less favored than those alcohol containing products, ranging from -94 to -104 kcal/mol. The addition of a •OH to the N_ζ radical is the least favored product, being ΔH_{aq}^{298} of -66 kcal/mol.

The products obtained by another •OH attack to the formed $Int_{Lys}^{C_\epsilon}$ can lead to alcohol ($Prod_{Lys}^{\epsilon oh}$) or an aldehyde ($Prod_{Lys}^{\epsilon o}$). The aldehyde lies about 10 kcal/mol lower than the corresponding alcohols; it is indeed the most stable product, and very close to the previously mentioned alcohols.

7.2.3 Amide containing amino acids

Asn and Gln have an amide group in the side chain. Little documentation about their oxidation is found, but are known to be a suitable site for the H atom abstraction.

7.2.3.1 Asparagine

Herein the possible oxidation mechanism for Asn by two •OH is analysed. The first •OH abstracts a H atom, while the second •OH generates the respective alcohols or the unsaturated products.

1st •OH can abstract a H atom from C_α , C_β or N_δ . The H abstraction from the backbone C_α has been considered as it could lead to the side chain dissociation. As shown in Figure 7.11 and Table C.8 the intermediate formed after the abstraction at C_α , $Int_{Asn}^{C_\alpha}$, is the most favored one. $Int_{Asn}^{C_\beta}$, a secondary radical, is about 7 kcal/mol less favored, and the abstraction of a H atom from N_δ , which leads to a primary radical ($Int_{Asn}^{N_\delta}$), showed to be about 30 kcal/mol higher than $Int_{Asn}^{C_\alpha}$.

Observing the spin densities of the first attack intermediates, the lowest value is obtained for $Int_{Asn}^{C_\alpha}$ due to the captodative effect. $Int_{Asn}^{C_\beta}$ displays a higher value, whereas the highest value is obtained for $Int_{Asn}^{N_\delta}$, the primary radical.

Side chain scission $Int_{Asn}^{C_\alpha}$ could dissociate the side chain homolytically to yield $Prod_{Asn}^{\alpha\beta}$, which contains a double bond between atoms C_α and C_β , and a radical specie ($\bullet CONH_2$). However, the relative enthalpies for the homolytic dissociation mechanism show that it is an endothermic reaction ($\Delta H_{aq}^{298} = 3.9$ kcal/mol). The formed radical specie ($\bullet CONH_2$) could at the same time abstract H atoms (in the same way as the $\bullet OH$) and to quantify its reactivity, relative enthalpy was computed with the reaction (6.3)



The obtained ΔH_{aq}^{298} for reaction (6.3) is 22.5 kcal/mol indicating that the $\bullet CONH_2$ capacity of abstracting H atoms compared with the $\bullet OH$ is much lower, probably due to delocalisation of the unpair electron along the radical, as the largest value of the spin density is 0.55 on the C atom.

However, we have considered the possibility by which $Prod_{Asn}^{\alpha\beta}$ gets oxidized by the radical obtained from the scission of the side chain, i.e. $\bullet CONH_2$. In this case the H abstraction from C_β position leads to the radical intermediates ($Int_{OAsn}^{C_\beta}$). The relative enthalpies indicate that the reaction is endothermic and therefore, the stages where the $\bullet CONH_2$ is involved are not prone to take place. Notice, that if the $Prod_{Asn}^{\alpha\beta}$ is oxidized by the $\bullet OH$, the reaction could not proceed but still is endothermic and the estimated ΔH_{aq}^{298} is about 1.5 kcal/mol.

2nd •OH can add itself to the already formed radical intermediate, in this case at C_β or N_δ . The addition to the former leads to two possible enantiomer products which show to be the most favored ones, $Prod_{Asn}^{r-\beta oh}$ ($\Delta H_{aq}^{298} = -111.7$ kcal/mol) and $Prod_{Asn}^{s-\beta oh}$ ($\Delta H_{aq}^{298} = -110.3$ kcal/mol). On the other hand, the addition at N_δ is less favored, lying about 40 kcal/mol higher than the previous reactions.

The second $\bullet OH$ can be also added to the radical ($Int_{OAsn}^{C_\beta}$) formed after the scission of the side chain. It renders two possible alcohol conformers ($Prod_{OAsn}^{cis-\beta oh}$ and $Prod_{OAsn}^{trans-\beta oh}$) and an aldehyde ($Prod_{OAsn}^{\beta o}$), obtained by the keto-enol tautomerisation of any of the isomers and shows to be slightly more favored than the enol tautomers.

7.2.3.2 Glutamine

As in the Asn case, the Gln oxidation mechanism proceeds through the H abstraction from C_β , C_γ or N_ϵ side chain atoms, and then a second $\bullet OH$ is added to form alcohols or abstract another H atom.

1st •OH In this case, the formation of $Int_{Gln}^{C_\gamma}$ ($\Delta H_{aq}^{298} = -26.7$ kcal/mol) is the most favorable one, being the $Int_{Gln}^{C_\beta}$ about 6 kcal/mol higher, both are secondary radicals. The H abstraction from N_ϵ leads to the formation of $Int_{Gln}^{N_\epsilon}$ which is about 23 kcal/mol higher than $Int_{Gln}^{C_\gamma}$.

Regarding to the spin densities, the primary radical $Int_{Gln}^{N_\epsilon}$ has the largest value, indicating the localisation at the unpair electron, while the secondary radicals have lower values as more stable the intermediate. In the other hand, the values close to 1 for the isomers reflect once again high reactivity of them (Table C.8).

Side chain scission $Int_{Gln}^{C_\beta}$ could proceed to the side chain splitting via homolytic dissociation. In this case, the product, $Prod_{Gln}^{\beta\gamma}$, has a double bond between C_β and C_γ , but once again the process is endothermic, $\Delta H_{aq}^{298} = 5.1$ kcal/mol. Subsequent oxidation with the $\bullet CONH_2$ to form the intermediates cis- and trans- $Int_{O_{Gln}}^{C_\gamma}$, proved to be an endothermic process, around 20 kcal/mol, as it was the case for Asn, while using the $\bullet OH$ to abstract the H atom makes the process slightly exothermic, around -0.5 kcal/mol.

2nd $\bullet OH$ The most favored products are obtained for the case in which the $\bullet OH$ is added to the C atom where the radical is centered, leading to the formation of alcohol containing products, Figure 7.12 (Table C.9). Observe that different enantiomers could be obtained with no significant energetic difference. The formation of a double bond occurs after a H atom is abstracted from C_γ or C_β of the $Int_{Gln}^{C_\beta}$ and $Int_{Gln}^{C_\gamma}$, respectively; generating the isomers, cis and trans, being the $Prod_{Gln}^{trans-\beta\gamma}$ the most favored one, by 3.6 kcal/mol. The addition of an $\bullet OH$ to the N_ϵ atom of $Int_{Gln}^{N_\epsilon}$ occurs to be the least favored one, lying about 40 kcal/mol higher than $Prod_{Gln}^{r-\beta oh}$.

Finally, the addition of an $\bullet OH$ to the intermediates $Int_{Gln}^{C_\gamma}$, produces the respective cis- and trans- alcohols and the keto tautomer, being this the most favored of them, but 19 kcal/mol less stable than the $Prod_{Gln}^{r-\beta oh}$.

7.3 Conclusions

In the present work we have provided the oxidation mechanism for acid, base and amide containing amino acid side chains. The simplified oxidation protocol is performed by the consecutive attack of two $\bullet OH$ to the amino acid side chains, which is divided and discussed into two stages. The attack of the first $\bullet OH$ produces the radical amino acids whose relative thermodynamic stabilisation is analysed in order to establish the most favorable reaction pathway. Then, the second attack of the $\bullet OH$ quenches the previously formed radical, leading to final oxidized products. This procedure helps rationalising experimentally observed oxidized products but also some other alternative ones which have been analysed.

Two dielectric constants were employed in order to simulate the reaction in water and a low dielectric environment. The conformational effect was taken into account performing the reaction in α -helix-like and β -sheet conformations. The obtained results do not vary in a significant way with these parameters so we conclude that the conformation and dielectric do not affect the reaction mechanisms herein discussed.

Most favored radical intermediates formed after the attack of the first $\bullet OH$ are the secondary ones, which are stabilised by the hyperconjugation effect. $Int_{Arg}^{C_\delta}$ has been observed to get even more stabilised due to the neighbouring N atom, whose lone pair further contributes to such stabilisation.

Asp can lead to side chain dissociation after abstracting a H atom from C_α or an e^- from the carboxylate group. The same is applicable to Glu, where the side chain dissociation can take place if a H atom is abstracted from C_β or an e^- from the carboxylate group. Arg could yield side chain dissociation if the $\bullet OH$ is added to the guanidinium C atom ($Int_{Arg}^{C_\zeta}$) or a H atom is abstracted from C_γ forming $Int_{Arg}^{C_\gamma}$. The addition mechanism and the side chain dissociation of $Int_{Arg}^{C_\gamma}$ are observed to be slightly endothermic and therefore

thermodynamically are not as favored as the other studied mechanisms. Lys can also lead to a side chain dissociation after the formation of $Int_{Lys}^{C\delta}$ but once again the dissociation mechanism is observed to be slightly endothermic.

Overall, the hydroperoxide formed in acid containing Asp, Asph, Glu and Gluh are shown to be the least favored products. Moreover, the formed intermediate (primary radical) is also the least favored one, remarking the little propensity for this pathway to take place. Arg and Lys most favorable products are aldehydes formed after the side chain scission. However, it has to be remarked that the intermediates from where they are formed are the least favorable ones, and therefore the reaction pathway is not the most favorable one.

In every case herein introduced, the formation of an alcohol group in the side chain is observed to be the most favored product obtained from the most stable intermediate. Therefore, in this work we have studied the mechanisms that render the experimentally observed products and we have proposed alternative reactions from where other products could be obtained.

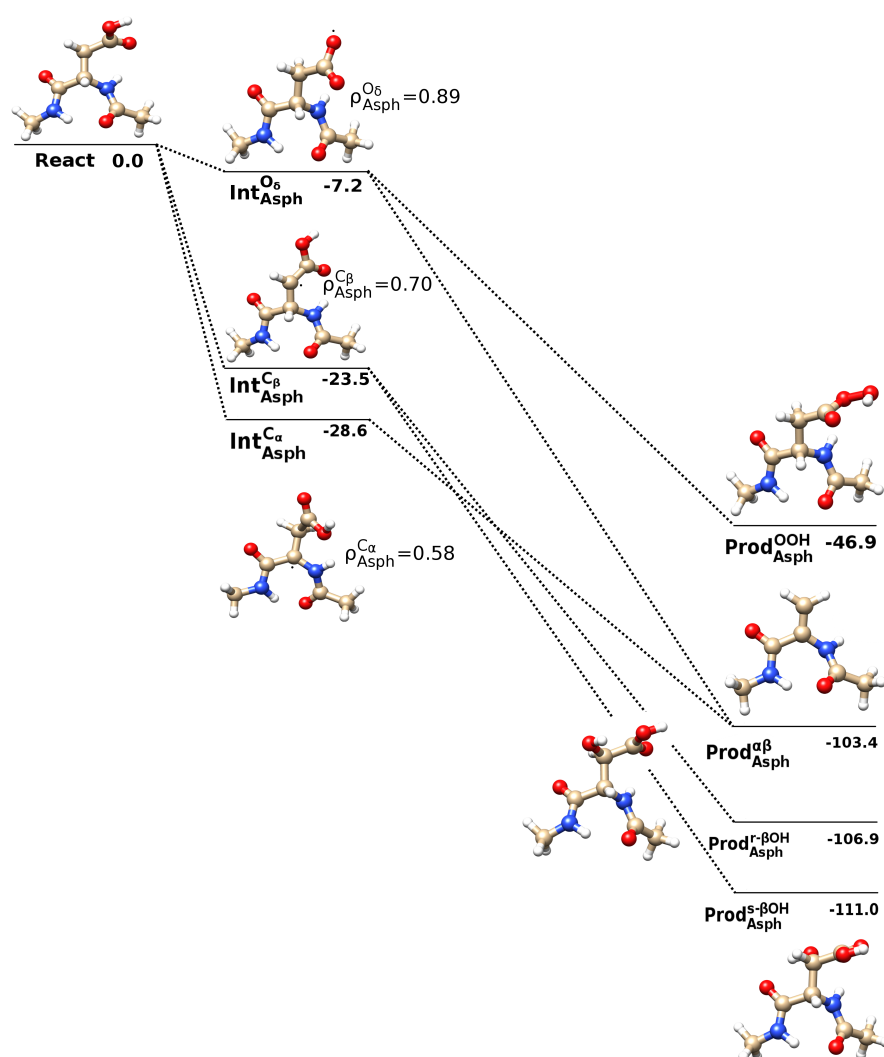


Figure 7.4: Schematic representation of Aspartic acid reaction pathway. Reactants (React), intermediates (Int) and products (Prod) are labelled depending on the attack site. Relative enthalpy values are given in kcal/mol. TFVC spin densities are shown for all Int.

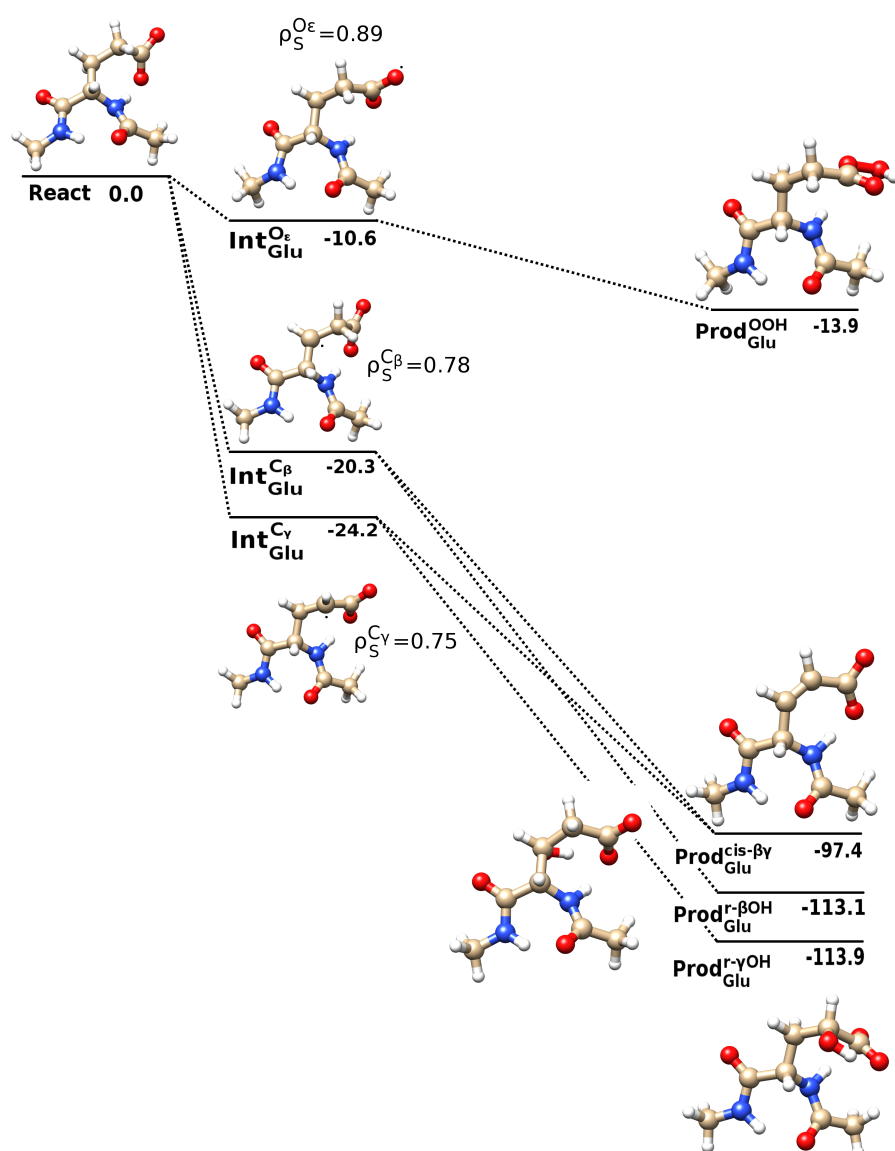


Figure 7.5: Scheme of Glutamate oxidation reaction pathway. Reactants (React), intermediates (Int) and products (Prod) are labelled depending on the attack site. Relative enthalpy values are given in kcal/mol. TFVC spin densities are shown for all Int.

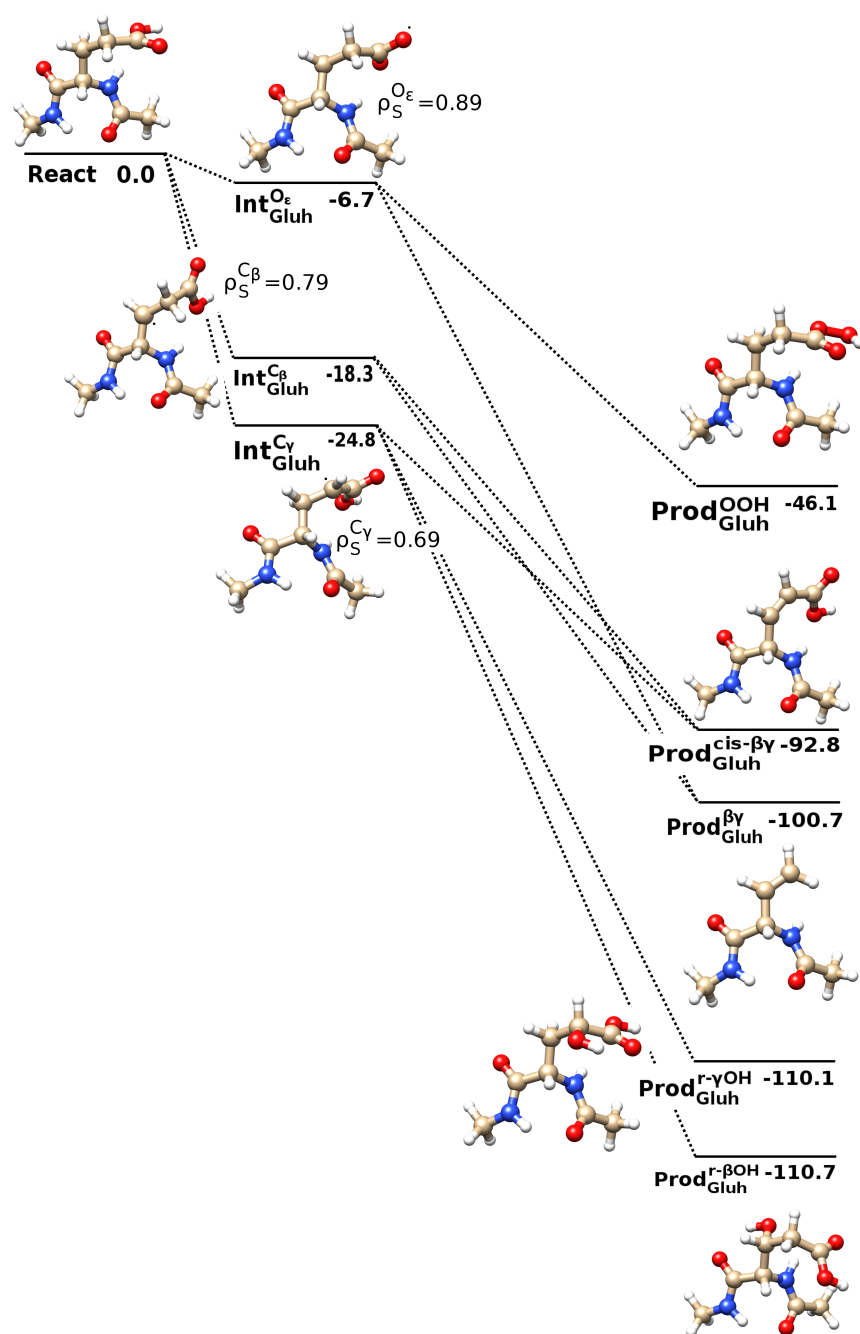


Figure 7.6: Schematic representation of Glutamic acid oxidation reaction mechanism. Reactants (React), intermediates (Int) and products (Prod) are labelled depending on the attack site. Relative enthalpy values are given in kcal/mol. TFVC spin densities are shown for all Int.

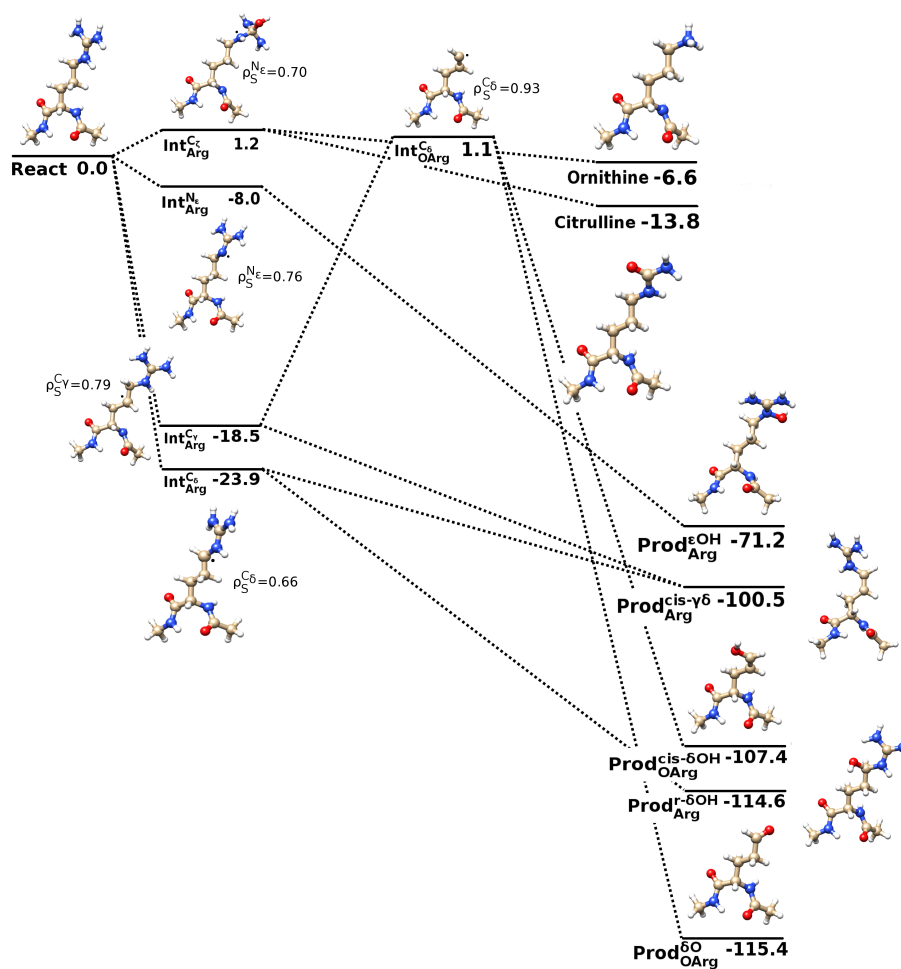


Figure 7.7: Schematic representation of Arg oxidation reaction pathway. Reactants (React), intermediates (Int) and products (Prod) are labelled depending on the attack site. Relative enthalpy values are given in kcal/mol. TFVC spin densities are shown for all Int.

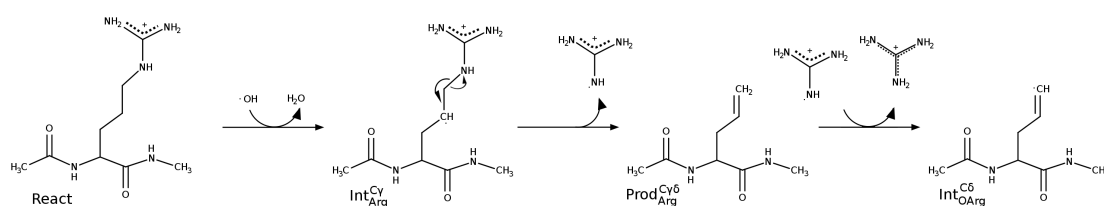


Figure 7.8: $Int_{Arg}^{C\gamma}$ homolytic dissociation of the side chain leading to a double bond formation in the amino acid ($Prod_{Arg}^{C\gamma\delta}$) and a guanidinium radical. $Int_{Arg}^{C\delta}$ formation by H abstraction of guanidinium radical.

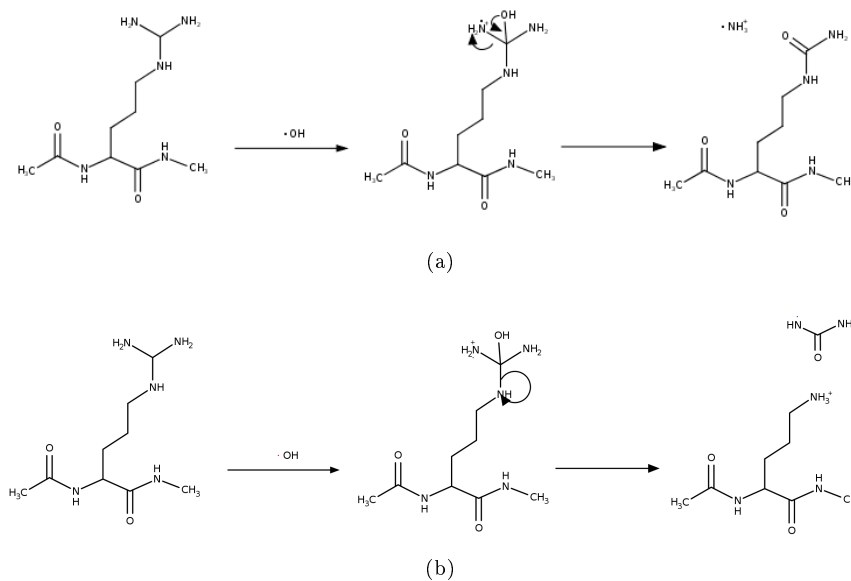


Figure 7.9: a) Citrulline product formation reaction pathway. b) Ornithine product formation reaction pathway.

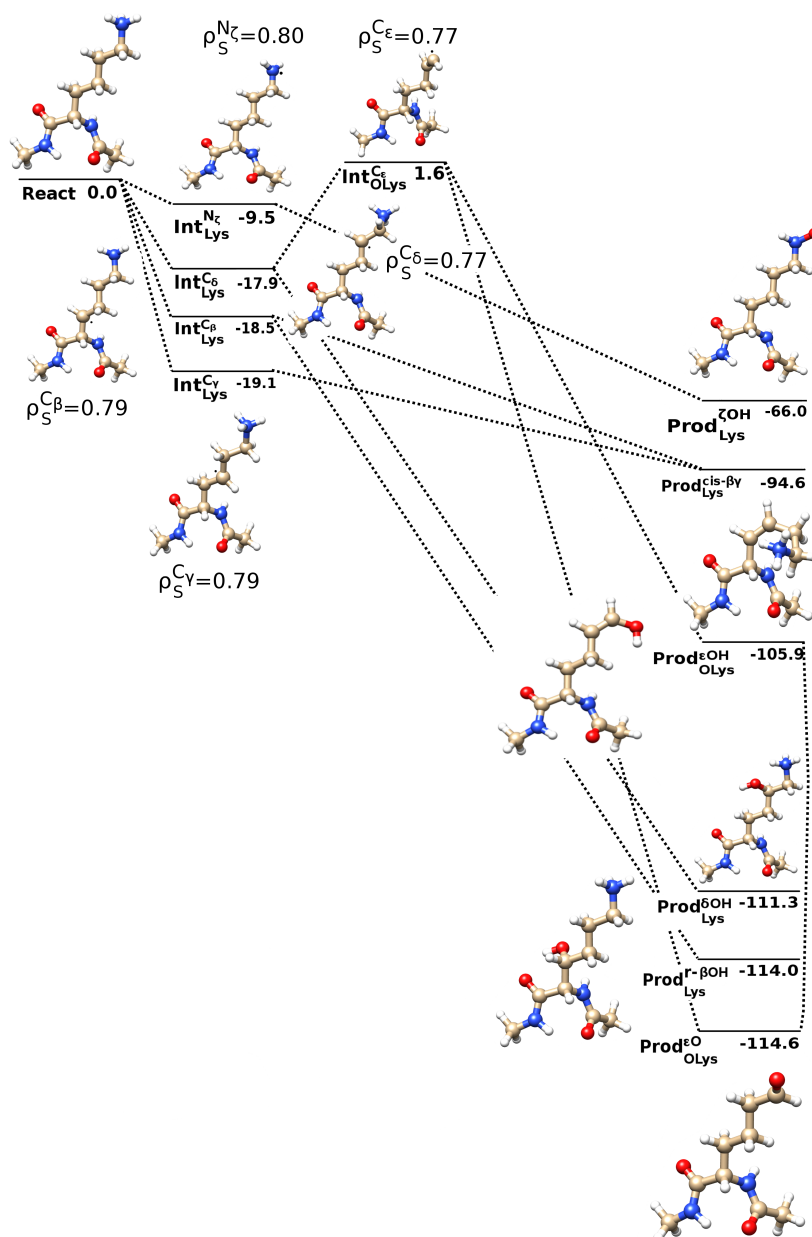


Figure 7.10: Schematic representation of Lys oxidation reaction pathway. Reactants (React), intermediates (Int) and products (Prod) are labelled depending on the attack site. Relative enthalpy values are given in kcal/mol. TFVC spin densities are shown for all Int.

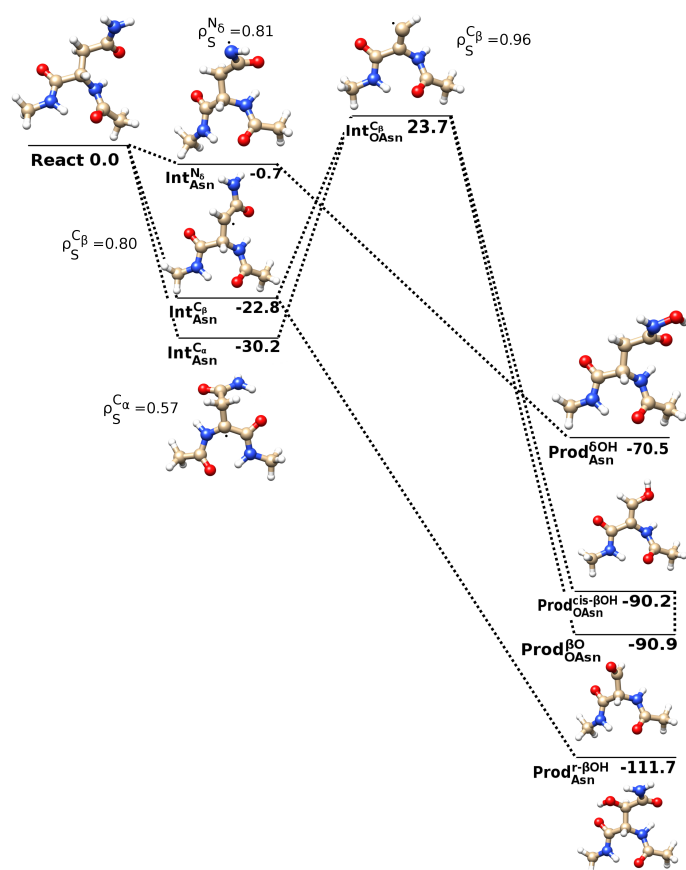


Figure 7.11: Schematic representation of Asn oxidation reaction pathway. Reactants (React), intermediates (Int) and products (Prod) are labelled depending on the attack site. Relative enthalpy values are given in kcal/mol. TFVC spin densities are shown for all Int.

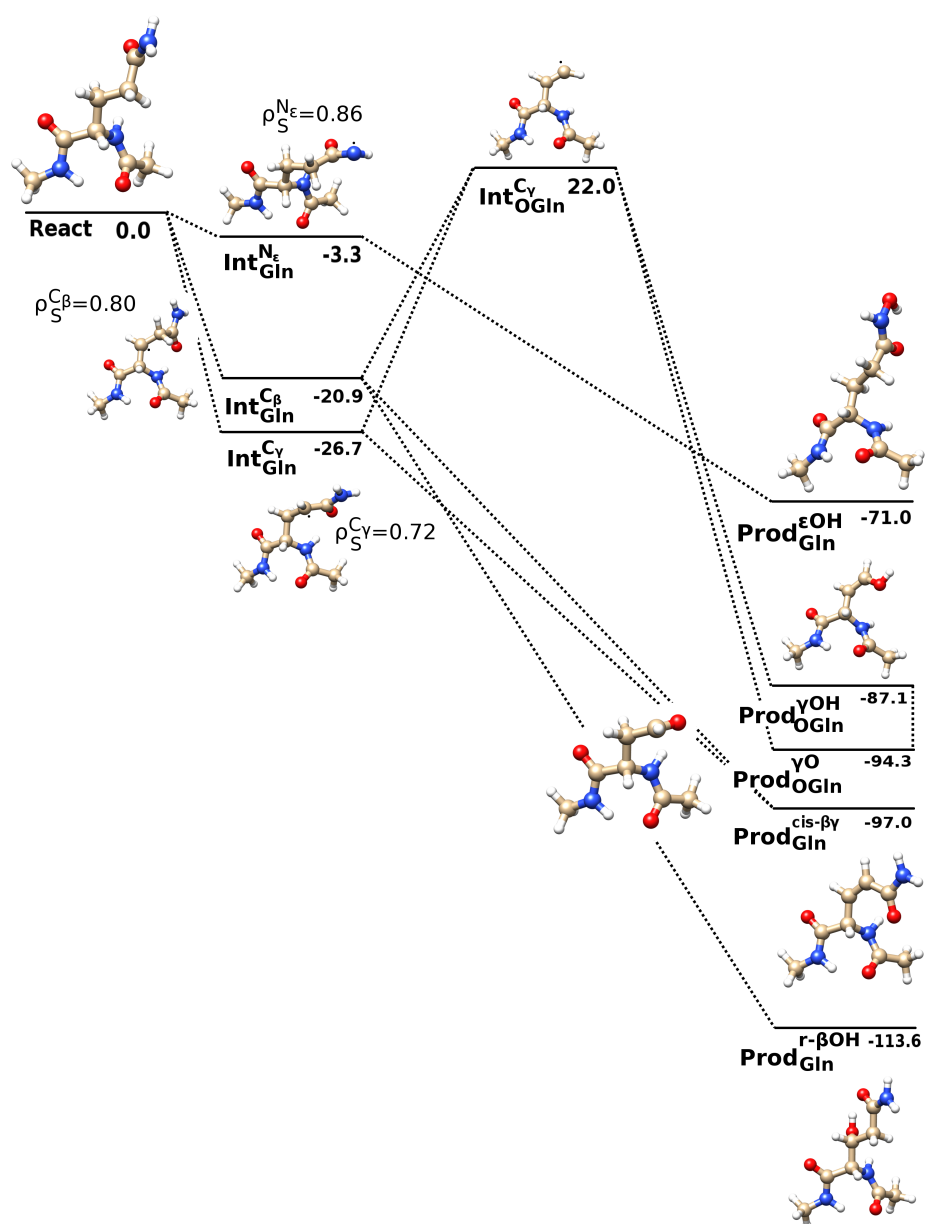


Figure 7.12: Schematic representation of Gln oxidation reaction mechanism. Reactants (React), intermediates (Int) and products (Prod) are labelled depending on the attack site. Relative enthalpy values are given in kcal/mol. TFVC spin densities are shown for all Int.

Chapter 8

Final Conclusions

This thesis work provides new insights towards the protein oxidation mechanisms by Reactive Oxygen Species, namely $\bullet OH$, which is an unavoidable event which causes many structural alterations at the protein. Herein, three reaction mechanisms are considered: i) H abstraction, ii) electron transfer and iii) $\bullet OH$ addition. Overall, the oxidation process is divided into two stages: in each step a $\bullet OH$ attacks the protein model under study. The reaction barriers for all these reaction steps show to be very small, hence, we conclude that thermodynamics is the main factor. Moreover, the observed transition barriers for different reactions does not vary in a significant way and we assume that the larger difference values obtained for the intermediates will influence in a more significant way to the reaction path. On the other hand, since the second step involves the reaction between two radical species, this step is known to be a barrierless process.

The effect of the environment is considered varying the dielectric continuum. A low dielectric constant is employed in order to mimic the buried regions of the proteins while water dielectric constant value is used with the purpose of representing solvent exposed residues. The observed difference is very low and therefore we conclude that the reaction mechanism is not influenced by this effect. However, the steric effects were not considered which could be important. In this sense, in the case that the residue is buried in the protein the oxidation event is more difficult to take place, as it is not accessible to the *reactive species*. Moreover, it is known that the backbone is a flexible part, hence, two different conformations were employed in the study, i.e. α -helix-like and β -sheet. It is observed that the effects of the conformation is small. Therefore, only the reactions characterized with the α -helix-like conformations are presented, while the reaction characterized with the β -sheet conformation are included in the Appendix.

Overall, the most stable intermediate radical formed after the H abstraction corresponds to C_α position (in the backbone), followed by the neighbour positions of the aromatic amino acids. Indeed, a correlation is observed between the radical spin density and the relative enthalpy values, as may be seen in Figure 8.1. The more delocalised the spin density of the intermediate the more stable the radical will be. Interestingly, the H abstraction from the N position of the aromatic moiety in Trp is very favored and the observed spin density is low. This occurs due to resonance structures which lowers the spin density and stabilises the intermediate. In the same way, the H abstraction from the O atom of Tyr brings a radical

which can delocalise its spin density through the aromatic moiety, lowering the radical at O atom. The rest of the H abstractions are favored for highest substituted atoms and the cases where a lone pair containing atom is nearby. The exception is the primary radical formed in Cys, which is favored due to the weak bond of SH. The mentioned three cases are marked in Figure 8.1.

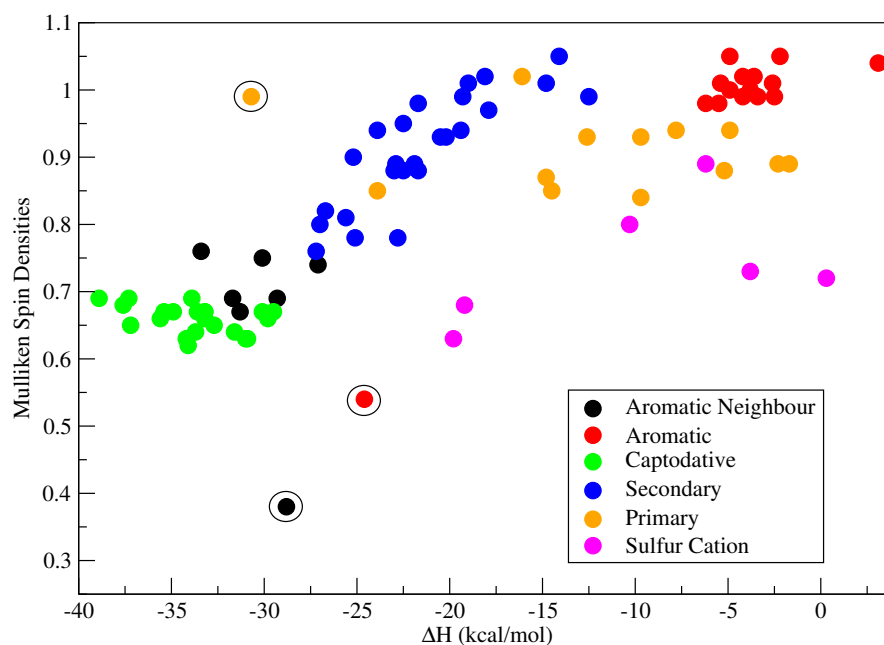


Figure 8.1: Mulliken spin densities respect to relative enthalpy values in kcal/mol for all studied intermediate radicals, obtained from the H and electron abstraction, in the β -sheet conformation and water dielectric.

The addition of $\bullet OH$ toward the aromatic ring leads to stable intermediates, even though the aromaticity is broken. It has to be noted that the most favored H abstraction are more stable than those type of additions, as the former are stabilised by delocalisation effects. The exception is the addition towards the C8 atom of Trp, where the aromaticity is broken but many possible resonance structures are possible.

The electron transfer mechanism, where an electron is abstracted from the S atom, in Met and Cys is shown to be highly dependent on the surrounding environment. In this sense, terminal amino acids with a carboxylate render the stablest intermediate radical cations. Among both amino acids, it is noted that Met display stabler intermediates as a result of the larger rings that can form. However, it has to be remarked that in the case of Cys and Met, H abstraction reactions lead to stabler intermediates than the electron transfer mechanism. Moreover, the oxidation mechanism of cystine showed that the first attack of $\bullet OH$ weakens the S-S bond. While, the second attack can lead to the breaking of the disulfide bond which in biology tends to render stability to the protein.

Concerning the products for the side chain oxidation, alcohol formation is usually favored.

However, the most stable product overall the work is observed to be the formation of a sulfur bridge, rendering the cystine. This is not a surprising result as it is employed in nature to bring chemical stability to proteins. On the other hand, Arg and Lys also show that the products obtained from side chain dissociation yield very stable products. Such side chain dissociation could also occur in Asp and Glu, but it is observed not to be as favored.

Finally, in regard to the alterations of the backbone structure, the C_α radicals show an increase of the backbone bonds, i.e. C_α -C and C_α -N, and so their dissociation is not plausible mechanism. The most notorious consequence of the creation of a radical at this position is the conformational change due to alterations in the dihedral angles, which tend to planar. On the other hand, the C_β radical intermediates can lead to homolytic dissociation mainly at C_α -C. The exception are Ser and Thr where C_α -N bond dissociation is a competitive reaction. The main reason for such mechanism to be possible in those two amino acids is the farther stabilisation obtained by the products. The dissociated products show a stabilising hydrogen bond which makes this reaction a real possibility.

Bibliography

- [1] B. Halliwell and J. Gutteridge. *Free radicals in Biology and Medicine*, volume 10.
- [2] H. D. Holland. The oxygenation of the atmosphere and oceans. *Philos. Trans. R. Soc. Lond. B. Biol. Sci.*, 361(1470):903–915, 2006.
- [3] B. Halliwell. Free radicals and antioxidants: a personal view. *Nutr. Rev.*, 52(8 Pt 1): 253–265, 1994.
- [4] K. Brieger, S. Schiavone, F. J. Miller, and K. H. Krause. Reactive oxygen species: from health to disease. *Swiss med. wkly.*, 142:w13659, 2012.
- [5] H. R. Griffiths. Antioxidants and protein oxidation. *Free radical res.*, 33 Suppl:S47–58, 2000.
- [6] C. L. Hawkins and M. J. Davies. Generation and propagation of radical reactions on proteins. *BBA-Bioenergetics*, 1504(2-3):196–219, 2001.
- [7] F. J. Corpas and J. B. Barroso. Reactive sulfur species (RSS): possible new players in the oxidative metabolism of plant peroxisomes. *Front. Plant Sci.*, 6(6):1803–1813, 2015.
- [8] V. I. Lushchak and H. M. Semchyshyn. *Oxidative Stress - Molecular Mechanisms and Biological Effects*. InTech, 2012.
- [9] V. I. Lushchak. Free radical oxidation of proteins and its relationship with functional state of organisms. *Biochemistry-Moscow+*, 72(8):809–827, 2007.
- [10] G. Lenaz, C. Bovina, M. D’Aurelio, R. Fato, G. Formigini, M. L. Genova, G. Giuliano, M. M. Pich, U. Paolucci, G. P. Castelli, and B. Ventura. Role of Mitochondria in Oxidative Stress and Aging. *Ann. NY. Acad. Sci.*, 959(1):199–213, 2006.
- [11] R. S. Balaban, S. Nemoto, and T. Finkel. Mitochondria, Oxidants, and Aging. *Cell*, 120(4):483–495, 2005.
- [12] J. F. Curtin, M. Donovan, and T. G. Cotter. Regulation and measurement of oxidative stress in apoptosis. *J. Immunol. Methods*, 265(1-2):49–72, 2002.
- [13] K. Heise, S. Puntarulo, H. O. Pörtner, and D. Abele. *Comp. Biochem. Physiol. C*, 134:79, 2003.

- [14] L. B. Valdez, S. Lores Arnaiz, J. Bustamante, S. Alvarez, L. E. Costa, and A. Boveris. Free radical chemistry in biological systems. *Biol. Res.*, 33(2):65–70, 2000.
- [15] M. D. Brand, C. Affourtit, T. C. Esteves, K. Green, A. J. Lambert, S. Miwa, J. L. Pakay, and N. Parker. Mitochondrial superoxide: production, biological effects, and activation of uncoupling proteins. *Free Radical Bio. Med.*, 37(6):755–767, 2004.
- [16] M. L. Genova, B. Ventura, G. Giuliano, C. Bovina, G. Formiggini, G. Parenti Castelli, and G. Lenaz. The site of production of superoxide radical in mitochondrial Complex I is not a bound ubiquinone but presumably iron-sulfur cluster N2. *FEBS Lett.*, 505(3):364–368, 2001.
- [17] M. P. Murphy. How mitochondria produce reactive oxygen species. *Biochem. J.*, 417(1):1–13, 2009.
- [18] H. Nohl, A. V. Kozlov, L. Gille, K. Staniek, and T. Grune. *Reactions, Processes: Oxidants and Antioxidant Defense Systems*. The Handbook of Environmental Chemistry 20. Springer-Verlag Berlin Heidelberg, 1 edition, 2005.
- [19] R. T. Dean, S. Fu, R. Stocker, and M. J. Davies. Biochemistry and pathology of radical-mediated protein oxidation. *Biochem. J.*, 324 (Pt 1):1–18, 1997.
- [20] A. Galano, J. R. Alvarez-Idaboy, A. Cruz-Torres, and M. E. Ruiz-Santoyo. Rate coefficients and mechanism of the gas phase OH hydrogen abstraction reaction from serine: a quantum mechanical approach. *J. Mol. Struct-Theochem*, 629(1-3):165–174, 2003.
- [21] H. J. H. Fenton. Oxidation of tartaric acid in presence of iron. *J. Chem. Soc. Trans.*, 65:899–910, 1894.
- [22] R. G. Zepp, B. C. Faust, and J. Hoigne. Hydroxyl radical formation in aqueous reactions (pH 3-8) of iron(II) with hydrogen peroxide: the photo-Fenton reaction. *Environ. Sci. Technol.*, 26(2):313–319, 1992.
- [23] F. Buda, B. Ensing, M. C. M. Gribnau, and E. J. Baerends. DFT study of the active intermediate in the Fenton reaction. *Chem-Eur. J.*, 7:2775–2783, 2001.
- [24] F. Buda, B. Ensing, M. C. M. Gribnau, and E. J. Baerends. O₂ evolution in the Fenton reaction. *Chem-Eur. J.*, 9(2):3436–3444, 2003.
- [25] A. S. Petit, R. C. R. Penniford, and J. N. Harvey. Electronic Structure and Formation of Simple Ferryl-oxo Complexes: Mechanism of the Fenton Reaction. *Inorg. Chem.*, 53(13):6473–6481, 2014.
- [26] W. H. Koppenol. The haber-weiss cycle 70 years later. *Redox Rep.*, 6(4):229–234, 2001.
- [27] C. C. Winterbourn and M. B. Hampton. Thiol chemistry and specificity in redox signaling. *Free Radical Bio. Med.*, 45(5):549–561, 2008.
- [28] M. D. Jacobson. Reactive oxygen species and programmed cell death. *Trends Biochem. Sci.*, 21(3):83–86, 1996.

- [29] W. Dröge. Free radicals in the physiological control of cell function. *Physiol. Rev.*, 82(1):47–95, 2002.
- [30] D. Harman. Aging: a theory based on free radical and radiation chemistry. *Journal of gerontology*, 11(3):298–300, 1956.
- [31] D. Harman. Prolongation of the normal life span by radiation protection chemicals. *Journal of gerontology*, 12(3):257–63, 1957.
- [32] D. Harman. The biologic clock: the mitochondria? *J. Am. Geriatr. Soc.*, 20(4):145–147, 1972.
- [33] S. Hekimi, J. Lapointe, and Y. Wen. Taking a "good" look at free radicals in the aging process. *Trends Cell Biol.*, 21(10):569–76, 2011.
- [34] D. J. Bonda, X. Wang, G. Perry, A. Nunomura, M. Tabaton, X. Zhu, and M. Smith. Oxidative stress in Alzheimer disease: a possibility for prevention. *Neuropharmacology*, 59(4-5):290–4, 2010.
- [35] A. Rauk. Why is the amyloid beta peptide of Alzheimer's disease neurotoxic? *Dalton T.*, (10):1273–82, 2008.
- [36] D. A. Butterfield, T. Reed, S. F. Newman, and R. Sultana. Roles of amyloid β -peptide-associated oxidative stress and brain protein modifications in the pathogenesis of Alzheimer's disease and mild cognitive impairment. *Free Radical Biol. Med.*, 43(5):658–677, 2007.
- [37] S. Varadarajan, S. Yatin, J. Kanski, F. Jahanshahi, and D. A. Butterfield. Methionine residue 35 is important in amyloid β -peptide-associated free radical oxidative stress. *Brain Res. Bull.*, 50(2):133–141, 1999.
- [38] D. G. Smith, R. Cappai, and K. J. Barnham. The redox chemistry of the Alzheimer's disease amyloid beta peptide. *BBA-Biomembranes*, 1768(8):1976–1990, 2007.
- [39] A. Rauk. The chemistry of Alzheimer's disease. *Chem. Soc. Rev.*, 38(9):2698–2715, 2009.
- [40] M. J. Davies. The oxidative environment and protein damage. *BBA-Proteins Proteom.*, 1703(2):93–109, 2005.
- [41] T. Özben. *Free radicals, oxidative stress, and antioxidants: pathological and physiological significance*, volume 296. Springer Science & Business Media, 1997.
- [42] B. Halliwell. Reactive oxygen species in living systems: Source, biochemistry, and role in human disease. *Am. J. Med.*, 91(3):S14–S22, 1991.
- [43] E. Piskounova, M. Agathocleous, M. M. Murphy, Z. Hu, S. E. Huddleston, Z. Zhao, A. M. Leitch, T. M. Johnson, R. J. DeBerardinis, and S. J. Morrison. Oxidative stress inhibits distant metastasis by human melanoma cells. *Nature*, 527(7577):186–191, 2015.

- [44] J. M. Matxain, M. Ristilä, A. Strid, and L. A. Eriksson. Theoretical study of the antioxidant properties of pyridoxine. *J. Phys. Chem. A*, 110(48):13068–13072, 2006.
- [45] J. M. Matxain, M. Ristilä, A. Strid, and L. A. Eriksson. Theoretical study of the reaction of vitamin B6 with $1O_2$. *Chem-Eur. J.*, 13(16):4636–4642, 2007.
- [46] J. I. Mujika and J. M. Matxain. Theoretical study of the pH-dependent antioxidant properties of vitamin C. *J. Mol. Model.*, 19(5):1945–52, 2012.
- [47] N. Chondrogianni, I. Petropoulos, S. Grimm, K. Georgila, B. Catalgol, B. Friguet, T. Grune, and E. S. Gonos. Protein damage, repair and proteolysis. *Mol. Aspects Med.*, 35(1):1–71, 2014.
- [48] Y. Zhou, J. S. Richardson, M. J. Mombourquette, and J. A. Weil. Free radical formation in autopsy samples of alzheimer and control cortex. *Neurosci. Lett.*, 195(2):89–92, 1995.
- [49] M. A. Smith, G. Perry, P. L. Richey, L. M. Sayre, V. E. Anderson, M. F. Beal, and N. Kowall. Oxidative damage in Alzheimer's. *Nature*, 382(6587):120–1, 1996.
- [50] W. R. Markesbery and J. M. Carney. Oxidative Alterations in Alzheimer's Disease. *Brain Pathol.*, 9(1):133–146, 1999.
- [51] R. S. Sohal and R. Weindruch. Oxidative Stress, Caloric Restriction, and Aging. *Science*, 273(5271):59–63, 1996.
- [52] K. M. Schaich. Co-oxidation of proteins by oxidizing lipids, 2008.
- [53] I. Dalle-Donne, R. Rossi, R. Colombo, D. Giustarini, and A. Milzani. Biomarkers of oxidative damage in human disease. *Clin. Chem.*, 52(4):601–623, 2006.
- [54] K. E. Holde. *Principles of physical biochemistry*. Prentice Hall, Upper Saddle River, N.J, 1998.
- [55] I. Verrastro, S. Pasha, K. Jensen, A. Pitt, and C. Spickett. Mass Spectrometry-Based Methods for Identifying Oxidized Proteins in Disease: Advances and Challenges. *Biomolecules*, 5(2):378–411, 2015.
- [56] E. Shacter. Quantification and significance of protein oxidation in biological samples. *Drug Metab. Rev.*, 32(3-4):307–26, 2000.
- [57] E. R. Stadtman. Metal ion-catalyzed oxidation of proteins: Biochemical mechanism and biological consequences. *Free Radical Bio. Med.*, 9(4):315–325, 1990.
- [58] J. R. Requena, R. L. Levine, C. Chao, and E. R. Stadtman. Glutamic and aminoadipic semialdehydes are the main carbonyl products of metal-catalyzed oxidation of proteins. *Proc. Natl. Acad. Sci. U. S. A.*, 98(1):69–74, 2001.
- [59] E. R. Stadtman and R. L. Levine. Free radical-mediated oxidation of free amino acids and amino acid residues in proteins. *Amino Acids*, 25(3-4):207–18, 2003.

- [60] M. F. Beal. Oxidatively Modified Proteins in Aging and Disease. *Free Radical Bio. Med.*, 32(9):797–803, 2002.
- [61] K. Hensley, N. Hall, R. Subramaniam, P. Cole, M. Harris, M. Aksenov, M. Aksenova, S. P. Gabbita, J. F. Wu, J. M. Carney, M. Lovell, W. R. Markesbery, and D. A. Butterfield. Brain Regional Correspondence Between Alzheimer’s Disease Histopathology and Biomarkers of Protein Oxidation. *J. Neurochem.*, 65(5):2146–2156, 1995.
- [62] K. Hensley, D. A. Butterfield, N. Hall, P. Cole, R. Subramaniam, R. Mark, M. P. Mattson, W. R. Markesbery, M. E. Harris, M. Akasenov, M. Aaksenova, J. F. Wu, and J. M. Carney. Reactive Oxygen Species as Causal Agents in the Neurotoxicity of the Alzheimer’s Disease-Associated Amyloid Beta Peptide. *Ann. NY. Acad. Sci.*, 786 (1 Near-Earth Ob):120–134, 1996.
- [63] G. Roos, F. De Proft, and P. Geerlings. Electron capture by the thiyl radical and disulfide bond: ligand effects on the reduction potential. *Chem-Eur. J.*, 19(16):5050–5060, 2013.
- [64] A. F. Choban, I. R. Yurchuk, and A. S. Lyavinets. Oxidation of dimethyl sulfoxide with hydrogen peroxide in the presence of potassium hydroxide. *Russ. J. Gen. Chem.*, 78(11):2071–2074, 2008.
- [65] H. Zipse. Radical Stability-A Theoretical Perspective. In *Radicals in Synthesis I*, pages 163–189. Springer-Verlag, Berlin/Heidelberg.
- [66] E. R. Stadtman. Oxidation of free amino acids and amino acid residues in proteins by radiolysis and by metal-catalyzed reactions. *Annu. Rev. Biochem.*, 62:797–821, 1993.
- [67] A. Amici, R. L. Levine, L. Tsai, and E. R. Stadtman. Conversion of amino acid residues in proteins and amino acid homopolymers to carbonyl derivatives by metal-catalyzed oxidation reactions. *J. Biol. Chem.*, 264(6):3341–3346, 1989.
- [68] E. R. Stadtman. Protein oxidation and aging. *Science*, 257(5074):1220–4, 1992.
- [69] J. E. Roseman and R. L. Levine. Purification of a protease from *Escherichia coli* with specificity for oxidized glutamine synthetase. *J. Biol. Chem.*, 262(5):2101–10, 1987.
- [70] J. Cervera and R. L. Levine. Modulation of the hydrophobicity of glutamine synthetase by mixed-function oxidation. *FASEB J.*, 2(10):2591–5, 1988.
- [71] R. J. Elias, S. S. Kellerby, and E. A. Decker. Antioxidant activity of proteins and peptides. *Crc. Rev. Food Sci.*, 48(5):430–41, 2008.
- [72] P. Hohenberg and W. Kohn. Density functional theory. *Phys. Rev. B*, 136:864–876, 1964.
- [73] W. Kohn and L. J. Sham. Self-consistent equations including exchange and correlation effects. *Phys. Rev.*, 140(4A):A1133, 1965.
- [74] Y. Zhao and D. G. Truhlar. Benchmark databases for nonbonded interactions and their use to test density functional theory. *J. Chem. Theory Comput.*, 1(3):415–432, 2005.

- [75] Y. Zhao, N. González-García, and D. G. Truhlar. Benchmark database of barrier heights for heavy atom transfer, nucleophilic substitution, association, and unimolecular reactions and its use to test theoretical methods. *J. Phys. Chem. A*, 109(9):2012–2018, 2005.
- [76] Y. Zhao, N. González-García, and D. G. Truhlar. Benchmark database of barrier heights for heavy atom transfer, nucleophilic substitution, association, and unimolecular reactions and its use to test theoretical methods. *J. Phys. Chem. A*, 110(14):4942–4942, 2006.
- [77] L. Goerigk and S. Grimme. A thorough benchmark of density functional methods for general main group thermochemistry, kinetics, and noncovalent interactions. *Phys. Chem. Chem. Phys.*, 13(14):6670, 2011.
- [78] Y. Zhao and D. G. Truhlar. Hybrid meta density functional theory methods for thermochemistry, thermochemical kinetics, and noncovalent interactions: the mpw1b95 and mpwblk models and comparative assessments for hydrogen bonding and van der waals interactions. *J. Phys. Chem. A*, 108(33):6908–6918, 2004.
- [79] M. J. Frisch, G. W. Trucks, H. B. Schlegel, G. E. Scuseria, M. A. Robb, J. R. Cheeseman, G. Scalmani, V. Barone, B. Mennucci, G. A. Petersson, H. Nakatsuji, M. Caricato, X. Li, H. P. Hratchian, A. F. Izmaylov, J. Bloino, G. Zheng, J. L. Sonnenberg, M. Hada, M. Ehara, K. Toyota, R. Fukuda, J. Hasegawa, M. Ishida, T. Nakajima, Y. Honda, O. Kitao, H. Nakai, T. Vreven, J. A. Montgomery, Jr., J. E. Peralta, F. Ogliaro, M. Bearpark, J. J. Heyd, E. Brothers, K. N. Kudin, V. N. Staroverov, R. Kobayashi, J. Normand, K. Raghavachari, A. Rendell, J. C. Burant, S. S. Iyengar, J. Tomasi, M. Cossi, N. Rega, J. M. Millam, M. Klene, J. E. Knox, J. B. Cross, V. Bakken, C. Adamo, J. Jaramillo, R. Gomperts, R. E. Stratmann, O. Yazyev, A. J. Austin, R. Cammi, C. Pomelli, J. W. Ochterski, R. L. Martin, K. Morokuma, V. G. Zakrzewski, G. A. Voth, P. Salvador, J. J. Dannenberg, S. Dapprich, A. D. Daniels, Ö. Farkas, J. B. Foresman, J. V. Ortiz, J. Cioslowski, and D. J. Fox. Gaussian 09 Revision A.1. Gaussian Inc. Wallingford CT 2009.
- [80] Z. Maskos, J. D. Rush, and W. H. Koppenol. The hydroxylation of phenylalanine and tyrosine: A comparison with salicylate and tryptophan. *Arch. Biochem. Biophys.*, 296(2):521–529, 1992.
- [81] M. B. Feeney and C. Schöneich. Tyrosine modifications in aging. *Antioxid. Redox Sign.*, 17(11):1571–9, 2012.
- [82] C. Giulivi, N. J. Traaseth, and K. J. A. Davies. Tyrosine oxidation products: Analysis and biological relevance. *Amino Acids*, 25(3-4):227–232, 2003.
- [83] Z. Maskos, J. D. Rush, and W. H. Koppenol. The hydroxylation of tryptophan. *Arch. Biochem. Biophys.*, 296(2):514–520, 1992.
- [84] J. R. Requena, R. L. Levine, and E. R. Stadtman. Recent advances in the analysis of oxidized proteins. *Amino acids*, 25(3-4):221–6, 2003.

- [85] W. Vogt. Oxidation of methionyl residues in proteins: Tools, targets, and reversal. *Free Radical Bio. Med.*, 18(1):93–105, 1995.
- [86] C. Jacob, G. I. Giles, N. M. Giles, and H. Sies. Sulfur and selenium: the role of oxidation state in protein structure and function. *Angew. Chem. Int. Edit.*, 42(39):4742–58, 2003.
- [87] G. Kim, S. J. Weiss, and R. L. Levine. Methionine oxidation and reduction in proteins. *BBA-Gen. Subjects*, 1840(2):901–905, 2014.
- [88] S. Carballal, B. Alvarez, L. Turell, H. Botti, B. Freeman, and R. Radi. Sulfenic acid in human serum albumin. *Amino acids*, 32(4):543–51, 2007.
- [89] M. Enescu and B. Cardey. Mechanism of cysteine oxidation by a hydroxyl radical: a theoretical study. *Chemphyschem*, 7(4):912–919, 2006.
- [90] M. Irani, U. Törnvall, S. Genheden, M. W. Larsen, R. Hatti-Kaul, and U. Ryde. Amino acid oxidation of *Candida antarctica* lipase B studied by molecular dynamics simulations and site-directed mutagenesis. *Biochemistry*, 52(7):1280–9, 2013.
- [91] C. Schöneich. Methionine oxidation by reactive oxygen species: reaction mechanisms and relevance to Alzheimer’s disease. *Biochim. Biophys. Acta*, 1703(2):111–9, 2005.
- [92] R. L. Levine, L. Mosoni, B. S. Berlett, and E. R. Stadtman. Methionine residues as endogenous antioxidants in proteins. *P. Natl. Acad. Sci-biol.*, 93(26):15036–40, 1996.
- [93] K. Bobrowski and C. Schöneich. Hydroxyl radical adduct at sulfur in substituted organic sulfides stabilized by internal hydrogen bond. *J. Chem. Soc. Chem. Comm.*, (9):795, 1993.
- [94] J. Bergès, P. Trouillas, and C. Houée-Levin. Oxidation of protein tyrosine or methionine residues: From the amino acid to the peptide. *J. Phys. Conf. Ser.*, 261:012003, 2011.
- [95] M. Ignasiak, D. Scuderi, P. de Oliveira, T. Pedzinski, Y. Rayah, and C. Houée Levin. Characterization by mass spectrometry and IRMPD spectroscopy of the sulfoxide group in oxidized methionine and related compounds. *Chem. Phys. Lett.*, 502(1-3):29–36, 2011.
- [96] I. Fourré, J. Bergès, B. Braïda, and C. Houée-Levin. Topological and spectroscopic study of three-electron bonded compounds as models of radical cations of methionine-containing dipeptides. *Chem. Phys. Lett.*, 467(1-3):164–169, 2008.
- [97] K. Bobrowski, G. L. Hug, D. Pogocki, B. Marciniak, and C. Schöneich. Stabilization of sulfide radical cations through complexation with the peptide bond: mechanisms relevant to oxidation of proteins containing multiple methionine residues. *J. Phys. Chem. B*, 111(32):9608–20, 2007.
- [98] I. Fourré, J. Bergès, and C. Houée-Levin. Structural and topological studies of methionine radical cations in dipeptides: electron sharing in two-center three-electron bonds. *J. Phys. Chem. A*, 114(27):7359–7368, 2010.

- [99] S. Varadarajan, J. Kanski, M. Aksenova, C. Lauderback, and D. A. Butterfield. Different Mechanisms of Oxidative Stress and Neurotoxicity for Alzheimer's A β (1-42) and A β (25-35). *J. Am. Chem. Soc.*, 123:5625–5631, 2001.
- [100] P. Brunelle and A. Rauk. One-electron oxidation of methionine in peptide environments: The effect of three-electron bonding on the reduction potential of the radical cation. *J. Phys. Chem. A*, 108(1):11032–11041, 2004.
- [101] M. Ignasiak, P. de Oliveira, C. H. Levin, and D. Scuderi. Oxidation of methionine-containing peptides by OH radicals: Is sulfoxide the only product? Study by mass spectrometry and IRMPD spectroscopy. *Chem. Phys. Lett.*, 590:35–40, 2013.
- [102] K. Bobrowski, C. Schöneich, J. Holcman, and K. Asmus. OH radical induced decarboxylation of methionine-containing peptides. Influence of peptide sequence and net charge. *J. Chem. Soc. Perk. T. 2*, (3):353–362, 1991.
- [103] T. Marino, C. Soriano-Correa, and N. Russo. Oxidation mechanism of methionine by HO^{*} radical: A theoretical study. *J. Phys. Chem. B*, 116(18):5349–5354, 2012.
- [104] A. Galano, J. R. Alvarez-Idaboy, A. Cruz-Torres, and Ma E. Ruiz-Santoyo. Kinetics and mechanism of the gas-phase OH hydrogen abstraction reaction from methionine: A quantum mechanical approach. *Int. J. Chem. Kinet.*, 35(5):212–221, 2003.
- [105] G. P. F. Wood, A. Sreedhara, J. M. Moore, J. Wang, and B. L. Trout. Mechanistic Insights into Radical-Mediated Oxidation of Tryptophan from ab Initio Quantum Chemistry Calculations and QM/MM Molecular Dynamics Simulations. *J. Phys. Chem. A*, page acs.jpca.6b02429, 2016.
- [106] J. W. Heinecke, W. Li, G. A. Francis, and J. A. Goldstein. Tyrosyl radical generated by myeloperoxidase catalyzes the oxidative cross-linking of proteins. *J. Clin. Invest.*, 91(6):2866, 1993.
- [107] H. Yeh, G. J. Gerfen, J. Wang, A. Tsai, and L. Wang. Characterization of the peroxidase mechanism upon reaction of prostacyclin synthase with peracetic acid. identification of a tyrosyl radical intermediate. *Biochemistry*, 48(5):917–928, 2009.
- [108] J. M. Anglada. Complex mechanism of the gas phase reaction between formic acid and hydroxyl radical. Proton coupled electron transfer versus radical hydrogen abstraction mechanisms. *J. Am. Chem. Soc.*, 126(31):9809–9820, 2004.
- [109] A. Galano, J. R. Alvarez-Idaboy, G. Bravo-Pérez, and Ma. E. Ruiz-Santoyo. Mechanism and rate coefficients of the gas phase OH hydrogen abstraction reaction from asparagine: a quantum mechanical approach. *J. Mol. Struct-Theochem*, 617(1-3):77–86, 2002.
- [110] A. Galano, J. R. Alvarez-Idaboy, E. Agacino-Valdés, and M. E. Ruiz-Santoyo. Quantum mechanical approach to isoleucine+OH gas phase reaction. Mechanism and kinetics. *J. Mol. Struct-Theochem*, 676(1-3):97–103, 2004.

- [111] A. Galano, J. R. Alvarez-Idaboy, L. Montero, and A. Vivier-Bunge. OH hydrogen abstraction reactions from alanine and glycine: A quantum mechanical approach. *J. Comput. Chem.*, 22(11):1138–1153, 2001.
- [112] H. G. Viehe, R. Merényi, L. Stella, and Z. Janousek. Cato-dative Substituent Effects in Syntheses with Radicals and Radicophiles [New synthetic methods (32)]. *Angew. Chem. Int. Ed.*, 18(1979):917–932, 1979.
- [113] A. Rauk, D. Yu, J. Taylor, G. V. Shustov, D. A. Block, and D. A. Armstrong. Effects of Structure on α C-H Bond Enthalpies of Amino Acid Residues: Relevance to H Transfers in Enzyme Mechanisms and in Protein Oxidation. *Biochemistry*, 38(28):9089–9096, 1999.
- [114] W. Cheng, S. Jang, C. Wu, R. Lin, H. Lu, and F. Li. Site specificity of the (alpha)C H bond dissociation energy for a naturally occurring beta-hairpin peptide-An ab initio study. *J. Comput. Chem.*, 30(3):407–414, 2009.
- [115] H. Q. Doan, A. C. Davis, and J. S. Francisco. Primary steps in the reaction of OH radicals with peptide systems: Perspective from a study of model amides. *J. Phys. Chem. A*, 114(16):5342–5357, 2010.
- [116] M. C. Owen, B. Viskolcz, and I. G. Csizmadia. Quantum Chemical Analysis of the Unfolding of a Penta-alanyl 310-Helix Initiated by HO, HO₂ and O₂-. *J. Phys. Chem. B*, 115(24):8014–8023, 2011.
- [117] G. Hart-Smith. A review of electron-capture and electron-transfer dissociation tandem mass spectrometry in polymer chemistry. *Anal. Chim. Acta*, 808:44–55, 2014.
- [118] R. A. Zubarev, N. L. Kelleher, and F. W. McLafferty. Electron Capture Dissociation of Multiply Charged Protein Cations. A Nonergodic Process. *J. Am. Chem. Soc.*, 120(13):3265–3266, 1998.
- [119] J. Simons. Mechanisms for S-S and N-C α bond cleavage in peptide ECD and ETD mass spectrometry. *Chem. Phys. Lett.*, 484(4-6):81–95, 2010.
- [120] E. A. Syrstad and F. Turecek. Toward a general mechanism of electron capture dissociation. *J. Am. Soc. Mass Spectrom.*, 16(2):208–224, 2005.
- [121] D. A. Thomas, C. H. Sohn, J. Gao, and J. L. Beauchamp. Hydrogen Bonding Constrains Free Radical Reaction Dynamics at Serine and Threonine Residues in Peptides. *J. Phys. Chem. A*, 118(37):8380–8392, 2014.
- [122] M. C. Owen, M. Szori, I. G. Csizmadia, and B. Viskolcz. Conformation-dependent ·OH/H₂O₂ hydrogen abstraction reaction cycles of Gly and Ala residues: a comparative theoretical study. *J. Phys. Chem. B.*, 116(3):1143–1154, 2012.
- [123] M. C. Owen, B. Viskolcz, and I. G. Csizmadia. Quantum chemical analysis of the unfolding of a penta-glycyl 3(10)-helix initiated by HO, HO₂, and O₂. *J. Chem. Phys.*, 135(2011):035101, 2011.

- [124] P. A. M. Dirac. On the Theory of Quantum Mechanics. *P. R. Soc. A*, 112(762): 661–677, 1926.
- [125] E. Schrödinger. An undulatory theory of the mechanics of atoms and molecules. *Phys. Rev.*, 28(6):1049, 1926.
- [126] W. Heisenberg. Über quantentheoretische Umdeutung kinematischer und mechanischer Beziehungen. *Z. Phys.*, 33(1):879–893, 1925.
- [127] W. Heisenberg. Über den anschaulichen inhalt der quantentheoretischen kinematik und mechanik. *Z. Phys.*, 43(3-4):172–198, 1927.
- [128] W. Pauli. Über den zusammenhang des abschlusses der elektronengruppen im atom mit der komplexstruktur der spektren. *Z. Phys.*, 31(1):765–783, 1925.
- [129] M. Born and R. Oppenheimer. Zur Quantentheorie der Molekeln. *Ann. Phys.*, 389(20):457–484, 1927.
- [130] D. R. Hartree. The wave mechanics of an atom with non-coulmbic central field: parts i, ii, and iii. In *Proc. Cambridge Philos. Soc.*, volume 24, page 89, 1928.
- [131] V. Fock. Näherungsmethode zur lösung des quantenmechanischen mehrkörperproblems. *Eur. Phys. J. A*, 61(1-2):126–148, 1930.
- [132] J. C. Slater. The theory of complex spectra. *Phys. Rev.*, 34(10):1293, 1929.
- [133] A. Szabo and N. S. Ostlund. *Modern quantum chemistry: introduction to advanced electronic structure theory*. Courier Corporation, 1989.
- [134] W. Heitler and F. London. Wechselwirkung neutraler atome und homöopolare bindung nach der quantenmechanik. *Z. Phys.*, 44(6-7):455–472, 1927.
- [135] L. Pauling. The nature of the chemical bond. application of results obtained from the quantum mechanics and from a theory of paramagnetic susceptibility to the structure of molecules. *J. Am. Chem. Soc.*, 53(4):1367–1400, 1931.
- [136] F. Hund. *Z. Phys.*, 73:1, 1931.
- [137] R. S. Mulliken. Electronic structures of polyatomic molecules and valence. ii. general considerations. *Phys. Rev.*, 41(1):49, 1932.
- [138] J. E. Lennard-Jones. The electronic structure of some diatomic molecules. *Trans. Faraday Soc.*, 25:668–686, 1929.
- [139] G. G. Hall. The Molecular Orbital Theory of Chemical Valency. VIII. A Method of Calculating Ionization Potentials. *P. R. Soc. A*, 205(1083):541–552, 1951.
- [140] C. C. J. Roothaan. New developments in molecular orbital theory. *Rev. Mod. Phys.*, 23(2):69, 1951.
- [141] S. F. Boys, G. B. Cook, C. M. Reeves, and I. Shavitt. Automatic Fundamental Calculations of Molecular Structure. *Nature*, 178(4544):1207–1209, 1956.

- [142] C. Møller and M. S. Plesset. Note on an approximation treatment for many-electron systems. *Phys. Rev.*, 46(7):618, 1934.
- [143] I. Shavitt. The history and evolution of configuration interaction. *Mol. Phys.*, 94(1): 3–17, 1998.
- [144] C. D. Sherrill and H. F. Schaefer. The configuration interaction method: Advances in highly correlated approaches. *Adv. Quantum Chem.*, 34:143–269, 1999.
- [145] J. A. Pople, R. Krishnan, H. B. Schlegel, and J. S. Binkley. Electron correlation theories and their application to the study of simple reaction potential surfaces. *Int. J. Quantum Chem.*, 14(5):545–560, 1978.
- [146] R. J. Bartlett and G. D. Purvis. Quadratic configuration interaction. a general technique for determining electron correlation energies. *Int. J. Quantum Chem.*, 14:516, 1978.
- [147] D. R. Yarkony. *Modern Electronic Structure Theory:(In 2 Parts)*, volume 2. World Scientific, 1995.
- [148] K. Andersson, P. A. Malmqvist, B. O. Roos, A. J. Sadlej, and K. Wolinski. Second-order perturbation theory with a casscf reference function. *J. Phys. Chem.*, 94(14): 5483–5488, 1990.
- [149] K. Andersson, P. A. Malmqvist, and B. O. Roos. Second-order perturbation theory with a complete active space self-consistent field reference function. *J. Chem. Phys.*, 96(2):1218–1226, 1992.
- [150] M. Levy. Universal variational functionals of electron densities, first-order density matrices, and natural spin-orbitals and solution of the v-representability problem. *Proc. Natl. Acad. Sci. U.S.A.*, 76(12):6062–6065, 1979.
- [151] E. H. Lieb. Variational Principle for Many-Fermion Systems. In *The Stability of Matter: From Atoms to Stars*, volume 55, pages 253–255. Springer Berlin Heidelberg, Berlin, Heidelberg, 1997.
- [152] M. C. Holthausen and W. Koch. A chemist’s guide to density functional theory, 2000.
- [153] E. S. Kryachko and E. V. Ludeña. *Energy density functional theory of many-electron systems*, volume 4. Springer Science & Business Media, 2012.
- [154] A. D. Becke. Density-functional thermochemistry. iii. the role of exact exchange. *J. Chem. Phys.*, 98(7):5648–5652, 1993.
- [155] A. D. Becke. A new mixing of hartree fock and local density-functional theories. *J. Chem. Phys.*, 98(2):1372–1377, 1993.
- [156] G. P. F. Wood, A. Sreedhara, J. M. Moore, and B. L. Trout. Reactions of benzene and 3-methylpyrrole with the OH and OOH radicals: An assessment of contemporary density functional theory methods. *J. Phys. Chem. A*, 118(14):2667–2682, 2014.

- [157] B. Liu and A. D. McLean. Accurate calculation of the attractive interaction of two ground state helium atoms. *J. Chem. Phys.*, 59(8):4557–4558, 1973.
- [158] N. R. Kestner. He-He Interaction in the SCF-MO Approximation. *J. Chem. Phys.*, 48(1):252–257, 1968.
- [159] J. R. Alvarez-Idaboy and A. Galano. Counterpoise corrected interaction energies are not systematically better than uncorrected ones: comparison with CCSD(T) CBS extrapolated values. *Theor. Chem. Acc.*, 126(1-2):75–85, 2010.
- [160] R. S. Mulliken. Electronic population analysis on lcao mo molecular wave functions. *J. Chem. Phys.*, 23(10):1833–1840, 1955.
- [161] F. L. Hirshfeld. Bonded-atom fragments for describing molecular charge densities. *Theor. Chem. Acc.*, 44(2):129–138, 1977.
- [162] P. Salvador and E. Ramos-Cordoba. Apost-3d program, 2012. Universitat de Girona (Spain).
- [163] P. Salvador and E. Ramos-Cordoba. Communication: An approximation to bader’s topological atom. *J. Chem. Phys.*, 139:071103, 2013.
- [164] A. D. Becke. A multicenter numerical integration scheme for polyatomic molecules. *J. Chem. Phys.*, 88:2547–2553, 1988.
- [165] I. Mayer and P. Salvador. Overlap populations, bond orders and valences for fuzzy atoms. *Chem. Phys. Lett.*, 383(3):368–375, 2004.
- [166] P. Politzer and J. S. Murray. *Quantitative treatments of solute/solvent interactions*, volume 1. Elsevier Science, 1994.
- [167] S. Miertuš, E. Scrocco, and J. Tomasi. Electrostatic interaction of a solute with a continuum. a direct utilization of ab initio molecular potentials for the prevision of solvent effects. *Chem. Phys.*, 55(1):117–129, 1981.
- [168] S. Miertuš and J. Tomasi. Approximate evaluations of the electrostatic free energy and internal energy changes in solution processes. *Chem. Phys.*, 65(2):239–245, 1982.
- [169] A. R. Leach. *Molecular modelling: principles and applications*. Pearson education, 2001.
- [170] Y. Zhao, B. J. Lynch, and D. G. Truhlar. Development and Assessment of a New Hybrid Density Functional Model for Thermochemical Kinetics. *J. Phys. Chem. A*, 108(14):2715–2719, 2004.
- [171] Y. Zhao, B. J. Lynch, and D. G. Truhlar. Doubly Hybrid Meta DFT: New Multi-Coefficient Correlation and Density Functional Methods for Thermochemistry and Thermochemical Kinetics. *J. Phys. Chem. A*, 108(21):4786–4791, 2004.
- [172] Y. Zhao, J. Pu, B. J. Lynch, and D. G. Truhlar. Tests of second-generation and third-generation density functionals for thermochemical kinetics. Electronic supplementary information (ESI) available: Mean errors for pure and hybrid DFT methods. *Phys. Chem. Chem. Phys.*, 6(4):673, 2004.

- [173] B. Mennucci and J. Tomasi. Continuum solvation models: A new approach to the problem of solute's charge distribution and cavity boundaries. *J. Chem. Phys.*, 106(12):5151, 1997.
- [174] J. Tomasi, B. Mennucci, and E. Cancès. The IEF version of the PCM solvation method: an overview of a new method addressed to study molecular solutes at the QM ab initio level. *J. Mol. Struct-Theochem*, 464(1-3):211–226, 1999.
- [175] X. Lopez, F. Ruipérez, M. Piris, J. M. Matxain, E. Matito, and J. M. Ugalde. Performance of pnof5 natural orbital functional for radical formation reactions: hydrogen atom abstraction and c-c and o-o homolytic bond cleavage in selected molecules. *J. Chem. Theory Comput.*, 8(8):2646–2652, 2012.
- [176] A. Rauk, D. A. Armstrong, and D. P. Fairlie. Is oxidative damage by beta-amyloid and prion peptides mediated by hydrogen atom transfer from glycine alpha-carbon to methionine sulfur within beta-sheets? *J. Am. Chem. Soc.*, 122(15):9761–9767, 2000.
- [177] R. M. Le Lacheur and W. H. Glaze. Reactions of Ozone and Hydroxyl Radicals with Serine. *Environ. Sci. Technol.*, 30(4):1072–1080, 1996.
- [178] M. Ignasiak, P. de Oliveira, C. H. Levin, and D. Scuderi. Oxidation of methionine-containing peptides by OH radicals: Is sulfoxide the only product? Study by mass spectrometry and IRMPD spectroscopy. *Chem. Phys. Lett.*, 590:35–40, 2013.
- [179] G. Roos and J. Messens. Protein sulfenic acid formation: from cellular damage to redox regulation. *Free Radical Bio. Med.*, 51(2):314–26, 2011.
- [180] A. Drazic and J. Winter. The physiological role of reversible methionine oxidation. *BBA-Proteins Proteom.*, 1844(8):1367–1382, 2014.
- [181] J. Chu, B. R. Brooks, and B. L. Trout. Oxidation of methionine residues in aqueous solutions: free methionine and methionine in granulocyte colony-stimulating factor. *J. Am. Chem. Soc.*, 126(50):16601–7, 2004.
- [182] D. M. Stanbury. Reduction potentials involving inorganic free radicals in aqueous solution. *Adv. Inorg. Chem.*, 33:69–138, 1989.
- [183] J. Bergès, P. de Oliveira, I. Fourré, and C. Houée-Levin. The one-electron reduction potential of methionine-containing peptides depends on the sequence. *J. Phys. Chem. B*, 116(31):9352–9362, 2012.
- [184] O. Augusto and S. Miyamoto. Oxygen radicals and related species. *Principles of free radical biomedicine*, 1:19–42, 2011.
- [185] C. Xipsiti and A. V. Nicolaidis. A computational study on the possible role of oxygen in the oxidation of methionine and dimethylsulfide initiated by OH radicals. *Comput. Theor. Chem.*, 1009:24–29, 2013.
- [186] B. O. Leung and A. Rauk. Dialkyl sulphur radical cations: competition between proton and methyl cation transfers to sulphur nucleophiles: an ab initio study. *Mol. Phys.*, 103(6-8):1201–1209, 2005.

- [187] J. I. Mujika, J. Uranga, and J. M. Matxain. Computational study on the attack of $\cdot\text{OH}$ radicals on aromatic amino acids. *Chem-Eur. J.*, 19(21):6862–73, 2013.
- [188] M. Roche, P. Rondeau, N. R. Singh, E. Tarnus, and E. Bourdon. The antioxidant properties of serum albumin. *Febs Lett.*, 582(13):1783–7, 2008.
- [189] V. Y. Reddy, P. E. Desrochers, S. V. Pizzo, S. L. Gonias, J. A. Sahakian, R. L. Levine, and S. J. Weiss. Oxidative dissociation of human α_2 -macroglobulin tetramers into dysfunctional dimers. *J Biol Chem*, 269:4683–4691, 1994.
- [190] M. Utrera, J. G. Rodríguez-Carpena, D. Morcuende, and M. Estévez. Formation of lysine-derived oxidation products and loss of tryptophan during processing of porcine patties with added avocado byproducts. *J. Agr. Food Chem.*, 60(15):3917–3926, 2012.

List of Publications

1. The nature of chemical bonds from PNOF5 calculations
Jon M. Matxain, Mario Piris, Jon Uranga, Xabier Lopez, Gabriel Merino, Jesus M. Ugalde
ChemPhysChem, 2012, 13, 2297
2. Can the protonation state of histidine residues be determined from molecular dynamics simulations?
Jon Uranga, Paulius Mikulskis, Samuel Genheden, Ulf Ryde
Comput. Theor. Chem., 2012, 1000, 75
3. Computational study on the attack of $\bullet OH$ radicals attack on aromatic amino acids
Jon I. Mujika, Jon Uranga, Jon M. Matxain
Chem-Eur J., 2013, 19, 6862
4. $\bullet OH$ Oxidation Towards S- and OH- Containing Amino Acids
Jon Uranga, Jon I. Mujika, Jon M. Matxain
J. Phys. Chem. B, 2015, 119, 15430
5. Computational Study of Radical Initiated Protein Backbone Homolytic Dissociation on All Natural Amino Acids
Jon Uranga, O. Lakuntza, E. Ramos-Cordoba, Jon M. Matxain, Jon I. Mujika
Phys. Chem. Chem. Phys., 2016, 18, 30972
6. Oxidation of acid, base and amide side chain amino acids via hydroxyl radical
Jon Uranga, Jon I. Mujika, Rafael Grande-Aztatzi, Jon M. Matxain
Submitted to Phys. Chem. Chem. Phys.
7. Can system truncation speed up ligand-binding calculations with periodic free-energy simulations
Francesco Manzoni, Jon Uranga, Samuel Genheden, Ulf Ryde
Submitted to J. Chem. Theory Comput.

8. Photosensitisation Mechanism of Cu(II) Porphyrins

Jon Uranga, Jon M. Matxain, Xabier Lopez, Jesus M. Ugalde, David Casanova

On process

Appendix for Chapter 4

	$\alpha - helix$			$\beta - sheet$			$\Delta\Delta H_{aq}^{\alpha-\beta}$
	ΔH_4	ΔH_{aq}	$\rho_s^{C_\alpha}$	ΔH_4	ΔH_{aq}	$\rho_s^{C_\alpha}$	
Asp	-34.0	-33.7	0.51	-31.2	-31.6	0.49	-2.1
Glu	-31.7	-31.3	0.51	-35.1	-35.6	0.51	4.3
Hip	-28.0	-28.5	0.54	-39.6	-38.9	0.53	10.4
Lys	-38.7	-33.3	0.52	-41.3	-37.6	0.52	4.3
Hid	-28.0	-28.2	0.59	-35.3	-34.9	0.50	6.7
Hie	-30.9	-30.9	0.56	-29.4	-31.0	0.53	0.1
Ser	-24.8	-26.0	0.56	-29.5	-29.8	0.51	3.8
Thr	-24.8	-25.9	0.53	-34.4	-33.6	0.52	7.7
Arg	-34.4	-31.6	0.53	-38.6	-37.3	0.52	5.7
Cys	-30.4	-30.9	0.56	-34.8	-34.2	0.50	3.3
Met	-29.7	-29.4	0.56	-31.9	-32.7	0.50	3.3
Asn	-30.7	-30.2	0.57	-38.6	-37.2	0.52	7.0
Gln	-28.2	-28.4	0.55	-36.6	-36.1	0.51	7.7
Phe	-27.9	-28.4	0.55	-34.2	-33.4	0.51	5.0
Trp	-29.3	-30.0	0.57	-32.9	-33.2	0.52	3.2
Tyr	-28.0	-28.4	0.54	-32.9	-33.2	0.51	4.5
Ala	-27.6	-28.5	0.57	-33.5	-33.7	0.51	5.0
Gly	-25.9	-27.1	0.49	-33.6	-33.9	0.53	6.5
Ile	-27.5	-28.4	0.56	-30.1	-30.1	0.51	1.7
Leu	-27.9	-28.9	0.55	-33.9	-34.1	0.50	5.2
Pro	-29.6	-30.7	0.54	-	-	-	-
Val	-25.1	-25.9	0.55	-29.4	-29.5	0.51	3.6

Table A.1: Relative enthalpies of the formed INT_{C_α} . Two different dielectric constants are shown ($\epsilon=4$ and $\epsilon=78.4$). The spin densities (Topological Fuzzy Voronoi Cells) of C_α at water dielectric are present.

	$\alpha - helix$			$\beta - sheet$			$\Delta\Delta H_{aq}^{\alpha-\beta}$
	ΔH_4	ΔH_{aq}	$\rho_s^{C_\alpha}$	ΔH_4	ΔH_{aq}	$\rho_s^{C_\alpha}$	
Asp	-22.7	-23.4	0.76	-22.2	-22.9	0.76	-0.5
Glu	-20.1	-20.3	0.78	-21.8	-22.5	0.77	2.2
Hip	-25.3	-25.4	0.59	-29.9	-30.1	0.60	4.7
Lys	-17.6	-17.8	0.79	-17.6	-18.1	0.79	0.3
Hid	-28.7	-29.5	0.55	-32.7	-33.4	0.60	3.9
Hie	-25.9	-27.0	0.60	-26.1	-27.1	0.58	0.1
Ser	-22.1	-22.7	0.67	-21.8	-21.9	0.66	-0.8
Thr	-23.9	-24.5	0.64	-26.6	-26.7	0.64	2.2
Arg	-18.0	-18.3	0.79	-18.4	-19.0	0.79	0.7
Cys	-24.5	-25.2	0.69	-25.7	-25.1	0.68	-0.1
Met	-17.9	-17.3	0.77	-18.5	-19.4	0.76	2.1
Asn	-22.5	-22.8	0.72	-21.2	-21.7	0.74	-1.1
Gln	21.2	20.9	0.80	-22.4	-21.7	0.79	0.8
Phe	-29.3	-29.6	0.60	-29.8	-29.3	0.58	-0.3
Trp	-31.3	-31.8	0.55	-31.5	-31.7	0.54	-0.1
Tyr	-30.0	-30.4	0.58	-30.9	-31.3	0.56	0.9
Ala	-14.3	-14.7	0.85	-13.8	-14.1	0.84	-0.6
Ile	-19.4	-19.9	0.75	-22.4	-22.5	0.74	2.6
Leu	-18.2	-18.5	0.78	-17.8	-17.9	0.77	-0.6
Pro	-18.8	-19.5	0.79	-	-	-	-
Val	-19.8	-20.3	0.75	-22.3	-23.0	0.74	2.7

Table A.2: Relative enthalpies of the formed INT_{C_β} . Two different dielectric constants are shown ($\epsilon=4$ and $\epsilon=78.4$). The spin densities (Topological Fuzzy Voronoi Cells) of C_β at water dielectric are present.

	AA $\Delta H_{aq}^{\alpha-\beta}$	$INT_{C\alpha}$ $\Delta H_{aq}^{\alpha-\beta}$	$INT_{C\beta}$ $\Delta H_{aq}^{\alpha-\beta}$
Asp	4.2	2.1	3.7
Glu	-1.9	2.4	0.3
Hip	-6.3	4.1	-1.6
Lys	-0.3	4.0	0.0
Hid	-2.0	4.7	2.0
Hie	1.7	2.7	1.8
Ser	-2.5	1.2	-3.3
Thr	-4.4	3.3	-2.3
Arg	-0.2	5.6	0.4
Cys	-0.5	2.8	-0.5
Met	-0.2	3.2	1.9
Asn	-0.5	6.6	-1.6
Gln	0.3	8.1	1.1
Phe	-0.1	4.7	-0.4
Trp	-0.7	2.5	-0.8
Tyr	0.0	4.7	-0.6
Ala	-0.3	5.0	-0.8
Gly	0.8	7.7	-
Ile	-0.2	1.5	2.3
Leu	-0.1	5.2	-0.7
Val	0.1	3.7	2.7
$\bar{\chi}$	-0.8	3.9	0.2
MAD	1.4	3.7	1.5

Table A.3: Relative enthalpies between α -*helix-like* and β -*sheet* conformations of AA, $INT_{C\alpha}$ and $INT_{C\beta}$, at water dielectric constant. Average value and MAD are also shown for each case.

	ΔH_{aq}	NH	ψ	φ	χ_1	
Ser	α - <i>helix-like</i>	0.0	2(6)	-84.3	71.5	53.8
	β - <i>sheet</i>	2.5	0	-156.1	178.2	64.3
	α - <i>helix</i>	7.4	1(6)	-171.6	-24.4	-171.8
	β - <i>sheet</i>	1.9	1(7)	-175.5	171.4	-96.7
Thr	α - <i>helix-like</i>	0.0	2(6)	-85.0	73.1	53.5
	β - <i>sheet</i>	4.4	0	-157.9	162.3	68.5
	α - <i>helix</i>	12.7	1(6)	-157.6	-22.3	-165.8
	β - <i>sheet</i>	2.9	1(7)	-163.2	149.6	-85.0

Table A.4: ΔH_{aq} (kcal/mol) with respect to α -*helix-like* for different conformations for Thr and Ser. NH specifies the number of hydrogen bonds present at the conformation and the number into parenthesis the atom number ring of the hydrogen bond between side chain alcohol and carbonyl of the backbone. ψ and φ are the dihedrals that define the conformation.

	$\alpha - helix$					$\beta - sheet$				
	ΔH_4^{TS}	ΔH_{water}^{TS}	r_{OH}^{TS}	r_{CH}^{TS}	ρ_s^O	ΔH_4^{TS}	ΔH_{water}^{TS}	r_{OH}^{TS}	r_{CH}^{TS}	ρ_s^O
Asp	-1.6	2.5	1.47	1.17	0.23	0.6	3.1	1.40	1.19	0.27
Glu	-1.9	1.6	1.45	1.17	0.23	3.3	2.7	1.39	1.18	0.28
Hip	0.7	2.9	1.33	1.19	0.32	2.0	7.0	1.35	1.18	0.29
Lys	0.5	2.8	1.35	1.19	0.30	-0.5	2.7	1.35	1.18	0.31
Hid	2.5	4.2	1.39	1.18	0.28	0.0	2.8	1.34	1.19	0.30
Hie	1.9	3.2	1.32	1.21	0.33	-1.3	0.9	1.38	1.18	0.27
Ser	1.2	3.0	1.32	1.20	0.34	-2.5	2.8	1.39	1.19	0.28
Thr	1.1	3.3	1.32	1.20	0.33	-2.8	3.0	1.37	1.19	0.30
Arg	-1.9	-0.9	1.34	1.20	0.31	-2.5	-1.4	1.35	1.18	0.31
Cys	1.8	3.9	1.35	1.19	0.31	-0.7	6.1	1.37	1.19	0.26
Met	0.7	2.7	1.35	1.19	0.31	0.1	3.4	1.36	1.18	0.30
Asn	0.2	3.4	1.40	1.17	0.27	-2.6	2.6	1.39	1.18	0.26
Glu	-2.4	2.1	1.40	1.18	0.28	0.4	3.2	1.37	1.18	0.29
Phe	1.2	4.0	1.37	1.19	0.27	-1.1	4.1	1.35	1.19	0.29
Trp	1.5	5.3	1.39	1.18	0.27	0.6	4.9	1.35	1.19	0.28
Tyr	1.0	3.9	1.38	1.18	0.27	-0.6	4.1	1.35	1.19	0.29
Ala	0.6	2.4	1.36	1.19	0.30	-0.9	2.4	1.38	1.17	0.27
Gly	0.4	1.7	1.33	1.20	0.34	-1.4	1.2	1.37	1.18	0.29
Ile	-1.1	1.0	1.36	1.19	0.28	-0.6	3.1	1.36	1.18	0.31
Leu	1.6	3.6	1.35	1.20	0.29	0.4	3.7	1.34	1.19	0.29
Pro	-0.7	1.2	1.39	1.18	0.30	-	-	-	-	-
Val	2.9	5.9	1.36	1.19	0.30	-0.7	2.5	1.31	1.20	0.35

Table A.5: Relative enthalpies of TS for the attack at C_α in different dielectric constants. Geometrical distances of the attack of $\bullet OH$ to the H of C_α . Mulliken spin densities of C_α and O atom of $\bullet OH$.

		α - helix - like		β - sheet		α - helix - like		β - sheet	
		cis				trans			
		ΔH_4	ΔH_{wat}	ΔH_4	ΔH_{wat}	ΔH_4	ΔH_{wat}	ΔH_4	ΔH_{wat}
Asp	$C_\alpha - NH$	12.2	11.0	15.8	15.3	15.1	11.1	18.7	15.3
	$C_\alpha - CO$	-5.0	-7.3	-1.3	-3.0	2.5	-3.1	6.2	1.2
Glu	$C_\alpha - NH$	20.7	16.1	18.5	14.2	18.8	15.1	16.6	13.2
	$C_\alpha - CO$	6.4	2.1	4.2	0.2	7.0	2.3	4.8	0.4
Hip	$C_\alpha - NH$	9.5	8.7	1.3	2.4	17.9	13.5	9.7	7.2
	$C_\alpha - CO$	7.1	2.6	-1.1	-3.7	2.8	-0.7	-5.4	-7.0
Lys	$C_\alpha - NH$	2.3	7.0	2.6	6.7	8.4	12.4	8.7	12.1
	$C_\alpha - CO$	1.3	-0.8	1.5	-1.0	-0.4	-1.6	-0.2	-1.8
Hid	$C_\alpha - NH$	7.7	7.0	5.3	5.0	11.2	9.2	8.7	7.2
	$C_\alpha - CO$	-0.4	-2.4	-2.8	-4.3	0.5	-2.3	-1.9	-4.3
Hie	$C_\alpha - NH$	11.5	10.4	13.8	12.2	9.6	7.1	11.9	8.8
	$C_\alpha - CO$	-1.6	-3.9	0.7	-2.2	-2.1	-4.2	0.2	-2.4
Ser	$C_\alpha - NH$	3.3	2.0	-0.4	-0.5	10.4	8.0	6.7	5.5
	$C_\alpha - CO$	4.2	1.5	0.4	-1.0	5.0	1.8	1.3	-0.7
Thr	$C_\alpha - NH$	-0.5	-1.8	-6.6	-6.3	9.1	7.0	3.0	2.6
	$C_\alpha - CO$	1.8	-0.9	-4.3	-5.3	2.4	-0.3	-3.7	-4.7
Arg	$C_\alpha - NH$	13.4	13.5	13.9	13.2	12.2	10.8	12.2	10.6
	$C_\alpha - CO$	10.9	10.9	11.4	10.6	7.4	6.6	8.0	6.4
Cys	$C_\alpha - NH$	11.2	10.2	9.6	9.7	12.1	10.5	10.6	10.0
	$C_\alpha - CO$	-0.6	-2.0	-2.2	-2.5	2.1	0.1	0.5	-0.4
Met	$C_\alpha - NH$	14.6	13.8	14.6	13.6	12.2	10.9	12.2	10.8
	$C_\alpha - CO$	-0.4	-1.4	-0.5	-1.6	-0.5	-2.0	-0.5	-2.1
Asn	$C_\alpha - NH$	19.1	17.8	17.7	17.4	18.6	16.3	17.2	15.8
	$C_\alpha - CO$	-4.2	-6.2	-5.6	-6.6	1.1	-1.5	-0.3	-1.9
Gln	$C_\alpha - NH$	13.0	12.6	13.6	12.9	12.7	10.7	13.3	11.1
	$C_\alpha - CO$	0.9	-1.1	1.6	-0.8	0.0	-1.5	0.6	-1.2
Phe	$C_\alpha - NH$	15.7	14.5	14.5	14.4	9.1	7.6	7.9	7.5
	$C_\alpha - CO$	-1.6	-3.0	-2.8	-3.1	-3.0	-4.9	-4.2	-5.0
Trp	$C_\alpha - NH$	10.6	9.6	9.9	8.8	8.1	6.2	7.4	5.4
	$C_\alpha - CO$	-1.4	-2.8	-2.1	-3.5	-2.3	-4.3	-3.0	-5.0
Tyr	$C_\alpha - NH$	14.3	9.6	12.6	11.9	8.3	6.6	6.6	5.2
	$C_\alpha - CO$	-1.4	-2.8	4.2	3.1	-3.0	-4.9	-4.7	-6.3
Ile	$C_\alpha - NH$	10.1	8.9	9.5	8.7	9.8	8.8	9.3	8.5
	$C_\alpha - CO$	-2.4	-4.1	-3.0	-4.3	-2.2	-3.9	-2.8	-4.1
Leu	$C_\alpha - NH$	17.8	17.0	17.7	16.9	11.4	10.2	11.3	10.1
	$C_\alpha - CO$	3.2	1.8	3.1	1.7	0.0	-1.6	-0.1	-1.6
Pro	$C_\alpha - NH$	5.7	4.6	-	-	3.1	1.6	-	-
	$C_\alpha - CO$	1.2	-0.5	-	-	-	-	-	-

Table A.6: Relative enthalpies of the backbone scission reactions departing from the amino acids and $\bullet OH$ in the two studied dielectrics.

	cis		trans	
	$\bar{\chi}$	MAD	$\bar{\chi}$	MAD
$C_\alpha - NH$	1.0	1.7	0.9	1.5
$C_\alpha - CO$	0.8	1.5	0.8	1.5

Table A.7: Average and MAD values of the $\Delta\Delta H_{wat}$ backbone scission reaction between two conformations.

		$\alpha - helix - like$		$\beta - sheet$	
		ΔH_4	ΔH_{wat}	ΔH_4	ΔH_{wat}
Ala	$C_\alpha - NH$	19.2	17.9	18.8	17.7
	$C_\alpha - CO$	4.0	2.6	3.6	2.4
Val	$C_\alpha - NH$	9.9	8.7	9.6	8.7
	$C_\alpha - CO$	-2.3	-4.0	-2.6	-4.0

Table A.8: Relative enthalpies of the backbone scission reactions departing from the amino acids and $\bullet OH$ in the two studied dielectrics.

X		α - helix - like		β - sheet	
		ΔBO_{N-C}	ΔBO_{C-C}	ΔBO_{N-C}	ΔBO_{C-C}
Ala	INT _{Cα}	0.19	0.16	0.22	0.16
	INT _{Cβ}	0.01	0.00	0.00	-0.01
Pro	INT _{Cα}	0.21	0.16	-	-
	INT _{Cβ}	0.02	-0.01	-	-
Iso	INT _{Cα}	0.18	0.16	0.20	0.14
	INT _{Cβ}	0.02	0.00	0.01	-0.02
Leu	INT _{Cα}	0.18	0.17	0.23	0.16
	INT _{Cβ}	0.00	0.00	0.00	-0.02
Val	INT _{Cα}	0.20	0.15	0.22	0.14
	INT _{Cβ}	0.00	0.00	0.01	-0.02
Gly	INT _{Cα}	0.14	0.31	0.23	0.15
	INT _{Cα}	0.24	0.18	0.18	0.14
Arg	INT _{Cβ}	0.01	0.00	0.08	-0.01
	INT _{Cα}	0.18	0.15	0.20	0.12
Asn	INT _{Cβ}	0.02	-0.01	0.00	-0.02
	INT _{Cα}	0.21	0.17	0.20	0.07
Gln	INT _{Cβ}	0.02	0.00	0.00	-0.09
	INT _{Cα}	0.21	0.17	0.22	0.16
Asp	INT _{Cβ}	0.02	-0.01	0.02	-0.02
	INT _{Cα}	0.19	0.17	0.22	0.15
Glu	INT _{Cβ}	0.00	0.00	0.01	0.00
	INT _{Cα}	0.22	0.17	0.21	0.12
Hip	INT _{Cβ}	0.00	0.00	-0.01	-0.02
	INT _{Cα}	0.23	0.20	0.19	0.12
Lys	INT _{Cβ}	0.00	0.00	0.00	0.00
	INT _{Cα}	0.19	0.12	0.21	0.14
Hid	INT _{Cβ}	0.00	-0.01	0.01	-0.02
	INT _{Cα}	0.21	0.16	0.20	0.14
Hie	INT _{Cβ}	-0.09	0.11	-0.01	-0.01
	INT _{Cα}	0.22	0.16	0.22	0.13
Thr	INT _{Cβ}	-0.03	0.01	0.01	-0.01
	INT _{Cα}	0.20	0.15	0.24	0.15
Ser	INT _{Cβ}	-0.02	0.01	0.01	-0.02
	INT _{Cα}	0.25	-0.04	0.23	0.14
Cys	INT _{Cβ}	0.09	-0.09	0.02	0.00
	INT _{Cα}	0.17	0.15	0.21	0.15
Met	INT _{Cβ}	0.00	0.01	0.00	-0.01
	INT _{Cα}	0.19	0.15	0.22	0.15
Phe	INT _{Cβ}	0.00	0.00	0.02	-0.01
	INT _{Cα}	0.19	0.15	0.24	0.16
Tyr	INT _{Cβ}	0.00	0.00	0.01	-0.01
	INT _{Cα}	0.20	0.15	0.23	0.18
Trp	INT _{Cβ}	0.00	0.01	0.00	0.00

Table A.9: Bond order difference between the formed intermediate and the correspondent reactant at water dielectric.

Appendix for Chapter 6

$\#n H_2O$	ΔG_{aq}^{298}	E^0
0	-111.8	0.4
1	-119.7	0.7
2	-127.9	1.1
3	-129.2	1.1
4	-127.9	1.1
5	-127.5	1.1
6	-130.3	1.2
7	-132.6	1.3
10	-133.1	1.3
15	-136.2	1.5
23	-143.7	1.8
Exp	-	1.9

Table B.1: Calculated ΔG_{aq}^{298} and E^0 reduction potential for the $\bullet OH/OH^-$ reduction process, as a function of the number of water molecules included explicitly.

	ΔH_4^{TS}	ΔH_{aq}^{TS}	ΔG_4^{TS}	ΔG_{aq}^{TS}	r_{OH}^{TS}	r_{XH}^{TS}	ρ_s^X	ρ_s^O
S-TS ₁ ^{Cβ} (α)	2.0	1.6	7.4	7.8	1.36	1.19	0.31	0.64
S-TS ₂ ^{Cβ} (α)	1.8	2.6	10.2	11.0	1.33	1.20	0.37	0.63
S-TS ₃ ^{Oγ} (α)	2.4	2.9	12.2	12.7	1.18	1.13	0.48	0.53
S-TS ₁ ^{Cβ} (β)	3.9	3.6	5.5	5.8	1.36	1.19	0.31	0.64
S-TS ₂ ^{Cβ} (β)	1.0	0.5	8.7	10.1	1.60	1.14	0.18	0.81
S-TS ₃ ^{Oγ} (β)	2.5	3.8	12.7	14.0	1.22	1.10	0.44	0.59
T-TS ₁ ^{Cβ} (α)	2.8	2.3	6.7	7.2	1.40	1.17	0.30	0.68
T-TS ₂ ^{Oγ} (α)	1.0	1.2	10.2	10.4	1.26	1.23	0.47	0.56
T-TS ₃ ^{Oγ} (α)	2.9	3.5	13.0	13.6	1.16	1.14	0.50	0.51
T-TS ₁ ^{Cβ} (β)	4.5	4.1	5.5	5.9	1.42	1.17	0.30	0.68
T-TS ₂ ^{Oγ} (β)	0.6	1.3	11.1	11.9	1.27	1.23	0.44	0.57
T-TS ₃ ^{Oγ} (β)	1.6	3.0	11.7	13.1	1.22	1.10	0.44	0.59
C-TS ₁ ^{Cβ} (α)	4.4	3.3	6.1	7.2	1.39	1.18	0.28	0.65
C-TS ₂ ^{Sγ} (α)	1.4	0.9	7.2	7.7	1.51	1.39	0.32	0.74
C-TS ₃ ^{Cβ} (α)	1.1	1.1	9.6	9.6	1.39	1.17	0.26	0.67
C-TS ₁ ^{Cβ} (β)	3.4	3.1	6.6	6.9	1.34	1.19	0.30	0.61
C-TS ₂ ^{Sγ} (β)	6.4	4.4	4.7	6.6	1.43	1.41	0.30	0.78
C-TS ₃ ^{Cβ} (β)	1.7	0.3	8.2	9.6	1.56	1.14	0.09	0.79
M-TS ₁ ^{Cϵ} (α)	3.3	3.2	6.9	7.0	1.32	1.20	0.34	0.58
M-TS ₂ ^{Cγ} (α)	3.7	2.6	4.6	5.6	1.52	1.14	0.18	0.72
M-TS ₃ ^{Cβ} (α)	2.1	1.7	7.1	7.5	1.30	1.21	0.41	0.60
M-TS ₄ ^{Cγ} (α)	1.0	0.9	5.9	6.0	1.48	1.15	0.22	0.71
M-TS ₅ ^{Cβ} (α)	1.1	1.4	9.9	10.3	1.34	1.20	0.36	0.64
M-TS ₁ ^{Cϵ} (β)	4.9	4.2	7.0	7.7	1.36	1.18	0.29	0.59
M-TS ₂ ^{Cβ} (β)	3.8	3.1	6.8	7.5	1.30	1.21	0.39	0.60
M-TS ₃ ^{Cγ} (β)	3.7	2.5	8.1	9.3	1.45	1.16	0.21	0.68
M-TS ₄ ^{Cβ} (β)	3.9	2.2	6.1	7.8	1.34	1.19	0.35	0.64
M-TS ₅ ^{Cγ} (β)	0.3	0.0	8.3	8.6	1.59	1.13	0.15	0.79

Table B.2: Computed enthalpy values (in kcal/mol) at dielectric constants of 4, and 80 (aqueous solution) of the transition states and radical intermediates for the attack of the $\bullet OH$ onto serine, in α -helix and β -sheet structures. R(XH, X=C,O)

	ΔH_4^{Int}	ΔH_{aq}^{Int}	ΔG_4^{Int}	ΔG_{aq}^{Int}	ρ_s^X
S-Int ₁ ^{Cβ} (α)	-22.1	-22.7	-23.6	-24.2	0.87
S-Int ₂ ^{Oγ} (α)	-11.1	-12.2	-13.0	-14.2	0.88
S-Int ₁ ^{Cβ} (β)	-21.8	-21.9	-22.8	-22.9	0.89
S-Int ₂ ^{Oγ} (β)	-14.4	-14.8	-15.4	-15.8	0.87
T-Int ₁ ^{Cβ} (α)	-23.9	-24.5	-26.0	-26.6	0.82
T-Int ₂ ^{Cγ} (α)	-14.6	-15.0	-16.0	-16.4	0.85
T-Int ₃ ^{Oγ} (α)	-10.2	-10.6	-12.2	-12.6	1.06
T-Int ₁ ^{Cβ} (β)	-26.0	-26.5	-26.1	-26.6	0.81
T-Int ₂ ^{Cγ} (β)	-16.1	-16.1	-16.9	-16.8	0.85
T-Int ₃ ^{Oγ} (β)	-14.1	-14.5	-14.9	-15.3	1.02
C-Int ₁ ^{Sγ} (α)	-30.9	-31.2	-32.2	-32.5	0.99
C-Int ₂ ^{Cβ} (α)	-24.6	-25.3	-25.7	-26.3	0.79
C-Int ₁ ^{Sγ} (β)	-30.3	-30.7	-31.5	-31.9	0.99
C-Int ₂ ^{Cβ} (β)	-23.1	-23.0	-24.9	-24.7	0.78
M-Int ₁ ^{Cγ} (α)	-28.4	-29.0	-30.6	-31.3	0.80
M-Int ₂ ^{Cϵ} (α)	-23.0	-23.2	-25.4	-25.6	0.83
M-Int ₃ ^{Cβ} (α)	-18.7	-19.2	-21.1	-21.5	0.98
M-Int ₁ ^{Cγ} (β)	-27.0	-27.2	-28.5	-28.7	0.76
M-Int ₂ ^{Cϵ} (β)	-23.5	-23.9	-25.7	-26.0	0.85
M-Int ₃ ^{Cβ} (β)	-19.7	-20.1	-20.3	-20.7	0.94

Table B.3: Computed enthalpy values (in kcal/mol) at dielectric constants of 4, and 80 (aqueous solution) of the transition states and radical intermediates for the attack of the $\bullet OH$ onto serine, in α -helix and β -sheet structures. R(XH, X=C,O)

	First·OH				Second·OH					
	ΔH_4^{Int}	ΔH_{aq}^{Int}	E_{aq}^0	r_{SX}^{Int1}	ρ_s^X	ΔH_4^{Int2}	ΔH_{aq}^{Int2}	$r_{O_{ac}H}^{Int2}$	$r_{O_{bb}H}^{Int2}$	r_{SX}^{Int2}
$S_O^+(\alpha)$	3.8	-11.1	1.32	2.33	0.72	-18.6	-47.1	0.96	4.41	2.34
$S_N^+(\alpha)$	-	-	-	-	-	-21.8	-50.1	1.05	1.38	3.23
$S_{N,ter}^+$	-0.2	-16.2	1.08	2.48	0.64	-20.5	-48.5	0.96	4.55	2.51
$S_{OH,ter}^+$	14.2	-1.8	1.72	2.52	0.88	-31.7	-61.2	1.49	1.08	3.46
$S_{O,ter}^+$	-22.3	-17.7	1.08	2.30	0.71	-11.1	-40.4	0.96	4.64	2.61
						-11.1	-40.3	0.98	1.67	3.28
						-39.9	-48.5	0.96	4.21	2.10
						-55.5	-63.2	3.39	0.96	3.66
$S_O^+(\beta)$	4.5	-10.7	1.43	2.39	0.80	-18.6	-47.7	0.96	4.60	2.51
$S_N^+(\beta)$	13.3	-1.8	1.80	2.58	0.71	-25.0	-53.7	1.04	1.42	3.20
						-20.1	-48.5	1.02	1.59	4.73
						-	-	-	-	-

Table B.4: Computed enthalpy values (in kcal/mol) at dielectric constants of 4 and 80 (aqueous solution) of the transition states and radical intermediates for the attack of the $\bullet OH$ onto methionine, in α -helix-like and β -sheet structures.

	ΔH_4	ΔH_{aq}	ΔG_4	ΔG_{aq}
S-Prod₁(α)	-117.4	-117.5	-107.0	-107.1
S-Prod₂(α)	-106.6	-108.0	-108.5	-109.8
S-Prod₃(α)	-47.5	-47.2	-37.2	-36.9
S-Prod₄(α)	-47.1	-48.2	-35.0	-36.0
S-Prod₁(β)	-118.4	-117.6	-107.2	-106.5
S-Prod₂(β)	-108.3	-109.9	-109.6	-111.2
S-Prod₃(β)	-51.1	-50.8	-40.3	-40.0
S-Prod₄(β)	-53.8	-52.8	-38.9	-37.9
C-Prod₁(α)	-122.5	-123.0	-110.8	-111.4
C-Prod₂(α)	-111.6	-111.3	-100.6	-100.3
C-Prod₃(α)	-103.6	-103.2	-92.0	-91.6
C-Prod₄(α)	-98.4	-99.1	-98.9	-99.6
C-Prod₅(α)	-86.8	-88.4	-76.6	-78.2
C-Prod₁(β)	-117.7	-117.4	-101.4	-101.2
C-Prod₂(β)	-109.4	-109.5	-98.0	-98.2
C-Prod₃(β)	-99.6	-99.3	-88.1	-87.8
C-Prod₄(β)	-96.5	-96.8	-97.0	-97.2
C-Prod₅(β)	-84.0	-83.7	-72.6	-72.2
T-Prod₁(α)	-117.5	-117.9	-107.3	-107.8
T-Prod₂(α)	-111.5	-112.8	-114.1	-115.3
T-Prod₃(α)	-110.1	-109.7	-98.9	-98.5
T-Prod₄(α)	-96.0	-98.3	-97.8	-100.2
T-Prod₁(β)	-124.4	-122.9	-112.9	-111.5
T-Prod₂(β)	-113.3	-114.6	-114.4	-115.8
T-Prod₃(β)	-110.3	-109.6	-99.8	-99.1
T-Prod₄(β)	-100.1	-101.4	-102.2	-103.5
M-Prod₁(α)	-108.4	-110.0	-101.4	-103.1
M-Prod₂(α)	-96.6	-97.6	-99.0	-100.0
M-Prod₃(α)	-97.7	-97.7	-87.0	-87.1
M-Prod₁(β)	-106.9	-107.5	-96.7	-97.4
M-Prod₂(β)	-100.6	-101.5	-100.7	-101.5
M-Prod₃(β)	-94.7	-95.2	-83.2	-83.7

Table B.5: Computed enthalpy values (in kcal/mol) at dielectric constants of 4, and 80 (aqueous solution) of the transition states and radical intermediates for the attack of the $\bullet OH$ onto serine, in α -helix and β -sheet structures. R(XH, X=C,O)

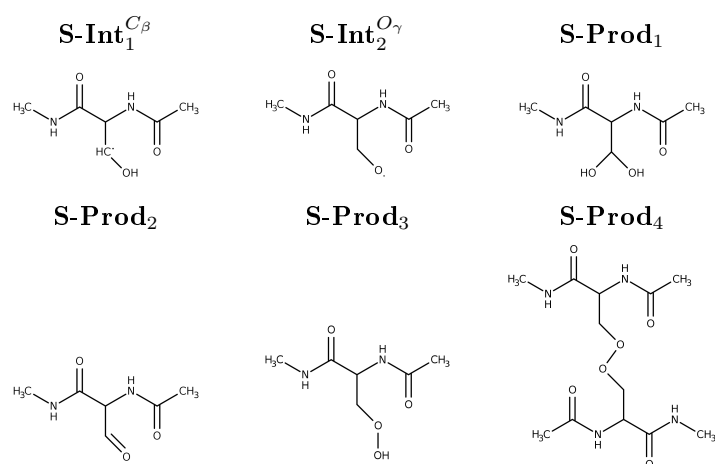


Figure B.1: 2D ChemDraw representations of serine intermediates and products

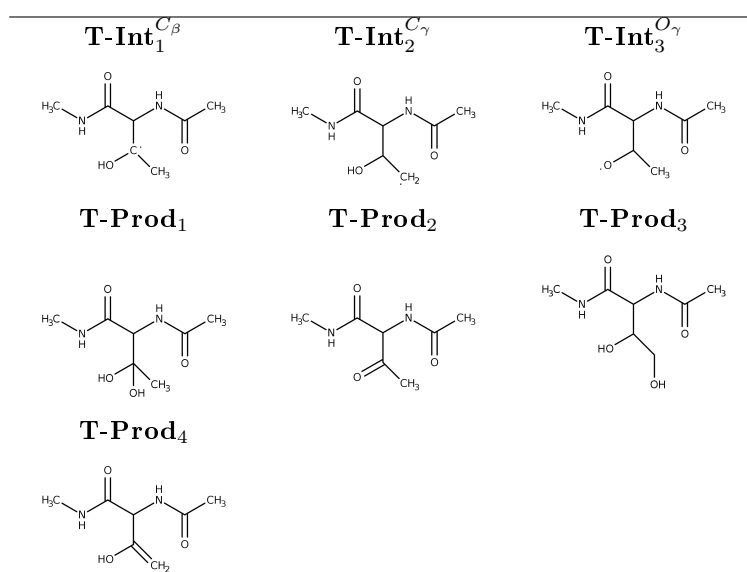


Figure B.2: 2D ChemDraw representations of threonine intermediates and products

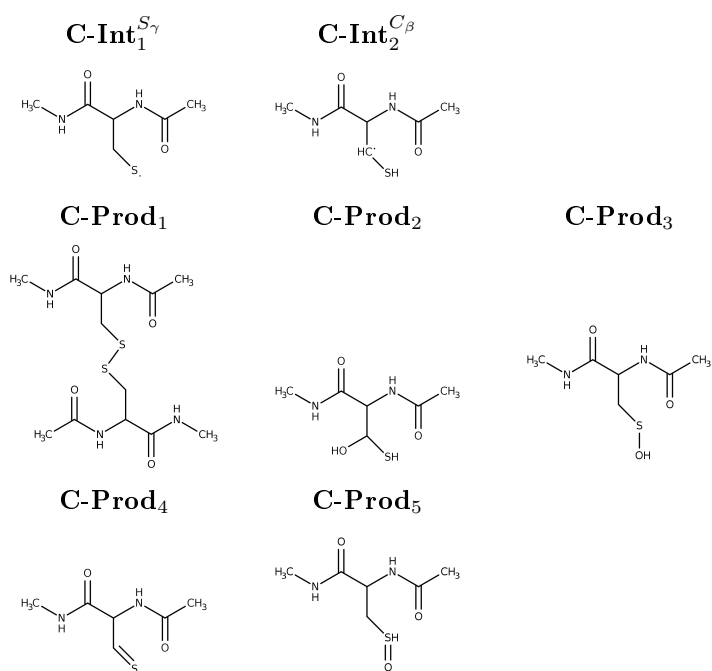


Figure B.3: 2D ChemDraw representations of cysteine intermediates and products

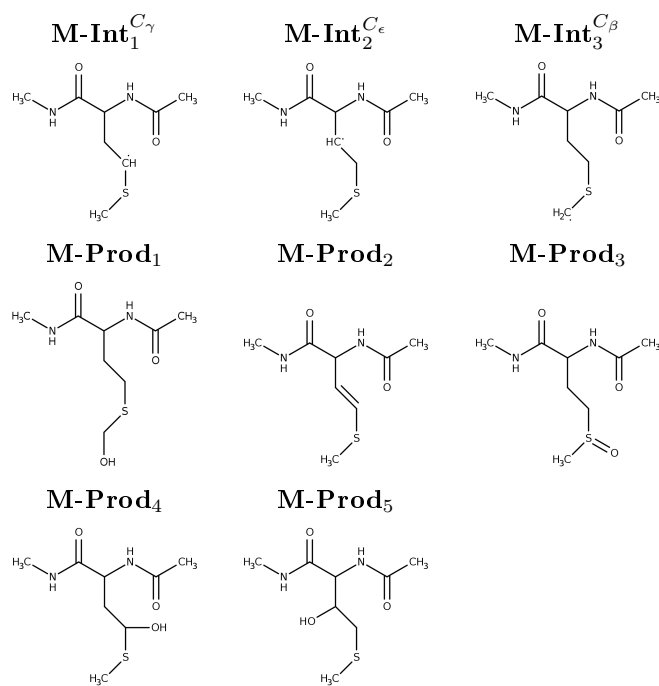


Figure B.4: 2D ChemDraw representations of methionine intermediates and products

Appendix for Chapter 7

	α – helix – like			β – sheet		
	ΔH_4^{298}	ΔH_{aq}^{298}	ρ_S^X	ΔH_4^{298}	ΔH_{aq}^{298}	ρ_S^X
$Int_{Asp}^{C\alpha}$	-34.0	-33.7	0.51	-31.2	-31.6	0.49
$Int_{Asp}^{C\beta}$	-22.7	-23.4	0.76	-22.1	-22.8	0.76
$Int_{Asp}^{O\delta}$	-15.8	-10.2	0.91	-13.9	-7.8	0.90
			$\rho_S^{C\alpha}$ $\rho_S^{C\beta}$			$\rho_S^{C\alpha}$ $\rho_S^{C\beta}$
$Int_{Asp}^{-\alpha\beta\ddagger}$	-20.8	-7.7	0.12 0.43	-5.1	-5.3	0.08 0.39
	α – helix – like			β – sheet		
	ΔH_4^{298}	ΔH_{aq}^{298}	ρ_S^X	ΔH_4^{298}	ΔH_{aq}^{298}	ρ_S^X
$Int_{Asp}^{C\alpha}$	-27.1	-28.6	0.58	-30.4	-30.9	0.50
$Int_{Asp}^{C\beta}$	-23.1	-23.5	0.70	-21.6	-22.8	0.69
$Int_{Asp}^{O\delta}$	-6.1	-7.2	0.89	-4.8	-4.9	0.90
			$\rho_S^{C\alpha}$ $\rho_S^{C\beta}$			$\rho_S^{C\alpha}$ $\rho_S^{C\beta}$
$Int_{Asp}^{-\alpha\beta\ddagger}$	8.5	7.3	0.12 0.43	23.0	8.0	0.08 0.39

Table C.1: Aspartate and Aspartic acid intermediates. Relative enthalpies with respect to the reactants and TFVC spin densities for the labelled atoms are shown. OH anion is treated with explicit 25 water molecules.

	α – helix – like		β – sheet	
	ΔH_4^{298}	ΔH_{aq}^{298}	ΔH_4^{298}	ΔH_{aq}^{298}
$Prod_{Asp}^{r-\beta oh}$	-111.3	-111.6	-112.3	-111.6
$Prod_{Asp}^{s-\beta oh}$	-115.6	-115.7	-105.0	-105.7
$Prod_{Asp}^{\alpha\beta}$	-112.2	-108.0	-113.8	-108.5
$Prod_{Asp}^{ooh}$	-8.3	-15.3	-4.6	-11.0
	α – helix – like		β – sheet	
	ΔH_4^{298}	ΔH_{aq}^{298}	ΔH_4^{298}	ΔH_{aq}^{298}
$Prod_{Asp}^{r-\beta oh}$	-106.5	-106.9	-105.9	-105.9
$Prod_{Asp}^{s-\beta oh}$	-111.1	-111.0	-106.6	-106.4
$Prod_{Asp}^{\alpha\beta}$	-101.9	-103.4	-104.6	-105.6
$Prod_{Asp}^{ooh}$	-47.3	-46.9	-44.8	-44.4

Table C.2: Aspartate and Aspartic acid products. Relative enthalpies with respect to the reactants are shown. OH anion is treated with explicit 25 water molecules.

	α - helix - like			β - sheet		
	ΔH_4^{298}	ΔH_{aq}^{298}	ρ_S^X	ΔH_4^{298}	ΔH_{aq}^{298}	ρ_S^X
$Int_{Glu}^{C\beta}$	-20.1	-20.3	0.78	-21.8	-22.5	0.77
$Int_{Glu}^{C\gamma}$	-23.6	-24.2	0.75	-24.4	-25.2	0.75
$Int_{Glu}^{O\varepsilon}$	-15.6	-10.6	0.89	-17.5	-12.6	0.89
	α - helix - like			β - sheet		
	ΔH_4^{298}	ΔH_{aq}^{298}	ρ_S^X	ΔH_4^{298}	ΔH_{aq}^{298}	ρ_S^X
$Int_{Glu}^{C\beta}$	-18.1	-18.3	0.79	-20.0	-20.5	0.78
$Int_{Glu}^{C\gamma}$	-24.6	-24.8	0.69	-26.5	-27.0	0.69
$Int_{Glu}^{O\varepsilon}$	-7.0	-6.7	0.89	-9.5	-9.7	0.89

Table C.3: Glutamate and Glutamic acid intermediates. Relative enthalpies with respect to the reactants and TFVC spin densities for the labelled atoms are shown. OH anion is treated with explicit 25 water molecules.

	α - helix - like		β - sheet	
	ΔH_4^{298}	ΔH_{aq}^{298}	ΔH_4^{298}	ΔH_{aq}^{298}
$Prod_{Glu}^{r-\beta oh}$	-113.6	-113.1	-115.1	-114.6
$Prod_{Glu}^{s-\beta oh}$	-113.8	-112.9	-111.1	-110.8
$Prod_{Glu}^{cis-\beta\gamma}$	-96.5	-97.4	-102.4	-104.1
$Prod_{Glu}^{trans-\beta\gamma}$	-92.3	-96.7	-95.9	-99.5
$Prod_{Glu}^{r-\gamma oh}$	-115.2	-113.9	-106.2	-106.6
$Prod_{Glu}^{s-\gamma oh}$	-116.6	-115.2	-116.6	-115.3
$Prod_{Glu}^{\beta\gamma}$	-109.0	-104.6	-110.5	-106.0
$Prod_{Glu}^{ooh}$	-6.5	-13.9	-5.9	-13.1
	α - helix - like		β - sheet	
	ΔH_4^{298}	ΔH_{aq}^{298}	ΔH_4^{298}	ΔH_{aq}^{298}
$Prod_{Glu}^{r-\beta oh}$	-111.6	-110.7	-117.1	-116.4
$Prod_{Glu}^{s-\beta oh}$	-109.1	-109.4	-113.0	-113.6
$Prod_{Glu}^{cis-\beta\gamma}$	-91.9	-92.8	-97.0	-98.2
$Prod_{Glu}^{trans-\beta\gamma}$	-98.8	-99.8	-100.6	-101.8
$Prod_{Glu}^{r-\gamma oh}$	-110.3	-110.1	-110.1	-110.5
$Prod_{Glu}^{s-\gamma oh}$	-104.4	-104.7	-110.7	-110.5
$Prod_{Glu}^{\beta\gamma}$	-100.4	-100.7	-102.5	-103.1
$Prod_{Glu}^{ooh}$	-47.2	-46.1	-47.2	-46.4

Table C.4: Glutamate and Glutamic acid products. Relative enthalpies with respect to the reactants are shown. OH anion is treated with explicit 25 water molecules.

	α - helix - like			β - sheet		
	ΔH_4^{298}	ΔH_{aq}^{298}	ρ_S^X	ΔH_4^{298}	ΔH_{aq}^{298}	ρ_S^X
$Int_{Arg}^{C\beta}$	-18.0	-18.3	0.79	-18.4	-19.0	0.79
$Int_{Arg}^{C\gamma}$	-18.1	-18.5	0.79	-22.3	-20.2	0.78
$Int_{Arg}^{C\delta}$	-23.2	-23.9	0.66	-23.2	-23.9	0.65
$Int_{Arg}^{N\epsilon}$	-7.0	-8.0	0.76	-6.5	-5.2	0.84
$Int_{Arg}^{C\zeta}$	0.3	1.2	0.70*	-1.0	1.6	0.65*
$Int_{Arg}^{N\eta}$	-1.4	-2.6	0.83	0.4	-0.8	0.83
$Int_{OArg}^{cis-C\delta}$	-8.1	1.1	0.93	-6.8	1.2	0.92
$Int_{OArg}^{trans-C\delta}$	-7.5	-7.2	0.91	-7.5	0.8	0.91
Citrulline	-21.5	-13.8	-	-21.1	-13.8	-
Ornithine	-3.0	-6.6	-	-3.5	-6.8	-
	α - helix - like			β - sheet		
	ΔH_4^{298}	ΔH_{aq}^{298}	ρ_S^X	ΔH_4^{298}	ΔH_{aq}^{298}	ρ_S^X
$Int_{Lys}^{C\beta}$	-18.0	-18.5	0.79	-17.6	-18.1	0.79
$Int_{Lys}^{C\gamma}$	-18.6	-19.1	0.79	-23.3	-19.3	0.79
$Int_{Lys}^{C\delta}$	-17.6	-17.9	0.77	-15.9	-12.5	0.79
$Int_{Lys}^{C\epsilon}$	-14.1	-14.7	0.77	-14.2	-14.8	0.77
$Int_{Lys}^{N\zeta}$	-9.8	-9.5	0.80	-10.3	-9.7	0.78
$Int_{OLys}^{cis-C\epsilon}$	28.9	1.6	0.92	29.5	1.6	0.92
$Int_{OLys}^{trans-C\epsilon}$	28.5	1.3	0.91	29.2	1.3	0.91

Table C.5: Arginine and Lysine intermediates. Relative enthalpies with respect to the reactants and TFVC spin densities for the labelled atoms are shown. * $N\epsilon$ spin density.

	α - helix - like		β - sheet	
	ΔH_4^{298}	ΔH_{aq}^{298}	ΔH_4^{298}	ΔH_{aq}^{298}
$Prod_{Arg}^{r-\beta oh}$	-115.5	-113.9	-112.8	-111.8
$Prod_{Arg}^{s-\beta oh}$	-107.6	-107.6	-110.3	-109.8
$Prod_{Arg}^{cis-\beta\gamma}$	-93.4	-93.2	-96.4	-95.0
$Prod_{Arg}^{trans-\beta\gamma}$	-95.8	-93.4	-97.7	-99.3
$Prod_{Arg}^{r-\gamma oh}$	-111.8	-110.3	-115.2	-113.9
$Prod_{Arg}^{s-\gamma oh}$	-111.5	-110.9	-109.4	-107.8
$Prod_{Arg}^{cis-\gamma\delta}$	-100.1	-100.5	-100.4	-99.6
$Prod_{Arg}^{trans-\gamma\delta}$	-99.2	-100.4	-100.4	-99.6
$Prod_{Arg}^{r-\delta oh}$	-114.9	-114.6	-115.4	-114.9
$Prod_{Arg}^{s-\delta oh}$	-114.0	-113.1	-114.0	-113.1
$Prod_{Arg}^{cis-\delta\epsilon}$	-93.7	-94.8	-92.0	-91.0
$Prod_{Arg}^{trans-\delta\epsilon}$	-95.9	-96.6	-103.0	-101.1
$Prod_{Arg}^{\xi oh}$	-71.0	-71.2	-70.5	-69.4
$Prod_{Arg}^{\eta oh}$	-68.7	-68.1	-69.0	-68.5
$Prod_{OArg}^{cis-\delta oh}$	-116.7	-107.4	-115.4	-107.0
$Prod_{OArg}^{trans-\delta oh}$	-116.4	-107.1	-115.0	-107.0
$Prod_{OArg}^{\delta o}$	-124.7	-115.4	-123.9	-115.6

Table C.6: Arginine products. Relative enthalpies with respect to the reactants are shown.

	α - helix - like		β - sheet	
	ΔH_4^{298}	ΔH_{aq}^{298}	ΔH_4^{298}	ΔH_{aq}^{298}
$Prod_{Lys}^{r-\beta oh}$	-115.5	-114.0	-112.8	-111.6
$Prod_{Lys}^{s-\beta oh}$	-113.2	-111.9	-111.3	-110.4
$Prod_{Lys}^{cis-\beta\gamma}$	-95.5	-94.6	-102.4	-99.9
$Prod_{Lys}^{trans-\beta\gamma}$	-97.3	-97.8	-108.5	-105.3
$Prod_{Lys}^{r-\gamma oh}$	-	-	-117.9	-113.4
$Prod_{Lys}^{s-\gamma oh}$	-110.9	-109.7	-110.8	-109.9
$Prod_{Lys}^{cis-\gamma\delta}$	-96.5	-95.9	-96.4	-97.4
$Prod_{Lys}^{trans-\gamma\delta}$	-98.5	-99.2	-106.8	-103.5
$Prod_{Lys}^{r-\delta oh}$	-112.9	-111.3	-113.1	-111.6
$Prod_{Lys}^{s-\delta oh}$	-113.0	-111.3	-112.7	-111.0
$Prod_{Lys}^{cis-\delta\epsilon}$	-93.7	-94.5	-106.7	-103.0
$Prod_{Lys}^{trans-\delta\epsilon}$	-95.7	-96.4	-95.9	-96.7
$Prod_{Lys}^{r-\epsilon oh}$	-111.7	-111.2	-110.9	-109.5
$Prod_{Lys}^{s-\epsilon oh}$	-111.8	-111.4	-111.0	-109.5
$Prod_{Lys}^{\epsilon\zeta}$	-104.5	-104.2	-105.0	-104.4
$Prod_{Lys}^{\zeta oh}$	-66.5	-66.0	-66.7	-66.4
$Prod_{OLys}^{cis-\epsilon oh}$	-79.1	-105.9	-78.7	-105.8
$Prod_{OLys}^{trans-\epsilon oh}$	-79.4	-106.3	-78.6	-106.2
$Prod_{OLys}^{\epsilon o}$	-87.4	-114.6	-86.9	-114.6

Table C.7: Lysine products. Relative enthalpies with respect to the reactants are shown.

	α - helix - like			β - sheet		
	ΔH_4^{298}	ΔH_{aq}^{298}	ρ_S^X	ΔH_4^{298}	ΔH_{aq}^{298}	ρ_S^X
$Int_{Asn}^{C\alpha}$	-30.7	-30.2	0.57	-38.6	-37.2	0.52
$Int_{Asn}^{C\beta}$	-22.5	-22.8	0.72	-21.2	-21.7	0.74
$Int_{Asn}^{N\delta}$	-1.0	-0.7	0.81	-2.1	-1.7	0.84
$Int_{OAsn}^{cis-C\beta}$	26.5	23.7	0.96	15.7	15.2	0.92
$Int_{OAsn}^{trans-C\beta}$	25.4	23.4	0.90	17.0	15.6	0.90
	α - helix - like			β - sheet		
	ΔH_4^{298}	ΔH_{aq}^{298}	ρ_S^X	ΔH_4^{298}	ΔH_{aq}^{298}	ρ_S^X
$Int_{Gln}^{C\beta}$	-21.2	-20.9	0.80	-22.4	-21.7	0.79
$Int_{Gln}^{C\gamma}$	-27.0	-26.7	0.72	-26.4	-25.6	0.70
$Int_{Gln}^{N\epsilon}$	-4.1	-3.3	0.86	-2.4	-2.3	0.84
$Int_{OGln}^{cis-C\gamma}$	23.0	22.0	0.96	22.9	21.6	0.92
$Int_{OGln}^{trans-C\gamma}$	21.6	20.9	0.90	22.5	20.9	0.92

Table C.8: Asparagine and Glutamine intermediates. Relative enthalpies with respect to the reactants and TFVC spin densities for the labelled atoms are shown.

	$\alpha - helix - like$		$\beta - sheet$	
	ΔH_4^{298}	ΔH_{aq}^{298}	ΔH_4^{298}	ΔH_{aq}^{298}
$Prod_{Asn}^{\alpha\beta}$	5.6	3.9	-0.9	-1.2
$Prod_{Asn}^{r-\beta oh}$	-113.1	-111.7	-113.9	-111.7
$Prod_{Asn}^{s-\beta oh}$	-110.3	-110.3	-110.3	-110.3
$Prod_{OAsn}^{cis-\beta oh}$	-88.4	-90.2	-87.5	-89.2
$Prod_{OAsn}^{trans-\beta oh}$	-83.3	-86.4	-92.0	-92.2
$Prod_{OAsn}^{\beta o}$	-89.1	-90.9	-95.8	-95.8
	$\alpha - helix - like$		$\beta - sheet$	
	ΔH_4^{298}	ΔH_{aq}^{298}	ΔH_4^{298}	ΔH_{aq}^{298}
$Prod_{Gln}^{r-\beta oh}$	-113.9	-113.6	-115.3	-114.4
$Prod_{Gln}^{s-\beta oh}$	-111.5	-111.6	-108.6	-109.1
$Prod_{Gln}^{cis-\beta\gamma}$	-96.7	-97.0	-95.4	-96.9
$Prod_{Gln}^{trans-\beta\gamma}$	-98.9	-100.6	-99.3	-100.9
$Prod_{Gln}^{r-\gamma oh}$	-112.2	-111.2	-108.5	-108.6
$Prod_{Gln}^{s-\gamma oh}$	-111.5	-111.3	-116.3	-115.4
$Prod_{Gln}^{\beta oh}$	-71.6	-71.0	-71.4	-70.7
$Prod_{OGln}^{cis-\gamma oh}$	-86.3	-87.1	-84.8	-86.3
$Prod_{OGln}^{trans-\gamma oh}$	-86.0	-87.1	-84.5	-86.3
$Prod_{OGln}^{\gamma o}$	-94.1	-94.3	-93.2	-94.7

Table C.9: Asparagine and Glutamine products. Relative enthalpies with respect to the reactants are shown.